



DISSERTATION / DOCTORAL THESIS

Titel der Dissertation / Title of the Doctoral Thesis

“Spaces of Functions of Variable Bandwidth
Parametrized by Piecewise Constant Functions”

verfasst von / submitted by

Mark Jason V. Celiz

angestrebter akademischer Grad / in partial fulfilment of the requirements for the degree of

Doktor der Naturwissenschaften (Dr. rer. nat.)

Wien, 2022 / Vienna 2022

Studienkennzahl lt. Studienblatt /
degree programme code as it appears on the student
record sheet:

UA 796 605 405

Dissertationsgebiet lt. Studienblatt /
field of study as it appears on the student record sheet:

Mathematik

Betreut von / Supervisor:

Univ.-Prof. Mag. Dr. Karlheinz Gröchenig

Acknowledgments

This dissertation project would not have been completed without the support of the following people and agencies:

First and foremost, I am greatly indebted to my adviser, Karlheinz Gröchenig for his overwhelming support and guidance throughout this project. I am equally grateful to Andreas Klotz who acted like a second supervisor during my study. Working with them was a humbling and inspiring experience, and I certainly learned a lot. Writing this dissertation was indeed a rough journey, but I could not just walk away and let them down. Without their support and encouragement, this thesis would not have been completed.

I offer my special regards to Monika Dörfler for giving me the opportunity to study at the University of Vienna. My stay was a lot less lonely with the company of NuHAG colleagues, Markus Faulhuber, Thomas Mejstrik, David Rottensteiner, Sarah Koppensteiner, Martin Rathmair, Jordy Timo van Velthoven, Dennis Elbrächter, Julius Berner, and Pavol Harar. I also got to meet Ralph Anthony Chan and Gervy Marie Angeles who are my fellow Filipino doctoral candidates.

I dedicate this dissertation to my Master's thesis adviser, the late Noli Reyes, for introducing me to the wonderful world of harmonic analysis. To my senior colleagues, Gino Angelo Velasco, Manuel Joseph Loquias, Marian Roque, Carlene Perpetua Pilar-Arceo, Jose Ernie Lope, Julius Basilla, and the rest of the UP Diliman Institute of Mathematics faculty, I sincerely thank you for putting your trust in me.

Special thanks to Dr. George Soo for being a good mentor and for taking care of me. Hope we can enjoy travelling Europe again.

Lastly, I would like to express my gratitude to my family, Antonio Celiz, Joan Mari Celiz-Del Rosario, Maria Shiela Rosana, and Angelyn Vidar for simply being my source of inspiration.

This project was supported by the OeAD-GmbH – Agency for Education and Internationalisation and the Austrian Science Fund (FWF) through the grant project P31887-N32

Abstract

The notion of variable bandwidth stems from the observation that it makes sense in time-frequency analysis to assign different local bandwidths to different segments of a signal. However, the problem in defining such a concept lies in the fact that bandwidth is a global property of a signal, and hence the idea of local bandwidth violates the uncertainty principle. In an attempt to formalize this concept, several definitions of variable bandwidth were presented by a number of mathematicians and engineers. In this thesis, we adopt the definition of spaces of functions of variable bandwidth as spectral subspaces of a Sturm-Liouville operator on the real line associated to a chosen bandwidth-parametrizing function. In particular, we study such spaces associated to piecewise constant parametrizing functions. As opposed to arbitrary parametrizing functions, with piecewise constant functions we obtain an explicit formula for the fundamental set of solutions of the corresponding Sturm-Liouville eigenvalue problem. From this the spectral measure of the operator can be derived, which in principle allows a direct evaluation of the reproducing kernel of spectral subspaces. Furthermore, the computation of the reproducing kernel is demonstrated in the case when the parametrizing function has two and three constant components. Afterwards, necessary density conditions for sets of sampling and interpolation and the reconstruction of functions of variable bandwidth are derived. The theory is confirmed by numerical simulations. The reconstruction algorithms are based on frame theory and regularization (since direct algorithms have stability problems). Notably, functions of variable bandwidth are much better approximated within this model than by classical bandlimited functions.

Zusammenfassung

Der Begriff der variablen Bandbreite beruht auf der Beobachtung, daß man verschiedenen Abschnitten eines Signals verschiedene Bandbreiten zuordnen kann. Das Problem dabei ist jedoch, daß Bandbreite eine globale Eigenschaft eines Signals ist und daher die Idee einer lokalen Bandbreite das Unschärfeprinzip verletzt. Der Versuch, diesen Begriff zu formalisieren, hat zu mehreren möglichen Definitionen von variabler Bandbreite durch Mathematiker und Ingenieure geführt. In dieser Arbeit benützen wir als Definition von Räumen variabler Bandbreite die spektralen Teilräume eines Sturm-Liouville-Operators auf der reellen Achse bezüglich einer geeigneten Parametrisierungsfunktion. Insbesondere untersuchen wir solche Räume, die einer stückweise konstanten Parametrisierungsfunktion zugeordnet sind. Im Gegensatz zu beliebigen Parametrisierungsfunktionen erhält man für stückweise konstante Funktionen explizite Formeln für die Fundamentallösungen des entsprechenden Sturm-Liouville-Problems. Daraus läßt sich das Spektralmaß des Operators ableiten, was im Prinzip eine direkte Auswertung des reproduzierenden Kerns der spektralen Teilräume erlaubt. Im weiteren wird gezeigt, wie der reproduzierende Kern im Fall von zwei und drei konstanten Komponenten der Parametrisierungsfunktion berechnet wird. Danach werden notwendige Dichtebedingungen für Abtast- und Interpolationsmengen und die Rekonstruktion von Funktionen variabler Bandbreite abgeleitet. Die Theorie wird durch numerische Simulationen bestätigt. Die Rekonstruktionsalgorithmen basieren auf Frame-Theorie und Regularisierung (da die direkten Algorithmen Stabilitätsprobleme haben). Insbesondere werden Funktionen variabler Bandbreite innerhalb dieses Modells viel besser approximiert als durch klassische bandbegrenzte Funktionen.

Contents

Acknowledgments	3
Abstract / Zusammenfassung	5
List of figures	11
1. Introduction	13
1.1. Motivation	13
1.2. Defining variable bandwidth	14
1.3. Piecewise constant parametrizing functions	16
1.4. Main results and overview	16
2. Preliminaries	21
2.1. Review of unbounded operators	22
2.2. Spectral theory of some self-adjoint Sturm-Liouville operators	25
3. Functions of variable bandwidth	37
3.1. Reproducing kernel Hilbert spaces	38
3.2. Necessary density conditions for sampling and interpolation	39
3.3. Non-uniform sampling	41
4. The space $PW_\Lambda(A_p)$ with piecewise constant p	43
4.1. Piecewise constant parametrizing functions	44
4.2. Construction of fundamental solutions	45
4.3. Wronskian determinants, resolvents and spectral matrix measure	53
4.4. Computing the reproducing kernel	59
4.4.1. Strategy for computing $k_\Lambda(x, y)$ numerically	61
5. Concrete Examples	67
5.1. Case $n = 1$: the toy example	68
5.2. Case $n = 2$: three-component p	71
5.2.1. Evaluating J : Series expansions	74
5.2.2. Piecewise Components of k_Λ	76
6. Density theorems in $PW_\Lambda(A_p)$	85
6.1. Density theorems for sampling and interpolation in reproducing kernel Hilbert spaces - variable bandwidth version	85
6.2. Conditions on the geometry of (\mathbb{R}, d, μ_p)	87
6.3. Properties of the reproducing kernel of $PW_\Lambda(A_p)$	88
6.3.1. The diagonal and averaged traces	89
6.3.2. Localization and approximation properties	94
6.4. Necessary density conditions for sampling and interpolation	99

7. Numerical implementation and simulations	101
7.1. General reconstruction theory	102
7.1.1. Finite-dimensional reconstruction algorithm	105
7.1.2. A note on selecting the regularization parameter	108
7.2. Generating sets of stable sampling	109
7.2.1. Sets of prescribed Beurling density	110
7.3. Numerical simulations	112
7.3.1. Simulations for two-component piecewise constant p	114
7.3.1.1. Reconstructing bandlimited functions in $PW_{\Lambda}(A_p)$	115
7.3.1.2. Reconstructing non-bandlimited functions in $PW_{\Lambda}(A_p)$	122
7.3.1.3. On the quality of regularized reconstruction on sets of stable sampling with near-critical densities	125
7.3.2. Numerical implementation for three-component piecewise constant p	127
8. Summary and outlook	131
8.1. Constructing orthonormal bases for $PW_{[0,\Omega]}(A_p)$	131
8.2. Subspace relations between variable bandwidth spaces	132
8.3. Reconstructions using other sets of stable sampling	133
Appendix	135
A. Matlab codes and additional plots	135
B. Evaluating J: complex analysis	141
C. Localization and approximation lemmas for general spectral sets	151
C.1. Weak localization property	151
C.2. Homogeneous approximation property	159

List of figures

4.1.	A five-component piecewise constant function	44
5.1.	Graph of the reproducing kernel $k_\Lambda(0, \cdot)$ when p has (a) two components, and (b) three components.	82
7.1.	Plots of E_{grid}^2 (col 1), E_{grid}^∞ (col 2), and $\ \hat{c}_\epsilon^{[2n,n]}\ _2$ (col 3) using the uniform sampling set $X_{\frac{1}{4}}$ and different values of p_1 approaching $p_1 = 1$	117
7.2.	Plots of E_{grid}^2 (col 1), E_{grid}^∞ (col 2), and $\ \hat{c}_\epsilon^{[2n,n]}\ _2$ (col 3) using the perturbed sampling set $\tilde{X}_{\frac{1}{4}, \frac{1}{8}}$ and noisy samples as well as different values of p_1 approaching $p_1 = 1$	117
7.3.	Plots of E_{grid}^2 (col 1), E_{grid}^∞ (col 2), and $\ \hat{c}_\epsilon^{[2n,n]}\ _2$ (col 3) using the uniform sampling set $X_{\frac{1}{4}}$, sampling rates $\varsigma = 2$ (row 1), $\varsigma = 1.75$ (row 2), $\varsigma = 1.5$ (row 3), $\varsigma = 1.25$ (row 4), and $p_1 \downarrow 1$	118
7.4.	Plots of E_{grid}^2 (col 1), E_{grid}^∞ (col 2), and $\ \hat{c}_\epsilon^{[n,n]}\ _2$ (col 3) using orthogonal reconstruction vectors and using multiples of a fixed parametrizing function.	122
7.5.	Plots of E_{grid}^2 (col 1), E_{grid}^∞ (col 2), and $\ \hat{c}_\epsilon^{[2n,n]}\ _2$ (col 3) when g is reconstructed in $PW_{[0,\pi^2]}(A_p)$ (row 1) and $PW_\pi(\mathbb{R})$ (row 2) using uniform sampling sets X_γ with increasing γ and MATLAB command <code>pinv</code>	124
7.6.	(Left) Plot of g and its regularized reconstructions $\tilde{g}_\epsilon^{[200,100]}$ using uniform sampling sets X_γ with increasing γ . (Right) A closer look at the reconstructions near $x = 0$	124
7.7.	Plots of E_{grid}^2 , E_{grid}^∞ , $\ \hat{c}_\epsilon^{[\lceil 100\varsigma \rceil, 100]}\ _2$, and $D_p^\pm(S_{\frac{4}{3},k})$ when g is reconstructed from sampling sets $S_{\frac{4}{3},k}$, $k = 0, \dots, 20$ whose Beurling densities approach the critical density 1 and taking decreasing sampling rates $\varsigma = 2, 1.75, 1.5, 1.25$	126
7.8.	Plot of $\kappa(G^{[\lceil 100\varsigma \rceil, 100]})$ when g is reconstructed from sampling sets $S_{\frac{4}{3},k}$, $k = 0, \dots, 20$ whose Beurling densities approach the critical density 1 and taking decreasing sampling rates $\varsigma = 2, 1.75, 1.5, 1.25$	126
7.9.	Graph of J_{real} for $\Omega = \pi^2$, $T = 6$, $p_0 = p_2 = 1$ and $p_1 = \frac{1}{4}$ on the interval $[-50, 50]$	128
7.10.	Plots of E_{grid}^2 (col 1), E_{grid}^∞ (col 2), $\ \hat{c}_\epsilon^{[2n,n]}\ _2$ (col 3) and the reconstructions (row 2) when g is reconstructed using the uniform sampling set $X_{\frac{1}{8}}$ and different values of p_1	129
7.11.	Plots of E_{grid}^2 (col 1), E_{grid}^∞ (col 2), $\ \hat{c}_\epsilon^{[2n,n]}\ _2$ (col 3), and the reconstructions (row 2) when g is reconstructed using the uniform sampling set $X_{\frac{1}{8}}$ and multiples of a fixed p	129
A.1.	Plots of E_{grid}^2 (col. 1), E_{grid}^∞ (col. 2), and $\ \hat{c}_\epsilon^{[2n,n]}\ _2$ (col. 3) using the uniform sampling set $X_{\frac{1}{4}}$ with different values of p_1 approaching $p_1 = 1$ and MATLAB command <code>lsqminnorm</code>	140
A.2.	Plots of E_{grid}^2 (col. 1), E_{grid}^∞ (col. 2), and $\ \hat{c}_\epsilon^{[n,n]}\ _2$ (col. 3) using the sampling set X_{onb} and different values of p_1 approaching $p_1 = 1$	140

B.1.	Contours γ^+ (in blue) and γ^- (in orange) enclosing the poles z_0^\pm of F_s . . .	145
B.2.	Contour γ^+ split into four oriented segments and the pole z_0^+ of F_s (in red dots) in the upper half-plane enclosed by γ^+	146
B.3.	Contour γ^- split into four oriented segments and the poles z_0^- of F (in red dots) in the lower half-plane enclosed by γ^-	147

1. Introduction

1.1. Motivation

The recovery of a continuous-time signal f from its samples $\{f(x_n)\}_{n \in \mathbb{Z}}$ is one of the central problems in signal processing. Without additional assumptions, this problem is ill-posed. For ω -bandlimited signals, i.e., signals whose Fourier transform

$$\mathcal{F}f(\xi) = \hat{f}(\xi) = \int_{\mathbb{R}} f(t)e^{-i\xi t} dt$$

vanishes outside the interval $[-\omega, \omega]$, perfect reconstruction is possible. Indeed, the uniform sampling theorem (see [49]) stipulates that ω -bandlimited signals can be perfectly recovered from its uniformly spaced samples $\{f(\frac{n\pi}{\omega})\}_{n \in \mathbb{Z}}$. An explicit reconstruction is given by the interpolation formula

$$f(x) = \sum_{n \in \mathbb{Z}} f\left(\frac{n\pi}{\omega}\right) \operatorname{sinc}(\omega x - n\pi) = \sum_{n \in \mathbb{Z}} f\left(\frac{n\pi}{\omega}\right) \frac{\sin(\omega x - n\pi)}{(\omega x - n\pi)}, \quad x \in \mathbb{R}$$

which converges absolutely in $L^2(\mathbb{R})$. This means that by taking sufficiently many uniform samples, any continuous-time bandlimited signal can be encoded as a discrete-time signal without loss of information. These ω -bandlimited functions form the so-called Paley-Wiener spaces $PW_{\omega}(\mathbb{R})$ and have been extensively studied due to its wide range of applications in various fields such as audio and image processing [36, 71, 74, 84], telecommunications [17, 51], medical and geophysical imaging [21, 58], etc.

An efficient sampling method is one that captures the essential features of a signal using a minimal number of samples. Furthermore, reconstruction algorithms should yield an output that is a faithful representation of these information. If a signal, particularly the non-bandlimited ones, consists of several bursts or pulses of varying duration, intensity and frequency, then uniform sampling and reconstruction methods may not be effective. Thus, it may be helpful to use alternative sampling strategies that make good use of additional information on the signal and develop reconstruction algorithms that use functions that share some of the signal's distinctive features.

Techniques in classical Fourier analysis are best suited for time-stationary signals, i.e., those whose range of frequencies, commonly known as its spectrum, does not change over time. For time-varying signals, techniques in time-frequency analysis are often used to depict a two-dimensional description that encodes temporal and spectral information of the given signal. One such description is the short-time Fourier transform $V_g f$ of f with respect to a fixed nonzero function $g \neq 0$, called a window, given by

$$V_g f(x, \xi) = \int_{\mathbb{R}} f(t) \overline{g(t-x)} e^{-i\xi t} dt, \quad x, \xi \in \mathbb{R}.$$

1. Introduction

If g is smooth, symmetric at the origin, and has compact support, then $V_g f(x, \cdot)$ is the Fourier transform of a smoothly tapered segment of f on a neighborhood of x and can be interpreted as the “local frequency content” of f around x . We can also form time-frequency representations of the signal from discrete samples of $V_g f$ using the theory of Gabor frames (see [22, 38] for a thorough discussion) and use them either as intermediate reconstructions of f or to derive from f other signals with certain desirable properties.

With information provided by time-frequency analytic methods it makes sense to assign “local bandwidths” to different segments of a signal. Signals with different local bandwidths are called functions of variable bandwidth, while bandlimited functions may also be called functions of constant bandwidth. Such functions may be sampled according to local bandwidth, i.e., high sampling rates on segments with large local bandwidths, low sampling rates on segments with small local bandwidths. With sufficiently many of these samples we may be able to perfectly recover the signal using reconstruction algorithms similar to those in [37].

Unfortunately, this intuitive approach of assigning local bandwidths violates the uncertainty principle (see [27]), which says that a nonzero signal cannot be simultaneously concentrated in time and frequency. This is exactly the same issue that we encounter in an attempt to define “instantaneous bandwidth” in time-frequency analysis (see [24, 67, 73] for further reading). It is now our task to find a satisfactory definition of variable bandwidth and exhibit concrete examples of functions of variable bandwidth. We also investigate some of its properties and prove relevant results that are comparable to fundamental results in Paley-Wiener spaces. Finally, we develop methods of sampling and reconstruction of functions of variable bandwidth.

1.2. Defining variable bandwidth

We are now confronted with the question: what exactly is local or variable bandwidth? Several approaches to define this concept already exist in the literature.

- (i) In [78], D. Wei and A.V. Oppenheim intuitively defined local bandwidth as the rate at which a signal varies locally. Two potential models for local bandwidth were proposed. The first is to consider locally bandlimited signals as being generated by a linear time-varying filter with additional properties. The second is based on the notion of time-warping (applying an invertible transformation on time) of bandlimited signals. Methods of sampling and reconstruction of signals according to local bandwidth are then developed. This is closely related to the work of [23] as well as other related papers [19, 43, 49, 64, 86] tackling problems related to time-varying systems.
- (ii) The papers [2, 3] of R. Aceska and H.G. Feichtinger define the space of functions of variable bandwidth as a weighted modulation space defined by a so-called variable bandwidth weight.
- (iii) The recent work [56] of R.T.W. Martin and A. Kempf generalizes the uniform sampling theory using self-adjoint extensions of regular simple symmetric operators with deficiency indices $(1, 1)$. Using techniques in spectral theory they were able to for-

mulate a notion of time-varying bandwidth and subsequently construct the so-called local bandlimit spaces whose properties resemble those of Paley-Wiener spaces.

In this thesis, we consider another definition of variable bandwidth proposed by K. Gröchenig and A. Klotz in their paper [39]. This definition can be seen in the context of I. Pesenson and A.I. Zayed's work on abstract Paley-Wiener spaces [45, 66]. The idea is based on the fact that the $L^2(\mathbb{R})$ -Fourier transform \mathcal{F} unitarily diagonalizes the differential operator $-D^2$. More precisely, it is known from the spectral theory of self-adjoint unbounded operators that in some dense subspace of \mathcal{D} of $L^2(\mathbb{R})$, the equation

$$-\mathcal{F}D^2\mathcal{F}^{-1}f(\xi) = \xi^2 f(\xi), \quad f \in \mathcal{D} \quad (1.2.1)$$

holds. By restricting the multiplier ξ^2 in (1.2.1) so that $0 \leq \xi^2 \leq \omega^2$, we get an orthogonal projection P_ω onto the spectral subspace

$$E_{[0, \omega^2]} = \{\varphi \in L^2(\mathbb{R}) : \text{supp}(\varphi) \subseteq [-\omega, \omega]\}$$

corresponding to the spectral set $[0, \omega^2]$, i.e., P_ω is essentially multiplication by the characteristic function $\chi_{[-\omega, \omega]}$. The orthogonal projection onto the Paley-Wiener space $PW_\omega(\mathbb{R})$ is therefore described by the operator $f \mapsto (\mathcal{F}^{-1}P_\omega\mathcal{F})f$, and

$$PW_\omega(\mathbb{R}) = \mathcal{F}^{-1}P_\omega\mathcal{F}(L^2(\mathbb{R})).$$

The transition to variable bandwidth spaces starts by replacing $-D^2$ by an elliptic differential operator τ_p of the form $\tau_p = -D(pD)$, where $p > 0$ is the so-called bandwidth-parametrizing function. As an unbounded operator, we take an appropriate dense subspace $\mathcal{D}(\tau_p)$ of $L^2(\mathbb{R})$ so that τ_p has a self-adjoint realization A_p . Consequently, we can find a unitary operator \mathcal{F}_{A_p} , referred to as the spectral Fourier transform in [45, 66], that unitarily diagonalizes A_p , i.e.,

$$-\mathcal{F}_{A_p}^{-1}A_p\mathcal{F}_{A_p}g(\lambda) = \lambda g(\lambda), \quad g \in \mathcal{D}(\tau_p).$$

In the same spirit, the Paley-Wiener space $PW_\Lambda(A_p)$ with respect to A_p and spectral set $\Lambda \subset \mathbb{R}_0^+$ is given by

$$PW_\Lambda(A_p) = \mathcal{F}_{A_p}^{-1}P_\Lambda\mathcal{F}_{A_p}(L^2(\mathbb{R})),$$

where P_Λ is the orthogonal projection onto the spectral subspace E_Λ (so that $\lambda \in \Lambda$) consisting of functions in $L^2(\mathbb{R})$ whose support is contained in Λ . This is the proposed definition of a space of functions of variable bandwidth. We refer the reader to Section 2.2 for a guided discussion of the relevant spectral theory and Chapter 3 on the complete derivation of the Paley-Wiener space $PW_\Lambda(A_p)$.

It turns out that this definition and the resulting theory capture three key features inherent to bandlimited functions in the form of sampling theorems, necessary density conditions, particularly on the existence of a critical density, and analyticity similar to the Paley-Wiener theorem [39]. A detailed comparison of all the existing notions of variable bandwidth is given in [39, Sec. 1.2].

1.3. Piecewise constant parametrizing functions

The ultimate goal of studying spaces of functions of variable bandwidth is to show that numerical signal reconstruction can be performed in these spaces. A sampling inequality based on local bandwidth was proved in [39, Thm. 5.2] and sufficient conditions for a set to yield stable reconstructions were identified. Among these conditions is the maximum gap condition

$$\delta = \sup_{j \in \mathbb{Z}} \frac{x_{j+1} - x_j}{\inf_{x \in [x_j, x_{j+1}]} \sqrt{p(x)}} < \frac{\pi}{\Omega^{1/2}}, \quad \Lambda \subseteq [0, \Omega]$$

on a set X which highlights the role of the parametrizing function p in variable bandwidth sampling. Consequently, we can formulate a number of algorithms (see e.g. [37]) on the recovery of a function of variable bandwidth given only its non-uniform point samples.

It was noted in [39, Sec. 8] that prior knowledge of the reproducing kernel k_Λ of $PW_\Lambda(A_p)$ is necessary to perform numerical reconstructions. For arbitrary parametrizing functions p , finding an explicit formula for k_Λ seems impossible. Nevertheless, it was demonstrated in [39, Sec. 4] that for $\Lambda = [0, \Omega]$ and

$$p(x) = \begin{cases} p_-, & x \leq 0, \\ p_+, & x > 0, \end{cases} \quad p_-, p_+ > 0,$$

an explicit formula for k_Λ can be derived. This gives us a hint that the computability of the reproducing kernel may be possible for any piecewise constant p . If this is indeed the case, then sampling and reconstruction is numerically feasible. It is for this reason that we focus our attention to spaces of functions of variable bandwidth parametrized by piecewise constant functions.

1.4. Main results and overview

This dissertation is a systematic study of the space of functions of variable bandwidth parametrized by a piecewise constant function. We demonstrate how such spaces can be constructed by identifying its reproducing kernel, prove a number of interesting properties, and compare theoretical results to known ones in Paley-Wiener spaces of constant bandwidth. We then present a regularized reconstruction method for functions of variable bandwidth and use it to perform a number of numerical simulations.

The thesis is structured as follows:

Chapter 2 is a review of the theory of unbounded operators with focus on the operator-theoretic aspects of Sturm-Liouville differential equations. We study self-adjoint realizations of Sturm-Liouville operators and derive some of their fundamental properties. We state the spectral representation theorem for Sturm-Liouville operators where the spectral transform, the spectral matrix measure, and the spectral projection are introduced. We then demonstrate that the Paley-Wiener space of bandlimited functions can be expressed as the range of a spectral projection. This observation motivates the definition of variable bandwidth in the next chapter.

Chapter 3 is a collection of some results from [39] on the general properties of Paley-Wiener spaces of variable bandwidth functions. We mention relevant facts about reproducing kernel Hilbert spaces and give a brief overview of necessary density conditions for sampling and interpolation as well as non-uniform sampling in $PW_\Lambda(A_p)$.

Chapter 4 is an extensive study of the fundamental aspects of functions of variable bandwidth parametrized by piecewise constant function. We prove several new results and draw a number of observations regarding the computability of important quantities.

- Section 4.1 gives a precise definition of the piecewise constant parametrizing function used in this thesis. We also prove some properties of the self-adjoint realization A_p of τ_p for such a choice of p .
- In Section 4.2, we show that for a piecewise constant p , the fundamental solutions $\Phi(z, \cdot) = (\Phi^+(z, \cdot), \Phi^-(z, \cdot))$ of $(\tau_p - z)f = 0, z \in \mathbb{C} \setminus (-\infty, 0]$ are completely determined by Λ and p . Theorem 4.2.2 presents an iterative, matrix-based procedure that solves the given differential equation locally on intervals I_k determined by the transition points (knots) of p . An explicit form of Φ is obtained by computing the “connection coefficients” a_k^\pm, b_k^\pm that continuously piece together all the local solutions of $(\tau_p - z)f = 0$ based on some continuity conditions. This direct computability of Φ is what makes piecewise constant functions a suitable choice for a parametrizing function.
- In Section 4.3, we prove a number of identities relating the quantities a_k^\pm, b_k^\pm using Wronskian determinants on each I_k . Together with methods on the spectral theory of Sturm-Liouville operators, these identities are used to prove an important result, Theorem 4.3.3, that gives an explicit form of the spectral matrix measure $d\mu$ for A_p . Such a result is a consequence of having explicit formulas for Φ , and it further justifies our point of choosing piecewise constant parametrizing functions.
- In Section 4.4, we discuss the computability of the reproducing kernel k_Λ of $PW_\Lambda(A_p)$ for piecewise constant p . By the computability of both Φ and $d\mu$, we show in Theorem 4.4.1 that k_Λ can be expressed as an integral whose integrand is completely determined by Λ and p . Previous results indicate that calculability of evaluations of k_Λ at any point is equivalent to the computability of an oscillatory parameter integral $J(s)$ for any $s \in \mathbb{R}$. We then study elementary properties of J and enumerate quadrature methods as well as numerical routines in MATLAB and Mathematica that are useful in computing $J(s)$ numerically. Issues on the accuracy of such numerical methods are then identified.

Chapter 5 demonstrates the computability of k_Λ when p has two or three piecewise constant components. First, the necessary quantities are directly computed using Theorems 4.2.2 and 4.3.3. Then, we show that J can be evaluated at any point using (i) an explicit formula when p has two piecewise components, and (ii) an infinite series (in terms of the cardinal sine functions) with geometric convergence when p has three piecewise components. Unlike the numerical methods mentioned in Chapter 4, in both cases we have an accurate and robust numerical evaluation of J , hence k_Λ , at any point.

- In Section 5.1, we consider the so-called toy example (two-component piecewise constant p , knot at 0) from [39, Sec. 4] and reproduce their computation of k_Λ in Theorem 5.1.1.
- In Section 5.2, we perform the same procedure to compute k_Λ when p is a three-component piecewise constant function whose knots are symmetric at the origin.

1. Introduction

Here, we illustrate the sudden increase in difficulty when the number of piecewise parameters of p is increased. In Theorem 5.2.3, we express J as a series expansion involving cardinal sine functions. We also show that for any $s \in \mathbb{R}$, the partial sums $J_M(s)$, $M \in \mathbb{N}$ of this expansion converge to $J(s)$ at a geometric rate. We then use this expansion to express the nine piecewise components of k_Λ in Theorem 5.2.5. We also show that degenerate forms of the resulting kernel are precisely the translates of the reproducing kernel in Section 5.1.

Chapter 6 is a discussion on the necessary density conditions for sampling and interpolation in $PW_\Lambda(A_p)$. We show that the natural assumptions on the geometry (i.e., continuity of metric, finiteness and non-degeneracy of balls, and weak annular decay) as well as the reproducing kernel (i.e., boundedness of diagonal, weak localization and homogeneous approximation properties) needed to apply the main result in [31] are indeed satisfied by $PW_\Lambda(A_p)$ with piecewise constant p . We also mention that in contrast to [39], our contributions do not require scattering theory to derive asymptotic estimates of the reproducing kernel.

- In Section 6.2, we prove in Lemma 6.2.1 that the measure μ_p generated by a piecewise constant p is equivalent to the Lebesgue measure, implying that the geometric assumptions are automatically satisfied.
- In Section 6.3, we prove that k_Λ satisfies the required kernel assumptions. First, we show in Theorem 6.3.2 that k_Λ has bounded diagonal. Next, Theorem 6.3.4 allows us to estimate averaged traces tr^\pm in terms of the averaged integral of the diagonal, and in turn yields an exact value of the critical density. Then, Lemma 6.3.5 states that for spectral sets that are compact intervals, k_Λ exhibits off-diagonal decay. Consequently, we prove the weak localization (Lemma 6.3.6) and homogeneous approximation (Lemma 6.3.8) for spectral sets that are compact intervals. A more general version of these properties are proved in Appendix C. In order to use the results in [31], Proposition 6.3.1 translates the above properties of k_Λ to the reproducing kernel of the correct space.
- In Section 6.4, we summarize our results and finally prove the density theorem in $PW_\Lambda(A_p)$ in Theorem 6.4.1.

Chapter 7 is concerned with the numerical aspects of sampling and reconstruction of function of variable bandwidth as well as the numerical implementation of reconstruction algorithms.

- In Section 7.1, we follow the discussion in [4, 5] and present frame-theoretic results on the numerical approximation of a function in some reproducing kernel Hilbert space. Given only point samples of a function we introduce a finite-dimensional regularized reconstruction method that is based on least squares approximation combined with truncation of singular values of finite sections of the Gramian. We also have a note on choosing an appropriate tolerance value for the regularization procedure.
- In Section 7.2, we generate sets of stable sampling that will be used in the forthcoming simulations. We mainly use uniform samples as well as perturbations of

uniform samples in our experiments. We also have an algorithm that generates a set of stable sampling that has uniform Beurling density and has almost uniform sampling on local intervals.

- In Section 7.3, we perform a number of simulations to test our theoretical results as well as to investigate from a numerical perspective a number of relevant problems in variable bandwidth. We restrict our experiments to the two- and three-component piecewise functions as we already have necessary quantities in Chapter 5 at our disposal. Our main point is to demonstrate that for functions where local bandwidth is present, approximation by functions of variable bandwidth performs better than approximation by bandlimited functions. We also take a look at how the quality of reconstruction is influenced by the parametrizing function as well as the density of sampling sets.

The **Appendix** contains calculations, theoretical results, as well as MATLAB codes and plots that serve as supplementary material to Chapters 5, 6, and 7, respectively.

- In Appendix A we collect some of the important routines used in the numerical simulations in Chapter 7 as well as plots showing the performance of the reconstruction as the piecewise parametrizing function varies.
- In Appendix B we show using complex analytic methods that for a special case of a three-component piecewise p , J can be expressed as a piecewise function that involves special functions. Such a formula serves as an alternative to a special case of Theorem 5.2.3 where we have an infinite series expansion to compute $J(s)$ for any $s \in \mathbb{R}$ up to desired accuracy.
- In Appendix C we present rather lengthy proofs of the weak localization and homogeneous approximation properties of the reproducing kernel of k_Λ when Λ is a bounded Borel set. These results are used in Theorem 6.4.1 as it allows us to extend the theorem to bounded spectral sets. The proofs are almost identical to the ones given in [39, Sec. 7] but with some adjustments.

2. Preliminaries

We have seen from Section 1.2 that the Paley-Wiener space $PW_\omega(\mathbb{R})$ of ω -bandlimited functions is the range of an orthogonal projection defined using the Fourier transform operator \mathcal{F} . Moreover, \mathcal{F} unitarily diagonalizes $-D^2$, i.e., equation (1.2.1) holds on some dense subspace of $L^2(\mathbb{R})$. This idea can be extended to differential operators $-D(pD)$ for some positive function p . Our goal is to find an operator which unitarily diagonalizes $-D(pD)$ and use it to construct an orthogonal projection whose range is then called a Paley-Wiener space of variable bandwidth functions. The spectral theory of self-adjoint Sturm-Liouville operators naturally comes as our main tool to solve the given problem.

In this chapter, we provide the necessary notation, definitions and some results that we shall use throughout the dissertation. These can be found in standard references on reproducing kernel Hilbert spaces, Fourier analysis, time-frequency analysis and frame theory (e.g. [10, 22, 38, 42, 75]), and on functional analysis with topics on unbounded operators (e.g. [20, 28, 59, 65, 68, 69, 77, 79, 81]), specifically on Sturm-Liouville operators (e.g. [50, 80, 82]). General results on the spectral theory of self-adjoint Sturm-Liouville operators are stated in the context of the operator $-D(pD)$. In particular, we apply the spectral representation theorem for self-adjoint Sturm-Liouville operators to a self-adjoint operator associated to $-D(pD)$ to derive the sought-after unitary operator. With this unitary operator we can precisely define the Paley-Wiener space of variable bandwidth functions corresponding to a choice of p .

The reader is assumed to be familiar with linear operators in Hilbert spaces, elementary differential equations, and complex analysis. Most proofs will be omitted and we refer the reader to the above references and cited literature for a detailed discussion.

We denote by \mathcal{H} a Hilbert space with the inner product $\langle \cdot, \cdot \rangle_{\mathcal{H}}$ and norm $\| \cdot \|_{\mathcal{H}}$ (or just $\langle \cdot, \cdot \rangle$, $\| \cdot \|$ if \mathcal{H} is clear from the context). We assume that \mathcal{H} is separable, and the inner product is linear in the first argument and conjugate linear in the second. Unless otherwise stated, operators between Hilbert spaces are assumed to be linear.

The following notations for known function spaces will be used throughout the manuscript.

- (i) For $1 \leq r \leq \infty$ and E a Lebesgue measurable set, the space $L^r(E)$ is the collection of (equivalence classes of) Lebesgue measurable functions $f : E \rightarrow \mathbb{C}$ for which the norm

$$\|f\|_r = \begin{cases} \left(\int_E |f(x)|^r dx \right)^{\frac{1}{r}}, & 1 \leq r < \infty \\ \text{ess sup}_{x \in E} |f(x)|, & r = \infty \end{cases}$$

is finite. We denote by χ_E the characteristic function of E and $|E| = \|\chi_E\|_1$ the Lebesgue measure of E .

- (ii) For $1 \leq r \leq \infty$, and X a non-empty set, the space $\ell^r(X)$ is the set of all complex-

2. Preliminaries

valued sequences $s = \{s(x)\}_{x \in X}$ for which the norm (by abuse of notation)

$$\|s\|_r = \begin{cases} \left(\sum_{x \in X} |s(x)|^r \right)^{\frac{1}{r}}, & 1 \leq r < \infty \\ \text{ess sup}_{x \in X} |s(x)|, & r = \infty \end{cases}$$

is finite.

(iii) The set of all locally p -integrable functions, denoted $L^p_{loc}(E)$, is given by

$$L^p_{loc}(E) = \{f : E \rightarrow \mathbb{C} \text{ measurable} : f|_K \in L^p(K) \forall K \subset E, K \text{ compact}\}.$$

(iv) Let $(a, b) \subseteq \mathbb{R}$ be an open interval. A function $f : (a, b) \rightarrow \mathbb{C}$ is said to be absolutely continuous on (a, b) if there exists another function $g \in L^1_{loc}(a, b)$ (uniquely determined a.e.) such that the fundamental theorem of calculus holds, i.e., there exists $c \in (a, b)$ such that

$$f(x) = f(c) + \int_c^x g(t) dt$$

for a.e. $x \in (a, b)$. We refer to g as the (weak) derivative of f , and we write $g = Df = f'$, with D as the differentiation operator. The vector space of absolutely continuous functions on (a, b) is denoted by $AC(a, b)$. For a compact interval $[a, b]$,

$$AC[a, b] = \{f \in AC(a, b) : f' \in L^1(a, b)\}.$$

(v) The set of locally absolutely continuous functions on \mathbb{R} , denoted $AC_{loc}(\mathbb{R})$, is the collection

$$AC_{loc}(\mathbb{R}) = \{f : \mathbb{R} \rightarrow \mathbb{C} : f \in AC[c, d] \text{ for all } [c, d] \subset \mathbb{R}\}.$$

2.1. Review of unbounded operators

We briefly review some notations and terminologies on unbounded operators. We follow parts of the discussion in [20, Chap. 6]. An **(unbounded) operator** in a Hilbert space \mathcal{H} is a pair $(A, \mathcal{D}(A))$, where the **domain** $\mathcal{D}(A) \subset \mathcal{H}$ is a linear subspace and $A : \mathcal{D}(A) \rightarrow \mathcal{H}$ is a linear map. For convenience, we may use the shorthand notation A to mean $(A, \mathcal{D}(A))$ but with the constant reminder that a domain $\mathcal{D}(A)$ is always implicitly meant to be defined alongside A . An operator A is **densely defined** if $\mathcal{D}(A)$ is dense in \mathcal{H} . We also say that A is **closed** if its graph

$$\text{graph}(A) = \{(x, Ax) : x \in \mathcal{D}(A)\}$$

is a closed linear subspace of $\mathcal{H} \times \mathcal{H}$ with respect to the product topology. An operator $(A_2, \mathcal{D}(A_2))$ is an **extension** of $(A_1, \mathcal{D}(A_1))$ if

$$\mathcal{D}(A_1) \subset \mathcal{D}(A_2) \text{ and } A_1x = A_2x \text{ for all } x \in \mathcal{D}(A_1).$$

Put in another perspective, we say that A_1 is the **restriction** of the map $A_2 : \mathcal{D}(A_2) \rightarrow \mathcal{H}$ onto $\mathcal{D}(A_1)$. We use the notation $A_1 \subset A_2$ to denote such relation. The operators A_1 and A_2 are **equal** if $A_1 \subset A_2$ and $A_2 \subset A_1$, and we denote this equality by $A_1 = A_2$.

Perhaps the most important concept that will be used here is the adjoint of an operator. Let A be a densely defined operator on \mathcal{H} . The **adjoint operator** $(A^*, \mathcal{D}(A^*))$ (or simply A^*) of A , where $\mathcal{D}(A^*) \subset \mathcal{H}$, $A^* : \mathcal{D}(A^*) \rightarrow \mathcal{H}$, is defined as follows. The domain $\mathcal{D}(A^*)$ is the linear subspace

$$\mathcal{D}(A^*) = \{y \in \mathcal{H} : \text{there exists } c > 0 \text{ such that } |\langle y, Ax \rangle| \leq c\|x\| \text{ for all } x \in \mathcal{D}(A)\},$$

and for $y \in \mathcal{D}(A^*)$, $A^*y \in \mathcal{H}$ is the unique element¹ of \mathcal{H} for which

$$\langle A^*y, x \rangle = \langle y, Ax \rangle$$

for all $x \in \mathcal{D}(A)$. For adjoints of extensions, it can be shown that if $A_1 \subset A_2$, then $A_2^* \subset A_1^*$.

We also consider classes of unbounded operators defined using the adjoint. A densely defined operator A on \mathcal{H} is called **symmetric** (or **Hermitian**) if $A \subset A^*$. This is equivalent to saying that

$$\langle Ay, x \rangle = \langle y, Ax \rangle$$

for all $x, y \in \mathcal{D}(A)$. Further classification of symmetric operators is as follows. We say that a symmetric operator A is

- (i) **positive** if $\langle Ax, x \rangle \geq 0$ for all $x \in \mathcal{D}(A)$,
- (ii) **self-adjoint** if $A = A^*$

Next, we define resolvents and spectrum for closed unbounded operators. Let A be a closed operator on \mathcal{H} . The **resolvent set** $\rho(A) \subset \mathbb{C}$ of A is given by

$$\rho(A) = \{z \in \mathbb{C} : A - z \text{ is bijective and } (A - z)^{-1} \text{ is bounded}\}.$$

By $A - z$ we mean $A - z \cdot \text{id}_{\mathcal{H}} : \mathcal{D}(A) \rightarrow \mathcal{H}$, where $\text{id}_{\mathcal{H}}(u) = u$ for all $u \in \mathcal{H}$. For $z \in \rho(A)$, we call $R_z(A) = (A - z)^{-1}$ the **resolvent** of A at z . The complement $\sigma(A) = \mathbb{C} \setminus \rho(A)$ of the resolvent set $\rho(A)$ in \mathbb{C} is called the **spectrum** of A . Elements of the spectrum include (if it has any) the **eigenvalues** of A , i.e., $\lambda \in \sigma(A)$ is an eigenvalue of A if there exists a nonzero $f \in \mathcal{D}(A)$ such that $Af = \lambda f$. We list the following relevant facts.

- (i) The resolvent set $\rho(A)$ is an open subset of \mathbb{C} , hence the spectrum $\sigma(A)$ is a closed subset of \mathbb{C} [79, Thm. 5.14].
- (ii) Self-adjoint operators are maximal in the sense that they do not have any proper self-adjoint extensions.
- (iii) If A is self-adjoint, then $\sigma(A) \subseteq \mathbb{R}$ [79, Thm. 5.23].

¹This means that A^* is well-defined and is a consequence of $\mathcal{D}(A)$ being dense and the Riesz representation theorem.

2. Preliminaries

(iv) A self-adjoint operator A is positive if and only if $\sigma(A) \subseteq [0, \infty)$ [59, Thm. 10.38a].

Example 2.1.1. Let (X, \mathcal{E}, μ) be a measure space and $g : X \rightarrow \mathbb{C}$ a measurable function. The **(maximal) multiplication operator** $(M_g, \mathcal{D}(M_g))$ is defined as

$$\begin{aligned}\mathcal{D}(M_g) &= \{\varphi \in L^2(X, \mu) : g\varphi \in L^2(X, \mu)\}, \\ M_g\varphi &= g\varphi, \quad \varphi \in \mathcal{D}(M_g).\end{aligned}$$

It follows that $M_g^* = M_{\bar{g}}$. In particular, M_g is self-adjoint if and only if g is real-valued a.e., and for a self-adjoint M_g , the spectrum is

$$\sigma(M_g) = \{x \in \mathbb{R} : \mu(g^{-1}((x - \epsilon, x + \epsilon))) > 0 \text{ for all } \epsilon > 0\}.$$

For additional facts on multiplication operators, see e.g. [65, Sec. 5.1]. △

The main fact about unbounded self-adjoint operators is the spectral theorem. This result can be seen as the generalization of the well-known unitary diagonalizability of Hermitian matrices [44, Thm. 2.5.6]. Several formulations of the spectral theorem exist in the literature, see for instance the versions found in [69, Sec. VIII]. One of the statements assert that self-adjoint operators are unitarily equivalent to a multiplication operator. We state a more precise statement of this result [81, Thm. 8.17].

Theorem 2.1.2. *Let $(A, \mathcal{D}(A))$ be a self-adjoint operator in a separable Hilbert space \mathcal{H} . Then there exists a σ -finite measure space (X, \mathcal{E}, μ) , a μ -measurable function $g : X \rightarrow \mathbb{R}$, and a unitary map $U : \mathcal{H} \rightarrow L^2(X, \mu)$ such that $UAU^{-1} = M_g$.*

We now see that self-adjoint operators associated to the operator $-D^2$ lead to the motivating observation (1.2.1). Since the procedure in defining Paley-Wiener spaces of variable bandwidth functions involves a transition from $-D^2$ to $-D(pD)$, it would be useful if we can get more information on the unitary map U corresponding to $-D(pD)$. Fortunately, there is the so-called spectral representation theorem for self-adjoint operators. This spectral representation takes the multiplier g of M_g to be the identity function in a certain Lebesgue space of square-integrable functions. We introduce this concept given in [81, Sec. 8.1]. Let A be a self-adjoint operator in \mathcal{H} . A unitary operator

$$U : \mathcal{H} \rightarrow \bigoplus_{j \in J} L^2(\mathbb{R}, \mu_j) = \left\{ (f_j)_{j \in J} \in \prod_{j \in J} L^2(\mathbb{R}, d\mu_j) : \sum_{j \in J} \|f_j\|_{L^2(\mathbb{R}, \mu_j)}^2 < \infty \right\}$$

with J an at most countably infinite index set and $\{\mu_j\}_{j \in J}$ a family of Borel measures on \mathbb{R} is called a **spectral representation** of A if $UAU^{-1} = M_{\text{id}}$, where id is the identity function in $\bigoplus_{j \in J} L^2(\mathbb{R}, \mu_j)$. We call U an **ordered spectral representation** of A if additionally, μ_{j+1} is absolutely continuous² with respect to μ_j for all $j \in J$.

We end this section by stating the following important result [81, Thm. 8.16].

Theorem 2.1.3 (Spectral representation theorem). *Every self-adjoint operator A in a separable Hilbert space has an (ordered) spectral representation U of A .*

For self-adjoint operators associated to differential operators, there is a straightforward method to derive the corresponding spectral representation. This will be tackled in the next section.

²Given two measures μ and ν on a measure space (X, \mathcal{E}) , we say μ is absolutely continuous with respect to ν , denoted $\mu \ll \nu$, if $\mu(E) = 0$ for every measurable set $E \in \mathcal{E}$ satisfying $\nu(E) = 0$.

2.2. Spectral theory of some self-adjoint Sturm-Liouville operators

We now discuss relevant aspects of the spectral theory of self-adjoint Sturm-Liouville operators. Our main references are [28, 77, 80, 82]. The formal³ second-order differential operator

$$(\tau f)(x) = -(pf')'(x) + q(x)f(x)$$

defined for a.e. $x \in (a, b) \subseteq \mathbb{R}$ and some real-valued functions p and q on (a, b) is called a **(formal) Sturm-Liouville operator**. Throughout the manuscript we only consider Sturm-Liouville operators on $(a, b) = \mathbb{R}$ of the form

$$(\tau_p f)(x) = -(pf')'(x),$$

where $p > 0$ a.e. and $\frac{1}{p} \in L^1_{loc}(\mathbb{R})$. We also have for a.e. $x \in \mathbb{R}$ and $z \in \mathbb{C}$ the Sturm-Liouville equation corresponding to τ_p given by

$$(\tau_p f)(x) = zf(x), \tag{2.2.1}$$

which we write as $(\tau_p - z)f = 0$ on \mathbb{R} .

With regularity conditions on p , (e.g. $p, p' \in AC_{loc}(\mathbb{R})$), a Sturm-Liouville operator may be transformed into a corresponding Schrödinger operator $\tilde{\tau}_q u = -u'' + qu$ for some q . Operators generated by $\tilde{\tau}_q$ admit properties similar to those of τ_p via unitary transformation (see some of the relevant properties in [39, Lem. 6.7]).

In the present work, we stick to τ_p since we will later consider a p where such a transformation cannot be applied. This distinguishes part of our work from [39]. It is for this reason that we state applications of general results for Sturm-Liouville operators exclusively to operators τ_p .

Functions that satisfy (2.2.1) play a crucial role in determining spectral representations of self-adjoint Sturm-Liouville operators. Let $z \in \mathbb{C}$. A **solution** of $(\tau_p - z)f = 0$ on \mathbb{R} is a function ϕ such that $\phi, p\phi' \in AC_{loc}(\mathbb{R})$ and satisfies $(\tau_p - z)\phi = 0$ a.e. For Sturm-Liouville initial value problems, we have the classical result on the existence and uniqueness of solutions [82, Cor. 13.3]. See also [77, Thm. 9.1], where an additional conclusion that the solutions are entire in z is added. The standard procedure in solving the homogeneous equation $(\tau_p - z)f = 0$ analytically is as follows. Since τ_p is a differential expression of order two, the set of solutions of $(\tau_p - z)f = 0$, $z \in \mathbb{C}$ fixed, forms a two-dimensional complex vector space of complex-valued functions. Among the solutions, we select two solutions u_z and v_z of $(\tau_p - z)f = 0$ such that the **(modified) Wronskian determinant**

$$W_x(u_z, v_z) = \begin{vmatrix} u_z(x) & v_z(x) \\ p(x)u'_z(x) & p(x)v'_z(x) \end{vmatrix} = u_z(x)(pv'_z)(x) - v_z(x)(pu'_z)(x) \tag{2.2.2}$$

is nonzero for some $x \in \mathbb{R}$. This is a necessary and sufficient condition for u_z and v_z to be linearly independent [77, Thm. 9.1], [80, Thm. 5.1]. With these linearly independent solutions the general solution y_z of $(\tau_p - z)f = 0$ takes the form

$$y_z(x) = c_1 u_z(x) + c_2 v_z(x) \text{ for a.e. } x \in \mathbb{R},$$

where $c_1, c_2 \in \mathbb{C}$ can be chosen arbitrarily.

³In the sense that we have not specified a dense domain on which the operator is well-defined and square-integrable.

2. Preliminaries

Remark 2.2.1. The Wronskian determinant of solutions of (2.2.1) is independent of x . Indeed, let $z \in \mathbb{C}$ be fixed. If u_z and v_z are solutions of $(\tau_p - z)f = 0$, differentiating $W_x(u_z, v_z)$ with respect to x yields

$$\frac{\partial}{\partial x} W_x(u_z, v_z) = u_z(x)(pv'_z)'(x) - v_z(x)(pu'_z)'(x) = 0$$

for a.e. $x \in \mathbb{R}$. This means that for a fixed $z \in \mathbb{C}$, $W_x(u_z, v_z)$ is constant in x . Hence, we may drop the variable x and simply write $W_x(u_z, v_z)$ as $W(u_z, v_z)$.

For $z \in \mathbb{C}$, any set $\{u_z, v_z\}$ of solutions of $(\tau_p - z)f = 0$ for which $W_x(u_z, v_z) \neq 0$ for some (hence for all by Remark 2.2.1) $x \in \mathbb{R}$ is called a **fundamental system** (or **fundamental set of solutions**) of $(\tau_p - z)f = 0$. In later discussions we conveniently denote a fundamental system $\{u_z, v_z\}$ by an ordered pair (u_z, v_z) . Most of the results stated later will assume that we have a fundamental system with continuous or analytic dependence in z .

We now go to relevant operator-theoretic aspects of Sturm-Liouville theory. To a given τ_p corresponds the **maximal operator** $(A_p, \mathcal{D}(A_p))$ given by

$$\begin{aligned} \mathcal{D}(A_p) &= \{f \in L^2(\mathbb{R}) : f, pf' \in AC_{loc}(\mathbb{R}) \text{ and } \tau_p f \in L^2(\mathbb{R})\}, \\ A_p f &= \tau_p f, \quad f \in \mathcal{D}(A_p). \end{aligned}$$

It was proved in [80, Thm. 3.7] that A_p is densely defined. We can think of the maximal operator A_p of τ_p as essentially the same τ_p defined on the largest subset of $L^2(\mathbb{R})$ for which $\tau_p f$ is well-defined and whose range is contained in $L^2(\mathbb{R})$.

In the succeeding discussions, we seek self-adjoint operators associated to τ_p . These operators are called **self-adjoint realizations** of τ_p and are restrictions of the maximal operator onto dense subspaces of $\mathcal{D}(A_p)$. See [80, Chap. 3] for an in-depth discussion. In particular, we investigate conditions for which the maximal operator A_p of τ_p is self-adjoint, i.e., A_p is the unique self-adjoint realization of τ_p . To this end, we introduce the following notions [82, Sec. 13.3], cf. [77, Sec. 9]. A Lebesgue measurable function $f : \mathbb{R} \rightarrow \mathbb{C}$ **lies right** in $L^2(\mathbb{R})$ if $f \in L^2(c, \infty)$ for some $c \in \mathbb{R}$. Correspondingly, we say f **lies left** in $L^2(\mathbb{R})$ if $f \in L^2(-\infty, c)$ for some $c \in \mathbb{R}$. An application of [80, Thm. 5.6], [82, Thm. 13.18] characterizes τ_p in terms of the behavior of the solutions of $(\tau_p - z)f = 0, z \in \mathbb{C}$ near $\pm\infty$

Theorem 2.2.2 (Weyl alternative). *Given the formal Sturm-Liouville operator τ_p , exactly one of the following must hold:*

- (i) *for every $z \in \mathbb{C}$, all solutions ϕ_z of $(\tau_p - z)f = 0$ lie right in $L^2(\mathbb{R})$, or*
- (ii) *for every $z \in \mathbb{C}$, there exists at least one solution ϕ_z of $(\tau_p - z)f = 0$ which does not lie right in $L^2(\mathbb{R})$. In this case, we have that for every $z \in \mathbb{C} \setminus \mathbb{R}$, there exists a unique (up to a constant factor) solution ϕ_z of $(\tau_p - z)f = 0$ which lies right in $L^2(\mathbb{R})$.*

The same result holds for “lies left in $L^2(\mathbb{R})$ ”.

We can now use the following terminologies, first introduced by H. Weyl in his paper [83]. We say that τ_p is in the **limit circle case** at ∞ if (i) of the Weyl alternative holds.

2.2. Spectral theory of some self-adjoint Sturm-Liouville operators

Otherwise, if (ii) holds, τ_p is in the **limit point case** at ∞ . The limit circle and limit point cases at $-\infty$ are defined analogously. The notions of limit circle and limit point at the endpoints allow us to classify τ_p in terms of its admissible self-adjoint realizations. In this thesis, only Sturm-Liouville operators in the limit point case at $\pm\infty$ will be considered. For this particular case, we have the following theorem [82, Thm. 13.21(a)] applied to τ_p .

Theorem 2.2.3. *If τ_p is in the limit point case at $\pm\infty$, then A_p is the only self-adjoint realization of τ_p .*

While it certainly is not straightforward to determine whether τ_p is in the limit circle or limit point case at an endpoint, we can use the so-called **limit point-limit circle criteria** that enumerates sufficient conditions for which τ_p is in the limit circle or limit point at an endpoint [82, Sec. 13.4]. For our purpose, we appeal to [82, Thm. 13.24, Cor. 13.25] applied to τ_p as well as Theorem 2.2.3 to derive the following criterion.

Theorem 2.2.4. *Let p be a function such that $p > 0$ a.e. and $\frac{1}{p} \in L^1_{loc}(\mathbb{R})$. Define for $x \in \mathbb{R}$ the function*

$$g(x) = \int_0^x \frac{1}{p(t)} dt.$$

If $g \notin L^2(0, \infty)$ and $g \notin L^2(-\infty, 0)$, then τ_p is in the limit point case at $\pm\infty$. Consequently, A_p is self-adjoint.

For instance, if $p > 0$ a.e. and is eventually constant (referred to as the **model case** in [39]), i.e.,

$$p(x) = \begin{cases} p_-, & x < -R, \\ p_+, & x > R \end{cases} \quad (2.2.3)$$

for some $p^+, p^-, R > 0$, then τ_p is in the limit point case at $\pm\infty$. Indeed, we know from the local integrability of $\frac{1}{p}$ that for $x \geq R$,

$$g(x) = \frac{1}{p_+}(x + c), \quad c = \int_0^R \frac{1}{p(t)} dt - \frac{R}{p_+} \in \mathbb{R}.$$

Consequently, $g \notin L^2(0, \infty)$ since

$$\int_0^\infty |g(x)|^2 dx \geq \frac{1}{p_+^2} \int_R^\infty (x + c)^2 dx = \infty.$$

A similar proof can be done to prove the other non-membership.

It is possible to draw conclusions on the spectrum $\sigma(A_p)$ of A_p if p satisfies additional conditions. We know that since A_p is positive, $\sigma(A_p) \subseteq [0, \infty)$. An application of a theorem [80, Thm. 15.1] to τ_p in the limit point case at $\pm\infty$ gives a sufficient condition for the reverse inclusion, hence set equality, to be true.

Theorem 2.2.5. *Let A_p be the self-adjoint realization of τ_p in the limit point case at $\pm\infty$. If there exist $C_1, C_2 > 0$ such that*

$$\liminf_{L \rightarrow \infty} \frac{1}{L} \int_0^L \left| 1 - \frac{C_1}{p(u)} \right| du = 0 = \liminf_{L \rightarrow \infty} \frac{1}{L} \int_{-L}^0 \left| 1 - \frac{C_2}{p(u)} \right| du,$$

then $\sigma(A_p) = [0, \infty)$.

2. Preliminaries

Now that the necessary results to establish self-adjointness of the maximal operator A_p are in place, we now discuss the spectral representation theorem for self-adjoint Sturm-Liouville operators. To state the theorem, we need the notion of square-integrable functions with respect to a matrix-valued measure. We adopt the definition in [28, Sec. XIII.5]. A family $\mu = \{\mu_{jl}\}_{j,l=1}^n$ of complex-valued set functions defined on bounded Borel subsets of \mathbb{R} is called an $n \times n$ **positive matrix measure** if

- (i) for every bounded Borel subset E of \mathbb{R} , the complex matrix $[\mu_{jl}(E)]_{j,l=1}^n$ is Hermitian and positive semi-definite, and
- (ii) for each sequence $\{E_m\}_{m=1}^\infty$ of disjoint, bounded Borel subsets of \mathbb{R} with bounded union, we have

$$\mu_{jl} \left(\bigcup_{m=1}^{\infty} E_m \right) = \sum_{m=1}^{\infty} \mu_{jl}(E_m) \quad \text{for } 1 \leq j, l \leq n.$$

In this thesis, it is enough to consider 2×2 positive matrix measures μ and the function space $L^2(\mathbb{R}, d\mu)$ of \mathbb{C}^2 -valued measurable functions $F = (F_1, F_2)$, $F_1, F_2 : \mathbb{R} \rightarrow \mathbb{C}$ for which

$$\|F\|_{L^2(\mathbb{R}, d\mu)} = \left\{ \sum_{j,l=1}^2 \int_{\mathbb{R}} F_j(\lambda) \overline{F_l(\lambda)} d\mu_{jl}(\lambda) \right\}^{1/2} < \infty.$$

This space is endowed with the inner product

$$\langle F, G \rangle_{L^2(\mathbb{R}, d\mu)} = \int_{\mathbb{R}} F(\lambda) \cdot \overline{G(\lambda)} d\mu(\lambda) = \sum_{j,l=1}^2 \int_{\mathbb{R}} F_j(\lambda) \overline{G_l(\lambda)} d\mu_{jl}(\lambda)$$

for $F = (F_1, F_2), G = (G_1, G_2) \in L^2(\mathbb{R}, d\mu)$. Of particular interest are 2×2 positive matrix measures μ whose components μ_{jl} are absolutely continuous with respect to the Lebesgue measure. In this case, we say that μ is absolutely continuous with respect to the Lebesgue measure. By the Radon-Nikodym Theorem, we can find positive Lebesgue measurable functions $\{\mathcal{M}_{jl}\}_{j,l=1}^2$ such that for every bounded Borel subset E of \mathbb{R} ,

$$\mu_{jl}(E) = \int_E \mathcal{M}_{jl}(\lambda) d\lambda, \quad 1 \leq j, l \leq 2.$$

Thus, we can write $d\mu$ as the matrix of densities

$$d\mu = \mathcal{M} d\lambda = \begin{bmatrix} \mathcal{M}_{11} & \mathcal{M}_{12} \\ \mathcal{M}_{21} & \mathcal{M}_{22} \end{bmatrix} d\lambda. \quad (2.2.4)$$

Moreover, the matrix \mathcal{M} is positive semi-definite a.e. [28, Lem. XIII.5.7].

We are now ready to state the spectral representation theorem for Sturm-Liouville operators. The statements in [77, Lem. 9.13], [82, Thm. 14.1] are direct applications of the spectral representation theorem in Theorem 2.1.3. However, instead of working on a direct sum of Hilbert spaces, the space $L^2(\mathbb{R}, d\mu)$ constructed using matrix measures as above will be used. In [80, Sec. 8] the notion of spectral representation of a self-adjoint

2.2. Spectral theory of some self-adjoint Sturm-Liouville operators

operator has been extended to the case where the spectral representation is a unitary operator of the form

$$U : L^2(\mathbb{R}) \rightarrow L^2(\mathbb{R}, d\mu)$$

with μ a positive matrix measure. See for instance [28, Thm. XIII.5.23], [77, Lem. 9.28], [79, Thm. 8.7], [82, Thm. 14.3] for the construction. We will adopt the following version [39, Thm. 2.3] of the spectral representation theorem for self-adjoint Sturm-Liouville operators below. The statement includes a Borel functional calculus that gives meaning to applying bounded Borel functions to self-adjoint operators.

Theorem 2.2.6. *Let A_p be the self-adjoint realization of τ_p in the limit point case at $\pm\infty$. Suppose*

$$\Phi(\lambda, x) = (\Phi_1(\lambda, x), \Phi_2(\lambda, x)), \quad \lambda, x \in \mathbb{R}$$

is a fundamental system of $(\tau_p - \lambda)u = 0$ that continuously depends on λ . Then there exists a 2×2 positive matrix measure μ such that the map

$$\mathcal{F}_{A_p} : L^2(\mathbb{R}) \rightarrow L^2(\mathbb{R}, d\mu), \quad \mathcal{F}_{A_p}f(\lambda) = \int_{\mathbb{R}} f(x) \overline{\Phi(\lambda, x)} dx \quad (2.2.5)$$

is a spectral representation of A_p , i.e., $\mathcal{F}_{A_p}A_p\mathcal{F}_{A_p}^{-1}G(\lambda) = \lambda G(\lambda)$ for all $G \in L^2(\mathbb{R}, d\mu)$. The inverse $\mathcal{F}_{A_p}^{-1}$ has the form

$$\mathcal{F}_{A_p}^{-1}G(x) = \int_{\mathbb{R}} G(\lambda) \cdot \Phi(\lambda, x) d\mu(\lambda) = \sum_{j,l=1}^2 \int_{\mathbb{R}} G_j(\lambda) \Phi_l(\lambda, x) d\mu_{jl}(\lambda), \quad G \in L^2(\mathbb{R}, d\mu).$$

Moreover, for any bounded Borel function g on \mathbb{R} ,

$$g(A_p)f(x) = \int_{\mathbb{R}} g(\lambda) \mathcal{F}_{A_p}f(\lambda) \cdot \Phi(\lambda, x) d\mu(\lambda), \quad f \in L^2(\mathbb{R}). \quad (2.2.6)$$

All integrals are assumed to be the $L^2(\mathbb{R})$ -limit of integrals $\lim_{\alpha \rightarrow -\infty}^{\beta \rightarrow \infty} \int_{\alpha}^{\beta}$. Equation (2.2.6) with $g = \chi_{\Lambda}$ for some Borel set $\Lambda \subseteq \mathbb{R}_0^+$ yields the expression

$$\chi_{\Lambda}(A_p)f(x) = \int_{\Lambda} \mathcal{F}_{A_p}f(\lambda) \cdot \Phi(\lambda, x) d\mu(\lambda) = \mathcal{F}_{A_p}^{-1}(\chi_{\Lambda} \mathcal{F}_{A_p}f)(x), \quad (2.2.7)$$

called the **spectral projection** from $L^2(\mathbb{R})$ onto the spectral subspace corresponding to spectral values in Λ . We refer the reader to [77, Chap. 9], [80, Chap. 8] on the fine details.

It is possible to use a fundamental system $\Phi(z, \cdot) = (\Phi_1(z, \cdot), \Phi_2(z, \cdot))$ of $(\tau_p - z)f = 0$ that is not defined in the entire complex plane. If the above fundamental system depends continuously in z in a neighborhood Q of an interval $\mathcal{I} \subset \mathbb{R}$, then the map

$$\mathcal{F}_{A_p} : L^2(\mathbb{R}) \rightarrow L^2(\mathcal{I}, d\mu), \quad \mathcal{F}_{A_p}f(\lambda) = \int_{\mathbb{R}} f(x) \overline{\Phi(\lambda, x)} dx$$

can be loosely described as a spectral representation of the part of A_p corresponding to spectral values⁴ in \mathcal{I} . Here, $L^2(\mathcal{I}, d\mu)$ can be viewed as isometrically embedded to

⁴Such a statement can be made precise by a thorough discussion of projection-valued measures as well as resolution of the identity (spectral families on Hilbert spaces). We refer the reader to [77, Sec. 3] and [79, Sec. 7.2].

2. Preliminaries

$L^2(\mathbb{R}, d\mu)$ by considering functions in $L^2(\mathcal{I}, d\mu)$ as functions in $L^2(\mathbb{R}, d\mu)$ whose components vanish outside \mathcal{I} . For a proof, see [28, Sec. XIII.5.12], [80, Thm. 9.7].

Following [45], we may refer to the spectral representation \mathcal{F}_{A_p} as the **spectral (Fourier) transform** of A_p . We refer to μ in the above theorem as the **spectral matrix⁵ measure** of A_p .

At this point, we already know how to form the spectral representation \mathcal{F}_{A_p} from a fundamental system $\{u_1(z, \cdot), u_2(z, \cdot)\}$. We now look for possible means to compute the matrix representation $d\mu$ as in (2.2.4). We apply the methods of [80, Chap. 9] (see also [28, Sec. XIII.5]) in our derivation. It turns out that two explicit forms of the resolvent $R_z(A_p)$ of A_p are the key tools in the derivation of μ . We now present two theorems which will be frequently used in Chapter 4.

The first theorem [80, Thm. 7.8] says that the resolvent can be expressed in terms of two solutions, one of which lies left and the other lies right in $L^2(\mathbb{R})$ in the case of τ_p in the limit point case at $\pm\infty$. We refer the reader to [82, Thm. 13.21] for a discussion in a broader setting.

Theorem 2.2.7. *Let A_p be the self-adjoint realization of τ_p in the limit point case at $\pm\infty$. Suppose $z \in \rho(A_p)$. Then there exist unique (up to a constant factor) solutions $u_1(z, \cdot)$ and $u_2(z, \cdot)$ of $(\tau_p - z)f = 0$ which lie right and lie left in $L^2(\mathbb{R})$, respectively. Moreover, the resolvent $R_z(A_p) = (A_p - z)^{-1}$ is given by*

$$R_z(A_p)g(x) = \frac{1}{W(u_1(z, \cdot), u_2(z, \cdot))} \left\{ u_1(z, x) \int_{-\infty}^x u_2(z, y)g(y) dy + u_2(z, x) \int_x^{\infty} u_1(z, y)g(y) dy \right\}.$$

We also define the **resolvent kernel** (or **Green's function**)

$$r_z(x, y) = \frac{1}{W(u_1(z, \cdot), u_2(z, \cdot))} \begin{cases} u_1(z, x)u_2(z, y), & y \leq x, \\ u_2(z, x)u_1(z, y), & y > x \end{cases} \quad (2.2.8)$$

for all $x, y \in \mathbb{R}$, so that $R_z(A_p)$ can be expressed as the integral operator

$$R_z(A_p)g(x) = \int_{\mathbb{R}} r_z(x, y)g(y) dy.$$

The next theorem [80, Thm. 7.7a] gives an alternative form of (2.2.8) and will later be used to describe the spectral matrix measure of A_p .

Theorem 2.2.8. *Let A_p be the self-adjoint realization of τ_p in the limit point case at $\pm\infty$ and $z \in \rho(A_p)$. Suppose $\{u_1(z, \cdot), u_2(z, \cdot)\}$ and $\{v_1(z, \cdot), v_2(z, \cdot)\}$ are fundamental systems of $(\tau_p - z)f = 0$ and $(\tau_p - \bar{z})f = 0$, respectively. Then there exist complex numbers $m_{jl}^{\pm}(z)$, $1 \leq j \leq n$, $z \in \mathbb{C} \setminus \mathbb{R}$ such that*

$$r_z(x, y) = \begin{cases} \sum_{j,l=1}^2 m_{jl}^+(z) \overline{v_j(z, x)} u_l(z, y), & y \leq x \\ \sum_{j,l=1}^2 m_{jl}^-(z) \overline{v_j(z, x)} u_l(z, y), & y > x \end{cases}$$

for all $x, y \in \mathbb{R}$.

⁵This is to distinguish it from the spectral measure generated by a spectral family. See [79, Sec. 7.2] for more details.

2.2. Spectral theory of some self-adjoint Sturm-Liouville operators

Let $(\alpha, \beta) \subset \mathbb{R}_0^+$ and $Q \subset \mathbb{C}$ a neighborhood of (α, β) . Suppose that $\{u_1(z, \cdot), u_2(z, \cdot)\}$ is a fundamental system of $(\tau_p - z)f = 0$ that continuously depends on z in Q . A straightforward choice for a fundamental system for $(\tau_p - \bar{z})f = 0$ is $\{u_1(\bar{z}, \cdot), u_2(\bar{z}, \cdot)\}$. For $z \in Q \cap \rho(A_p)$, the resolvent kernel in Theorem 2.2.8 can be rewritten as

$$r_z(x, y) = \begin{cases} \sum_{j,l=1}^2 m_{jl}^+(z) \overline{u_j(\bar{z}, x)} u_l(z, y), & y \leq x \\ \sum_{j,l=1}^2 m_{jl}^-(z) \overline{u_j(\bar{z}, x)} u_l(z, y), & y > x \end{cases} \quad (2.2.9)$$

for all $x, y \in \mathbb{R}$. Thus, using a single fundamental system, we can derive the 2×2 complex matrix functions $m^\pm(z) = [m_{jl}^\pm(z)] \in \mathbb{C}^{2 \times 2}$ for $z \in \mathbb{C} \setminus \mathbb{R}$.

We now take a look at the interaction between Theorem 2.2.7 and (2.2.9). Observe that since τ_p has real coefficients,

$$\overline{(\tau_p - \bar{z})f} = (\tau_p - z)f$$

holds. This means that if $\{u_1(z, \cdot), u_2(z, \cdot)\}$ is a fundamental system of $(\tau_p - z)f = 0$ which continuously depends on z , $\{\overline{u_1(\bar{z}, \cdot)}, \overline{u_2(\bar{z}, \cdot)}\}$ is also a fundamental system of $(\tau_p - z)f = 0$. Hence, we can write $u_1(z, x)$ and $u_2(z, x)$ as a linear combination of $\overline{u_1(\bar{z}, x)}$ and $\overline{u_2(\bar{z}, x)}$, say

$$u_j(z, x) = c_j(z) \overline{u_1(\bar{z}, x)} + d_j(z) \overline{u_2(\bar{z}, x)}, \quad j = 1, 2.$$

for some functions $c_j, d_j, j = 1, 2$. Upon substituting the above quantities to corresponding factors in (2.2.8), we have for instance

$$r_z(x, y) = \begin{cases} c_1(z) \overline{u_1(\bar{z}, x)} u_2(z, y) + d_1(z) \overline{u_2(\bar{z}, x)} u_2(z, y), & y \leq x \\ c_2(z) \overline{u_1(\bar{z}, x)} u_1(z, y) + d_2(z) \overline{u_2(\bar{z}, x)} u_1(z, y), & y > x. \end{cases}$$

This yields the matrices

$$m^+(z) = \begin{bmatrix} 0 & c_1(z) \\ 0 & d_1(z) \end{bmatrix}, \quad m^-(z) = \begin{bmatrix} c_2(z) & 0 \\ d_2(z) & 0 \end{bmatrix}.$$

The final step is to find a connection between the spectral measure μ and the matrices m^\pm . We have the following result [82, Thm. 14.5], cf. [28, Thm. XIII.5.18], [80, Thm. 9.4].

Theorem 2.2.9 (Weyl-Titchmarsh-Kodaira Formula). *Let $(\alpha, \beta) \subseteq \mathbb{R}_0^+$, $Q \subset \mathbb{C}$ a neighborhood of (α, β) , and $\{u_1(z, \cdot), u_2(z, \cdot)\}$ a fundamental system of $(\tau_p - z)f = 0$ that depends continuously on $z \in Q$. With the normalization $\mu(\gamma) = 0$ for some $\gamma \in (\alpha, \beta)$, the equation*

$$\mu_{jl}((\gamma, \lambda]) = \frac{1}{2\pi i} \lim_{\delta \downarrow 0} \lim_{\epsilon \downarrow 0} \int_{\gamma+\delta}^{\lambda+\delta} (m_{jl}^\pm(t + i\epsilon) - m_{jl}^\pm(t - i\epsilon)) dt$$

holds for all $\lambda \in (\alpha, \beta)$, $j, l = 1, 2$.

2. Preliminaries

This means that we can derive the matrix measure $\mu = \{\mu_{ij}\}_{j,l=1}^2$ using either $m^+(z) - m^+(\bar{z})$ or $m^-(z) - m^-(\bar{z})$ for $\text{Im}z > 0$. In our computations, we prefer using the matrix m^+ . If the fundamental system is further assumed to be analytically dependent on $z \in Q$, the entries of m^\pm are analytic in $Q \cap \rho(A_p)$ [28, Thm. XIII.5.18]. If μ is absolutely continuous with respect to the Lebesgue measure, the matrix \mathcal{M} of densities in (2.2.4) is precisely

$$\mathcal{M}(\lambda) = \lim_{\epsilon \downarrow 0} \frac{1}{2\pi i} (m^\pm(\lambda + \epsilon i) - m^\pm(\lambda - \epsilon i)).$$

We note here that one has to be careful when deriving the matrices $m^\pm(z)$ for $\text{Im}z > 0$ and $\text{Im}z < 0$; it can happen that the properties “lies left” and “lies right” of the respective solutions are swapped when $\text{Im}z > 0$ is changed to $\text{Im}z < 0$.

What remains as far as the spectral matrix measure μ is concerned is to guarantee that it is in fact absolutely continuous with respect to the Lebesgue measure. We can uniquely decompose the Borel measure μ as a sum (see [70, Sec. 18.4], [77, Secs. 3, A.7]) of three mutually singular⁶ measures

$$\mu = \mu_{pp} + \mu_{sc} + \mu_{ac}$$

defined as follows:

- μ_{pp} , the pure point part of μ , is a discrete measure, i.e., there exists a sequence $\{a_j\}_{j \in I}$ indexed by an at most countably infinite set I such that $\mu_{pp}(\mathbb{R} \setminus \{a_j\}_{j \in I}) = 0$. In other words, μ_{pp} is supported⁷ on $\{a_j\}_{j \in I}$.
- μ_{sc} , the singular continuous part of μ , is the part of μ that is supported on a set of Lebesgue measure zero and satisfies $\mu_{sc}(\{a\}) = 0$ for all $a \in \mathbb{R}$.
- μ_{ac} , the absolutely continuous part of μ , is absolutely continuous with respect to Lebesgue measure, i.e., $d\mu$ can be written as (2.2.4).

For the spectral matrix measure μ obtained from the spectral representation of A_p , we have in [82, Ex. 12.5] the decomposition of $L^2(\mathbb{R}, d\mu)$ as

$$L^2(\mathbb{R}, d\mu) = L^2(\mathbb{R}, d\mu_{pp}) \oplus L^2(\mathbb{R}, d\mu_{sc}) \oplus L^2(\mathbb{R}, d\mu_{ac}),$$

and the spectrum of A_p can be decomposed [69, Sec. VII.2] as

$$\sigma(A_p) = \overline{\sigma_{pp}(A_p)} \cup \sigma_{sc}(A_p) \cup \sigma_{ac}(A_p),$$

where $\sigma_{pp}(A_p)$ is the set of all eigenvalues of A_p , while $\sigma_{sc}(A_p)$ and $\sigma_{ac}(A_p)$ are the supports of μ_{sc} and μ_{ac} , respectively. Thus, to prove $\mu = \mu_{ac}$, we show $\mu_{pp} = 0$, i.e., A_p has no eigenvalues, and $\mu_{sc} = 0$. To this end, an application of [80, Thm. 10.14] to τ_p provides a sufficient condition on the absence of singular continuous spectrum.

⁶Two measures μ and ν on a measure space (X, \mathcal{E}) are said to be mutually singular if there exists a measurable set $N \in \mathcal{E}$ such that $\mu(N) = 0$ and $\nu(X \setminus N) = 0$. We denote this relation by $\mu \perp \nu$.

⁷A support for a measure μ in a measure space (X, \mathcal{E}) is a set $E \in \mathcal{E}$ such that $\mu(X \setminus E) = 0$. If X is a topological space and \mathcal{E} is the Borel σ -algebra, then the (topological) support of μ is the set of all points $x \in X$ such that $\mu(E_x) > 0$ for every open neighborhood $E_x \in \mathcal{E}$ of x . The topological support of μ is closed. See [77, Sec. A.1] for more details.

2.2. Spectral theory of some self-adjoint Sturm-Liouville operators

Theorem 2.2.10. *Let A_p be the self-adjoint realization of τ_p . Let $(\alpha, \beta) \subset \mathbb{R}$ and $Q \subset \mathbb{C}$ an open neighborhood of (α, β) . Assume that for $z \in Q$ there exist solutions $u_1(z, \cdot)$ and $u_2(z, \cdot)$ of $(\tau_p - z)f = 0$ analytically dependent on z such that for $z \in Q^+ = \{z \in Q : \text{Im}z > 0\}$, $u_1(z, \cdot)$ and $u_2(z, \cdot)$ lies right and lies left in $L^2(\mathbb{R})$, respectively. Then $\sigma_{pp}(A_p)$ has no accumulation point in (α, β) and $\sigma_{sc}(A_p) \cap (\alpha, \beta) = \emptyset$.*

To illustrate the whole procedure, we give an example on the derivation of the spectral representation and spectral measure of a simple differential operator. Some parts of the calculations can be found on [77, Secs. 7.2, 9.3], [82, Ex. 14.9]

Example 2.2.11. Let $p \equiv 1$ a.e. so that $\tau_p = -D^2$ on \mathbb{R} . We first note some preliminary observations.

- (i) By Theorem 2.2.4, τ_p is in the limit point case at $\pm\infty$. Hence, by Theorem 2.2.3, τ_p has a unique self-adjoint realization A_p which is nothing but its maximal operator, i.e.,

$$\mathcal{D}(A_p) = \{f \in L^2(\mathbb{R}) : f, f' \in AC_{loc}(\mathbb{R}), f'' \in L^2(\mathbb{R})\}, \quad A_p f = -f''.$$

- (ii) A_p is a positive operator with $\sigma(A_p) = [0, \infty)$ by Theorem 2.2.5.

Next, we see that the solutions of the equation $-u'' - zu = 0$, $z \in \mathbb{C} \setminus (-\infty, 0]$ are completely determined by linear combinations of

$$u_1(z, x) = e^{i\sqrt{z}x} \quad \text{and} \quad u_2(z, x) = e^{-i\sqrt{z}x}$$

since $W(u_1(z, \cdot), u_2(z, \cdot)) = -2i\sqrt{z} \neq 0$ for all $z \in \mathbb{C} \setminus (-\infty, 0]$. Here, \sqrt{z} is conveniently defined to have the branch cut at $(-\infty, 0]$ so that \sqrt{z} is analytic with $\text{Im}z \cdot \text{Im}\sqrt{z} \geq 0$ for all $z \in \mathbb{C} \setminus (-\infty, 0]$. Thus, for $z \in \mathbb{C} \setminus (-\infty, 0]$, $u_1(z, \cdot)$ and $u_2(z, \cdot)$ are analytic and form a fundamental system of $-u'' - zu = 0$. Moreover, A_p has no eigenvalues in $[0, \infty)$. Indeed, if $\lambda \in (0, \infty)$, then any nontrivial linear combination of $u_1(\lambda, \cdot)$ and $u_2(\lambda, \cdot)$ cannot be in $L^2(\mathbb{R})$. The case $\lambda = 0$ shares a similar fate, since a fundamental system of $-f'' = 0$ is $\{1, x\}$. Therefore, $\mu_{pp} = 0$.

For the spectral matrix measure μ of A_p , we proceed as follows.

- If $\text{Im}z > 0$, $u_1(z, \cdot)$ lies right and $u_2(z, \cdot)$ lies left in $L^2(\mathbb{R})$. Moreover, we have $\overline{u_1(\bar{z}, \cdot)} = u_2(z, \cdot)$ and $\overline{u_2(\bar{z}, \cdot)} = u_1(z, \cdot)$. Equation (2.2.8) becomes

$$r_z(x, y) = -\frac{1}{2i\sqrt{z}}u_1(z, x)u_2(z, y) = \frac{1}{2i\sqrt{z}}\overline{u_2(\bar{z}, x)}u_2(z, y), \quad y \leq x.$$

- If $\text{Im}z < 0$, $u_2(z, \cdot)$ lies right and $u_1(z, \cdot)$ lies left in $L^2(\mathbb{R})$. Equation (2.2.8) becomes

$$r_z(x, y) = \frac{1}{2i\sqrt{z}}u_2(z, x)u_1(z, y) = \frac{1}{2i\sqrt{z}}\overline{u_1(\bar{z}, x)}u_1(z, y), \quad y \leq x.$$

From (2.2.9), we have the matrices

$$m^+(z) = \frac{1}{2i} \begin{bmatrix} 0 & 0 \\ 0 & -\frac{1}{\sqrt{z}} \end{bmatrix}, \text{Im}z > 0 \quad \text{and} \quad m^+(z) = \frac{1}{2i} \begin{bmatrix} \frac{1}{\sqrt{z}} & 0 \\ 0 & 0 \end{bmatrix}, \text{Im}z < 0.$$

2. Preliminaries

By Theorem 2.2.10, $\sigma_{sc}(A_p) \cap (0, \infty) = \emptyset$ and consequently, $(0, \infty) \subseteq \sigma_{ac}(A_p)$. Since μ_{sc} cannot be supported on $\{0\}$, it follows that $\sigma(A_p) = \sigma_{ac}(A_p) = [0, \infty)$. Hence, μ is absolutely continuous with respect to the Lebesgue measure on $[0, \infty)$. In turn, Theorem 2.2.9 (Weyl-Titchmarsh-Kodaira formula) yields the matrix of densities

$$d\mu = \mathcal{M}(\lambda)d\lambda = \frac{1}{4\pi} \begin{bmatrix} \frac{1}{\sqrt{\lambda}} & 0 \\ 0 & \frac{1}{\sqrt{\lambda}} \end{bmatrix} d\lambda.$$

Finally, by Theorem 2.2.6, the spectral representation $\mathcal{F}_{A_p} : L^2(\mathbb{R}) \rightarrow L^2([0, \infty), d\mu)$ can be expressed as the column vector

$$\mathcal{F}_{A_p}f(\lambda) = \begin{bmatrix} \int_{\mathbb{R}} e^{-i\sqrt{\lambda}x} f(x) dx \\ \int_{\mathbb{R}} e^{i\sqrt{\lambda}x} f(x) dx \end{bmatrix}, \quad \lambda \in \sigma(A_p) = [0, \infty).$$

On the other hand, for $G \in L^2([0, \infty), d\mu)$,

$$\begin{aligned} \mathcal{F}_{A_p}^{-1}G(x) &= \frac{1}{4\pi} \int_0^\infty \frac{1}{\sqrt{\lambda}} (G_1(\lambda)e^{i\sqrt{\lambda}x} + G_2(\lambda)e^{-i\sqrt{\lambda}x}) d\lambda \\ &= \frac{1}{2\pi} \int_0^\infty (G_1(\xi^2)e^{i\xi x} + G_2(\xi^2)e^{-i\xi x}) d\xi, \quad \xi = \sqrt{\lambda}. \end{aligned} \quad (2.2.10)$$

△

Now that most of the technical details needed from Sturm-Liouville theory are established, we can now demonstrate how the Paley-Wiener space of bandlimited functions can be derived via the spectral transform of the self-adjoint realization of $-D^2$ on \mathbb{R} . This procedure will be used to define Paley-Wiener spaces of variable bandwidth functions as a generalization of the classical Paley-Wiener spaces of bandlimited functions. The **Fourier transform** $\mathcal{F}f = \widehat{f}$ of $f \in L^2(\mathbb{R})$ is defined as the $L^2(\mathbb{R})$ -limit

$$\mathcal{F}f(\xi) = \widehat{f}(\xi) = \int_{\mathbb{R}} f(x)e^{-i\xi x} dx = \lim_{N \rightarrow \infty} \int_{-N}^N f(x)e^{-i\xi x} dx, \quad \text{for a.e. } \xi \in \mathbb{R}.$$

Its inverse \mathcal{F}^{-1} , called the **inverse Fourier transform**, is given by

$$\mathcal{F}^{-1}\varphi(x) = \frac{1}{2\pi} \widehat{\varphi}(-x) = \frac{1}{2\pi} \int_{\mathbb{R}} \varphi(\xi)e^{i\xi x} d\xi = \lim_{N \rightarrow \infty} \frac{1}{2\pi} \int_{-N}^N \varphi(\xi)e^{i\xi x} d\xi, \quad \text{for a.e. } x \in \mathbb{R}.$$

The **support** of a function $f : \mathbb{R} \rightarrow \mathbb{C}$, denoted $\text{supp}(f)$, is the smallest closed subset of \mathbb{R} for which f does not vanish, i.e.,

$$\text{supp}(f) = \overline{\{x \in \mathbb{R} : f(x) \neq 0\}}.$$

Fix $\omega > 0$. The **Paley-Wiener space of ω -bandlimited functions** (or **Paley-Wiener space of constant bandwidth functions**), denoted $PW_\omega(\mathbb{R})$, is the closed subspace of $L^2(\mathbb{R})$ given by

$$PW_\omega(\mathbb{R}) = \{f \in L^2(\mathbb{R}) : \text{supp}(\widehat{f}) \subseteq [-\omega, \omega]\}.$$

2.2. Spectral theory of some self-adjoint Sturm-Liouville operators

Using the orthogonal projection $P_\omega : L^2(\mathbb{R}) \rightarrow PW_\omega(\mathbb{R})$ defined as $P_\omega f = \chi_{[-\omega, \omega]} f$, we have that

$$PW_\omega(\mathbb{R}) = \mathcal{F}^{-1} P_\omega \mathcal{F}(L^2(\mathbb{R})).$$

We claim that $PW_\omega(\mathbb{R})$ can also be written using \mathcal{F}_A of the self-adjoint realization A ($= A_p$, $p \equiv 1$) of $-D^2$ on \mathbb{R} via the spectral projection $\chi_{[0, \omega^2]}(A)$ given in (2.2.7). More precisely,

$$PW_\omega(\mathbb{R}) = \chi_{[0, \omega^2]}(A)(L^2(\mathbb{R})) = \mathcal{F}_A^{-1}(\chi_{[0, \omega^2]} \mathcal{F}_A)(L^2(\mathbb{R})). \quad (2.2.11)$$

Indeed, direct computation of (2.2.6) with $g = \chi_{[0, \omega^2]}$ and mimicking the derivation of (2.2.10) with $G = \chi_{[0, \omega^2]} \cdot \mathcal{F}_A f$ for $f \in L^2(\mathbb{R})$ yields (note $\mathcal{F}_A f(\xi^2) = (\mathcal{F} f(\xi), \mathcal{F} f(-\xi))$)

$$\begin{aligned} \mathcal{F}_A^{-1}(\chi_{[0, \omega^2]} \mathcal{F}_A f)(x) &= \frac{1}{2\pi} \int_0^\infty \chi_{[0, \omega^2]}(\xi^2) (\mathcal{F} f(\xi) e^{i\xi x} + \mathcal{F} f(-\xi) e^{-i\xi x}) d\xi \\ &= \frac{1}{2\pi} \int_{-\omega}^\omega \mathcal{F} f(\xi) e^{i\xi x} d\xi, \quad \chi_{[0, \omega^2]}(\xi^2) = \chi_{[-\omega, \omega]}(\xi) \\ &= (\mathcal{F}^{-1} P_\omega \mathcal{F} f)(x) \end{aligned}$$

for a.e. $x \in \mathbb{R}$. We also have the freedom to use any nonempty subset of \mathbb{R} to define other Paley-Wiener spaces with various supports as above.

It is clear that the standard Paley-Wiener spaces can be derived from Theorem 2.2.6. We can now extend this procedure to the operator τ_p to define Paley-Wiener spaces of variable bandwidth functions.

3. Functions of variable bandwidth

In this chapter we formally introduce the notion of variable bandwidth given in [39]. Using formulas for the spectral transform \mathcal{F}_{A_p} and its inverse $\mathcal{F}_{A_p}^{-1}$ from Theorem 2.2.6, we can use the Borel functional calculus (2.2.6) to compute spectral projections onto spectral subspaces. Let $\Lambda \subset \mathbb{R}_0^+$ be a Borel set of finite measure and A_p the self-adjoint realization of τ_p in the limit point case at $\pm\infty$. We recall from (2.2.7) the spectral projection $\chi_\Lambda(A_p) : L^2(\mathbb{R}) \rightarrow L^2(\mathbb{R})$ corresponding to the spectral set Λ given by

$$\chi_\Lambda(A_p)f(x) = \int_\Lambda \mathcal{F}_{A_p}f(\lambda) \cdot \Phi(\lambda, x) d\mu(\lambda) = \mathcal{F}_{A_p}^{-1}(\chi_\Lambda \mathcal{F}_{A_p}f)(x) \quad (3.0.1)$$

for all $f \in L^2(\mathbb{R})$. With such a projection operator we define the following.

Definition 3.0.1. Let A_p be the self-adjoint realization of τ_p in the limit point case at $\pm\infty$ and $\Lambda \subset \mathbb{R}_0^+$ be of finite measure. The **Paley-Wiener space of variable bandwidth functions** (or **Λ -bandlimited functions with respect to A_p**), denoted $PW_\Lambda(A_p)$, is the range of the spectral projection $\chi_\Lambda(A_p)$, i.e.,

$$PW_\Lambda(A_p) = \chi_\Lambda(A_p)(L^2(\mathbb{R})).$$

We refer to Λ as the **spectral set** and the a.e. positive function p the **bandwidth-parametrizing function**. Equivalently, a function $f \in L^2(\mathbb{R})$ belongs to $PW_\Lambda(A_p)$ if $f = \chi_\Lambda(A_p)f$.

We have seen at the end of Section 2.2 in conjunction with Example 2.2.11 that the classical Paley-Wiener space of ω -bandlimited functions $PW_\omega(\mathbb{R})$ can be expressed in the above form. Definition 3.0.1 falls under the abstract notion of bandlimited vectors introduced by I. Pesenson and A. Zayed in [45, 66]. We appeal to the result [39, Prop. 3.2] that enumerates basic properties of variable bandwidth functions that resemble those of bandlimited functions.

Proposition 3.0.2. *Let $\Lambda \subset \mathbb{R}_0^+$ be of finite measure and A_p the self-adjoint realization of τ_p in the limit point case at $\pm\infty$. Let μ and \mathcal{F}_{A_p} be the spectral matrix measure and spectral transform of A_p , respectively. The following are equivalent:*

- (i) $f \in PW_\Lambda(A_p)$,
- (ii) $\text{supp } \mathcal{F}_{A_p}f \subseteq \Lambda$,
- (iii) there exists a function $F \in L^2(\mathbb{R}, d\mu)$ such that

$$f(x) = \int_\Lambda F(\lambda) \cdot \Phi(\lambda, x) d\mu(\lambda) \quad \text{for a.e. } x \in \mathbb{R}.$$

3. Functions of variable bandwidth

If additionally, $\Lambda = [0, \Omega]$, the following conditions are equivalent to the first three:

$$(iv) \quad \|A_p^k f\| \leq \Omega^k \|f\| \text{ for all } k \in \mathbb{N},$$

(v) for all $g \in L^2(\mathbb{R})$, the function $z \mapsto \langle e^{zA_p} f, g \rangle$ is an entire function of exponential type Ω , i.e., for any $\epsilon > 0$, there exists $C_\epsilon > 0$ such that

$$|\langle e^{zA_p} f, g \rangle| \leq C_\epsilon e^{(\Omega+\epsilon)|\text{Im}z|}, \quad z \in \mathbb{C}.$$

3.1. Reproducing kernel Hilbert spaces

The central theme of this thesis revolves around a particular class of Hilbert spaces. Let E be a non-empty set. A function $k : E \times E \rightarrow \mathbb{C}$ is a **reproducing kernel** of a Hilbert space \mathcal{H} of functions from E to \mathbb{C} if

(i) for every $x \in E$, $k(x, \cdot) \in \mathcal{H}$, and

(ii) for every $x \in E$ and for every $\varphi \in \mathcal{H}$, $\varphi(x) = \langle \varphi, k(x, \cdot) \rangle$.

It follows from the above conditions that

$$k(x, y) = \langle k(x, \cdot), k(y, \cdot) \rangle$$

for all $x, y \in E$. A Hilbert space of complex functions that possesses a reproducing kernel is called a **reproducing kernel Hilbert space**. The following result [10, Thm. 1] is an elementary characterization of reproducing kernel Hilbert spaces. For an extensive study, consult [8, 10].

Theorem 3.1.1. *A Hilbert space of functions from E to \mathbb{C} is a reproducing kernel Hilbert space if and only if for every $x \in E$, the evaluation functional $f \mapsto f(x)$, $f \in \mathcal{H}$ is continuous.*

As a consequence, norm convergence of a sequence of functions in a reproducing kernel Hilbert space implies pointwise convergence [10, Cor. 1]. Moreover, it was proved in [60, Prop. 3.1] that boundedness of the so-called diagonal $k(x, x)$, $x \in \mathbb{R}$ of k implies uniform convergence.

The next proposition ([39, Prop. 3.3], see also [28, Thm. VIII.5.14(ii)] for the case of compact spectral sets) asserts that Paley-Wiener spaces of variable bandwidth functions are reproducing kernel Hilbert spaces.

Proposition 3.1.2. *Let $\Lambda \subset \mathbb{R}_0^+$ be of finite measure and A_p the self-adjoint realization of τ_p in the limit point case at $\pm\infty$. Let $\Phi(\lambda, \cdot) = (\Phi_1(\lambda, \cdot), \Phi_2(\lambda, \cdot))$ be a fundamental system of $(\tau_p - \lambda)f = 0$ which continuously depends on λ . Then the following holds:*

(i) *The Paley-Wiener space $PW_\Lambda(A_p)$ is a closed subspace of $L^2(\mathbb{R})$ and every function in $PW_\Lambda(A_p)$ is continuous.*

3.2. Necessary density conditions for sampling and interpolation

(ii) If Λ is compact, then $PW_\Lambda(A_p)$ is a reproducing kernel Hilbert space with kernel

$$k_\Lambda(x, y) = \int_\Lambda \overline{\Phi(\lambda, x)} \cdot \Phi(\lambda, y) d\mu(\lambda) = \sum_{j,l=1}^2 \int_\Lambda \overline{\Phi_j(\lambda, x)} \Phi_l(\lambda, y) d\mu_{jl}(\lambda). \quad (3.1.1)$$

Moreover, k_Λ is the integral kernel of the spectral projection $\chi_\Lambda(A_p)$ from $L^2(\mathbb{R})$ onto $PW_\Lambda(A_p)$.

Finally, we mention the local behavior of functions in $PW_{[0,\Omega]}(A_p)$. The Bernstein space B_Ω consists of all functions whose distributional Fourier transforms are supported in $[-\Omega, \Omega]$. See [62] for further reading. The following theorem claims that functions in $PW_{[0,\Omega]}(A_p)$ behave locally like functions in some Bernstein space.

Proposition 3.1.3. *If $p(x) = p_0$ for all x on an open interval I , then on I every $f \in PW_{[0,\Omega]}(A_p)$ coincides with a function in $B_{\sqrt{\Omega/p_0}}$ restricted to I .*

This proposition serves as one of our motivations in choosing a particular class of parametrizing functions. We defer the discussion on this matter until Chapter 4.

3.2. Necessary density conditions for sampling and interpolation

Let \mathcal{H} be a reproducing kernel Hilbert space of functions from \mathbb{R} to \mathbb{C} and $X \subset \mathbb{R}$ be at most countably infinite. We say X is a **set of stable sampling** for \mathcal{H} if there exist $C_1, C_2 > 0$ such that

$$C_1 \|f\|_{\mathcal{H}}^2 \leq \sum_{x \in X} |f(x)|^2 \leq C_2 \|f\|_{\mathcal{H}}^2$$

for all $f \in \mathcal{H}$. The above inequality implies an element of \mathcal{H} is uniquely determined by its samples on X , and a small error in sample values corresponds to a small reconstruction error. On the other hand, X is a **set of interpolation** for \mathcal{H} if for every $c \in \ell^2(X)$ there exists $f \in \mathcal{H}$ such that $f(x) = c_x$ for all $x \in X$.

If $\mathcal{H} = PW_S(\mathbb{R})$ with $S \subset \mathbb{R}$ a single interval, Beurling [12, 13] characterized sets of stable sampling and sets of interpolation using the concept of upper and lower uniform densities. Shortly after, Landau [52] extended the necessary implications of Beurling's results to higher dimensions and general bandwidths. For our purpose, we consider a measurable set $S \subset \mathbb{R}$ and the space

$$\mathcal{H} = PW_S(\mathbb{R}) = \{f \in L^2(\mathbb{R}) : \text{supp } \widehat{f} \subseteq S\}.$$

The one-dimensional version of Landau's necessary conditions is as follows [52, Thms. 3,4].

(i) Let $S \subset \mathbb{R}$ and X a set of stable sampling for $PW_S(\mathbb{R})$. Then

$$D^-(X) = \liminf_{r \rightarrow \infty} \inf_{x \in \mathbb{R}} \frac{\#(X \cap B_r(x))}{2r} \geq \frac{|S|}{2\pi}.$$

3. Functions of variable bandwidth

(ii) Let $S \subset \mathbb{R}$ be bounded and X a set of interpolation for $PW_S(\mathbb{R})$. Then

$$D^+(X) = \limsup_{r \rightarrow \infty} \sup_{x \in \mathbb{R}} \frac{\#(X \cap B_r(x))}{2r} \leq \frac{|S|}{2\pi}.$$

The quantities $D^-(X)$ and $D^+(X)$ are called **lower and upper Beurling densities** of X , respectively, and the **critical density** $\frac{|S|}{2\pi}$ separates sets of stable sampling from sets of interpolation. In particular, for signals bandlimited to $S = [-\omega, \omega]$ for some $\omega > 0$, the critical density is precisely the Nyquist rate $\frac{\omega}{\pi}$, i.e., the minimum sampling rate at which a bandlimited signal in $PW_\omega(\mathbb{R})$ must be sampled for stable reconstruction to happen. The Nyquist rate is also the maximum transmission rate at which a sequence may be represented as the samples of a bandlimited signal in $PW_\omega(\mathbb{R})$. Further discussion on Beurling densities and the Nyquist rate can be found in [53].

Landau's necessary conditions form the so-called ‘‘density theorem’’ for sampling and interpolation of functions of exponential type. Several mathematicians also proved versions of the density theorem to other function spaces as well. Some of these spaces are the bandlimited functions [40, 52, 53] (see also [1] for a Hankel transform version), de Branges spaces [57], and Bargmann-Fock spaces [72, 87], to name a few. In essence, the theorem states that sets of stable sampling must be sufficiently dense, while sets of interpolation must be sufficiently sparse. We can use the density theorem as a rough guide to determine which sets may be used for stable sampling and reconstruction and which ones are for interpolation.

In the style of Landau, we present a density theorem for sampling and interpolation in $PW_\Lambda(A_p)$ for a certain choice of p as discussed in [39, Sec. 6.1]. We introduce a new measure, namely

$$\mu_p(I) = \int_I \frac{dx}{\sqrt{p(x)}}, \quad I \subseteq \mathbb{R} \text{ measurable}$$

generated by a parametrizing function p . The rationale behind this came from the observation that if p is a constant p_j on some interval I_j , then the required number of samples to reconstruct $f \in PW_{[0,\Omega]}(A_p)$ in I_j , viewed as an element of the Bernstein space $B_{\sqrt{\Omega/p_j}}$ by Proposition 3.1.3, is roughly

$$\frac{\#(X \cap I_j)}{|I_j|} \sim \sqrt{\frac{\Omega}{p_j}}. \quad (3.2.1)$$

Hence, the quantity $|I_j|p_j^{-1/2}$ may be viewed as a way to measure the length of I_j . With this measure, we define the concept of Beurling density for $PW_\Lambda(A_p)$. Suppose $p^{-1/2} \in L^1_{loc}(\mathbb{R})$ and $X \subseteq \mathbb{R}$ is μ_p -separated, i.e.,

$$\inf\{\mu_p([x, z]) : x, z \in X, x < z\} > 0.$$

The **upper and lower A_p -Beurling densities** $D_p^+(X)$ and $D_p^-(X)$ are defined as follows:

$$D_p^+(X) = \limsup_{r \rightarrow \infty} \sup_{\mu_p(I)=r} \frac{\#\{X \cap I : I \subset \mathbb{R} \text{ closed interval}\}}{r} \quad (3.2.2)$$

$$D_p^-(X) = \liminf_{r \rightarrow \infty} \inf_{\mu_p(I)=r} \frac{\#\{X \cap I : I \subset \mathbb{R} \text{ closed interval}\}}{r}. \quad (3.2.3)$$

With the additional assumption that p is the model case (2.2.3) and $p, p' \in AC_{loc}(\mathbb{R})$, the following necessary density conditions for sampling and interpolation hold [39, Thms. 6.2, 6.3].

Theorem 3.2.1. *Let $\Lambda \subset \mathbb{R}_0^+$ be of finite Lebesgue measure. Suppose p is the model case*

$$p(x) = \begin{cases} p_-, & x < -R, \\ p_+, & x > R \end{cases}$$

for some $R > 0$ such that $p, p' \in AC_{loc}(\mathbb{R})$ and A_p the self-adjoint realization of τ_p in the limit point case at $\pm\infty$.

- If X is a set of stable sampling for $PW_\Lambda(A_p)$, then $D_p^-(X) \geq \frac{|\Lambda^{1/2}|}{\pi}$.
- If X is a set of interpolation for $PW_\Lambda(A_p)$, then $D_p^+(X) \leq \frac{|\Lambda^{1/2}|}{\pi}$.

In this thesis, we will prove an analogue of the above density theorem for a particular choice of p that does not satisfy $p, p' \in AC_{loc}(\mathbb{R})$, i.e., Theorem 3.2.1 does not apply. This will be the main theme of Chapter 6.

3.3. Non-uniform sampling

We present a sampling theorem for $PW_\Lambda(A_p)$ where $\Lambda \subseteq [0, \Omega] \subset \mathbb{R}$ that is consistent with our observation in (3.2.1). Let $X = \{x_j\}_{j \in \mathbb{Z}} \subset \mathbb{R}$ be a non-uniform, increasingly ordered sampling set and define the **maximum gap**

$$\delta(X, p) = \sup_{j \in \mathbb{Z}} \frac{x_{j+1} - x_j}{\inf_{x \in [x_j, x_{j+1}]} \sqrt{p(x)}}.$$

The following theorem is a weighted sampling inequality [39, Thm. 5.2] for $PW_\Lambda(A_p)$. We made minor corrections in the original statement by adding boundedness of $x_{j+1} - x_j$ for $j \in \mathbb{Z}$.

Theorem 3.3.1. *Let $\Lambda \subseteq [0, \Omega] \subset \mathbb{R}_0^+$ and assume $\inf_{x \in \mathbb{R}} p(x) > 0$. If $\delta = \delta(X, p) < \pi/\Omega^{1/2}$, then for all $f \in PW_\Lambda(A_p)$, we have*

$$\left(1 - \frac{\delta\Omega^{1/2}}{\pi}\right)^2 \|f\|^2 \leq \sum_{j \in \mathbb{Z}} \frac{x_{j+1} - x_{j-1}}{2} |f(x_j)|^2 \leq \left(1 + \frac{\delta\Omega^{1/2}}{\pi}\right)^2 \|f\|^2.$$

If, in addition, there exist $\gamma_1, \gamma_2 > 0$ such that $\gamma_1 \leq x_{j+1} - x_j \leq \gamma_2$ for all $j \in \mathbb{Z}$, then X is a set of stable sampling for $PW_\Lambda(A_p)$ with lower and upper bounds $\gamma_2^{-1} \left(1 - \frac{\delta\Omega^{1/2}}{\pi}\right)^2$ and $\gamma_1^{-1} \left(1 + \frac{\delta\Omega^{1/2}}{\pi}\right)^2$, respectively.

With the above sampling inequality, one can formulate several reconstruction algorithms to recover $f \in PW_\Lambda(A_p)$ from its samples. We refer the reader to [39, Thm. 5.3] for a projection-based iterative reconstruction algorithm. However, as mentioned in [39, Sec. 8],

3. Functions of variable bandwidth

any reconstruction procedure requires the knowledge of the reproducing kernel. For special parametrizing functions such as

$$p(x) = \begin{cases} p_-, & x \leq 0, \\ p_+, & x > 0 \end{cases}$$

with $p_-, p_+ > 0$, an explicit formula for the reproducing kernel was derived in [39, Sec. 4]. It is then natural to ask if the derivation can be extended to piecewise constant functions of the form

$$p(x) = \begin{cases} p_0, & x \in (-\infty, t_1], \\ p_1, & x \in (t_1, t_2], \\ \vdots & \vdots \\ p_{n-1}, & x \in (t_{n-1}, t_n], \\ p_n, & x \in (t_n, \infty), \end{cases}$$

for some $n \in \mathbb{N}$, $\{p_k\}_{k=0}^n \subset (0, \infty)$ and $-\infty < t_1 \leq t_2 \leq \dots \leq t_n < \infty$. This will be thoroughly discussed in the next chapter.

4. The space $PW_\Lambda(A_p)$ with piecewise constant p

Among all possible parametrizing functions, piecewise constant functions offer a straightforward and practical approach of assigning local bandwidths to segments of a signal. Let $n \in \mathbb{N}$ and $\Omega > 0$. Consider a finite partition $\{I_k\}_{k=0}^n$ of subintervals of \mathbb{R} and a finite sequence $\{p_k\}_{k=0}^n \subset (0, \infty)$. Now, define the piecewise function $p : \mathbb{R} \rightarrow (0, \infty)$ by $p(x) = p_k$ if $x \in I_k$, for $k = 0, \dots, n$. If A_p is the self-adjoint realization of $\tau_p = -D(pD)$ on \mathbb{R} in the limit point case at $\pm\infty$, Proposition 3.1.3 asserts that every $f \in PW_{[0, \Omega]}(A_p)$ coincides with a function in $B_{(\Omega/p_k)^{1/2}}$ on the interior of I_k for all k . This means that for each k , p prescribes the local bandwidth $(\Omega/p_k)^{1/2}$ on the interior of I_k . Hence, $PW_{[0, \Omega]}(A_p)$ can be viewed as the space of functions with different local bandwidths determined by p and whose spectral Fourier transform has support contained in $[0, \Omega]$.

One of the main goals of this thesis is to show that numerical signal reconstruction can be performed in some class of variable bandwidth spaces. As observed in [39, Sec. 8], any reconstruction procedure requires the knowledge of the reproducing kernel k_Λ of $PW_\Lambda(A_p)$. For general parametrizing functions, finding k_Λ is an arduous task. Indeed, evaluating $k_\Lambda(x, y)$ for any $x, y \in \mathbb{R}$ using formula (3.1.1) demands explicit formulas of the fundamental system $\Phi(z, \cdot) = (\Phi_1(z, \cdot), \Phi_2(z, \cdot))$ of $(\tau_p - z)f = 0$ as well as the spectral measure μ , both of which are difficult to compute in general. The use of piecewise constant parametrizing functions is motivated by the hope that if p is such a function, direct evaluations of k_Λ can in principle be performed. We draw inspiration from the so-called toy example [39, Sec. 4], where $\Lambda = [0, \Omega]$ and p is of the form

$$p(x) = \begin{cases} p_-, & x \leq 0 \\ p_+, & x > 0, \end{cases} \quad p_-, p_+ > 0.$$

With this p , a closed-form expression of the fundamental system of $(\tau_p - z)f = 0$ as well as the spectral matrix measure were derived (see [39, Sec. 4, Appx. A] for a sketch of the calculations), and consequently, an explicit form of k_Λ was computed. This gave us an insight that for a general piecewise constant functions, the corresponding reproducing kernel might also be directly computable.

In this chapter, we discuss the fundamental aspects of functions of variable bandwidth parametrized by piecewise constant functions. The theory revolves around the Sturm-Liouville operator τ_p with p a piecewise constant function. More precisely, we consider its self-adjoint realization A_p to define the abstract Paley-Wiener space $PW_\Lambda(A_p)$ with spectral set $\Lambda \subset \mathbb{R}_0^+$. Following the model case (2.2.3), all parametrizing functions in the subsequent discussions are always assumed to be positive and eventually constant. This assumption is convenient as p can only have a finite number of piecewise components, and thus computations require only a finite number of steps. We shall shortly see that for

4. The space $PW_\Lambda(A_p)$ with piecewise constant p

piecewise constant parametrizing functions, calculations starting from the construction of solutions up to finding the reproducing kernel can be made explicit. This observation brings us closer to our goal of using variable bandwidth spaces for numerical signal reconstruction.

4.1. Piecewise constant parametrizing functions

Definition 4.1.1. Fix $n \in \mathbb{N}$. Let $\{t_k\}_{k=1}^n \subset \mathbb{R}$ be strictly increasing and $\{p_k\}_{k=0}^n \subset (0, \infty)$. Set $I_0 = (-\infty, t_1]$, $I_n = (t_n, \infty)$, $I_k = (t_k, t_{k+1}]$ for $1 \leq k \leq n-1$ and χ_k the characteristic function of I_k for $0 \leq k \leq n$. An $(n+1)$ -**component piecewise constant function** p is a function of the form

$$p(x) = \sum_{k=0}^n p_k \chi_k(x), \quad x \in \mathbb{R}.$$

We call $\{t_k\}_{k=1}^n$ and $\{p_k\}_{k=0}^n$ the **knots** and **components** of p , respectively.

If the number of components of p is immaterial in the discussion, we will refer to p as a piecewise constant function.

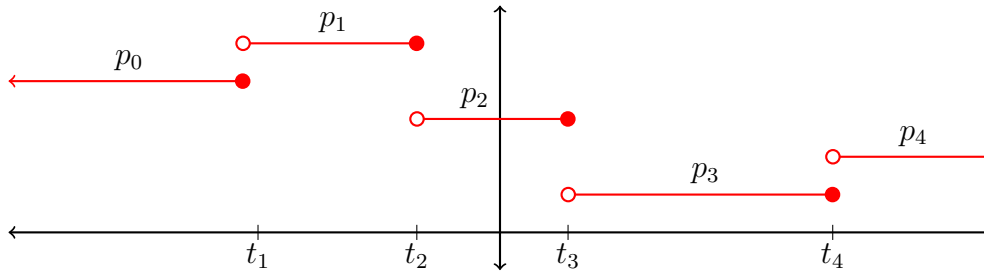


Figure 4.1.: A five-component piecewise constant function

With only the piecewise constant assumption on p , we can instantly deduce some properties of τ_p as well as its self-adjoint realization A_p .

Proposition 4.1.2. *Let p be a piecewise constant function. Then the following statements hold.*

- (i) *The Sturm-Liouville operator $\tau_p = -D(pD)$ on \mathbb{R} is in the limit point case at $\pm\infty$. Moreover, τ_p has a unique self-adjoint realization A_p given by*

$$\begin{aligned} \mathcal{D}(A_p) &= \{f \in L^2(\mathbb{R}) : f, pf' \in AC_{loc}(\mathbb{R}) \text{ and } -(pf')' \in L^2(\mathbb{R})\}, \\ A_p f &= -(pf')'. \end{aligned}$$

- (ii) *The spectrum of A_p is $\sigma(A_p) = [0, \infty)$.*

Proof. Let $n \in \mathbb{N}$ and p an $(n+1)$ -component piecewise constant function.

- (i) We have τ_p in the limit point case at $\pm\infty$ by applying Theorem 2.2.4 at both endpoints $\pm\infty$. By Theorem 2.2.3, τ_p has a unique self-adjoint realization A_p which is equal to the maximal operator of τ_p .

(ii) Suppose $t_n \geq 0$. With $C_1 = p_n$, we have

$$\liminf_{L \rightarrow \infty} \frac{1}{L} \int_0^L \left| 1 - \frac{C_1}{p(u)} \right| du = \liminf_{L \rightarrow \infty} \frac{1}{L} \int_0^{t_n} \left| 1 - \frac{C_1}{p(u)} \right| du = 0$$

as the integral is independent of L . On the other hand, if $t_n < 0$, then $[0, L] \subset I_n$ and the integrand is trivially zero. Analogously, taking $C_2 = p_0$ proves that

$$\liminf_{L \rightarrow \infty} \frac{1}{L} \int_{-L}^0 \left| 1 - \frac{C_2}{p(u)} \right| du = 0.$$

Therefore, $\sigma(A_p) = [0, \infty)$ by Theorem 2.2.5.

□

4.2. Construction of fundamental solutions

Recall from Theorem 2.2.6 that the spectral representation \mathcal{F}_{A_p} defined in (2.2.5) requires the knowledge of a fundamental system $\Phi(z, x) = (\Phi_1(z, x), \Phi_2(z, x))$ of $(\tau_p - z)f = 0$ for $z \in \mathbb{C}, x \in \mathbb{R}$. While finding analytic expressions of a fundamental system may be difficult, if not impossible, for arbitrary parametrizing functions, we shall see that in the case of a piecewise constant p , a closed-form expression for Φ can be derived and is completely determined by p . The derivation of solutions of $(\tau_p - z)f = 0$ is similar to the construction of splines where continuity conditions on the knots are prescribed.

In this section, we find an explicit formula for the general solutions of $(\tau_p - z)f = 0$, $z \in \mathbb{C} \setminus (-\infty, 0]$ for piecewise constant functions p . We know from Theorem 2.2.2 (Weyl alternative) and Proposition 4.1.2 that for $\text{Im}z \neq 0$, we can find a unique (up to a constant factor) pair of solutions, one of which lies left and the other lies right in $L^2(\mathbb{R})$. A particular pair will be used to form the spectral transform \mathcal{F}_{A_p} and will be derived in the next section.

We now briefly discuss the strategy to find a fundamental system of $(\tau_p - z)f = 0$. Let $n \in \mathbb{N}$ and assume p is an $(n + 1)$ -piecewise constant function and A_p the self-adjoint realization of $\tau_p = -D(pD)$. By solving the $n + 1$ equations

$$(-p_k D^2 - z)f = 0, \quad x \in I_k, 0 \leq k \leq n$$

for fixed $z \in \mathbb{C} \setminus (-\infty, 0]$, we obtain $n + 1$ local general solutions of the form

$$a_k e^{i\sqrt{z/p_k}x} + b_k e^{-i\sqrt{z/p_k}x}, \quad x \in I_k$$

for some $a_k, b_k \in \mathbb{C}, 0 \leq k \leq n$, i.e., these functions solve the original equation $(\tau_p - z)f = 0$ restricted to $x \in I_k$. We conveniently take the branch cut on the nonpositive real axis of the complex plane so that the principal square root⁸ \sqrt{z} of $z \in \mathbb{C} \setminus (-\infty, 0]$ is well-defined and satisfies $\text{Im}z \cdot \text{Im}\sqrt{z} \geq 0$. By carefully choosing the coefficients a_k, b_k , out of these local solutions we can form global solutions that solve the original equation $(\tau_p - z)f = 0$ on \mathbb{R} .

⁸If $z = re^{i\theta} \in \mathbb{C} \setminus (-\infty, 0]$ with $r > 0$ and $-\pi < \theta < \pi$, $\sqrt{z} = \sqrt{r}e^{i\theta/2}$ is the principal square root of z .

4. The space $PW_\Lambda(A_p)$ with piecewise constant p

From this point onward, we will always assume p is a piecewise constant function as in Definition 4.1.1 and A_p the self-adjoint realization of τ_p . Since the components $\{p_k\}_{k=0}^n$ of p will appear frequently as denominators in most of the computations, we set

$$q_k = p_k^{-1/2}, \quad 0 \leq k \leq n. \quad (4.2.1)$$

This notation will be used throughout the entire manuscript. We also define for $1 \leq k \leq n$, $z \in \mathbb{C} \setminus (-\infty, 0]$ the matrices

$$L_k(z) = \frac{1}{2} \begin{bmatrix} \left(1 + \frac{q_k}{q_{k-1}}\right) e^{it_k(q_{k-1}-q_k)\sqrt{z}} & \left(1 - \frac{q_k}{q_{k-1}}\right) e^{-it_k(q_{k-1}+q_k)\sqrt{z}} \\ \left(1 - \frac{q_k}{q_{k-1}}\right) e^{it_k(q_{k-1}+q_k)\sqrt{z}} & \left(1 + \frac{q_k}{q_{k-1}}\right) e^{-it_k(q_{k-1}-q_k)\sqrt{z}} \end{bmatrix} \quad (4.2.2)$$

$$\begin{aligned} R_k(z) &= L_k^{-1}(z) \\ &= \frac{1}{2} \begin{bmatrix} \left(1 + \frac{q_{k-1}}{q_k}\right) e^{-it_k(q_{k-1}-q_k)\sqrt{z}} & \left(1 - \frac{q_{k-1}}{q_k}\right) e^{-it_k(q_{k-1}+q_k)\sqrt{z}} \\ \left(1 - \frac{q_{k-1}}{q_k}\right) e^{it_k(q_{k-1}+q_k)\sqrt{z}} & \left(1 + \frac{q_{k-1}}{q_k}\right) e^{it_k(q_{k-1}-q_k)\sqrt{z}} \end{bmatrix} \end{aligned} \quad (4.2.3)$$

which will be used to generate solutions of $(\tau_p - z)f = 0$. It may also be convenient to rewrite L_k and R_k as follows. Define for $1 \leq k \leq n$ the quantities

$$\gamma_k^{-1} = \left(\frac{q_k}{q_{k-1}}\right)^{1/2}, \quad \eta_k = t_k(q_{k-1} - q_k) \quad \text{and} \quad \theta_k = t_k(q_{k-1} + q_k).$$

We can then express (4.2.2) as

$$L_k(z) = \gamma_k^{-1} \begin{bmatrix} \frac{\gamma_k + \gamma_k^{-1}}{2} e^{i\eta_k \sqrt{z}} & \frac{\gamma_k - \gamma_k^{-1}}{2} e^{-i\theta_k \sqrt{z}} \\ \frac{\gamma_k - \gamma_k^{-1}}{2} e^{i\theta_k \sqrt{z}} & \frac{\gamma_k + \gamma_k^{-1}}{2} e^{-i\eta_k \sqrt{z}} \end{bmatrix}, \quad \det L_k(z) = \gamma_k^{-2} \quad (4.2.4)$$

and (4.2.3) as

$$R_k(z) = \gamma_k \begin{bmatrix} \frac{\gamma_k + \gamma_k^{-1}}{2} e^{-i\eta_k \sqrt{z}} & -\frac{\gamma_k - \gamma_k^{-1}}{2} e^{-i\theta_k \sqrt{z}} \\ -\frac{\gamma_k - \gamma_k^{-1}}{2} e^{i\theta_k \sqrt{z}} & \frac{\gamma_k + \gamma_k^{-1}}{2} e^{i\eta_k \sqrt{z}} \end{bmatrix}, \quad \det R_k(z) = \gamma_k^2. \quad (4.2.5)$$

Lemma 4.2.1. *Let $n \in \mathbb{N}$ and assume p is an $(n+1)$ -piecewise constant function. Then for $z \in \mathbb{C} \setminus (-\infty, 0]$, the piecewise function $\varphi(z, \cdot) : \mathbb{R} \rightarrow \mathbb{C}$ of the form*

$$\varphi(z, x) = a_k e^{iq_k \sqrt{z}x} + b_k e^{-iq_k \sqrt{z}x}, \quad x \in I_k, q_k = p_k^{-1/2}$$

for some coefficients $a_k, b_k \in \mathbb{C}$, $0 \leq k \leq n$ solves $(\tau_p - z)f = 0$ on \mathbb{R} if and only if

$$\begin{bmatrix} a_k \\ b_k \end{bmatrix} = L_k(z) \begin{bmatrix} a_{k-1} \\ b_{k-1} \end{bmatrix} \quad (4.2.6)$$

holds for $1 \leq k \leq n$.

Proof. Fix $z \in \mathbb{C} \setminus (-\infty, 0]$. We start with the local solutions of $(\tau_p - z)f = 0$. Let $0 \leq k \leq n$. Since $\tau_p f = -p_k f''$ on I_k , we know that the functions

$$u_k(z, x) = e^{i\sqrt{z/p_k}x} = e^{iq_k \sqrt{z}x}, \quad v_k(z, x) = e^{-i\sqrt{z/p_k}x} = e^{-iq_k \sqrt{z}x}, \quad q_k = p_k^{-1/2} \quad (4.2.7)$$

4.2. Construction of fundamental solutions

solve $-p_k f'' - z f = -\frac{1}{q_k^2} f'' - z f = 0$ for $x \in I_k$. Moreover, the Wronskian $W(u_k(z, \cdot), v_k(z, \cdot))$ in (2.2.2) computed on I_k is

$$W(u_k(z, \cdot), v_k(z, \cdot)) = \det \begin{bmatrix} e^{iq_k \sqrt{z} x} & e^{-iq_k \sqrt{z} x} \\ i \frac{\sqrt{z}}{q_k} e^{iq_k \sqrt{z} x} & -i \frac{\sqrt{z}}{q_k} e^{-iq_k \sqrt{z} x} \end{bmatrix} = -\frac{2i\sqrt{z}}{q_k} \neq 0. \quad (4.2.8)$$

Thus, $u_k(z, x)$ and $v_k(z, x)$ form a fundamental system of $-p_k f'' - z f = 0$ on I_k . Hence, the local solutions $\varphi_k(z, \cdot)$ of $(\tau_p - z)f = 0$ on I_k take the form

$$\varphi_k(z, x) = a_k u_k(z, x) + b_k v_k(z, x) = a_k e^{iq_k \sqrt{z} x} + b_k e^{-iq_k \sqrt{z} x}, \quad x \in I_k \quad (4.2.9)$$

for some constants $a_k, b_k \in \mathbb{C}$, $0 \leq k \leq n$.

Now, since the collection $\{I_k\}_{k=0}^n$ is a disjoint partition of \mathbb{R} , consider the piecewise function $\varphi(z, \cdot) : \mathbb{R} \rightarrow \mathbb{C}$ defined as

$$\varphi(z, x) = \varphi_k(z, x), \quad x \in I_k$$

for some choice of scalars $a_k, b_k \in \mathbb{C}$, $0 \leq k \leq n$ in (4.2.9). Then $\varphi(z, \cdot), p(\cdot)\varphi'(z, \cdot) \in AC_{loc}(\mathbb{R})$ if and only if both are continuous at each knot t_k . This condition can be expressed in matrix form (in conjunction with $p(t_k) = p_{k-1} = \frac{1}{q_{k-1}^2}$, $\lim_{x \downarrow t_k} p(x) = p_k = \frac{1}{q_k^2}$) as

$$\begin{bmatrix} \varphi_{k-1}(z, t_k) \\ \frac{1}{q_{k-1}^2} \varphi'_{k-1}(z, t_k) \end{bmatrix} = \begin{bmatrix} \varphi(z, t_k) \\ p(t_k) \varphi'(z, t_k) \end{bmatrix} = \lim_{x \downarrow t_k} \begin{bmatrix} \varphi(z, x) \\ p(x) \varphi'(z, x) \end{bmatrix} = \begin{bmatrix} \varphi_k(z, t_k) \\ \frac{1}{q_k^2} \varphi'_k(z, t_k) \end{bmatrix}$$

$$\begin{bmatrix} e^{iq_{k-1} \sqrt{z} t_k} & e^{iq_{k-1} \sqrt{z} t_k} \\ i \frac{\sqrt{z}}{q_{k-1}} e^{iq_{k-1} \sqrt{z} t_k} & -i \frac{\sqrt{z}}{q_{k-1}} e^{iq_{k-1} \sqrt{z} t_k} \end{bmatrix} \begin{bmatrix} a_{k-1} \\ b_{k-1} \end{bmatrix} = \begin{bmatrix} e^{iq_k \sqrt{z} t_k} & e^{iq_k \sqrt{z} t_k} \\ i \frac{\sqrt{z}}{q_k} e^{iq_k \sqrt{z} t_k} & -i \frac{\sqrt{z}}{q_k} e^{iq_k \sqrt{z} t_k} \end{bmatrix} \begin{bmatrix} a_k \\ b_k \end{bmatrix}.$$

For $1 \leq k \leq n$, $z \in \mathbb{C} \setminus (-\infty, 0]$, set

$$L_k(z) = \begin{bmatrix} e^{iq_k \sqrt{z} t_k} & e^{iq_k \sqrt{z} t_k} \\ i \frac{\sqrt{z}}{q_k} e^{iq_k \sqrt{z} t_k} & -i \frac{\sqrt{z}}{q_k} e^{iq_k \sqrt{z} t_k} \end{bmatrix}^{-1} \begin{bmatrix} e^{iq_{k-1} \sqrt{z} t_k} & e^{iq_{k-1} \sqrt{z} t_k} \\ i \frac{\sqrt{z}}{q_{k-1}} e^{iq_{k-1} \sqrt{z} t_k} & -i \frac{\sqrt{z}}{q_{k-1}} e^{iq_{k-1} \sqrt{z} t_k} \end{bmatrix}.$$

A straightforward computation of L_k yields

$$\begin{aligned} L_k(z) &= \frac{q_k}{2i\sqrt{z}} \begin{bmatrix} i \frac{\sqrt{z}}{q_k} e^{-iq_k \sqrt{z} t_k} & e^{-iq_k \sqrt{z} t_k} \\ i \frac{\sqrt{z}}{q_k} e^{iq_k \sqrt{z} t_k} & -e^{iq_k \sqrt{z} t_k} \end{bmatrix} \begin{bmatrix} e^{iq_{k-1} \sqrt{z} t_k} & e^{-iq_{k-1} \sqrt{z} t_k} \\ i \frac{\sqrt{z}}{q_{k-1}} e^{iq_{k-1} \sqrt{z} t_k} & -i \frac{\sqrt{z}}{q_{k-1}} e^{-iq_{k-1} \sqrt{z} t_k} \end{bmatrix} \\ &= \frac{q_k}{2} \begin{bmatrix} \left(\frac{1}{q_{k-1}} + \frac{1}{q_k}\right) e^{it_k(q_{k-1}-q_k)\sqrt{z}} & \left(-\frac{1}{q_{k-1}} + \frac{1}{q_k}\right) e^{-it_k(q_{k-1}+q_k)\sqrt{z}} \\ \left(-\frac{1}{q_{k-1}} + \frac{1}{q_k}\right) e^{it_k(q_{k-1}+q_k)\sqrt{z}} & \left(\frac{1}{q_{k-1}} + \frac{1}{q_k}\right) e^{-it_k(q_{k-1}-q_k)\sqrt{z}} \end{bmatrix} \end{aligned}$$

which equals (4.2.2). By construction, $\varphi(z, \cdot)$ is a solution of $(\tau_p - z)f = 0$ on \mathbb{R} if and only if (4.2.6) holds. \square

Although there are $2(n+1)$ constants involved in forming the above solutions, only two of them can be arbitrarily chosen. In fact, for a fixed $z \in \mathbb{C} \setminus (-\infty, 0]$ one can construct a plethora of solutions of $(\tau_p - z)f = 0$ by setting arbitrary constants $c_1, c_2 \in \mathbb{C}$ as a_k and b_k on a chosen interval I_k . The remaining coefficients are obtained from Lemma 4.2.1 by either forward or backward iterative calculation. We summarize below how exactly the solutions of $(\tau_p - z)f = 0$ are generated.

4. The space $PW_\Lambda(A_p)$ with piecewise constant p

- Starting from the leftmost interval I_0 with $a_0 = c_1, b_0 = c_2$, we have

$$\begin{bmatrix} a_j \\ b_j \end{bmatrix} = L_j(z)L_{j-1}(z) \cdots L_1(z) \begin{bmatrix} c_1 \\ c_2 \end{bmatrix}, \quad 1 \leq j \leq n. \quad (4.2.10)$$

- Starting from the rightmost interval I_n with $a_n = c_1, b_n = c_2$, we left-multiply the inverse $R_k(z)$ of $L_k(z)$ on both sides of (4.2.6) to obtain

$$\begin{bmatrix} a_l \\ b_l \end{bmatrix} = R_{l+1}(z)R_l(z) \cdots R_n(z) \begin{bmatrix} c_1 \\ c_2 \end{bmatrix}, \quad 0 \leq l \leq n-1. \quad (4.2.11)$$

- We start from one of the middle intervals I_k , $0 < k < n$ and $a_k = c_1, b_k = c_2$ and then take a combination of the two procedures above, i.e.,

$$\begin{bmatrix} a_r \\ b_r \end{bmatrix} = \begin{cases} L_r(z)L_{r-1}(z) \cdots L_{k+1}(z) \begin{bmatrix} c_1 \\ c_2 \end{bmatrix}, & k+1 \leq r \leq n, \\ R_{r+1}(z)R_r(z) \cdots R_k(z) \begin{bmatrix} c_1 \\ c_2 \end{bmatrix}, & 0 \leq r \leq k-1. \end{cases} \quad (4.2.12)$$

By writing $\begin{bmatrix} c_1 \\ c_2 \end{bmatrix}$ as $c_1 \begin{bmatrix} 1 \\ 0 \end{bmatrix} + c_2 \begin{bmatrix} 0 \\ 1 \end{bmatrix}$, (4.2.10), (4.2.11) and (4.2.12) are equivalent to taking linear combinations (cf. (4.2.7))

$$c_1 \varphi^+(z, \cdot) + c_2 \varphi^-(z, \cdot), \quad c_1, c_2 \in \mathbb{R}, 0 \leq k \leq n,$$

where $\varphi^\pm(z, x) = e^{\pm iq_k \sqrt{z}x}$ for $x \in I_k$ and extended to the whole of \mathbb{R} via Lemma 4.2.1. By construction, $\{\varphi^+, \varphi^-\}$ is a fundamental system of $(\tau_p - z)f = 0$ on \mathbb{R} and thus all solutions of $(\tau_p - z)f = 0$ are formed by way of Lemma 4.2.1. In the forthcoming discussions, we only generate solutions using formulas (4.2.10) and (4.2.11). Formula (4.2.12) is useful in some situations (cf. the proof of [39, Prop. 3.5]) but will not be used anywhere in this thesis.

As τ_p is in the limit point case at $\pm\infty$, Theorem 2.2.2(ii) (Weyl alternative) and Proposition 4.1.2 state that for all $z \in \mathbb{C} \setminus \mathbb{R}$ we can always find two unique (up to a constant factor) solutions of $(\tau_p - z)f = 0$, one of which lies left and the other lies right in $L^2(\mathbb{R})$. With the help of (4.2.10) and (4.2.11), we can determine the exact form of such a pair of solutions.

Theorem 4.2.2. *Let p be an $(n+1)$ -component piecewise constant function. Define the functions $a_l^+, b_l^+, a_j^-, b_j^-$, $0 \leq l \leq n-1, 1 \leq j \leq n$ from $\mathbb{C} \setminus (-\infty, 0]$ to \mathbb{C} by*

$$\begin{bmatrix} a_l^+(z) \\ b_l^+(z) \end{bmatrix} = R_{l+1}(z)R_l(z) \cdots R_n(z) \begin{bmatrix} 1 \\ 0 \end{bmatrix}, \quad 0 \leq l \leq n-1 \quad (4.2.13)$$

$$\begin{bmatrix} a_j^-(z) \\ b_j^-(z) \end{bmatrix} = L_j(z)L_{j-1}(z) \cdots L_1(z) \begin{bmatrix} 0 \\ 1 \end{bmatrix}, \quad 1 \leq j \leq n. \quad (4.2.14)$$

Then the functions $\Phi(z, \cdot) = (\Phi^+(z, \cdot), \Phi^-(z, \cdot))$ given by

$$\Phi^+(z, x) = \begin{cases} a_l^+(z)e^{iq_l \sqrt{z}x} + b_l^+(z)e^{-iq_l \sqrt{z}x}, & x \in I_l, 0 \leq l \leq n-1 \\ e^{iq_n \sqrt{z}x}, & x \in I_n \end{cases} \quad (4.2.15)$$

$$\Phi^-(z, x) = \begin{cases} e^{-iq_0 \sqrt{z}x}, & x \in I_0 \\ a_j^-(z)e^{iq_j \sqrt{z}x} + b_j^-(z)e^{-iq_j \sqrt{z}x}, & x \in I_j, 1 \leq j \leq n \end{cases} \quad (4.2.16)$$

4.2. Construction of fundamental solutions

are solutions of $(\tau_p - z)f = 0$ for all $z \in \mathbb{C} \setminus (-\infty, 0]$ that are analytic in z . Furthermore,

- if $\text{Im}z > 0$, then $\Phi(z, \cdot) = (\Phi^+(z, \cdot), \Phi^-(z, \cdot))$ is a fundamental system of $(\tau_p - z)f = 0$ satisfying

$$\Phi^-(z, \cdot) \in L^2(-\infty, c) \quad \text{and} \quad \Phi^+(z, \cdot) \in L^2(c, \infty)$$

for all $c \in \mathbb{R}$

- if $\text{Im}z < 0$, then $\overline{\Phi(\bar{z}, \cdot)} = (\overline{\Phi^+(\bar{z}, \cdot)}, \overline{\Phi^-(\bar{z}, \cdot)})$ is a fundamental system of $(\tau_p - z)f = 0$ satisfying

$$\overline{\Phi^-(\bar{z}, \cdot)} \in L^2(-\infty, c) \quad \text{and} \quad \overline{\Phi^+(\bar{z}, \cdot)} \in L^2(c, \infty)$$

for all $c \in \mathbb{R}$.

Proof. By construction, we have from Lemma 4.2.1 as well as (4.2.10) and (4.2.11) that $\Phi^\pm(z, \cdot)$ are solutions of $(\tau_p - z)f = 0$ for all $z \in \mathbb{C} \setminus (-\infty, 0]$. Since p is real-valued, $\overline{\Phi^\pm(\bar{z}, \cdot)}$ are solutions of $(\tau_p - z)f = 0$ as well. Since $z \mapsto e^{\pm iq_k \sqrt{z}x}$ is analytic for all $x \in \mathbb{R}$, it follows that the entries of L_j and R_l for $0 \leq l \leq n-1, 1 \leq j \leq n$, the coefficients a_k^\pm, b_k^\pm for $0 \leq k \leq n$, and ultimately the fundamental solutions $\Phi^\pm(\cdot, x)$ for all $x \in \mathbb{R}$, are analytic as well. We next prove the second conclusion of the theorem. Observe that

$$|e^{\pm iq \sqrt{z}x}| = e^{\mp q \text{Im}\sqrt{z}x}, \quad x \in \mathbb{R}, q > 0, z \in \mathbb{C} \setminus (-\infty, 0]. \quad (4.2.17)$$

Note the following.

- If $\text{Im}z > 0$, then $\text{Im}\sqrt{z} > 0$. By (4.2.17), we have $\Phi^-(z, x) = e^{-iq_0 \sqrt{z}x} \in L^2(I_0)$ and $\Phi^+(z, x) = e^{iq_n \sqrt{z}x} \in L^2(I_n)$. Thus, $\Phi^-(z, \cdot)$ lies left and $\Phi^+(z, \cdot)$ lies right in $L^2(\mathbb{R})$.
- If $\text{Im}z < 0$, then $\text{Im}\sqrt{z} < 0$. Since $\sqrt{\bar{z}} = \overline{\sqrt{z}}$ for all $z \in \mathbb{C} \setminus (-\infty, 0]$, (4.2.17) implies

$$|\overline{e^{\pm iq \sqrt{z}x}}| = |e^{\pm iq \sqrt{\bar{z}}x}| = e^{\pm q \text{Im}\sqrt{\bar{z}}x}, \quad x \in \mathbb{R}, q > 0, z \in \mathbb{C} \setminus (-\infty, 0].$$

Hence $\overline{\Phi^-(\bar{z}, \cdot)}$ lies left and $\overline{\Phi^+(\bar{z}, \cdot)}$ lies right in $L^2(\mathbb{R})$.

Now, suppose there exists $z_0 \in \mathbb{C} \setminus (-\infty, 0]$ with $\text{Im}z_0 > 0$ such that $\Phi(z_0, \cdot)$ is linearly dependent, i.e., $\Phi^+(z_0, \cdot)$ is a scalar multiple of $\Phi^-(z_0, \cdot)$. Then $(\tau_p - z_0)f = 0$ has a nontrivial solution in $\mathcal{D}(A_p) \subset L^2(\mathbb{R})$, i.e., an eigenvector corresponding to the eigenvalue z_0 . Thus, $z_0 \in \sigma(A_p) = [0, \infty)$ by Proposition 4.1.2, which is a contradiction. Therefore, $\Phi(z, \cdot)$ is linearly independent for all $z \in \mathbb{C} \setminus (-\infty, 0]$ with $\text{Im}z > 0$. The same proof works for $\overline{\Phi(\bar{z}, \cdot)}$, $\text{Im}z < 0$. \square

Remark 4.2.3. For $z \in (0, \infty)$ and $1 \leq k \leq n$, $\gamma_k L_k(z)$ and $\gamma_k^{-1} R_k(z)$ are elements of the group

$$SU(1, 1) = \left\{ \begin{bmatrix} a & \bar{b} \\ b & \bar{a} \end{bmatrix} : a, b \in \mathbb{C} \text{ and } |a|^2 - |b|^2 = 1 \right\}$$

with group multiplication given by matrix multiplication. This follows from the fact that $e^{iz} = e^{-iz}$ if and only if $z \in \mathbb{R}$. Hence,

$$\gamma_j L_j(z) \cdots \gamma_1 L_1(z) = \left(\prod_{k=1}^j \gamma_k \right) \begin{bmatrix} \overline{b_j^-(z)} & a_j^-(z) \\ a_j^-(z) & \overline{b_j^-(z)} \end{bmatrix}$$

4. The space $PW_\Lambda(A_p)$ with piecewise constant p

and therefore

$$L_j(z) \cdot \dots \cdot L_1(z) = \begin{bmatrix} \overline{b_j^-(z)} & a_j^-(z) \\ a_j^-(z) & \overline{b_j^-(z)} \end{bmatrix}, \quad 1 \leq j \leq n. \quad (4.2.18)$$

By the same token, it can be shown that

$$R_{l+1}(z) \cdot \dots \cdot R_n(z) = \begin{bmatrix} a_l^+(z) & \overline{b_l^+(z)} \\ b_l^+(z) & \overline{a_l^+(z)} \end{bmatrix}, \quad 0 \leq l \leq n-1. \quad (4.2.19)$$

In spite of a group structure, the left-hand side of (4.2.18) and (4.2.19) cannot be simplified further, even with the help of known matrix product decompositions.

We can now prove that the spectrum of A_p is purely absolutely continuous.

Lemma 4.2.4. *Let p be a piecewise constant function and A_p the self-adjoint realization of τ_p in the limit point case at $\pm\infty$. Then A_p has purely absolutely continuous spectrum, i.e.,*

$$\sigma(A_p) = \sigma_{ac}(A_p) = [0, \infty), \quad \sigma_{pp}(A_p) = \sigma_{sc}(A_p) = \emptyset.$$

Proof. Recall from Proposition 4.1.2 that $\sigma(A_p) = [0, \infty)$. First, we prove that $\sigma_{pp}(A_p) = \emptyset$, i.e., A_p has no eigenvalues. Let p be an $(n+1)$ -component piecewise constant function for some $n \in \mathbb{N}$. Fix $\lambda \in (0, \infty)$. By Lemma 4.2.1, the solutions $\varphi(\lambda, \cdot) : \mathbb{R} \rightarrow \mathbb{C}$ of $(\tau_p - \lambda)f = 0$ are of the form

$$\varphi(\lambda, x) = a_k e^{iq_k \sqrt{\lambda} x} + b_k e^{-iq_k \sqrt{\lambda} x}, \quad x \in I_k, q_k = p_k^{-1/2},$$

where the coefficients $a_k, b_k \in \mathbb{C}$, $0 \leq k \leq n$ satisfy (4.2.6). Observe that $\varphi(\lambda, \cdot) \in L^2(\mathbb{R})$ if and only if $\varphi(\lambda, \cdot)|_{I_0} \in L^2(I_0)$ and $\varphi(\lambda, \cdot)|_{I_n} \in L^2(I_n)$. Since I_0 is unbounded, $\varphi(\lambda, \cdot)|_{I_0}$ is periodic on I_0 , and $e^{iq_k \sqrt{\lambda} x}$ and $e^{-iq_k \sqrt{\lambda} x}$ are linearly independent, it follows that $\varphi(\lambda, \cdot)|_{I_0} \in L^2(I_0)$ if and only if $a_0 = b_0 = 0$. Consequently, (4.2.6) implies $a_k = b_k = 0$ for $0 \leq k \leq n$, i.e., $\varphi(\lambda, \cdot) = 0$. Hence, λ cannot be an eigenvalue. We obtain the same conclusion if we instead start from I_n .

On the other hand, if $\lambda = 0$, it can be shown as in the proof of Lemma 4.2.1 that all solutions of $\tau_p f = (\tau_p - 0)f = 0$ are piecewise functions $\varphi(0, \cdot) : \mathbb{R} \rightarrow \mathbb{C}$ of the form

$$\varphi(0, x) = a_k + b_k x, \quad x \in I_k,$$

where the coefficients $a_k, b_k \in \mathbb{C}$, $1 \leq k \leq n$ satisfy

$$\begin{bmatrix} a_k \\ b_k \end{bmatrix} = \frac{1}{p_k} \begin{bmatrix} p_k & t_k(p_k - p_{k-1}) \\ 0 & p_{k-1} \end{bmatrix} \begin{bmatrix} a_{k-1} \\ b_{k-1} \end{bmatrix}.$$

It is clear that $\tau_p f = 0$ has no nontrivial solution in $L^2(\mathbb{R})$, hence 0 is not an eigenvalue of A_p . Thus, $\sigma_{pp}(A_p) = \emptyset$.

Finally, by Theorem 2.2.10 and Theorem 4.2.2, $\sigma_{sc}(A_p) \cap (0, \infty) = \emptyset$. Therefore, $(0, \infty) \subseteq \sigma_{ac}(A_p)$. Since $\sigma_{sc}(A_p)$ cannot be supported on $\{0\}$, we conclude that $\sigma_{sc}(A_p) = \emptyset$ and $\sigma_{ac}(A_p) = [0, \infty)$. \square

4.2. Construction of fundamental solutions

We refer to the analytic functions a_k^\pm and b_k^\pm defined in (4.2.13) and (4.2.14) with initial conditions $a_n^+(z) = b_0^-(z) = 1$, $a_0^-(z) = b_n^+(z) = 0$ for all $z \in \mathbb{C} \setminus (-\infty, 0]$ as the **connection coefficients** of Φ . These functions are defined to continuously piece together local solutions of $(\tau_p - z)f = 0$ on I_k to form the global solutions $\Phi^\pm(z, \cdot)$ of $(\tau_p - z)f = 0$ on \mathbb{R} .

With the more neat expressions (4.2.4) and (4.2.5) for L_k and R_k , respectively, it is clear that the connection coefficients a_k^\pm and b_k^\pm can be written as a finite sum $\sum_k \alpha_k e^{i\beta_k \sqrt{z}}$ for some $\alpha_k \in \mathbb{C}$, $\beta_k \in \mathbb{R}$. Such functions are called **almost periodic polynomials** (in our case, in \sqrt{z}). These functions belong to a larger class of functions, called almost periodic functions and was first studied by H. Bohr [18] and later generalized by other mathematicians. See e.g. [6, 11] for further reading on almost periodic functions.

Lemma 4.2.5. *The analytic functions $a_j^-, b_j^-, a_l^+, b_l^+$ defined as in (4.2.13) and (4.2.14) are almost periodic polynomials in \sqrt{z} with real coefficients.*

Proof. This follows from the definition of $a_j^-, b_j^-, a_l^+, b_l^+$ together with the fact that the space of almost periodic polynomials is an algebra over \mathbb{R} . \square

The iterative procedure presented in the proof of Lemma 4.2.5 is best programmed using matrix operations. We have Algorithm 1 for the routine that computes all the connection coefficients a_k^\pm, b_k^\pm .

Algorithm 1 Computing the connection coefficients $a_k^\pm(\lambda), b_k^\pm(\lambda)$

Input: Components $p = [p_0 \ p_1 \ \cdots \ p_n]$ and knots $t = [t_1 \ t_2 \ \cdots \ t_n]$
Output: Matrices $C^+(\lambda)$ and $C^-(\lambda)$ of connection coefficients $a_k^\pm(\lambda), b_k^\pm(\lambda)$

- 1: **function** CONNCOEFF(t, p)
- 2: Set symbolic variable λ
- 3: Assign $n = \text{length}(t)$
- 4: Let $C^-(\lambda) = 0^{2 \times (n+1)} = C^+(\lambda)$ $\triangleright C^-$ for a_k^-, b_k^- , C^+ for a_k^+, b_k^+
- 5: Set $C_{2,1}^-(\lambda) = 1 = C_{1,n+1}^+(\lambda)$ \triangleright Initial conditions
- 6: **for** $k = 1$ to n **do**
- 7: Compute $L_k(\lambda)$ and $R_{n-k+1}(\lambda)$
- 8: $C_{:,k+1}^-(\lambda) = L_k(\lambda)C_{:,k}^-(\lambda)$ \triangleright Forward iteration
- 9: $C_{:,n-k+1}^+(\lambda) = R_{n-k+1}(\lambda)C_{:,n-k+2}^+(\lambda)$ \triangleright Backward iteration
- 10: **end for**
- 11: **return** $[C^+(\lambda) \ C^-(\lambda)]$
- 12: **end function**

The connection coefficients $a_k^\pm, b_k^\pm, 0 \leq k \leq n$ are computed and stored in matrices

$$C^\pm(\lambda) = \begin{bmatrix} a_0^\pm(\lambda) & a_1^\pm(\lambda) & \cdots & a_n^\pm(\lambda) \\ b_0^\pm(\lambda) & b_1^\pm(\lambda) & \cdots & b_n^\pm(\lambda) \end{bmatrix}.$$

4. The space $PW_\Lambda(A_p)$ with piecewise constant p

Hence, each piecewise component of $\Phi^\pm(\lambda, x)$ can be quickly retrieved as

$$\begin{aligned}\Phi^\pm(\lambda, x) &= a_k^\pm(\lambda)e^{iq_k\sqrt{\lambda}x} + b_k^\pm(\lambda)e^{-iq_k\sqrt{\lambda}x}, \quad x \in I_k, 0 \leq k \leq n \\ &= \begin{bmatrix} e^{iq_k\sqrt{\lambda}x} & e^{-iq_k\sqrt{\lambda}x} \end{bmatrix} \begin{bmatrix} a_k^\pm(\lambda) \\ b_k^\pm(\lambda) \end{bmatrix} \\ &= \begin{bmatrix} e^{iq_k\sqrt{\lambda}x} & e^{-iq_k\sqrt{\lambda}x} \end{bmatrix} C_{:,k+1}^\pm(\lambda).\end{aligned}\tag{4.2.20}$$

We end this section by stating the following result. As a consequence of the computability of the connection coefficients a_k^\pm and b_k^\pm via (4.2.13) and (4.2.14), we can prove uniform boundedness of Φ in $\mathbb{R}^+ \times \mathbb{R}$.

Lemma 4.2.6. *Let $\Phi = (\Phi^+, \Phi^-)$ be defined as in Theorem 4.2.2. Then Φ is uniformly bounded on $\mathbb{R}^+ \times \mathbb{R}$.*

Proof. It is clear from the definition of Φ that for $0 \leq k \leq n$ and $(\lambda, x) \in \mathbb{R}^+ \times I_k$,

$$|\Phi^\pm(\lambda, x)| \leq |a_k^\pm(\lambda)| + |b_k^\pm(\lambda)| = \left\| \begin{bmatrix} a_k^+(\lambda) & b_k^+(\lambda) \end{bmatrix}^T \right\|_1.$$

Define $\|\cdot\|_1$ to be the matrix norm subordinate to the vector norm $\|\cdot\|_1$. From (4.2.13) and (4.2.14), we have that for $(\lambda, x) \in \mathbb{R}^+ \times \mathbb{R}$,

$$\begin{aligned}|\Phi^+(\lambda, x)| &\leq \max_{0 \leq k \leq n} \left\| \begin{bmatrix} a_k^+(\lambda) & b_k^+(\lambda) \end{bmatrix}^T \right\|_1 \leq \max \left\{ \max_{1 \leq k \leq n} \|R_k R_{k-1} \cdots R_n\|_1, 1 \right\} \\ |\Phi^-(\lambda, x)| &\leq \max_{0 \leq k \leq n} \left\| \begin{bmatrix} a_k^-(\lambda) & b_k^-(\lambda) \end{bmatrix}^T \right\|_1 \leq \max \left\{ 1, \max_{1 \leq k \leq n} \|L_k L_{k-1} \cdots L_1\|_1 \right\}.\end{aligned}$$

Since $\|\cdot\|_1$ is submultiplicative, i.e., $\|AB\|_1 \leq \|A\|_1 \|B\|_1$ for $A, B \in \mathbb{C}^{2 \times 2}$, we obtain

$$\begin{aligned}|\Phi^+(\lambda, x)| &\leq \max \left\{ \max_{1 \leq k \leq n} \{ \|R_k\|_1 \|R_{k-1}\|_1 \cdots \|R_n\|_1 \}, 1 \right\} \\ |\Phi^-(\lambda, x)| &\leq \max \left\{ 1, \max_{1 \leq k \leq n} \{ \|L_k\|_1 \|L_{k-1}\|_1 \cdots \|L_1\|_1 \} \right\}.\end{aligned}$$

From (4.2.2) and (4.2.3), we have for $1 \leq k \leq n$ that

$$\begin{aligned}\|L_k\|_1 &= \frac{1}{2} \left(\left| 1 + \frac{q_k}{q_{k-1}} \right| + \left| 1 - \frac{q_k}{q_{k-1}} \right| \right) \leq 1 + \frac{q_k}{q_{k-1}} \\ \|R_k\|_1 &= \frac{1}{2} \left(\left| 1 + \frac{q_{k-1}}{q_k} \right| + \left| 1 - \frac{q_{k-1}}{q_k} \right| \right) \leq 1 + \frac{q_{k-1}}{q_k}.\end{aligned}$$

Finally, since both upper bounds above are always at least one, we conclude that for every $(\lambda, x) \in \mathbb{R}^+ \times \mathbb{R}$,

$$|\Phi^\pm(\lambda, x)| \leq \max \left\{ \prod_{k=1}^n \left(1 + \frac{q_{k-1}}{q_k} \right), \prod_{k=1}^n \left(1 + \frac{q_k}{q_{k-1}} \right) \right\},$$

proving uniform boundedness of Φ on $\mathbb{R}^+ \times \mathbb{R}$. \square

4.3. Wronskian determinants, resolvents and spectral matrix measure

We establish a number of identities on the connection coefficients $a_k^\pm(z)$ and $b_k^\pm(z)$ of $\Phi(z, \cdot) = (\Phi^+(z, \cdot), \Phi^-(z, \cdot))$ for $z \in \mathbb{C} \setminus (-\infty, 0]$. This is done by evaluating at each interval I_k the Wronskian determinant of pairs of solutions of $(\tau_p - z)f = 0$ derived from $\Phi(z, \cdot)$. Since the Wronskian determinant of solutions of $(\tau_p - z)f = 0$ is independent of x by Remark 2.2.1, all Wronskian determinants evaluated on the local intervals I_k are equal. We then use some of these identities on the resolvent kernels $r_z(x, y)$ to extract from (2.2.9) the matrices $m^\pm(z)$, which in turn yields the spectral matrix measure μ via Theorem 2.2.9 (Weyl-Titchmarsh-Kodaira formula) via limiting procedure.

We start with the identities arising from independence of the Wronskian determinant on x .

Lemma 4.3.1. *Let $n \in \mathbb{N}$ and $a_k^\pm, b_k^\pm, 0 \leq k \leq n$ be defined as in (4.2.13) and (4.2.14). Then the following identities hold.*

(i) *If $z \in \mathbb{C} \setminus (-\infty, 0]$, then*

$$\begin{aligned} \frac{a_0^+(z)}{q_0} &= \frac{1}{q_1} (a_1^+(z)b_1^-(z) - a_1^-(z)b_1^+(z)) = \dots \\ &= \frac{1}{q_{n-1}} (a_{n-1}^+(z)b_{n-1}^-(z) - a_{n-1}^-(z)b_{n-1}^+(z)) = \frac{b_n^-(z)}{q_n}. \end{aligned} \quad (4.3.1)$$

(ii) *If $\lambda \in (0, \infty)$, then for all $0 \leq k \leq n$,*

$$|b_k^-(\lambda)|^2 - |a_k^-(\lambda)|^2 = \frac{q_k}{q_0} \quad (4.3.2)$$

$$|a_k^+(\lambda)|^2 - |b_k^+(\lambda)|^2 = \frac{q_k}{q_n}. \quad (4.3.3)$$

Consequently,

$$\frac{|a_k^+(\lambda)|^2}{q_0} + \frac{|a_k^-(\lambda)|^2}{q_n} = \frac{|b_k^+(\lambda)|^2}{q_0} + \frac{|b_k^-(\lambda)|^2}{q_n}. \quad (4.3.4)$$

(iii) *If $\lambda \in (0, \infty)$, then*

$$\begin{aligned} \frac{b_0^+(\lambda)}{q_0} &= \frac{1}{q_1} (b_1^+(\lambda)\overline{b_1^-(\lambda)} - a_1^+(\lambda)\overline{a_1^-(\lambda)}) = \dots \\ &= \frac{1}{q_{n-1}} (b_{n-1}^+(\lambda)\overline{b_{n-1}^-(\lambda)} - a_{n-1}^+(\lambda)\overline{a_{n-1}^-(\lambda)}) = -\frac{\overline{a_n^-(\lambda)}}{q_n}. \end{aligned} \quad (4.3.5)$$

Proof. We prove the three statements by evaluating the Wronskian determinant of pairs of solutions derived from $\Phi = (\Phi^+, \Phi^-)$ of Theorem 4.2.2 on each subinterval I_k . Equalities are then established by the constancy of the Wronskian determinant in x .

4. The space $PW_\Lambda(A_p)$ with piecewise constant p

(i) Let $z \in \mathbb{C} \setminus (-\infty, 0]$. Then for $x \in I_k, 0 \leq k \leq n$,

$$\begin{aligned} W(\Phi^+(z, x), \Phi^-(z, x)) &= W\left(a_k^+(z)e^{iq_k\sqrt{z}x} + b_k^+(z)e^{-iq_k\sqrt{z}x}, a_k^-(z)e^{iq_k\sqrt{z}x} + b_k^-(z)e^{-iq_k\sqrt{z}x}\right) \\ &= a_k^+(z)b_k^-(z)W\left(e^{iq_k\sqrt{z}x}, e^{-iq_k\sqrt{z}x}\right) + b_k^+(z)a_k^-(z)W\left(e^{-iq_k\sqrt{z}x}, e^{iq_k\sqrt{z}x}\right) \\ &= -\frac{2i\sqrt{z}}{q_k}\left(a_k^+(z)b_k^-(z) - a_k^-(z)b_k^+(z)\right). \end{aligned} \quad (4.3.6)$$

On the unbounded intervals I_0 and I_n , (4.3.6) reduces to

$$W(\Phi^+(z, x), \Phi^-(z, x)) = -\frac{2i\sqrt{z}}{q_0}a_0^+(z) \quad (k=0 : a_0^-(z) = 0, b_0^-(z) = 1) \quad (4.3.7)$$

$$W(\Phi^+(z, x), \Phi^-(z, x)) = -\frac{2i\sqrt{z}}{q_n}b_n^-(z) \quad (k=n : a_n^+(z) = 1, b_n^+(z) = 0). \quad (4.3.8)$$

Equating (4.3.6), (4.3.7) and (4.3.8) yields (4.3.1) for all $z \in \mathbb{C} \setminus (-\infty, 0]$.

(ii) Let $\lambda \in (0, \infty)$. We can infer from p being real-valued that $(\Phi^+(\lambda, \cdot), \overline{\Phi^+(\lambda, \cdot)})$ and $(\Phi^-(\lambda, \cdot), \overline{\Phi^-(\lambda, \cdot)})$ are pairs of solutions of $(\tau_p - \lambda)f = 0$. For $x \in I_k, 0 \leq k \leq n$ and doing a similar computation as in the previous case,

$$\begin{aligned} W(\Phi^\pm(\lambda, x), \overline{\Phi^\pm(\lambda, x)}) &= W\left(a_k^\pm(\lambda)e^{iq_k\sqrt{\lambda}x} + b_k^\pm(\lambda)e^{-iq_k\sqrt{\lambda}x}, \overline{a_k^\pm(\lambda)}e^{-iq_k\sqrt{\lambda}x} + \overline{b_k^\pm(\lambda)}e^{iq_k\sqrt{\lambda}x}\right) \\ &= |a_k^\pm(\lambda)|^2W(e^{iq_k\sqrt{\lambda}x}, e^{-iq_k\sqrt{\lambda}x}) + |b_k^\pm(\lambda)|^2W(e^{-iq_k\sqrt{\lambda}x}, e^{iq_k\sqrt{\lambda}x}) \\ &= \frac{2i\sqrt{\lambda}}{q_k}\left(|b_k^\pm(\lambda)|^2 - |a_k^\pm(\lambda)|^2\right). \end{aligned}$$

Hence, using the initial conditions $a_n^+(\lambda) = b_0^-(\lambda) = 1, a_0^-(\lambda) = b_n^+(\lambda) = 0$, we obtain for $a_k^-(\lambda)$ and $b_k^-(\lambda)$ the equations

$$\begin{aligned} 0 \neq \frac{2i\sqrt{\lambda}}{q_0} &= \frac{2i\sqrt{\lambda}}{q_1}\left(|b_1^-(\lambda)|^2 - |a_1^-(\lambda)|^2\right) = \dots \\ &= \frac{2i\sqrt{\lambda}}{q_k}\left(|b_k^-(\lambda)|^2 - |a_k^-(\lambda)|^2\right) = \dots = \frac{2i\sqrt{\lambda}}{q_n}\left(|b_n^-(\lambda)|^2 - |a_n^-(\lambda)|^2\right), \end{aligned}$$

while for $a_k^+(\lambda)$ and $b_k^+(\lambda)$, we have

$$\begin{aligned} 0 \neq -\frac{2i\sqrt{\lambda}}{q_n} &= \frac{2i\sqrt{\lambda}}{q_{n-1}}\left(|b_{n-1}^+(\lambda)|^2 - |a_{n-1}^+(\lambda)|^2\right) = \dots \\ &= \frac{2i\sqrt{\lambda}}{q_k}\left(|b_k^+(\lambda)|^2 - |a_k^+(\lambda)|^2\right) = \dots = \frac{2i\sqrt{\lambda}}{q_0}\left(|b_0^+(\lambda)|^2 - |a_0^+(\lambda)|^2\right). \end{aligned}$$

The above computations imply (4.3.2) and (4.3.3), respectively. Moreover, solving for q_k yields

$$q_0\left(|b_k^-(\lambda)|^2 - |a_k^-(\lambda)|^2\right) = q_k = q_n\left(|a_k^+(\lambda)|^2 - |b_k^+(\lambda)|^2\right).$$

Dividing both sides by q_0q_n and rearranging the terms give (4.3.4).

(iii) Let $\lambda \in (0, \infty)$. We now consider the pair $(\Phi^+(\lambda, \cdot), \overline{\Phi^-(\lambda, \cdot)})$ of solutions of $(\tau_p - \lambda)f = 0$. Then for $x \in I_k, 0 \leq k \leq n$,

$$\begin{aligned} W(\Phi^+(\lambda, x), \overline{\Phi^-(\lambda, x)}) &= W\left(a_k^+(\lambda)e^{iq_k\sqrt{\lambda}x} + b_k^+(\lambda)e^{-iq_k\sqrt{\lambda}x}, \overline{a_k^-(\lambda)}e^{-iq_k\sqrt{\lambda}x} + \overline{b_k^-(\lambda)}e^{iq_k\sqrt{\lambda}x}\right) \\ &= a_k^+(\lambda)\overline{a_k^-(\lambda)}W(e^{iq_k\sqrt{\lambda}x}, e^{-iq_k\sqrt{\lambda}x}) + b_k^+(\lambda)\overline{b_k^-(\lambda)}W(e^{-iq_k\sqrt{\lambda}x}, e^{iq_k\sqrt{\lambda}x}) \\ &= \frac{2i\sqrt{\lambda}}{q_k}\left(b_k^+(\lambda)\overline{b_k^-(\lambda)} - a_k^+(\lambda)\overline{a_k^-(\lambda)}\right) \end{aligned}$$

which finally yields the last identity (4.3.5).

□

A shorter proof of (4.3.2) and (4.3.3) is possible using Remark 4.2.3. Let $z \in (0, \infty)$. If $k = 0$, then $a_0^-(z) = 0$, $b_0^-(z) = 1$ and (4.3.2) trivially holds. Now, suppose $1 \leq k \leq n$. By taking the determinant of both sides of (4.2.18) and with $j = k$, we derive

$$|b_k^-(z)|^2 - |a_k^-(z)|^2 = \gamma_k^{-2} \cdots \gamma_1^{-2} = \frac{q_k}{q_0},$$

proving (4.3.2). Identity (4.3.3) is analogously proved from (4.2.19).

An immediate consequence of the previous theorem is that $|a_0^+|$ and $|b_n^-|$ are bounded below on $(0, \infty)$.

Corollary 4.3.2. *Let $n \in \mathbb{N}$ and p an $(n + 1)$ -component piecewise constant function. Suppose $\lambda \in (0, \infty)$ and $\Phi(\lambda, \cdot) = (\Phi^+(\lambda, \cdot), \Phi^-(\lambda, \cdot))$ is defined as in Theorem 4.2.2 with connection coefficients $a_k^\pm(\lambda), b_k^\pm(\lambda), 0 \leq k \leq n$. Then for all $\lambda \in (0, \infty)$,*

$$\frac{|b_0^+(\lambda)|^2}{q_0^2} + \frac{1}{q_0 q_n} = \frac{|a_0^+(\lambda)|^2}{q_0^2} = \frac{|b_n^-(\lambda)|^2}{q_n^2} = \frac{1}{q_0 q_n} + \frac{|a_n^-(\lambda)|^2}{q_n^2}.$$

Proof. Let $\lambda \in (0, \infty)$. Taking the squared moduli of the leftmost and rightmost sides of (4.3.1) gives the innermost equation

$$\frac{|a_0^+(\lambda)|^2}{q_0^2} = \frac{|b_n^-(\lambda)|^2}{q_n^2}.$$

On the other hand, for $k = 0$ and $k = n$, (4.3.4) becomes

$$\frac{|a_0^+(\lambda)|^2}{q_0} = \frac{|b_0^+(\lambda)|^2}{q_0} + \frac{1}{q_n}, \quad (k = 0 : a_0^-(\lambda) = 0, b_0^-(\lambda) = 1), \quad (4.3.9)$$

$$\frac{|b_n^-(\lambda)|^2}{q_n} = \frac{1}{q_0} + \frac{|a_n^-(\lambda)|^2}{q_n}, \quad (k = n : a_n^+(\lambda) = 1, b_n^+(\lambda) = 0). \quad (4.3.10)$$

Multiplying (4.3.9) by $\frac{1}{q_0}$ and (4.3.10) by $\frac{1}{q_n}$ proves the assertion. □

With all the necessary identities in place, we are now ready to derive the spectral transform \mathcal{F}_{A_p} and spectral matrix measure μ of the self-adjoint realization A_p of τ_p with p a piecewise constant function. Recall from Theorem 4.2.2 that for $\text{Im} z > 0$, $\Phi^+(z, \cdot)$ and $\Phi^-(z, \cdot)$ lies right and lies left in $L^2(\mathbb{R})$, respectively, and form a fundamental system of $(\tau_p - z)f = 0$. In the same way, for $\text{Im} z < 0$, $\overline{\Phi^+(\bar{z}, \cdot)}$ and $\overline{\Phi^-(\bar{z}, \cdot)}$ lies right and lies left in $L^2(\mathbb{R})$, respectively, and also form a fundamental system of $(\tau_p - z)f = 0$. Using (2.2.8) and (2.2.9), we can then derive expressions for the resolvent kernel $r_z(x, y)$, $x, y \in \mathbb{R}$ for $\text{Im} z > 0$ and $\text{Im} z < 0$, and the spectral matrix measure μ can be described by a matrix of densities that are computed via Theorem 2.2.9 (Weyl-Titchmarsh-Kodaira formula).

The following theorem is a restatement of Theorem 2.2.6 in the context of piecewise constant parametrizing functions as well as an explicit form of the spectral matrix measure.

4. The space $PW_\Lambda(A_p)$ with piecewise constant p

Theorem 4.3.3. *Let $n \in \mathbb{N}$ and p an $(n+1)$ -component piecewise constant function. Suppose $\Phi = (\Phi^+, \Phi^-)$ is defined as in Theorem 4.2.2 with connection coefficients a_k^\pm, b_k^\pm , $0 \leq k \leq n$. Then the 2×2 positive matrix measure μ given by*

$$d\mu(\lambda) = \frac{1}{4\pi\kappa(\sqrt{\lambda})} \begin{bmatrix} \frac{1}{q_0} & 0 \\ 0 & \frac{1}{q_n} \end{bmatrix} \frac{d\lambda}{\sqrt{\lambda}}, \quad \kappa(\sqrt{\lambda}) = \frac{|a_0^+(\lambda)|^2}{q_0^2} = \frac{|b_n^-(\lambda)|^2}{q_n^2} \geq \frac{1}{q_0 q_n} \quad (4.3.11)$$

yields the spectral transform

$$\mathcal{F}_{A_p} : L^2(\mathbb{R}) \longrightarrow L^2([0, \infty), d\mu), \quad \mathcal{F}_{A_p} f(\lambda) = \int_{\mathbb{R}} f(x) \overline{\Phi(\lambda, x)} dx \quad (4.3.12)$$

which is a spectral representation of A_p . The inverse $\mathcal{F}_{A_p}^{-1}$ takes the form

$$\begin{aligned} \mathcal{F}_{A_p}^{-1} G(x) &= \int_0^\infty G(\lambda) \cdot \Phi(\lambda, x) d\mu(\lambda) \\ &= \frac{1}{4\pi} \int_0^\infty \frac{\frac{1}{q_0} G_1(\lambda) \Phi^+(\lambda, x) + \frac{1}{q_n} G_2(\lambda) \Phi^-(\lambda, x)}{\kappa(\sqrt{\lambda})} \frac{d\lambda}{\sqrt{\lambda}} \end{aligned} \quad (4.3.13)$$

for all $G = (G_1, G_2) \in L^2([0, \infty), d\mu)$.

Proof. The result is an application of Theorem 2.2.6, but as Φ is explicitly given in Theorem 4.2.2, together with Theorem 4.3.1 we can proceed one step further to compute the spectral matrix measure μ . The succeeding calculations closely follow some of the computable examples in [80, Chap. 17] and [82, Sec. 23.2].

Without loss of generality, let $z \in \mathbb{C} \setminus (-\infty, 0]$ such that $\text{Im} z > 0$. By Theorem 4.2.2, $\Phi(z, \cdot) = (\Phi^+(z, \cdot), \Phi^-(z, \cdot))$ is a fundamental system of $(\tau_p - z)f = 0$, where $\Phi^+(z, \cdot)$ lies right and $\Phi^-(z, \cdot)$ lies left in $L^2(\mathbb{R})$, respectively. By (2.2.8) and (4.3.7)

$$\begin{aligned} r_z(x, y) &= \frac{1}{W(\Phi^+(z, \cdot), \Phi^-(z, \cdot))} \begin{cases} \Phi^+(z, x) \Phi^-(z, y), & y \leq x, \\ \Phi^-(z, x) \Phi^+(z, y), & y > x \end{cases} \\ &= \frac{iq_0}{2a_0^+(z)\sqrt{z}} \begin{cases} \Phi^+(z, x) \Phi^-(z, y), & y \leq x, \\ \Phi^-(z, x) \Phi^+(z, y), & y > x. \end{cases} \end{aligned} \quad (4.3.14)$$

On the other hand, since $\text{Im} \bar{z} < 0$, $\overline{\Phi(z, \cdot)} = (\overline{\Phi^+(z, \cdot)}, \overline{\Phi^-(z, \cdot)})$ is a fundamental system of $(\tau_p - \bar{z})f = 0$ where $\overline{\Phi^+(z, \cdot)}$ lies right and $\overline{\Phi^-(z, \cdot)}$ lies left in $L^2(\mathbb{R})$, respectively. Moreover, by (2.2.8) and (4.3.8),

$$\begin{aligned} r_{\bar{z}}(x, y) &= \frac{1}{W(\overline{\Phi^+(z, \cdot)}, \overline{\Phi^-(z, \cdot)})} \begin{cases} \overline{\Phi^+(z, x) \Phi^-(z, y)}, & y \leq x \\ \overline{\Phi^-(z, x) \Phi^+(z, y)}, & y > x \end{cases} \\ &= \frac{-iq_n}{2b_n^-(z)\sqrt{\bar{z}}} \begin{cases} \overline{\Phi^+(z, x) \Phi^-(z, y)}, & y \leq x \\ \overline{\Phi^-(z, x) \Phi^+(z, y)}, & y > x \end{cases} \\ &= \overline{r_z(x, y)}. \end{aligned} \quad (4.3.15)$$

By the piecewise nature of Φ , there are $(n+1)^2$ possible expressions for $r_z(x, y)$ depending on where x and y are located. We choose the unbounded intervals I_0 and I_n in the succeeding computations as the expressions for $\Phi^\pm(z, x)$ are simpler compared to those found in the finite intervals $I_k, 1 \leq k \leq n-1$.

4.3. Wronskian determinants, resolvents and spectral matrix measure

- For $x \in I_0$, we observe that

$$\Phi^+(\bar{z}, x) = a_0^+(\bar{z})e^{iq_0\sqrt{\bar{z}}x} + b_0^+(\bar{z})e^{-iq_0\sqrt{\bar{z}}x}, \quad \Phi^-(\bar{z}, x) = e^{-iq_0\sqrt{\bar{z}}x}.$$

Thus,

$$\overline{\Phi^-(z, x)} = \overline{e^{-iq_0\sqrt{z}}} = e^{iq_0\sqrt{\bar{z}}x} = \frac{1}{a_0^+(\bar{z})}\Phi^+(\bar{z}, x) - \frac{b_0^+(\bar{z})}{a_0^+(\bar{z})}\Phi^-(\bar{z}, x), \quad x \in I_0. \quad (4.3.16)$$

- Similarly, for $x \in I_n$, we get

$$\overline{\Phi^+(z, x)} = e^{-iq_n\sqrt{z}x}, \quad \overline{\Phi^-(z, x)} = \overline{a_n^-(z)}e^{-iq_n\sqrt{\bar{z}}x} + \overline{b_n^-(z)}e^{iq_n\sqrt{\bar{z}}x}$$

and consequently,

$$\Phi^+(z, x) = e^{iq_n\sqrt{z}x} = \frac{1}{\overline{b_n^-(z)}}\overline{\Phi^-(z, x)} - \frac{\overline{a_n^-(z)}}{\overline{b_n^-(z)}}\overline{\Phi^+(z, x)}, \quad x \in I_n. \quad (4.3.17)$$

Therefore, for $\text{Im } z > 0$, substituting (4.3.16) to (4.3.15) and (4.3.17) to (4.3.14) yields

$$r_z(x, y) = \frac{iq_0}{2a_0^+(z)\overline{b_n^-(z)}\sqrt{z}} \left\{ \overline{\Phi^-(z, x)} - \overline{a_n^-(z)} \overline{\Phi^+(z, x)} \right\} \Phi^-(z, y) \quad (4.3.18)$$

for $x \in I_n, y \leq x$ and

$$r_{\bar{z}}(x, y) = \frac{-iq_n}{2a_0^+(\bar{z})\overline{b_n^-(z)}\sqrt{\bar{z}}} \overline{\Phi^+(z, x)} \left\{ \Phi^+(z, y) - b_0^+(\bar{z})\Phi^-(z, y) \right\} \quad (4.3.19)$$

for $x \in I_0, y \leq x$, respectively. Recall that for $\text{Im } z > 0$, the resolvent kernel $r_z(x, y)$ has the expression (2.2.9) which can be written as (we use here $\Phi_1 = \Phi^+, \Phi_2 = \Phi^-$)

$$r_z(x, y) = \sum_{j,l=1}^2 m_{jl}^+(z) \overline{\Phi_j(z, x)} \Phi_l(z, y), \quad y \leq x,$$

$$r_{\bar{z}}(x, y) = \sum_{j,l=1}^2 m_{jl}^+(\bar{z}) \overline{\Phi_j(z, x)} \Phi_l(\bar{z}, y), \quad y \leq x,$$

where each m_{jl}^+ is independent of x and y . One sees from (4.3.18) and (4.3.19) that for $\text{Im } z > 0$, m^+ takes the form

$$m^+(z) = \frac{iq_0}{2a_0^+(z)\overline{b_n^-(z)}\sqrt{z}} \begin{bmatrix} 0 & -\overline{a_n^-(z)} \\ 0 & 1 \end{bmatrix},$$

$$m^+(\bar{z}) = \frac{-iq_n}{2a_0^+(\bar{z})\overline{b_n^-(z)}\sqrt{\bar{z}}} \begin{bmatrix} 1 & -b_0^+(\bar{z}) \\ 0 & 0 \end{bmatrix}.$$

Hence, for $\text{Im } z > 0$,

$$m^+(z) - m^+(\bar{z}) = \begin{bmatrix} \frac{iq_n}{2a_0^+(\bar{z})\overline{b_n^-(z)}\sqrt{\bar{z}}} & \frac{-iq_0\overline{a_n^-(z)}}{2a_0^+(z)\overline{b_n^-(z)}\sqrt{z}} - \frac{iq_nb_0^+(\bar{z})}{2a_0^+(\bar{z})\overline{b_n^-(z)}\sqrt{\bar{z}}} \\ 0 & \frac{iq_0}{2a_0^+(z)\overline{b_n^-(z)}\sqrt{z}} \end{bmatrix}. \quad (4.3.20)$$

4. The space $PW_\Lambda(A_p)$ with piecewise constant p

By Lemma 4.2.4, μ is absolutely continuous with respect to the Lebesgue measure on $[0, \infty)$. Consequently, by Theorem 2.2.9 (Weyl-Titchmarsh-Kodaira), the matrix \mathcal{M} of densities has entries

$$\mathcal{M}_{jl}(\lambda) = \frac{d\mu_{jl}}{d\lambda} = \lim_{\epsilon \downarrow 0} \frac{1}{2\pi i} (m_{jk}^+(\lambda + i\epsilon) - m_{jk}^+(\lambda - i\epsilon)).$$

Applying (4.3.1), (4.3.5) and Corollary 4.3.2 to (4.3.20) with $z = \lambda + i\epsilon$, $\epsilon \downarrow 0$ yields

$$\begin{aligned} \frac{d\mu_{11}}{d\lambda} &= \frac{q_n}{4\pi\sqrt{\lambda}a_0^+(\lambda)\overline{b_n^-(\lambda)}} = \frac{q_0}{4\pi\sqrt{\lambda}|a_0^+(\lambda)|^2}, \\ \frac{d\mu_{22}}{d\lambda} &= \frac{q_0}{4\pi\sqrt{\lambda}a_0^+(\lambda)\overline{b_n^-(\lambda)}} = \frac{q_n}{4\pi\sqrt{\lambda}|b_n^-(\lambda)|^2} = \frac{q_0}{q_n} \frac{d\mu_{11}}{d\lambda}, \\ \frac{d\mu_{12}}{d\lambda} &= 0, \\ \frac{d\mu_{21}}{d\lambda} &= -\frac{q_0q_n \left(\frac{1}{q_n}\overline{a_n^-(\lambda)} + \frac{1}{q_0}b_0^+(\lambda) \right)}{4\pi a_0^+(\lambda)\overline{b_n^-(\lambda)}\sqrt{\lambda}} = 0. \end{aligned}$$

By definition of κ and by Corollary 4.3.2, $\kappa(\sqrt{\lambda}) \geq \frac{1}{q_0q_n} > 0$ for all $\lambda \in (0, \infty)$ and

$$d\mu(\lambda) = \mathcal{M}(\lambda) d\lambda = \frac{1}{4\pi\kappa(\sqrt{\lambda})} \begin{bmatrix} \frac{1}{q_0} & 0 \\ 0 & \frac{1}{q_n} \end{bmatrix} \frac{d\lambda}{\sqrt{\lambda}}.$$

The expression for \mathcal{F}_{A_p} now follows. □

The argument $\sqrt{\lambda}$ of κ in (4.3.11) is intentional as we will be employing the change of variables $\lambda = u^2$ when we go to the actual computations. We also define

$$\Lambda^{1/2} = \{\omega \geq 0 : \omega^2 \in \Lambda\}.$$

With this prescribed substitution, (4.3.11) and (4.3.13) read as

$$d\mu(u^2) = \frac{1}{2\pi\kappa(u)} \begin{bmatrix} \frac{1}{q_0} & 0 \\ 0 & \frac{1}{q_n} \end{bmatrix} du, \quad (4.3.21)$$

$$\mathcal{F}_{A_p}^{-1}G(x) = \frac{1}{2\pi} \int_0^\infty \frac{\frac{1}{q_0}G_1(u^2)\Phi^+(u^2, x) + \frac{1}{q_n}G_2(u^2)\Phi^-(u^2, x)}{\kappa(u)} du. \quad (4.3.22)$$

We see that the entries of $d\mu(u^2)$ are bounded on $(0, \infty)$. In addition, the spectral projection $\chi_\Lambda(A_p) : L^2(\mathbb{R}) \rightarrow PW_\Lambda(A_p)$ can be written as

$$\chi_\Lambda(A_p)f(x) = \frac{1}{2\pi} \int_{\Lambda^{1/2}} \frac{\frac{1}{q_0}F_1(u^2)\Phi^+(u^2, x) + \frac{1}{q_n}F_2(u^2)\Phi^-(u^2, x)}{\kappa(u)} du, \quad (4.3.23)$$

where $F = (F_1, F_2) = \mathcal{F}_{A_p}f$.

Remark 4.3.4. It follows from Lemma 4.2.5 and upon expanding the formula for κ in (4.3.11) that there exist $r \in \mathbb{N}$ (that increases as the number of piecewise components of p increases) and $c_0, \dots, c_r, \lambda_1, \dots, \lambda_r \in \mathbb{R}$ such that

$$\kappa(u) = c_0 + \sum_{j=1}^r c_j \cos(\lambda_j u), \quad u \in (0, \infty).$$

In summary, Theorem 4.3.3 asserts that piecewise constant parametrizing functions yield explicit spectral matrix measures determined by the components $\{p_k\}_{k=0}^n$ of p . However, one clearly sees from (4.2.13) and (4.2.14) that the expression for κ becomes more complicated as n increases. This presents the problem of how integrals involving the spectral measure μ can be calculated. In particular, we wish to know how the reproducing kernel k_Λ of $PW_\Lambda(A_p)$ are computed, at least numerically. We shall deal with this main obstacle in the next section.

4.4. Computing the reproducing kernel

Recall from Definition 3.0.1 that for a spectral set $\Lambda \subset \mathbb{R}_0^+$ of finite measure, the Paley-Wiener space $PW_\Lambda(A_p)$ of variable bandwidth functions with spectral set Λ is the range of the spectral projection $\chi_\Lambda(A_p)$, i.e., the space

$$PW_\Lambda(A_p) = \chi_\Lambda(A_p)(L^2(\mathbb{R}))$$

which consists of functions $f \in L^2(\mathbb{R})$ given by

$$f(x) = \chi_\Lambda(A_p)f(x) = \int_\Lambda \mathcal{F}_{A_p}f(\lambda) \cdot \Phi(\lambda, x) d\mu(\lambda), \quad x \in \mathbb{R}. \quad (4.4.1)$$

Moreover, Proposition 3.1.2 shows that for compact spectral sets, $PW_\Lambda(A_p)$ is a reproducing kernel Hilbert space with reproducing kernel

$$k_\Lambda(x, y) = \int_\Lambda \overline{\Phi(\lambda, x)} \cdot \Phi(\lambda, y) d\mu(\lambda), \quad x, y \in \mathbb{R}. \quad (4.4.2)$$

Theorem 4.2.2 shows that if p is a piecewise constant function, explicit forms of the fundamental solutions $\Phi(z, \cdot) = (\Phi^+(z, \cdot), \Phi^-(z, \cdot))$ of $(\tau_p - z)f = 0$, $z \in \mathbb{C} \setminus (-\infty, 0]$ can be derived. Consequently, in Theorem 4.3.3 these expressions were used to directly compute both the spectral representation \mathcal{F}_{A_p} of the self-adjoint realization A_p of τ_p and the 2×2 positive matrix measure μ as stated in Theorem 4.3.3. Putting all these facts together, we now have the following result (cf. Proposition 3.1.2 and its proof in [39, Prop. 3.3]).

Theorem 4.4.1. *Let $n \in \mathbb{N}$ and $\Lambda \subset \mathbb{R}_0^+$ be of finite measure. Suppose p is an $(n+1)$ -component piecewise constant function. Then $PW_\Lambda(A_p)$ is a closed subspace of $L^2(\mathbb{R})$ whose elements are continuous. Moreover, if $\Phi = (\Phi^+, \Phi^-)$ is defined as in Theorem 4.2.2 with connection coefficients a_j^\pm, b_j^\pm , $0 \leq j \leq n$ and κ is given by (4.3.11), then $PW_\Lambda(A_p)$ is a reproducing kernel Hilbert space with kernel*

$$k_\Lambda(x, y) = \frac{1}{4\pi} \int_\Lambda \left(\frac{q_0 \overline{\Phi^+(\lambda, x)} \Phi^+(\lambda, y)}{|a_0^+(\lambda)|^2} + \frac{q_n \overline{\Phi^-(\lambda, x)} \Phi^-(\lambda, y)}{|b_n^-(\lambda)|^2} \right) \frac{d\lambda}{\sqrt{\lambda}} \quad (4.4.3)$$

$$= \frac{1}{2\pi} \int_{\Lambda^{1/2}} \frac{\frac{1}{q_0} \cdot \overline{\Phi^+(u^2, x)} \Phi^+(u^2, y) + \frac{1}{q_n} \cdot \overline{\Phi^-(u^2, x)} \Phi^-(u^2, y)}{\kappa(u)} du, \quad (4.4.4)$$

for every $x, y \in \mathbb{R}$.

4. The space $PW_\Lambda(A_p)$ with piecewise constant p

Proof. We first claim that the set $\{\|\Phi(\cdot, x)\|_{L^2(\Lambda, d\mu)}\}_{x \in \mathbb{R}}$ is bounded. Indeed, Theorem 4.3.3 implies that for all $x \in \mathbb{R}$,

$$\begin{aligned} \|\Phi(\cdot, x)\|_{L^2(\Lambda, d\mu)} &= \left\{ \frac{1}{2\pi} \int_{\Lambda^{1/2}} \frac{\frac{1}{q_0} |\Phi^+(u^2, x)|^2 + \frac{1}{q_n} |\Phi^-(u^2, x)|^2}{\kappa(u)} du \right\}^{1/2} \\ &\leq \operatorname{ess\,sup}_{u \in \Lambda^{1/2}} |\Phi^\pm(u^2, x)| \left\{ \frac{1}{2\pi} \int_{\Lambda^{1/2}} \frac{q_0 + q_n}{q_0 q_n \kappa(u)} du \right\}^{1/2}. \end{aligned}$$

By (4.3.11), $\kappa(u) \geq \frac{1}{q_0 q_n}$ for $u \in (0, \infty)$, so that

$$\|\Phi(\cdot, x)\|_{L^2(\Lambda, d\mu)} \leq \operatorname{ess\,sup}_{u \in \Lambda^{1/2}} |\Phi^\pm(u^2, x)| \left(\frac{q_0 + q_n}{2\pi} \right)^{1/2} |\Lambda^{1/2}|^{1/2}.$$

Thus, by Lemma 4.2.6 and by assumption, there exists $C > 0$ such that $\|\Phi(\cdot, x)\|_{L^2(\Lambda, d\mu)} \leq C$ for all $x \in \mathbb{R}$.

We now prove the first assertion. Observe that

- for all $x \in \mathbb{R}$, $\mathcal{F}_{A_p} f(\cdot) \cdot \Phi(\cdot, x) \in L^1(\Lambda, d\mu)$ by Cauchy-Schwartz inequality and the claim,
- for almost every $\lambda \in \Lambda$, $\mathcal{F}_{A_p} f(\lambda) \cdot \Phi(\lambda, \cdot)$ is continuous on \mathbb{R} by Theorem 4.2.2, and
- for all $x \in \mathbb{R}$, $|\mathcal{F}_{A_p} f(\cdot) \cdot \Phi(\cdot, x)| \leq C' |\mathcal{F}_{A_p} f| \in L^1(\Lambda, d\mu)$ for some $C' > 0$ by Lemma 4.2.6.

By a standard result on continuity of parameter integrals (see e.g. [25, Thm. 14.3.1] and [29, Thm. 5.6]), we conclude that functions $f \in PW_\Lambda(A_p)$ defined in (4.4.1) are continuous. That $PW_\Lambda(A_p)$ is closed also follows from (4.4.1) and the unitarity of \mathcal{F}_{A_p} . To prove the second assertion, let $x \in \mathbb{R}$. By the claim and by unitarity of \mathcal{F}_{A_p} ,

$$|f(x)| \leq \|\Phi(\cdot, x)\|_{L^2(\Lambda, d\mu)} \|\mathcal{F}_{A_p} f\|_{L^2(\Lambda, d\mu)} = \|\Phi(\cdot, x)\|_{L^2(\Lambda, d\mu)} \|f\|_2 \leq C \|f\|_2$$

for all $f \in PW_\Lambda(A_p)$. Hence, for every $x \in \mathbb{R}$, the evaluation map $f \mapsto f(x)$ for $f \in PW_\Lambda(A_p)$ is continuous. By Theorem 3.1.1, $PW_\Lambda(A_p)$ is a reproducing kernel Hilbert space. The formula for the reproducing kernel k_Λ is exactly (4.4.2) and is derived as follows (see [28, Thm. XIII.5.24]). Let $f \in PW_\Lambda(A_p)$. Then for $x \in \mathbb{R}$,

$$\begin{aligned} f(x) &= (\chi_\Lambda(A_p) f)(x) = \int_\Lambda \mathcal{F}_{A_p} f(\lambda) \cdot \Phi(\lambda, x) d\mu(\lambda) \\ &= \int_\Lambda \int_{\mathbb{R}} f(y) \overline{\Phi(\lambda, y)} \cdot \Phi(\lambda, x) dy d\mu(\lambda) \\ &= \int_{\mathbb{R}} f(y) \int_\Lambda \overline{\Phi(\lambda, y)} \cdot \Phi(\lambda, x) d\mu(\lambda) dy \\ &= \int_{\mathbb{R}} f(y) \overline{k_\Lambda(x, y)} dy. \end{aligned}$$

The interchange of integrals is justified by Fubini-Tonelli Theorem (see e.g. [15, Thm. 18.3] and [26, Thms. 14.1, 14.2]). Formulas (4.4.3) and (4.4.4) now follow from the computable expressions of the spectral matrix measure (4.3.11) and (4.3.21), respectively. \square

What we have above is a description of $PW_\Lambda(A_p)$ with piecewise constant p as a reproducing kernel Hilbert space with kernel k_Λ . Constructing $PW_\Lambda(A_p)$ from k_Λ can also be done via the Moore-Aronszajn Theorem [8, Thm. 3]: $PW_\Lambda(A_p)$ is the completion of the pre-Hilbert space

$$\mathcal{H}_0 = \text{span}\{k_\Lambda(x, \cdot) : x \in \mathbb{R}\}$$

with inner product

$$\langle f, g \rangle_{\mathcal{H}_0} = \sum_{l=1}^r \sum_{j=1}^m \alpha_l \overline{\beta_j} k_\Lambda(y_l, x_j),$$

where $f = \sum_{l=1}^r \alpha_l k_\Lambda(y_l, \cdot)$, $g = \sum_{j=1}^m \beta_j k_\Lambda(x_j, \cdot) \in \mathcal{H}_0$.

In Chapter 7, our numerical reconstruction method is based on approximating a function by elements of finite-dimensional subspaces of $PW_\Lambda(A_p)$ spanned by $k_\Lambda(x_j, \cdot)$ with finitely many j . Hence, we can translate the reconstruction procedure into a linear algebra problem that can be implemented in MATLAB.

4.4.1. Strategy for computing $k_\Lambda(x, y)$ numerically

The computability of the reproducing kernel k_Λ at any point translates to feasibility of numerical reconstruction methods in variable bandwidth spaces. We now explore how to numerically evaluate $k_\Lambda(x, y)$ for any $x, y \in \mathbb{R}$. Algorithm 1 shows that we can compute the connection coefficients a_k^\pm, b_k^\pm as well as the local solutions

$$\Phi^\pm(u^2, x) = a_k^\pm(u^2) e^{iq_k u x} + b_k^\pm(u^2) e^{-iq_k u x},$$

where $u > 0$, $x \in I_k$, and $q_k = p_k^{-1/2}$, $0 \leq k \leq n$. For convenience, we adopt the notation

$$\vartheta(u, x, y) = \frac{1}{q_0} \overline{\Phi^+(u^2, x)} \Phi^+(u^2, y) + \frac{1}{q_n} \overline{\Phi^-(u^2, x)} \Phi^-(u^2, y), \quad (4.4.5)$$

so that (4.4.4) can be compactly written as

$$k_\Lambda(x, y) = \frac{1}{2\pi} \int_{\Lambda^{1/2}} \frac{\vartheta(u, x, y)}{\kappa(u)} du, \quad x, y \in \mathbb{R}. \quad (4.4.6)$$

By expanding ϑ , we can try possible methods to calculate the reproducing kernel. Fix $x, y \in \mathbb{R}$. By Lemma 4.2.5, there exist a positive integer $m(x, y)$ and real numbers $\alpha_k(x, y), \beta_k(x, y)$, $1 \leq k \leq m(x, y)$ such that

$$\vartheta(u, x, y) = \sum_{k=1}^{m(x, y)} \alpha_k(x, y) e^{i\beta_k(x, y)u}. \quad (4.4.7)$$

Remark 4.4.2. By looking at the matrices (4.2.2) and (4.2.3) as well as the iterative expressions (4.2.13) and (4.2.14), the nonzero coefficients $\alpha_k(x, y)$, $x \in I_j$, $y \in I_l$ for $0 \leq j, l \leq n$ are obtained by taking products of some of the expressions

$$\frac{1}{q_0}, \frac{1}{q_n}, 1 \pm \frac{q_r}{q_{r-1}}, 1 \pm \frac{q_{s+1}}{q_s}, \quad 1 \leq r \leq j \text{ and } l \leq s \leq n-1.$$

4. The space $PW_\Lambda(A_p)$ with piecewise constant p

For out-of-range index values, i.e., $j = 0$ or $l = n$, we take 1 as the factor. We see here that each $\alpha_k(x, y)$ does not directly depend on the values of x and y , but rather on the intervals I_j and I_l in which x and y are located. Hence, for $0 \leq j, l \leq n$ fixed, the coefficients $\alpha_k(x, y), x \in I_j, y \in I_l$ are merely constants. Similarly, if algebraic simplifications are skipped, we have for $0 \leq j, l \leq n$ fixed that $m(x, y), x \in I_j, y \in I_l$ is also a fixed natural number. In contrast, the exponents $\beta_k(x, y), x \in I_j, y \in I_l$ are of the form

$$c_k \pm q_j x \pm q_l y, \quad (4.4.8)$$

where the scalars $c_k \in \mathbb{R}$ are dependent on $\{t_r\}_{r=1}^n$ and $\{q_r\}_{r=0}^n$. Such statements are best illustrated by examples in Chapter 5 where we derive computable formulas for the reproducing kernel when $n = 1$ and $n = 2$.

Meanwhile, since κ is bounded below on $(0, \infty)$ and Λ has finite Lebesgue measure, the integral

$$J(s) = \frac{1}{2\pi} \int_{\Lambda^{1/2}} \frac{e^{isu}}{\kappa(u)} du, \quad s \in \mathbb{R} \quad (4.4.9)$$

is well-defined. By (4.4.6) and (4.4.7), we can write the reproducing kernel k_Λ as

$$\begin{aligned} k_\Lambda(x, y) &= \frac{1}{2\pi} \sum_{k=1}^{m(x,y)} \alpha_k(x, y) \int_{\Lambda^{1/2}} \frac{e^{i\beta_k(x,y)u}}{\kappa(u)} du \\ &= \sum_{k=1}^{m(x,y)} \alpha_k(x, y) J(\beta_k(x, y)). \end{aligned} \quad (4.4.10)$$

Thus, an important step in the numerical evaluation of the reproducing kernel is the numerical evaluation of J . Ideally, we want an explicit formula for J . However, the potentially complicated form of κ as mentioned in Remark 4.3.4 renders J difficult to calculate using standard techniques of integration. Assuming we have a separate routine to calculate $J(s)$ for any $s \in \mathbb{R}$, we have in Algorithm 2 a pseudocode that computes $k_\Lambda(x, y)$ for any $x, y \in \mathbb{R}$.

We now investigate the integral J . First, we observe some of its basic properties.

Lemma 4.4.3. *Let $\Lambda \subset \mathbb{R}_0^+$ be of finite measure and define*

$$J(s) = \frac{1}{2\pi} \int_{\Lambda^{1/2}} \frac{e^{isu}}{\kappa(u)} du, \quad s \in \mathbb{R}.$$

Then the following hold.

- (i) $J(-s) = \overline{J(s)}$ for all $s \in \mathbb{R}$.
- (ii) $\text{supp } \mathcal{F}J = \overline{\Lambda^{1/2}}$.
- (iii) If Λ is a compact interval, then there exists $M > 0$ such that $|J(s)| \leq M|s|^{-1}$ for all $s \neq 0$.

Proof. Let $\Lambda \subset \mathbb{R}_0^+$ be of finite measure.

Algorithm 2 Calculating $k_\Lambda(x, y)$ for any $x, y \in \mathbb{R}$.

Input: Components $p = [p_0 \ p_1 \ \cdots \ p_n]$ and knots $t = [t_1 \ t_2 \ \cdots \ t_n]$
 Spectral set $\Lambda \subset \mathbb{R}_0^+$ and points $x, y \in \mathbb{R}$

Output: Evaluation $k_\Lambda(x, y)$

- 1: **function** VBREPKER(t, p, Λ, x, y)
 - 2: Assign $n = \text{length}(t)$.
 - 3: Set $q_k = p_k^{-1/2}$, $0 \leq k \leq n$.
 - 4: Let $0 \leq j, l \leq n$ such that $(x, y) \in I_j \times I_l$.
 - 5: Compute $[C^+(u^2) \ C^-(u^2)] = \text{CONNCOEFF}(t, p)$. ▷ Algorithm 1
 - 6: Compute $\kappa(u) = \frac{|a_0^+(u^2)|^2}{q_0^2} = \frac{|C_{1,1}^+(u^2)|^2}{q_0^2}$. ▷ Formula (4.3.11)
 - 7: Calculate $\Phi^+(u^2, x) = [e^{iq_j ux} \ e^{-iq_j ux}] C_{:,j+1}^+(u^2)$. ▷ Using (4.2.20)
 - 8: Calculate $\Phi^-(u^2, y) = [e^{iq_l uy} \ e^{-iq_l uy}] C_{:,l+1}^-(u^2)$. ▷ Using (4.2.20)
 - 9: Evaluate $\vartheta(u, x, y) = \frac{1}{q_0} \overline{\Phi^+(u^2, x)} \Phi^+(u^2, y) + \frac{1}{q_n} \overline{\Phi^-(u^2, x)} \Phi^-(u^2, y)$.
 - 10: Write $\vartheta(u, x, y)$ as $\sum_{k=1}^m \alpha_k e^{i\beta_k u}$ for some positive integer $m = m(x, y)$ and real constants $\alpha_k = \alpha_k(x, y)$, $\beta_k = \beta_k(x, y)$. ▷ As in (4.4.7)
 - 11: Extract the coefficient-exponent pairs $[\alpha_k \ \beta_k]_{k=1}^m \in \mathbb{C}^{m \times 2}$.
 - 12: Compute $k_\Lambda(x, y) = \frac{1}{2\pi} \sum_{k=1}^m \alpha_k \int_{\Lambda^{1/2}} \frac{e^{i\beta_k u}}{\kappa(u)} du = \sum_{k=1}^m \alpha_k J(\beta_k)$ ▷ As in (4.4.10).
 - 13: **return** $k_\Lambda(x, y)$
 - 14: **end function**
-

(i) This follows from the property of integration of functions of a real variable.

(ii) By definition, $J = \mathcal{F}^{-1}(\chi_{\Lambda^{1/2}} \cdot \frac{1}{\kappa})$, which means $\text{supp } \mathcal{F}J = \overline{\Lambda^{1/2}}$.

(iii) Without loss of generality, assume $\Lambda = [0, \Omega]$ for some $\Omega > 0$. By Remark 4.3.4, κ is (infinitely) differentiable on $(0, \infty)$ with bounded derivatives and $0 < \frac{1}{\kappa(u)} \leq q_0 q_n$ for all $u \in (0, \infty)$. Consequently, integration by parts yields

$$J(s) = \frac{1}{2\pi i s} \left(\frac{e^{is\Omega^{1/2}}}{\kappa(\Omega^{1/2})} - \frac{1}{\kappa(0^+)} \right) + \frac{1}{2\pi i s} \int_0^{\Omega^{1/2}} \frac{\kappa'(u)}{(\kappa(u))^2} e^{isu} \quad (4.4.11)$$

$$|J(s)| \leq \frac{1}{2\pi |s|} \left\{ \frac{1}{|\kappa(\Omega^{1/2})|} + \frac{1}{|\kappa(0^+)|} + \int_0^{\Omega^{1/2}} \frac{|\kappa'(u)|}{(\kappa(u))^2} du \right\},$$

where $\kappa(0^+) = \lim_{u \downarrow 0} \kappa(u)$. Therefore, for all $s \neq 0$,

$$|J(s)| \leq \frac{q_0 q_n}{2\pi |s|} \left(2 + q_0 q_n \Omega^{1/2} \text{ess sup}_{0 \leq u \leq \Omega^{1/2}} |\kappa'(u)| \right).$$

□

If explicit formulas for J are not available, we settle for approximations of $J(s)$ with satisfactory error bounds for any $s \in \mathbb{R}$. Such an approximation can potentially be derived

4. The space $PW_\Lambda(A_p)$ with piecewise constant p

by applying integration by parts several times to (4.4.11). Let $g = \frac{1}{\kappa}$. Then for $m \in \mathbb{N}$ and $s \neq 0$,

$$J(s) = \frac{1}{2\pi} \sum_{k=0}^{m-1} \frac{(-1)^k}{(is)^k} (g^{(k)}(\Omega^{1/2})e^{isu} - g^{(k)}(0^+)) + \frac{(-1)^m}{2\pi(is)^m} \int_0^{\Omega^{1/2}} g^{(m)}(u)e^{isu} du.$$

Assuming we have access to derivatives

$$g^{(k)}(0^+) = \lim_{u \downarrow 0} g^{(k)}(u) \text{ and } g^{(k)}(\Omega^{1/2}), \quad k = 0, \dots, m-1,$$

define the m^{th} approximation J_m of J as

$$J_m(s) = \frac{1}{2\pi} \sum_{k=0}^{m-1} \frac{(-1)^k}{(is)^k} (g^{(k)}(\Omega^{1/2})e^{isu} - g^{(k)}(0^+)).$$

Then the error $E_m(s)$, $s \neq 0$ is computed as

$$E_m(s) = |J(s) - J_m(s)| \leq \frac{1}{2\pi|s|^m} \int_0^{\Omega^{1/2}} g^{(m)}(u)e^{isu} du \leq \frac{\Omega^{1/2}}{2\pi|s|^m} \operatorname{ess\,sup}_{0 \leq u \leq \Omega^{1/2}} |g^{(m)}(u)| < \infty.$$

Clearly, the accuracy of the proposed approximation improves as we take larger $|s|$ and use higher order derivatives. However, for small to moderate values of s , the errors may be large. Alternatively, we can evaluate $J(s)$ for any $s \in \mathbb{R}$ using efficient quadrature methods for oscillatory integrals, i.e., integrals of the form

$$\int_a^b f(u)e^{isg(u)} du,$$

where $-\infty < a < b < \infty$, both f (the amplitude function) and g (the phase function; $e^{isg(u)}$ is the oscillatory term) are sufficiently smooth functions, and $s \in \mathbb{R}$. Several methods and software packages are available for such computations. We list the basic ones below. We refer the reader to [30, 46, 47, 54, 55] for an introductory study of numerical quadratures on evaluating oscillatory integrals.

- MATLAB's `integral` (essentially the same as `quadgk`) command uses high-order adaptive quadrature and can handle small to moderate values of $|s|$, but fails to correctly approximate $J(s)$ for large $|s|$.
- The Filon quadrature [30, 46, 48] is a numerical integration method specifically designed to calculate highly oscillatory integrals, i.e., when $|s|$ is large. We approximate $\frac{1}{\kappa}$ by an interpolating polynomial P_F of degree at most $m-1$ using interpolation nodes $c_1, \dots, c_m \in [a, b]$ and compute

$$Q_F(s) = \frac{1}{2\pi} \int_a^b P_F(u)e^{isu} du.$$

This only requires computing the moments

$$\int_a^b x^j e^{isu} du, \quad j = 0, \dots, \deg P_F.$$

A complete error analysis of the Filon method for the non-oscillatory, mildly oscillatory, and highly oscillatory cases can be found in [47, Sec. 3].

- Mathematica's `NIntegrate`⁹ command uses the `OscillatorySelection` preprocessor to select the most appropriate method to evaluate highly oscillatory integrals. For small to moderate values of $|s|$, `NIntegrate` can evaluate $J(s)$ with ease. For large $|s|$, it uses the `LevinRule` that is based on the Levin collocation method [54, 85]. Let $s \in \mathbb{R}$. The idea is if there exists a function ϕ such that

$$\phi'(u) + is\phi(u) = \frac{1}{\kappa(u)}, \quad a \leq u \leq b,$$

then with $\Lambda = [a, b] \subset \mathbb{R}_0^+$,

$$J(s) = \frac{1}{2\pi} \int_a^b (\phi'(u) + is\phi(u))e^{isu} du = \frac{1}{2\pi}(\phi(b)e^{isb} - \phi(a)e^{isa}).$$

Instead of finding such ϕ , we choose interpolation nodes $c_1, \dots, c_m \in [a, b]$ for some $m \in \mathbb{N}$ to find an interpolating polynomial P_L of degree at most $m-1$ which satisfies

$$P'_L(c_j) + isP_L(c_j) = \frac{1}{\kappa(c_j)}, \quad j = 1, \dots, m.$$

Then the quantity

$$Q_L(s) = \frac{1}{2\pi} \int_a^b (P'_L(u) + isP_L(u))e^{isu} du = \frac{1}{2\pi}(P_L(b)e^{isb} - P_L(a)e^{isa})$$

is an approximation of $J(s)$. In a more general context, it was proved in [55, Thm. 3.1] that the accuracy of the approximation increases as $|s|$ increases. It also follows as a special case of [85, Thms. 2.1, 2.2] that for $s \in \mathbb{R}$ and with the same m interpolating nodes, $Q_L(s) = Q_F(s)$ and with the same error bound

$$E(s) \leq \frac{3(1+m)\|D^m \frac{1}{\kappa}\|_\infty (b-a)^m}{|s|m!}.$$

It should be noted as in [54, 55] that the above quadrature methods for oscillatory integrals are effective when s is large and the amplitude function is not highly oscillatory, which by Remark 4.3.4 may not be true for $\frac{1}{\kappa}$. We can still use these methods by forcing software packages to identify e^{isu} as the only oscillatory term of J . However, if $\frac{1}{\kappa}$ oscillates much faster than $|s|$, then we may get incorrect values. This is because the interpolating polynomials P_F and P_L may fail to capture the true oscillatory behavior of $\frac{1}{\kappa}$. We can interpolate $\frac{1}{\kappa}$ using a preferred class of orthogonal polynomials (e.g. Hermite, Chebyshev, Legendre) and, if necessary, add more or choose special interpolation nodes to improve the approximation at the cost of increased computational effort.

In the next chapter, we investigate the cases $n = 1$ (two-component p) and $n = 2$ (three-component p) where the resulting κ has a simple formula. We show that for $n = 1$, we can find an explicit formula for J , while for $n = 2$, we give a series expansion of $J(s)$ for any $s \in \mathbb{R}$ and whose partial sums converge geometrically to the correct value. These

⁹More information on `NIntegrate` integration rules can be found on Wolfram's web page: <https://reference.wolfram.com/language/tutorial/NIntegrateIntegrationRules.html>.

4. The space $PW_\Lambda(A_p)$ with piecewise constant p

formulas save effort in demonstrating the accuracy of actual numerical computations in Chapter 7 and avoid complications that may arise from using any numerical quadrature for oscillatory integrals. Consequently, for $n = 1$ we have an exact formula for k_Λ and a computable formula for k_Λ for the case $n = 2$. In Appendix B, we will use the theory of residues to investigate the integral J for a rather special case of parameters.

As a final note, we see that the aforementioned numerical quadrature methods may be useful in the case $n > 2$ (p has at least four piecewise components) where there is absolute necessity to perform all symbolic calculations (i.e., computing Φ^\pm , κ and $d\mu$) using a computer. Nonetheless, additional work is needed here to show accuracy of computational results. This case is computationally intensive and is beyond the scope of this thesis.

5. Concrete Examples

A key ingredient in the computation of the reproducing kernel k_Λ of $PW_\Lambda(A_p)$ with an $(n + 1)$ -component piecewise constant p is the evaluation the integral

$$J(s) = \frac{1}{2\pi} \int_{\Lambda^{1/2}} \frac{e^{isu}}{\kappa(u)} du.$$

Remark 4.3.4 pointed out the complexity of the form of κ , hence the difficulty in calculating $J(s)$ for any $s \in \mathbb{R}$. In this chapter, we take a look at the following concrete examples where evaluations of J can be accurately computed. Assume that $\Lambda = [0, \Omega]$ for some $\Omega > 0$.

- When $n = 1$ and p is the function

$$p(x) = \begin{cases} p_0, & x \leq 0, \\ p_1, & x > 0, \end{cases} \quad p_0, p_1 > 0,$$

we show that κ is a constant. Hence, $J(s)$ is a constant multiple of the Fourier transform of $\chi_{\Lambda^{1/2}} = \chi_{[0, \Omega^{1/2}]}$ evaluated at $-s$, and therefore can be expressed in terms of cardinal sine functions. Using the general theory of Chapter 4, we reproduce the result in [39, Sec. 4] where an exact formula for the corresponding k_Λ was derived.

- When $n = 2$ and p is the function

$$p(x) = \begin{cases} p_0, & x \in (-\infty, -\frac{T}{2}], \\ p_1, & x \in (-\frac{T}{2}, \frac{T}{2}], \\ p_2, & x \in (\frac{T}{2}, \infty), \end{cases} \quad p_0, p_1, p_2, T > 0,$$

we prove that $\kappa(s) = C + K \cos \zeta s$, where C, K and ζ are constants determined by p . Using series expansions, we show that

$$J(s) = \frac{1}{2\pi} \int_{\Lambda^{1/2}} \frac{e^{isu}}{C + K \cos \zeta s} du$$

can be written as an infinite series of cardinal sine functions. Moreover, for any $s \in \mathbb{R}$, the corresponding sequence of partial sums evaluated at s converges to $J(s)$ at a geometric rate. We then partially compute the piecewise components of the corresponding k_Λ in terms of J . Note that such a series expansion for J allows us to numerically evaluate $k_\Lambda(x, y)$ at any point $(x, y) \in \mathbb{R}^2$ up to desired accuracy.

To aid us with the computations, we recall from (4.4.5) the notation

$$\vartheta(u, x, y) = \frac{1}{q_0} \overline{\Phi^+(u^2, x)} \Phi^+(u^2, y) + \frac{1}{q_n} \overline{\Phi^-(u^2, x)} \Phi^-(u^2, y), \quad x, y \in \mathbb{R}$$

5. Concrete Examples

so that the reproducing kernel k_Λ in (4.4.4) reads as

$$k_\Lambda(x, y) = \frac{1}{2\pi} \int_{\Lambda^{1/2}} \frac{\vartheta(u, x, y)}{\kappa(u)} du, \quad x, y \in \mathbb{R}.$$

We will see shortly that upon expanding ϑ and applying identities from Lemma 4.3.1, most of its terms are of the form

$$e^{isu} + e^{-isu} = 2 \cos(su), \quad s \in \mathbb{R}.$$

Thus, when computing for k_Λ , we mainly use the real (also even) part J_{real} of J given by

$$J_{\text{real}}(s) = \frac{J(s) + J(-s)}{2} = \frac{1}{2\pi} \int_{\Lambda^{1/2}} \frac{\cos(su)}{\kappa(u)} du.$$

5.1. Case $n = 1$: the toy example

We consider the simplest case of a two-component piecewise constant p having the origin as its only knot. This is called a *toy example* in [39, Sec. 4]. We then rederive the reproducing kernel as part of the general theory of Chapter 4.

Theorem 5.1.1. *Let $\Omega, p_0, p_1 > 0$. Set $\Lambda = [0, \Omega]$. Define p to be the piecewise constant function*

$$p(x) = \begin{cases} p_0, & x \leq 0, \\ p_1, & x > 0 \end{cases}$$

and the constants $q_k = p_k^{-1/2}$, $k = 0, 1$. Then the reproducing kernel of $PW_\Lambda(A_p)$ is given by

$$k_\Lambda(x, y) = \begin{cases} \frac{q_0 \Omega^{1/2}}{\pi} \left(\text{sinc } q_0 \Omega^{1/2}(x - y) - \frac{q_0 - q_1}{q_0 + q_1} \text{sinc } q_0 \Omega^{1/2}(x + y) \right), & x, y \leq 0, \\ \frac{q_1 \Omega^{1/2}}{\pi} \left(\text{sinc } q_1 \Omega^{1/2}(x - y) + \frac{q_0 - q_1}{q_0 + q_1} \text{sinc } q_1 \Omega^{1/2}(x + y) \right), & x, y > 0, \\ \frac{2q_0 q_1 \Omega^{1/2}}{\pi(q_0 + q_1)} \text{sinc } \Omega^{1/2}(q_0 x - q_1 y), & x \leq 0, y > 0, \\ \frac{2q_0 q_1 \Omega^{1/2}}{\pi(q_0 + q_1)} \text{sinc } \Omega^{1/2}(q_1 x - q_0 y), & x > 0, y \leq 0. \end{cases}$$

The above formula for k_Λ is equivalent to the one given in [39, Sec. 4] if written purely in terms of p_0 and p_1 . We reproduce this result.

Proof. We first prepare the necessary quantities for quick reference. By Theorem 4.2.2, the fundamental system $\Phi(u^2, \cdot) = (\Phi^+(u^2, \cdot), \Phi^-(u^2, \cdot))$, $u \in (0, \infty)$ is of the form (using $n = 1$, $t_1 = 0$, $q_0 = p_0^{-1/2}$, $q_1 = p_1^{-1/2}$)

$$\Phi^+(u^2, x) = \begin{cases} a_0^+(u^2) e^{iq_0 x u} + b_0^+(u^2) e^{-iq_0 x u}, & x \leq 0, \\ e^{iq_1 x u}, & x > 0, \end{cases}$$

$$\Phi^-(u^2, x) = \begin{cases} e^{-iq_0 x u}, & x \leq 0, \\ a_1^-(u^2) e^{iq_1 x u} + b_1^-(u^2) e^{-iq_1 x u}, & x > 0. \end{cases}$$

5.1. Case $n = 1$: the toy example

We now need $L_1(u^2)$ and $R_1(u^2)$ to compute $a_1^-(u^2)$, $b_1^-(u^2)$ and $a_0^+(u^2)$, $b_0^+(u^2)$. By (4.2.4) and (4.2.5),

$$L_1(u^2) = \frac{1}{2} \begin{bmatrix} 1 + \frac{q_1}{q_0} & 1 - \frac{q_1}{q_0} \\ 1 - \frac{q_1}{q_0} & 1 + \frac{q_1}{q_0} \end{bmatrix} \quad \text{and} \quad R_1(u^2) = \frac{1}{2} \begin{bmatrix} 1 + \frac{q_0}{q_1} & 1 - \frac{q_0}{q_1} \\ 1 - \frac{q_0}{q_1} & 1 + \frac{q_0}{q_1} \end{bmatrix}.$$

Thus,

$$\begin{bmatrix} a_1^-(u^2) \\ b_1^-(u^2) \end{bmatrix} = \frac{1}{2} \begin{bmatrix} 1 + \frac{q_1}{q_0} & 1 - \frac{q_1}{q_0} \\ 1 - \frac{q_1}{q_0} & 1 + \frac{q_1}{q_0} \end{bmatrix} \begin{bmatrix} 0 \\ 1 \end{bmatrix} = \frac{1}{2} \begin{bmatrix} 1 - \frac{q_1}{q_0} \\ 1 + \frac{q_1}{q_0} \end{bmatrix}, \quad (5.1.1)$$

$$\begin{bmatrix} a_0^+(u^2) \\ b_0^+(u^2) \end{bmatrix} = \frac{1}{2} \begin{bmatrix} 1 + \frac{q_0}{q_1} & 1 - \frac{q_0}{q_1} \\ 1 - \frac{q_0}{q_1} & 1 + \frac{q_0}{q_1} \end{bmatrix} \begin{bmatrix} 1 \\ 0 \end{bmatrix} = \frac{1}{2} \begin{bmatrix} 1 + \frac{q_0}{q_1} \\ 1 - \frac{q_0}{q_1} \end{bmatrix}. \quad (5.1.2)$$

By Theorem 4.3.3 and (4.3.21),

$$\kappa(u) = \frac{|a_0^+(u^2)|^2}{q_0^2} = \frac{|b_1^-(u^2)|^2}{q_1^2} = \frac{(q_0 + q_1)^2}{4q_0^2q_1^2}, \quad d\mu(u^2) = \frac{2q_0q_1}{\pi(q_0 + q_1)^2} \begin{bmatrix} q_1 & 0 \\ 0 & q_0 \end{bmatrix} du. \quad (5.1.3)$$

Hence, with $\Lambda = [0, \Omega]$, the integral J can be expressed as

$$\begin{aligned} J(s) &= \frac{1}{2\pi} \int_{\Lambda^{1/2}} \frac{e^{isu}}{\kappa(u)} du = \frac{2q_0^2q_1^2}{\pi(q_0 + q_1)^2} \int_0^{\Omega^{1/2}} e^{isu} du = \frac{2q_0^2q_1^2}{\pi(q_0 + q_1)^2} \frac{e^{i\Omega^{1/2}s} - 1}{is} \\ &= \frac{2q_0^2q_1^2\Omega^{1/2}e^{i\frac{\Omega^{1/2}s}{2}}}{\pi(q_0 + q_1)^2} \operatorname{sinc}\left(\frac{\Omega^{1/2}s}{2}\right), \quad s \in \mathbb{R}. \end{aligned} \quad (5.1.4)$$

The real part J_{real} of J is

$$J_{\text{real}}(s) = \frac{2q_0^2q_1^2}{\pi(q_0 + q_1)^2} \int_0^{\Omega^{1/2}} \cos(su) du = \frac{2q_0^2q_1^2\Omega^{1/2}}{\pi(q_0 + q_1)^2} \operatorname{sinc} \Omega^{1/2}s, \quad s \in \mathbb{R}. \quad (5.1.5)$$

We now compute the piecewise components of k_Λ . We partition \mathbb{R} as the union of intervals $I_0 = (-\infty, 0]$ and $I_1 = (0, \infty)$.

- Suppose $x, y \leq 0$. Then $x, y \in I_0$, i.e., $j = l = 0$ and

$$\begin{aligned} \vartheta(u, x, y) &= \frac{1}{q_0} \overline{\Phi^+(u^2, x)} \Phi^+(u^2, y) + \frac{1}{q_n} \overline{\Phi^-(u^2, x)} \Phi^-(u^2, y) \\ &= \frac{1}{q_0} \overline{(a_0^+(u^2)e^{-iq_0xu} + b_0^+(u^2)e^{iq_0xu})} (a_0^+(u^2)e^{iq_0yu} + b_0^+(u^2)e^{-iq_0yu}) \\ &\quad + \frac{1}{q_1} e^{iq_0xu} e^{-iq_0yu}. \end{aligned}$$

From (5.1.1) and (5.1.2), we have

$$\begin{aligned} \vartheta(u, x, y) &= \frac{1}{4q_0} \left\{ \left(1 - \frac{q_0^2}{q_1^2}\right) (e^{iq_0(x+y)u} + e^{-iq_0(x+y)u}) + \left(1 + \frac{q_0}{q_1}\right)^2 e^{-iq_0(x-y)u} \right. \\ &\quad \left. + \left[\left(1 - \frac{q_0}{q_1}\right)^2 + \frac{4q_0}{q_1} \right] e^{iq_0(x-y)u} \right\} \\ &= \frac{1}{2q_0} \left\{ \left(1 - \frac{q_0^2}{q_1^2}\right) \cos(q_0(x+y)u) + \left(1 + \frac{q_0}{q_1}\right)^2 \cos(q_0(x-y)u) \right\}. \end{aligned}$$

5. Concrete Examples

Dividing both sides of the above equation by $2\pi\kappa(u)$ in (5.1.3) and integrating with respect to u over the interval $[0, \Omega^{1/2}]$ yields

$$\begin{aligned} k_\Lambda(x, y) &= \frac{1}{2\pi} \int_0^{\Omega^{1/2}} \frac{\vartheta(u, x, y)}{\kappa(u)} du \\ &= \frac{1}{2q_0} \left(1 - \frac{q_0^2}{q_1^2}\right) \cdot \int_0^{\Omega^{1/2}} \frac{\cos(q_0(x+y)u)}{\kappa(u)} du + \frac{1}{2q_0} \left(1 + \frac{q_0}{q_1}\right)^2 \cdot \int_0^{\Omega^{1/2}} \frac{\cos(q_0(x-y)u)}{\kappa(u)} du \\ &= \frac{1}{2q_0} \left(1 - \frac{q_0^2}{q_1^2}\right) J_{\text{real}}(q_0(x+y)) + \frac{1}{2q_0} \left(1 + \frac{q_0}{q_1}\right)^2 J_{\text{real}}(q_0(x-y)). \end{aligned}$$

By (5.1.5),

$$\begin{aligned} \frac{1}{2q_0} \left(1 - \frac{q_0^2}{q_1^2}\right) J_{\text{real}}(q_0(x+y)) &= \frac{1}{2q_0} \left(1 - \frac{q_0^2}{q_1^2}\right) \frac{2q_0^2 q_1^2 \Omega^{1/2}}{\pi(q_0 + q_1)^2} \text{sinc}(q_0 \Omega^{1/2}(x+y)) \\ &= \frac{q_0 \Omega^{1/2}}{\pi} \frac{q_1 - q_0}{q_0 + q_1} \text{sinc}(q_0 \Omega^{1/2}(x+y)), \\ \frac{1}{2q_0} \left(1 + \frac{q_0}{q_1}\right)^2 J_{\text{real}}(q_0(x-y)) &= \frac{1}{2q_0} \left(1 + \frac{q_0}{q_1}\right)^2 \frac{2q_0^2 q_1^2 \Omega^{1/2}}{\pi(q_0 + q_1)^2} \text{sinc}(q_0 \Omega^{1/2}(x-y)) \\ &= \frac{q_0 \Omega^{1/2}}{\pi} \text{sinc}(q_0 \Omega^{1/2}(x-y)). \end{aligned}$$

Therefore,

$$k_\Lambda(x, y) = \frac{q_0 \Omega^{1/2}}{\pi} \left(\text{sinc}(q_0 \Omega^{1/2}(x-y)) - \frac{q_0 - q_1}{q_0 + q_1} \text{sinc}(q_0 \Omega^{1/2}(x+y)) \right), \quad x, y \leq 0.$$

- Suppose $x, y > 0$. Then $x, y \in I_1$, i.e., $j = l = 1$ and

$$\begin{aligned} \vartheta(u, x, y) &= \frac{1}{q_0} e^{-iq_1 x u} e^{iq_1 y u} \\ &\quad + \frac{1}{q_1} (\overline{a_1^-(u^2)} e^{-iq_1 x u} + \overline{b_1^-(u^2)} e^{iq_1 x u}) (a_1^-(u^2) e^{iq_1 y u} + b_1^-(u^2) e^{-iq_1 y u}). \end{aligned}$$

Performing the same procedure as in the previous case yields the similar formula

$$k_\Lambda(x, y) = \frac{q_0 \Omega^{1/2}}{\pi} \left(\text{sinc}(q_0 \Omega^{1/2}(x-y)) + \frac{q_0 - q_1}{q_0 + q_1} \text{sinc}(q_0 \Omega^{1/2}(x+y)) \right), \quad x, y > 0.$$

- Suppose $x \leq 0, y > 0$. Then $x \in I_0, y \in I_1$, i.e., $j = 0, l = 1$ and

$$\begin{aligned} \vartheta(u, x, y) &= \frac{1}{q_0} (\overline{a_0^+(u^2)} e^{-iq_0 x u} + \overline{b_0^+(u^2)} e^{iq_0 x u}) e^{iq_1 y u} \\ &\quad + \frac{1}{q_1} e^{iq_0 x u} (a_1^-(u^2) e^{iq_1 y u} + b_1^-(u^2) e^{-iq_1 y u}). \end{aligned}$$

Again, by (5.1.1) and (5.1.2) we get

$$\begin{aligned} \vartheta(u, x, y) &= \left(\frac{1}{2q_0} \left(1 - \frac{q_0}{q_1} \right) + \frac{1}{2q_1} \left(1 - \frac{q_1}{q_0} \right) \right) e^{i(q_0x + q_1y)u} \\ &\quad + \frac{1}{2q_1} \left(1 + \frac{q_1}{q_0} \right) e^{i(q_0x - q_1y)u} + \frac{1}{2q_0} \left(1 + \frac{q_0}{q_1} \right) e^{-i(q_0x - q_1y)u} \\ &= \frac{q_0 + q_1}{q_0q_1} \cos((q_0x - q_1y)u). \end{aligned}$$

Hence, by (5.1.5),

$$k_\Lambda(x, y) = \frac{q_0 + q_1}{q_0q_1} J_{\text{real}}(q_0x - q_1y) = \frac{2q_0q_1\Omega^{1/2}}{\pi(q_0 + q_1)} \text{sinc}(\Omega^{1/2}(q_0x - q_1y)), \quad x \leq 0, y > 0.$$

- Suppose $x > 0, y \leq 0$. Then $x \in I_1, y \in I_0$, i.e., $j = 1, l = 0$. By the previous case,

$$\begin{aligned} k_\Lambda(x, y) &= \overline{k_\Lambda(y, x)} = \frac{2q_0q_1\Omega^{1/2}}{\pi(q_0 + q_1)} \text{sinc}(\Omega^{1/2}(q_0y - q_1x)) \\ &= \frac{2q_0q_1\Omega^{1/2}}{\pi(q_0 + q_1)} \text{sinc}(\Omega^{1/2}(q_1x - q_0y)), \quad x > 0, y \leq 0. \end{aligned}$$

By inspection, all four cases match the formula for k_Λ in Theorem 5.1.1. \square

If $p_0 = p_1$ ($q_0 = q_1$), the reproducing kernel k_Λ reduces to

$$k_\Lambda(x, y) = \frac{q_0\Omega^{1/2}}{\pi} \text{sinc}(q_0\Omega^{1/2}(x - y)), \quad x, y \in \mathbb{R}$$

which we know as the reproducing kernel for the Paley-Wiener space $PW_{q_0\Omega^{1/2}}(\mathbb{R})$ of $q_0\Omega^{1/2}$ -bandlimited functions.

The previous computations demonstrate that complete derivation the reproducing kernel k_Λ is possible if we know an explicit formula for J . We shall see in the next example that finding a formula for J becomes more difficult as $n \geq 2$. We illustrate the case $n = 2$ in the next section where we only have a series expansion for J .

5.2. Case $n = 2$: three-component p

We consider a three-component piecewise function p where the middle interval I_1 is centered at the origin. Unlike the toy example where we have an explicit formula for J , we settle for a series expansion as the computations are more complicated.

Lemma 5.2.1. *Let $p_0, p_1, p_2, T > 0$ and $\Lambda \subset \mathbb{R}_0^+$ be of finite measure. Define p by*

$$p(x) = \begin{cases} p_0, & x \in (-\infty, -\frac{T}{2}], \\ p_1, & x \in (-\frac{T}{2}, \frac{T}{2}], \\ p_2, & x \in (\frac{T}{2}, \infty), \end{cases}$$

5. Concrete Examples

the constants $q_k = p_k^{-1/2}$, $k = 0, 1, 2$,

$$C = \frac{1}{16q_0^2} \left[\left(1 + \frac{q_0}{q_1}\right)^2 \left(1 + \frac{q_1}{q_2}\right)^2 + \left(1 - \frac{q_0}{q_1}\right)^2 \left(1 - \frac{q_1}{q_2}\right)^2 \right], \quad (5.2.1)$$

$$K = \frac{1}{8q_0^2} \left(1 - \frac{q_0^2}{q_1^2}\right) \left(1 - \frac{q_1^2}{q_2^2}\right), \quad (5.2.2)$$

and $\zeta = 2q_1T$. Then

$$J(s) = \frac{1}{2\pi} \int_{\Lambda^{1/2}} \frac{e^{isu}}{C + K \cos \zeta u} du, \quad s \in \mathbb{R}.$$

Proof. We proceed as in the toy example. By Theorem 4.2.2, the fundamental system $\Phi(u^2, \cdot) = (\Phi^+(u^2, \cdot), \Phi^-(u^2, \cdot))$, $u \in (0, \infty)$ is of the form

$$\Phi^+(u^2, x) = \begin{cases} a_0^+(u^2)e^{iq_0xu} + b_0^+(u^2)e^{-iq_0xu}, & x \in (-\infty, -\frac{T}{2}] \\ a_1^+(u^2)e^{iq_1xu} + b_1^+(u^2)e^{-iq_1xu}, & x \in (-\frac{T}{2}, \frac{T}{2}] \\ e^{iq_2xu}, & x \in (\frac{T}{2}, \infty) \end{cases}$$

$$\Phi^-(u^2, x) = \begin{cases} e^{-iq_0xu}, & x \in (-\infty, -\frac{T}{2}] \\ a_1^-(u^2)e^{iq_1xu} + b_1^-(u^2)e^{-iq_1xu}, & x \in (-\frac{T}{2}, \frac{T}{2}] \\ a_2^-(u^2)e^{iq_2xu} + b_2^-(u^2)e^{-iq_2xu}, & x \in (\frac{T}{2}, \infty). \end{cases}$$

To obtain the rest of the connection coefficients, we need the matrices

$$L_1(u^2) = \frac{1}{2} \begin{bmatrix} \left(1 + \frac{q_1}{q_0}\right) e^{-i\frac{T}{2}(q_0-q_1)u} & \left(1 - \frac{q_1}{q_0}\right) e^{i\frac{T}{2}(q_0+q_1)u} \\ \left(1 - \frac{q_1}{q_0}\right) e^{-i\frac{T}{2}(q_0+q_1)u} & \left(1 + \frac{q_1}{q_0}\right) e^{i\frac{T}{2}(q_0-q_1)u} \end{bmatrix},$$

$$L_2(u^2) = \frac{1}{2} \begin{bmatrix} \left(1 + \frac{q_2}{q_1}\right) e^{i\frac{T}{2}(q_1-q_2)u} & \left(1 - \frac{q_2}{q_1}\right) e^{-i\frac{T}{2}(q_1+q_2)u} \\ \left(1 - \frac{q_2}{q_1}\right) e^{i\frac{T}{2}(q_1+q_2)u} & \left(1 + \frac{q_2}{q_1}\right) e^{-i\frac{T}{2}(q_1-q_2)u} \end{bmatrix},$$

$$R_1(u^2) = \frac{1}{2} \begin{bmatrix} \left(1 + \frac{q_0}{q_1}\right) e^{i\frac{T}{2}(q_0-q_1)u} & \left(1 - \frac{q_0}{q_1}\right) e^{i\frac{T}{2}(q_0+q_1)u} \\ \left(1 - \frac{q_0}{q_1}\right) e^{-i\frac{T}{2}(q_0+q_1)u} & \left(1 + \frac{q_0}{q_1}\right) e^{-i\frac{T}{2}(q_0-q_1)u} \end{bmatrix},$$

$$R_2(u^2) = \frac{1}{2} \begin{bmatrix} \left(1 + \frac{q_1}{q_2}\right) e^{-i\frac{T}{2}(q_1-q_2)u} & \left(1 - \frac{q_1}{q_2}\right) e^{-i\frac{T}{2}(q_1+q_2)u} \\ \left(1 - \frac{q_1}{q_2}\right) e^{i\frac{T}{2}(q_1+q_2)u} & \left(1 + \frac{q_1}{q_2}\right) e^{i\frac{T}{2}(q_1-q_2)u} \end{bmatrix}.$$

Now, by Theorem 4.2.2, we have

$$\begin{bmatrix} a_1^+(u^2) \\ b_1^+(u^2) \end{bmatrix} = R_2(u^2) \begin{bmatrix} 1 \\ 0 \end{bmatrix}, \quad \begin{bmatrix} a_0^+(u^2) \\ b_0^+(u^2) \end{bmatrix} = R_1(u^2)R_2(u^2) \begin{bmatrix} 1 \\ 0 \end{bmatrix} = R_1(u^2) \begin{bmatrix} a_1^+(u^2) \\ b_1^+(u^2) \end{bmatrix},$$

$$\begin{bmatrix} a_1^-(u^2) \\ b_1^-(u^2) \end{bmatrix} = L_1(u^2) \begin{bmatrix} 0 \\ 1 \end{bmatrix}, \quad \begin{bmatrix} a_2^-(u^2) \\ b_2^-(u^2) \end{bmatrix} = L_2(u^2)L_1(u^2) \begin{bmatrix} 0 \\ 1 \end{bmatrix} = L_2(u^2) \begin{bmatrix} a_1^-(u^2) \\ b_1^-(u^2) \end{bmatrix}.$$

Therefore,

$$\begin{aligned}
 & \bullet \begin{bmatrix} a_0^-(u^2) \\ b_0^-(u^2) \end{bmatrix} = \begin{bmatrix} 0 \\ 1 \end{bmatrix}, \quad \begin{bmatrix} a_2^+(u^2) \\ b_2^+(u^2) \end{bmatrix} = \begin{bmatrix} 1 \\ 0 \end{bmatrix}, \\
 & \bullet \begin{bmatrix} a_1^-(u^2) \\ b_1^-(u^2) \end{bmatrix} = \frac{1}{2} \begin{bmatrix} \left(1 - \frac{q_1}{q_0}\right) e^{i\frac{T}{2}(q_0+q_1)u} \\ \left(1 + \frac{q_1}{q_0}\right) e^{i\frac{T}{2}(q_0-q_1)u} \end{bmatrix}, \quad \begin{bmatrix} a_1^+(u^2) \\ b_1^+(u^2) \end{bmatrix} = \frac{1}{2} \begin{bmatrix} \left(1 + \frac{q_1}{q_2}\right) e^{-i\frac{T}{2}(q_1-q_2)u} \\ \left(1 - \frac{q_1}{q_2}\right) e^{i\frac{T}{2}(q_1+q_2)u} \end{bmatrix}, \\
 & \bullet \begin{bmatrix} a_2^-(u^2) \\ b_2^-(u^2) \end{bmatrix} = \frac{1}{4} \begin{bmatrix} \left(1 - \frac{q_1}{q_0}\right) \left(1 + \frac{q_2}{q_1}\right) e^{i\frac{T}{2}(q_0+2q_1-q_2)u} + \left(1 + \frac{q_1}{q_0}\right) \left(1 - \frac{q_2}{q_1}\right) e^{i\frac{T}{2}(q_0-2q_1-q_2)u} \\ \left(1 - \frac{q_1}{q_0}\right) \left(1 - \frac{q_2}{q_1}\right) e^{i\frac{T}{2}(q_0+2q_1+q_2)u} + \left(1 + \frac{q_1}{q_0}\right) \left(1 + \frac{q_2}{q_1}\right) e^{i\frac{T}{2}(q_0-2q_1+q_2)u} \end{bmatrix}, \\
 & \begin{bmatrix} a_0^+(u^2) \\ b_0^+(u^2) \end{bmatrix} = \frac{1}{4} \begin{bmatrix} \left(1 + \frac{q_0}{q_1}\right) \left(1 + \frac{q_1}{q_2}\right) e^{i\frac{T}{2}(q_0-2q_1+q_2)u} + \left(1 - \frac{q_0}{q_1}\right) \left(1 - \frac{q_1}{q_2}\right) e^{i\frac{T}{2}(q_0+2q_1+q_2)u} \\ \left(1 - \frac{q_0}{q_1}\right) \left(1 + \frac{q_1}{q_2}\right) e^{i\frac{T}{2}(-q_0-2q_1+q_2)u} + \left(1 + \frac{q_0}{q_1}\right) \left(1 - \frac{q_1}{q_2}\right) e^{i\frac{T}{2}(-q_0+2q_1+q_2)u} \end{bmatrix}.
 \end{aligned}$$

Using the constants C and K as in (5.2.1) and (5.2.2), we can write $\kappa(u)$ as

$$\begin{aligned}
 \kappa(u) &= \frac{|a_0^+(u^2)|^2}{q_0^2} = \frac{1}{16q_0^2} \left\{ \left(1 + \frac{q_0}{q_1}\right)^2 \left(1 + \frac{q_1}{q_2}\right)^2 + \left(1 - \frac{q_0}{q_1}\right)^2 \left(1 - \frac{q_1}{q_2}\right)^2 \right. \\
 &\quad \left. + 2 \left(1 - \frac{q_0^2}{q_1^2}\right) \left(1 - \frac{q_1^2}{q_2^2}\right) \cos(2Tq_1u) \right\} \\
 &= C + K \cos \zeta u.
 \end{aligned}$$

Therefore,

$$J(s) = \frac{1}{2\pi} \int_{\Lambda^{1/2}} \frac{e^{isu}}{C + K \cos \zeta u} du$$

for any $s \in \mathbb{R}$. □

According to Theorem 4.3.3, one can also use $\kappa(u) = \frac{|b_2^-(u^2)|^2}{q_2^2}$ to compute κ . Indeed, in this simple case we see from the similarity of the expressions $a_0^+(u^2)$ and $b_2^-(u^2)$ that

$$\begin{aligned}
 \kappa(u) &= \frac{|b_2^-(u^2)|^2}{q_2^2} = \frac{1}{16q_2^2} \left\{ \left(1 + \frac{q_1}{q_0}\right)^2 \left(1 + \frac{q_2}{q_1}\right)^2 + \left(1 - \frac{q_1}{q_0}\right)^2 \left(1 - \frac{q_2}{q_1}\right)^2 \right. \\
 &\quad \left. + 2 \left(1 - \frac{q_1^2}{q_0^2}\right) \left(1 - \frac{q_2^2}{q_1^2}\right) \cos \zeta u \right\}.
 \end{aligned}$$

By distributing $\frac{1}{q_2^2}$ and factoring out $\frac{1}{q_0^2}$, we arrive at the same expression for κ .

Remark 5.2.2. We have the following observations.

(i) It is clear that $C > 0$ and

$$C \pm K = \frac{1}{16q_0^2} \left[\left(1 + \frac{q_0}{q_1}\right) \left(1 + \frac{q_1}{q_2}\right) \pm \left(1 - \frac{q_0}{q_1}\right) \left(1 - \frac{q_1}{q_2}\right) \right]^2 \geq 0.$$

Moreover, $C = K$ if and only if $q_1^2 + q_0q_2 = 0$ and $C = -K$ if and only if $q_0 + q_2 = 0$. Since both conditions cannot happen as $q_1, q_2, q_3 > 0$, we conclude that $C > |K|$, which also confirms for $n = 2$ that $\kappa(u)$ does not vanish for $u \in (0, \infty)$, cf. Corollary 4.3.2.

5. Concrete Examples

(ii) We can also take a look at degenerate forms of $n = 2$ where consecutive components of p are equal. If $\Lambda = [0, \Omega]$ and $p_1 = p_2$ ($q_1 = q_2$), i.e., the only knot is at $t_1 = -\frac{T}{2}$, then $C = \frac{(q_0+q_1)^2}{4q_0^2q_1^2}$ and $K = 0$. Hence,

$$J(s) = \frac{1}{2\pi} \int_0^{\Omega^{1/2}} \frac{e^{isu}}{C} du = \frac{2q_0^2q_1^2}{\pi(q_0+q_1)^2} \int_0^{\Omega^{1/2}} e^{isu} du = \frac{2q_0^2q_1^2\Omega^{1/2}e^{i\frac{\Omega^{1/2}s}{2}}}{\pi(q_0+q_1)^2} \operatorname{sinc} \frac{\Omega^{1/2}s}{2}$$

and

$$J_{\text{real}}(s) = \frac{2q_0^2q_1^2\Omega^{1/2}}{\pi(q_0+q_1)^2} \operatorname{sinc} \Omega^{1/2}s. \quad (5.2.3)$$

Analogously, if $p_0 = p_1$ ($q_0 = q_1$), i.e., the only knot is at $t_2 = \frac{T}{2}$, then $C = \frac{(q_1+q_2)^2}{4q_1^2q_2^2}$ and $K = 0$. Therefore

$$J(s) = \frac{1}{2\pi} \int_0^{\Omega^{1/2}} \frac{e^{isu}}{C} du = \frac{2q_1^2q_2^2}{\pi(q_1+q_2)^2} \int_0^{\Omega^{1/2}} e^{isu} du = \frac{2q_1^2q_2^2\Omega^{1/2}e^{i\frac{\Omega^{1/2}s}{2}}}{\pi(q_1+q_2)^2} \operatorname{sinc} \frac{\Omega^{1/2}s}{2}$$

and

$$J_{\text{real}}(s) = \frac{2q_1^2q_2^2\Omega^{1/2}}{\pi(q_1+q_2)^2} \operatorname{sinc} \Omega^{1/2}s. \quad (5.2.4)$$

Up to a shift by $\frac{T}{2}$, these formulas coincide with the closed-form expressions for J and J_{real} in (5.1.4) and (5.1.5), respectively. If it turns out in both cases above (even including the toy example) that $p_0 = p_1 = p_2$ ($q_0 = q_1 = q_2$), then for $s \in \mathbb{R}$,

$$J(s) = \frac{q_0^2\Omega^{1/2}}{2\pi} e^{i\frac{\Omega^{1/2}s}{2}} \operatorname{sinc} \frac{\Omega^{1/2}s}{2}, \quad J_{\text{real}}(s) = \frac{q_0^2\Omega^{1/2}}{2\pi} \operatorname{sinc} \Omega^{1/2}s.$$

5.2.1. Evaluating J : Series expansions

To our knowledge, J in Lemma 5.2.1 does not belong to any class of special functions. We first discuss a series expansion that will be used in Chapter 7 for the numerical evaluation of J .

Theorem 5.2.3. *Let $\Omega, T, q_0, q_1, q_2 > 0$. Set $\Lambda = [0, \Omega]$ and the constants*

$$C = \frac{1}{16q_0^2} \left[\left(1 + \frac{q_1}{q_2}\right)^2 \left(1 + \frac{q_0}{q_1}\right)^2 + \left(1 - \frac{q_1}{q_2}\right)^2 \left(1 - \frac{q_0}{q_1}\right)^2 \right],$$

$$K = \frac{1}{8q_0^2} \left(1 - \frac{q_1^2}{q_2^2}\right) \left(1 - \frac{q_0^2}{q_1^2}\right),$$

$\zeta = 2q_1T$ and $r = \frac{K}{C}$. Then for $s \in \mathbb{R}$,

$$\begin{aligned} J(s) &= \frac{1}{2\pi} \int_{\Lambda^{1/2}} \frac{e^{isu}}{C + K \cos \zeta u} du \\ &= \frac{1}{2C\pi} \sum_{m=0}^{\infty} \left(\sum_{l=0}^m \left(-\frac{r}{2}\right)^m \binom{m}{l} \frac{e^{i(s+(m-2l)\zeta)\Omega^{1/2}} - 1}{i(s+(m-2l)\zeta)} \right) \\ &= \frac{\Omega^{1/2}}{2C\pi} \sum_{m=0}^{\infty} \sum_{l=0}^m \left(-\frac{r}{2}\right)^m \binom{m}{l} e^{i\frac{\Omega^{1/2}}{2}(s+(m-2l)\zeta)} \operatorname{sinc} \left(\frac{\Omega^{1/2}}{2}(s+(m-2l)\zeta)\right). \end{aligned}$$

Moreover, if J_M is the M^{th} partial sum of J , then

$$|J(s) - J_M(s)| \leq \frac{\Omega^{1/2} |r|^{M+1}}{2C\pi (1 - |r|)}, \quad s \in \mathbb{R}.$$

Proof. By Remark 5.2.2, $|r| < 1$. By Lemma 5.2.1, we have that for $s \in \mathbb{R}$,

$$\begin{aligned} J(s) &= \frac{1}{2C\pi} \int_0^{\Omega^{1/2}} \frac{e^{isu}}{1 - (-r \cos \zeta u)} du = \frac{1}{2C\pi} \int_0^{\Omega^{1/2}} \sum_{m=0}^{\infty} (-r)^m e^{isu} \cos^m \zeta u du \\ &= \frac{1}{2C\pi} \sum_{m=0}^{\infty} (-r)^m \int_0^{\Omega^{1/2}} e^{isu} \cos^m \zeta u du. \end{aligned} \quad (5.2.5)$$

For $m \in \mathbb{N}_0$, define the bandlimited function

$$F_m(s) = \int_0^{\Omega^{1/2}} e^{isu} \cos^m \zeta u du, \quad s \in \mathbb{R}$$

so that $J = \frac{1}{2C\pi} \sum_{m=0}^{\infty} (-r)^m F_m$. To compute F_m , we write cosine using complex exponentials:

$$\begin{aligned} F_m(s) &= \int_0^{\Omega^{1/2}} e^{isu} \cos^m \zeta u du = \int_0^{\Omega^{1/2}} e^{isu} \cdot \left(\frac{e^{i\zeta u} + e^{-i\zeta u}}{2} \right)^m du \\ &= \frac{1}{2^m} \sum_{l=0}^m \binom{m}{l} \int_0^{\Omega^{1/2}} e^{isu} e^{i(m-l)\zeta u} \cdot e^{-il\zeta u} du \\ &= \frac{1}{2^m} \sum_{l=0}^m \binom{m}{l} \int_0^{\Omega^{1/2}} e^{i(s+(m-2l)\zeta)u} du. \end{aligned}$$

Since

$$\begin{aligned} \int_0^{\Omega^{1/2}} e^{i(s+(m-2l)\zeta)u} du &= \frac{e^{i\Omega^{1/2}(s+(m-2l)\zeta)} - 1}{i(s + (m-2l)\zeta)} \\ &= \Omega^{1/2} e^{i\frac{\Omega^{1/2}}{2}(s+(m-2l)\zeta)} \operatorname{sinc} \left(\frac{\Omega^{1/2}}{2}(s + (m-2l)\zeta) \right) \end{aligned}$$

for any $s \in \mathbb{R}$, we have

$$F_m(s) = \frac{1}{2^m} \sum_{l=0}^m \binom{m}{l} \frac{e^{i\Omega^{1/2}(s+(m-2l)\zeta)} - 1}{i(s + (m-2l)\zeta)} \quad (5.2.6)$$

$$= \frac{\Omega^{1/2}}{2^m} \sum_{l=0}^m \binom{m}{l} e^{i\frac{\Omega^{1/2}}{2}(s+(m-2l)\zeta)} \operatorname{sinc} \left(\frac{\Omega^{1/2}}{2}(s + (m-2l)\zeta) \right). \quad (5.2.7)$$

Substituting either (5.2.6) or (5.2.7) to (5.2.5) gives the first conclusion. Now, since $|F_m(s)| \leq \Omega^{1/2}$ for all $m \in \mathbb{N}_0$, then for $M \in \mathbb{N}_0$,

$$|J(s) - J_M(s)| = \frac{1}{2C\pi} \left| \sum_{m=M+1}^{\infty} (-r)^m F_m(s) \right| \leq \frac{\Omega^{1/2}}{2C\pi} \sum_{m=M+1}^{\infty} |r|^m = \frac{\Omega^{1/2} |r|^{M+1}}{2C\pi (1 - |r|)}, \quad s \in \mathbb{R}.$$

This completes the proof. \square

5. Concrete Examples

For bounded spectral sets, we replace $[0, \Omega]$ by Λ in (5.2.5). However, expressions for $\mathcal{F}^{-1}(\chi_{\Lambda^{1/2}} \cos^m \zeta u)$ without integrals for all $m \in \mathbb{N}_0$ may be difficult to derive.

The real part J_{real} of J is given by

$$\begin{aligned} J_{\text{real}}(s) &= \frac{J(s) + J(-s)}{2} \\ &= \frac{\Omega^{1/2}}{2C\pi} \sum_{m=0}^{\infty} \sum_{l=0}^m \left(-\frac{r}{2}\right)^m \binom{m}{l} \cos\left(\frac{\Omega^{1/2}}{2}(s + (m-2l)\zeta)\right) \operatorname{sinc}\left(\frac{\Omega^{1/2}}{2}(s + (m-2l)\zeta)\right). \end{aligned}$$

Observe that for $\theta \in \mathbb{R}$,

$$\cos \frac{\theta}{2} \operatorname{sinc} \frac{\theta}{2} = \cos \frac{\theta}{2} \cdot \frac{\sin \frac{\theta}{2}}{\frac{\theta}{2}} = \frac{2 \sin \frac{\theta}{2} \cos \frac{\theta}{2}}{\theta} = \frac{\sin \theta}{\theta} = \operatorname{sinc} \theta.$$

Taking $\theta = \Omega^{1/2}(s + (m-2l)\zeta)$ yields

$$J_{\text{real}}(s) = \frac{\Omega^{1/2}}{2C\pi} \sum_{m=0}^{\infty} \sum_{l=0}^m \left(-\frac{r}{2}\right)^m \binom{m}{l} \operatorname{sinc}\left(\Omega^{1/2}(s + (m-2l)\zeta)\right), \quad s \in \mathbb{R}.$$

Remark 5.2.4. An alternative expansion for J_{real} can be derived using the connection between binomial coefficients and Pascal's triangle. Writing the first few terms of J_{real} in the above series expansion yields

$$\begin{aligned} J_{\text{real}}(s) &= \frac{\Omega^{1/2}}{2C\pi} \left\{ \underbrace{\operatorname{sinc}(\Omega^{1/2}s)}_{m=0} - \frac{r}{2} \underbrace{(\operatorname{sinc}(\Omega^{1/2}(s-\zeta)) + \operatorname{sinc}(\Omega^{1/2}(s+\zeta)))}_{m=1} \right. \\ &\quad \left. + \frac{r^2}{4} \underbrace{(\operatorname{sinc}(\Omega^{1/2}(s-2\zeta)) + 2\operatorname{sinc}(\Omega^{1/2}s) + \operatorname{sinc}(\Omega^{1/2}(s+2\zeta)))}_{m=2} - \dots \right\}. \end{aligned}$$

Considering the sum of entries found in the k th column of Pascal's triangle we define

$$c_k = \frac{\Omega^{1/2}}{2C\pi} \sum_{j=0}^{\infty} \binom{2j+|k|}{j} \left(-\frac{r}{2}\right)^{2j+|k|}, \quad k \in \mathbb{Z}, \quad (5.2.8)$$

so that

$$J_{\text{real}}(s) = \sum_{k=-\infty}^{\infty} c_k \operatorname{sinc}(\Omega^{1/2}(s - k\zeta)).$$

In Appendix B we give a special case where we get an explicit formula for J using the theory of residues as well as special functions.

5.2.2. Piecewise Components of k_{Λ}

We now partially compute the piecewise components of the reproducing kernel k_{Λ} for $n = 2$. Since we do not have a formula for J in this case, the best we can do to compute k_{Λ}

5.2. Case $n = 2$: three-component p

is to manually expand $\vartheta(u, x, y)$ for any $x, y \in \mathbb{R}$. Afterwards, we express the components of k_Λ in terms of J . Instead of considering all nine possible expressions for k_Λ , we appeal to the symmetry $k_\Lambda(x, y) = \overline{k_\Lambda(y, x)}$ for all $x, y \in \mathbb{R}$ to reduce the number of components to compute. Once these partial computations are performed, we use Theorem 5.2.3 to accurately evaluate J at any point.

Theorem 5.2.5. *Let $\Omega, p_0, p_1, p_2, T > 0$ and set $\Lambda = [0, \Omega]$. Let $I_0 = (-\infty, -\frac{T}{2}]$, $I_1 = (-\frac{T}{2}, \frac{T}{2}]$, $I_2 = (\frac{T}{2}, \infty)$ and $\chi_j = \chi_{I_j}$ the characteristic function on I_j , $j = 0, 1, 2$. Define p by*

$$p(x) = \sum_{j=0}^2 p_j \chi_j(x) = \begin{cases} p_0, & x \in I_0, \\ p_1, & x \in I_1, \\ p_2, & x \in I_2, \end{cases}$$

the constants $q_k = p_k^{-1/2}$, $0 \leq k \leq 2$, and the real part J_{real} of J by

$$J_{real}(s) = \frac{\Omega^{1/2}}{2C\pi} \sum_{m=0}^{\infty} \sum_{l=0}^m \left(-\frac{r}{2}\right)^m \binom{m}{l} \operatorname{sinc}(\Omega^{1/2}(s + (m-2l)\zeta)), \quad s \in \mathbb{R}. \quad (5.2.9)$$

Furthermore, we define the functions $k_{\Lambda, jl}$, $0 \leq j, l \leq 2$ by

$$\begin{aligned} k_{\Lambda, 00}(x, y) &= \frac{q_0 \Omega^{1/2}}{\pi} \operatorname{sinc}(q_0 \Omega^{1/2}(x-y)) + \frac{1}{4q_0} \left(1 - \frac{q_0^2}{q_1^2}\right) \left(1 + \frac{q_1^2}{q_2^2}\right) J_{real}(q_0(x+y+T)) \\ &\quad + \frac{1}{8q_0} \left(1 - \frac{q_0}{q_1}\right)^2 \left(1 - \frac{q_1^2}{q_2^2}\right) J_{real}(q_0(x+y+T) + 2q_1 T) \\ &\quad + \frac{1}{8q_0} \left(1 + \frac{q_0}{q_1}\right)^2 \left(1 - \frac{q_1^2}{q_2^2}\right) J_{real}(q_0(x+y+T) - 2q_1 T), \\ k_{\Lambda, 11}(x, y) &= \frac{1}{2} \left[\frac{1}{q_0} \left(1 + \frac{q_1^2}{q_2^2}\right) + \frac{1}{q_2} \left(1 + \frac{q_1^2}{q_0^2}\right) \right] J_{real}(q_1(x-y)) \\ &\quad + \frac{1}{2q_0} \left(1 - \frac{q_1^2}{q_2^2}\right) J_{real}(q_1(x+y-T)) + \frac{1}{2q_2} \left(1 - \frac{q_1^2}{q_0^2}\right) J_{real}(q_1(x+y+T)), \\ k_{\Lambda, 22}(x, y) &= \frac{q_2 \Omega^{1/2}}{\pi} \operatorname{sinc}(q_2 \Omega^{1/2}(x-y)) + \frac{1}{4q_2} \left(1 + \frac{q_1^2}{q_0^2}\right) \left(1 - \frac{q_2^2}{q_1^2}\right) J_{real}(q_2(x+y-T)) \\ &\quad + \frac{1}{8q_2} \left(1 - \frac{q_1^2}{q_0^2}\right) \left(1 - \frac{q_2}{q_1}\right)^2 J_{real}(q_2(x+y-T) - 2q_1 T) \\ &\quad + \frac{1}{8q_2} \left(1 - \frac{q_1^2}{q_0^2}\right) \left(1 + \frac{q_2}{q_1}\right)^2 J_{real}(q_2(x+y-T) + 2q_1 T), \\ k_{\Lambda, 01}(x, y) &= k_{\Lambda, 10}(y, x) \\ &= \frac{1}{4q_0} \left(1 + \frac{q_0}{q_1}\right) \left(1 + \frac{q_1}{q_2}\right)^2 J_{real}(q_0(x + \frac{T}{2}) - q_1(y + \frac{T}{2})) \\ &\quad + \frac{1}{4q_0} \left(1 - \frac{q_0}{q_1}\right) \left(1 - \frac{q_1}{q_2}\right)^2 J_{real}(q_0(x + \frac{T}{2}) + q_1(y + \frac{T}{2})) \\ &\quad + \frac{1}{4q_0} \left(1 + \frac{q_0}{q_1}\right) \left(1 - \frac{q_1^2}{q_2^2}\right) J_{real}(q_0(x + \frac{T}{2}) + q_1(y - \frac{3T}{2})) \end{aligned}$$

5. Concrete Examples

$$\begin{aligned}
& + \frac{1}{4q_0} \left(1 - \frac{q_0}{q_1}\right) \left(1 - \frac{q_1^2}{q_2^2}\right) J_{\text{real}}\left(q_0\left(x + \frac{T}{2}\right) - q_1\left(y - \frac{3T}{2}\right)\right), \\
k_{\Lambda,02}(x, y) & = k_{\Lambda,20}(y, x) \\
& = \frac{1}{2q_0} \left(1 - \frac{q_0}{q_1}\right) \left(1 - \frac{q_1}{q_2}\right) J_{\text{real}}\left(q_0\left(x + \frac{T}{2}\right) + q_1T - q_2\left(y - \frac{T}{2}\right)\right) \\
& + \frac{1}{2q_0} \left(1 + \frac{q_0}{q_1}\right) \left(1 + \frac{q_1}{q_2}\right) J_{\text{real}}\left(q_0\left(x + \frac{T}{2}\right) - q_1T - q_2\left(y - \frac{T}{2}\right)\right), \\
k_{\Lambda,12}(x, y) & = k_{\Lambda,21}(y, x) \\
& = \frac{1}{4q_2} \left(1 + \frac{q_1}{q_0}\right)^2 \left(1 + \frac{q_2}{q_1}\right) J_{\text{real}}\left(q_1\left(x - \frac{T}{2}\right) - q_2\left(y - \frac{T}{2}\right)\right) \\
& + \frac{1}{4q_2} \left(1 - \frac{q_1}{q_0}\right)^2 \left(1 - \frac{q_2}{q_1}\right) J_{\text{real}}\left(q_1\left(x - \frac{T}{2}\right) + q_2\left(y - \frac{T}{2}\right)\right) \\
& + \frac{1}{4q_2} \left(1 - \frac{q_1^2}{q_0^2}\right) \left(1 + \frac{q_2}{q_1}\right) J_{\text{real}}\left(q_1\left(x + \frac{3T}{2}\right) + q_2\left(y - \frac{T}{2}\right)\right) \\
& + \frac{1}{4q_2} \left(1 - \frac{q_1^2}{q_0^2}\right) \left(1 - \frac{q_2}{q_1}\right) J_{\text{real}}\left(q_1\left(x + \frac{3T}{2}\right) - q_2\left(y - \frac{T}{2}\right)\right).
\end{aligned}$$

Then the reproducing kernel of $PW_{[0,\Omega]}(A_p)$ is

$$k_{\Lambda}(x, y) = \sum_{j,l=0}^2 k_{\Lambda,jl}(x, y) \chi_j(x) \chi_l(y), \quad x, y \in \mathbb{R}.$$

Proof. Initially, we have nine cases to consider:

$$(j, l) \in \{(0, 0), (0, 1), (0, 2), (1, 0), (1, 1), (1, 2), (2, 0), (2, 1), (2, 2)\}.$$

By the symmetry $k_{\Lambda}(x, y) = \overline{k_{\Lambda}(y, x)}$ for all $x, y \in \mathbb{R}$, (1, 0) follows from (0, 1), (2, 0) follows from (0, 2), and (2, 1) follows from (1, 2). Furthermore, since the knots of p are symmetric at the origin, (2, 2) follows from (0, 0) and (1, 2) follows from (0, 1) by applying the replacement rule $(x, y, T, q_0, q_1, q_2) \rightarrow (y, x, -T, q_2, q_1, q_0)$. Therefore, it suffices to take the four cases

$$(j, l) \in \{(0, 0), (0, 1), (0, 2), (1, 1)\}.$$

- Suppose $x, y \leq -\frac{T}{2}$, i.e., $(j, l) = (0, 0)$. Then

$$\begin{aligned}
\vartheta(u, x, y) & = \frac{1}{q_0} \overline{\Phi^+(u^2, x)} \Phi^+(u^2, y) + \frac{1}{q_n} \overline{\Phi^-(u^2, x)} \Phi^-(u^2, y) \\
& = \frac{1}{q_0} (\overline{a_0^+(u^2)} e^{-iq_0xu} + \overline{b_0^+(u^2)} e^{iq_0xu}) (a_0^+(u^2) e^{iq_0yu} + b_0^+(u^2) e^{-iq_0yu}) \\
& + \frac{1}{q_2} e^{iq_0xu} e^{-iq_0yu} \\
& = \frac{|a_0^+(u^2)|^2}{q_0} e^{-iq_0(x-y)u} + \left(\frac{1}{q_2} + \frac{|b_0^+(u^2)|^2}{q_0}\right) e^{iq_0(x-y)u} \\
& + \frac{1}{q_0} \left(a_0^+(u^2) \overline{b_0^+(u^2)} e^{iq_0(x+y)u} + \overline{a_0^+(u^2)} b_0^+(u^2) e^{-iq_0(x+y)u}\right). \tag{5.2.10}
\end{aligned}$$

5.2. Case $n = 2$: three-component p

By Corollary 4.3.2 and by definition of κ in Theorem 4.3.3,

$$\frac{1}{q_2} + \frac{|b_0^+(u^2)|^2}{q_0} = \frac{|a_0^+(u^2)|^2}{q_0} = q_0 \kappa(u).$$

Consequently, the sum of the first two terms equals $2q_0 \kappa(u) \cos(q_0(x - y)u)$. Upon expanding the remaining connection coefficients using the values computed in the proof of Lemma 5.2.1, we get

$$\begin{aligned} \vartheta(u, x, y) &= 2q_0 \kappa(u) \cos(q_0(x - y)u) + \frac{1}{4q_0} \left(1 + \frac{q_1^2}{q_2^2}\right) \left(1 - \frac{q_0^2}{q_1^2}\right) \cos(q_0(x + y + T)u) \\ &\quad + \frac{1}{8q_0} \left(1 - \frac{q_1^2}{q_2^2}\right) \left(1 - \frac{q_0}{q_1}\right)^2 \cos((q_0(x + y + T) + 2q_1 T)u) \\ &\quad + \frac{1}{8q_0} \left(1 - \frac{q_1^2}{q_2^2}\right) \left(1 + \frac{q_0}{q_1}\right)^2 \cos((q_0(x + y + T) - 2q_1 T)u). \end{aligned}$$

Hence,

$$\begin{aligned} k_\Lambda(x, y) &= \frac{1}{2\pi} \int_{\Lambda^{1/2}} \frac{\vartheta(u, x, y)}{\kappa(u)} du \\ &= \frac{q_0 \Omega^{1/2}}{\pi} \text{sinc}(q_0 \Omega^{1/2}(x - y)) + \frac{1}{4q_0} \left(1 + \frac{q_1^2}{q_2^2}\right) \left(1 - \frac{q_0^2}{q_1^2}\right) J_{\text{real}}(q_0(x + y + T)) \\ &\quad + \frac{1}{8q_0} \left(1 - \frac{q_1^2}{q_2^2}\right) \left(1 - \frac{q_0}{q_1}\right)^2 J_{\text{real}}(q_0(x + y + T) + 2q_1 T) \\ &\quad + \frac{1}{8q_0} \left(1 - \frac{q_1^2}{q_2^2}\right) \left(1 + \frac{q_0}{q_1}\right)^2 J_{\text{real}}(q_0(x + y + T) - 2q_1 T) \\ &= k_{\Lambda, 00}(x, y). \end{aligned}$$

- Suppose $x \leq -\frac{T}{2}$, $-\frac{T}{2} < y \leq \frac{T}{2}$, i.e., $(j, l) = (0, 1)$. Then

$$\begin{aligned} \vartheta(u, x, y) &= \frac{1}{q_0} (\overline{a_0^+(u^2)} e^{-iq_0 x u} + \overline{b_0^+(u^2)} e^{iq_0 x u}) (a_1^+(u^2) e^{iq_1 y u} + b_1^+(u^2) e^{-iq_1 y u}) \\ &\quad + \frac{1}{q_2} e^{iq_0 x u} (a_1^-(u^2) e^{iq_1 y u} + b_1^-(u^2) e^{-iq_1 y u}) \\ &= \frac{\overline{a_0^+(u^2)} a_1^+(u^2)}{q_0} e^{-i(q_0 x - q_1 y)u} + \frac{\overline{a_0^+(u^2)} b_1^+(u^2)}{q_0} e^{-i(q_0 x + q_1 y)u} \\ &\quad + \left(\frac{\overline{b_0^+(u^2)} b_1^+(u^2)}{q_0} + \frac{b_1^-(u^2)}{q_2} \right) e^{i(q_0 x - q_1 y)u} + \left(\frac{\overline{b_0^+(u^2)} a_1^+(u^2)}{q_0} + \frac{a_1^-(u^2)}{q_2} \right) e^{i(q_0 x + q_1 y)u}. \end{aligned}$$

5. Concrete Examples

The coefficients are as follows:

$$\begin{aligned}\frac{\overline{a_0^+(u^2)}a_1^+(u^2)}{q_0} &= \frac{1}{8q_0} \left[\left(1 + \frac{q_1}{q_2}\right)^2 \left(1 + \frac{q_0}{q_1}\right) e^{-i\frac{T}{2}(q_0-q_1)u} + \left(1 - \frac{q_1^2}{q_2^2}\right) \left(1 - \frac{q_0}{q_1}\right) e^{-i\frac{T}{2}(q_0+3q_1)u} \right], \\ \frac{\overline{a_0^+(u^2)}b_1^+(u^2)}{q_0} &= \frac{1}{8q_0} \left[\left(1 - \frac{q_1^2}{q_2^2}\right) \left(1 + \frac{q_0}{q_1}\right) e^{-i\frac{T}{2}(q_0-3q_1)u} + \left(1 - \frac{q_1}{q_2}\right)^2 \left(1 - \frac{q_0}{q_1}\right) e^{-i\frac{T}{2}(q_0+q_1)u} \right], \\ \frac{\overline{b_0^+(u^2)}b_1^+(u^2)}{q_0} + \frac{b_1^-(u^2)}{q_2} &= \frac{1}{8q_0} \left[\left(1 - \frac{q_1^2}{q_2^2}\right) \left(1 - \frac{q_0}{q_1}\right) e^{i\frac{T}{2}(q_0+3q_1)u} + \left(1 + \frac{q_1}{q_2}\right)^2 \left(1 + \frac{q_0}{q_1}\right) e^{i\frac{T}{2}(q_0-q_1)u} \right], \\ \frac{\overline{b_0^+(u^2)}a_1^+(u^2)}{q_0} + \frac{a_1^-(u^2)}{q_2} &= \frac{1}{8q_0} \left[\left(1 - \frac{q_1^2}{q_2^2}\right) \left(1 + \frac{q_0}{q_1}\right) e^{i\frac{T}{2}(q_0-3q_1)u} + \left(1 - \frac{q_1}{q_2}\right)^2 \left(1 - \frac{q_0}{q_1}\right) e^{i\frac{T}{2}(q_0+q_1)u} \right].\end{aligned}$$

Careful expansion and combining relevant terms eventually give

$$\begin{aligned}\vartheta(u, x, y) &= \frac{1}{4q_0} \left(1 + \frac{q_1}{q_2}\right)^2 \left(1 + \frac{q_0}{q_1}\right) \cos\left(\left(q_0\left(x + \frac{T}{2}\right) - q_1\left(y + \frac{T}{2}\right)\right)u\right) \\ &+ \frac{1}{4q_0} \left(1 - \frac{q_1}{q_2}\right)^2 \left(1 - \frac{q_0}{q_1}\right) \cos\left(\left(q_0\left(x + \frac{T}{2}\right) + q_1\left(y + \frac{T}{2}\right)\right)u\right) \\ &+ \frac{1}{4q_0} \left(1 - \frac{q_1^2}{q_2^2}\right) \left(1 + \frac{q_0}{q_1}\right) \cos\left(\left(q_0\left(x + \frac{T}{2}\right) + q_1\left(y - \frac{3T}{2}\right)\right)u\right) \\ &+ \frac{1}{4q_0} \left(1 - \frac{q_1^2}{q_2^2}\right) \left(1 - \frac{q_0}{q_1}\right) \cos\left(\left(q_0\left(x + \frac{T}{2}\right) - q_1\left(y - \frac{3T}{2}\right)\right)u\right).\end{aligned}$$

Consequently,

$$\begin{aligned}k_\Lambda(x, y) &= \frac{1}{4q_0} \left(1 + \frac{q_1}{q_2}\right)^2 \left(1 + \frac{q_0}{q_1}\right) J_{\text{real}}\left(q_0\left(x + \frac{T}{2}\right) - q_1\left(y + \frac{T}{2}\right)\right) \\ &+ \frac{1}{4q_0} \left(1 - \frac{q_1}{q_2}\right)^2 \left(1 - \frac{q_0}{q_1}\right) J_{\text{real}}\left(q_0\left(x + \frac{T}{2}\right) + q_1\left(y + \frac{T}{2}\right)\right) \\ &+ \frac{1}{4q_0} \left(1 - \frac{q_1^2}{q_2^2}\right) \left(1 + \frac{q_0}{q_1}\right) J_{\text{real}}\left(q_0\left(x + \frac{T}{2}\right) + q_1\left(y - \frac{3T}{2}\right)\right) \\ &+ \frac{1}{4q_0} \left(1 - \frac{q_1^2}{q_2^2}\right) \left(1 - \frac{q_0}{q_1}\right) J_{\text{real}}\left(q_0\left(x + \frac{T}{2}\right) - q_1\left(y - \frac{3T}{2}\right)\right) \\ &= k_{\Lambda,01}(x, y).\end{aligned}$$

- Suppose $x \leq -\frac{T}{2}, y > \frac{T}{2}$, i.e., $(j, l) = (0, 2)$. Then

$$\begin{aligned}\vartheta(u, x, y) &= \frac{1}{q_0} \overline{a_0^+(u^2)} e^{-iq_0xu} + \overline{b_0^+(u^2)} e^{iq_0xu} e^{iq_2yu} + \frac{1}{q_2} e^{iq_0xu} \overline{a_2^-(u^2)} e^{iq_2yu} + b_2^-(u^2) e^{-iq_2yu} \\ &= \left(\frac{\overline{b_0^+(u^2)}}{q_0} + \frac{a_2^-(u^2)}{q_2} \right) e^{i(q_0x+q_2y)u} + \frac{\overline{a_0^+(u^2)}}{q_0} e^{-i(q_0x-q_2y)u} + \frac{b_2^-(u^2)}{q_2} e^{i(q_0x-q_2y)u} \\ &= \frac{\overline{a_0^+(u^2)}}{q_0} e^{-i(q_0x-q_2y)u} + \frac{a_0^+(u^2)}{q_0} e^{i(q_0x-q_2y)u}\end{aligned}\tag{5.2.11}$$

by identities (4.3.1) and (4.3.5). Therefore,

$$\begin{aligned}\vartheta(u, x, y) &= \frac{1}{2q_0} \left(1 - \frac{q_1}{q_2}\right) \left(1 - \frac{q_0}{q_1}\right) \cos\left(\left(q_0\left(x + \frac{T}{2}\right) + q_1T - q_2\left(y - \frac{T}{2}\right)\right)u\right) \\ &\quad + \frac{1}{2q_0} \left(1 + \frac{q_1}{q_2}\right) \left(1 + \frac{q_0}{q_1}\right) \cos\left(\left(q_0\left(x + \frac{T}{2}\right) - q_1T - q_2\left(y - \frac{T}{2}\right)\right)u\right)\end{aligned}$$

which implies

$$\begin{aligned}k_\Lambda(x, y) &= \frac{1}{2q_0} \left(1 - \frac{q_1}{q_2}\right) \left(1 - \frac{q_0}{q_1}\right) J_{\text{real}}\left(q_0\left(x + \frac{T}{2}\right) + q_1T - q_2\left(y - \frac{T}{2}\right)\right) \\ &\quad + \frac{1}{2q_0} \left(1 + \frac{q_1}{q_2}\right) \left(1 + \frac{q_0}{q_1}\right) J_{\text{real}}\left(q_0\left(x + \frac{T}{2}\right) - q_1T - q_2\left(y - \frac{T}{2}\right)\right) \\ &= k_{\Lambda,02}(x, y).\end{aligned}$$

- Finally, suppose $-\frac{T}{2} < x, y \leq \frac{T}{2}$, i.e., $(j, l) = (1, 1)$. Then

$$\begin{aligned}\vartheta(u, x, y) &= \frac{1}{q_0} \left(\overline{a_1^+(u^2)} e^{-iq_1xu} + \overline{b_1^+(u^2)} e^{iq_1xu}\right) \left(a_1^+(u^2) e^{iq_1yu} + b_1^+(u^2) e^{-iq_1yu}\right) \\ &\quad + \frac{1}{q_2} \left(\overline{a_1^-(u^2)} e^{-iq_1xu} + \overline{b_1^-(u^2)} e^{iq_1xu}\right) \left(a_1^-(u^2) e^{iq_1yu} + b_1^-(u^2) e^{-iq_1yu}\right) \\ &= \left(\frac{|a_1^+(u^2)|^2}{q_0} + \frac{|a_1^-(u^2)|^2}{q_2}\right) e^{-iq_1(x-y)u} + \left(\frac{|b_1^+(u^2)|^2}{q_0} + \frac{|b_1^-(u^2)|^2}{q_2}\right) e^{iq_1(x-y)u} \\ &\quad + \left(\frac{a_1^+(u^2)\overline{b_1^+(u^2)}}{q_0} + \frac{a_1^-(u^2)\overline{b_1^-(u^2)}}{q_2}\right) e^{iq_1(x+y)u} \\ &\quad + \left(\frac{a_1^+(u^2)\overline{b_1^+(u^2)}}{q_0} + \frac{a_1^-(u^2)\overline{b_1^-(u^2)}}{q_2}\right) e^{-iq_1(x+y)u}.\end{aligned}$$

Upon substituting the corresponding values of the connection coefficients, we have

$$\begin{aligned}\frac{|a_1^+(u^2)|^2}{q_0} + \frac{|a_1^-(u^2)|^2}{q_2} &= \frac{1}{4} \left[\frac{1}{q_0} \left(1 + \frac{q_1}{q_2}\right)^2 + \frac{1}{q_2} \left(1 - \frac{q_1}{q_0}\right)^2 \right] \\ &= \frac{1}{4} \left[\frac{1}{q_0} \left(1 + \frac{q_1^2}{q_2^2}\right) + \frac{1}{q_2} \left(1 + \frac{q_1^2}{q_0^2}\right) \right], \\ \frac{|b_1^+(u^2)|^2}{q_0} + \frac{|b_1^-(u^2)|^2}{q_2} &= \frac{1}{4} \left[\frac{1}{q_0} \left(1 - \frac{q_1}{q_2}\right)^2 + \frac{1}{q_2} \left(1 + \frac{q_1}{q_0}\right)^2 \right] \\ &= \frac{1}{4} \left[\frac{1}{q_0} \left(1 + \frac{q_1^2}{q_2^2}\right) + \frac{1}{q_2} \left(1 + \frac{q_1^2}{q_0^2}\right) \right], \\ \frac{a_1^+(u^2)\overline{b_1^+(u^2)}}{q_0} + \frac{a_1^-(u^2)\overline{b_1^-(u^2)}}{q_2} &= \frac{1}{4} \left[\frac{1}{q_0} \left(1 - \frac{q_1^2}{q_2^2}\right) e^{-iq_1Tu} + \frac{1}{q_2} \left(1 - \frac{q_1^2}{q_0^2}\right) e^{iq_1Tu} \right].\end{aligned}$$

Therefore,

$$\begin{aligned}\vartheta(u, x, y) &= \frac{1}{2} \left[\frac{1}{q_0} \left(1 + \frac{q_1^2}{q_2^2}\right) + \frac{1}{q_2} \left(1 + \frac{q_1^2}{q_0^2}\right) \right] \cos(q_1(x-y)u) \\ &\quad + \frac{1}{2q_0} \left(1 - \frac{q_1^2}{q_2^2}\right) \cos(q_1(x+y-T)u) + \frac{1}{2q_2} \left(1 - \frac{q_1^2}{q_0^2}\right) \cos(q_1(x+y+T)u),\end{aligned}$$

5. Concrete Examples

which means that

$$\begin{aligned} k_\Lambda(x, y) &= \frac{1}{2} \left[\frac{1}{q_0} \left(1 + \frac{q_1^2}{q_2^2} \right) + \frac{1}{q_2} \left(1 + \frac{q_1^2}{q_0^2} \right) \right] J_{\text{real}}(q_1(x - y)) \\ &\quad + \frac{1}{2q_0} \left(1 - \frac{q_1^2}{q_2^2} \right) J_{\text{real}}(q_1(x + y - T)) + \frac{1}{2q_2} \left(1 - \frac{q_1^2}{q_0^2} \right) J_{\text{real}}(q_1(x + y + T)) \\ &= k_{\Lambda,11}(x, y). \end{aligned}$$

The remaining piecewise components follow from the symmetry $k_\Lambda(x, y) = \overline{k_\Lambda(y, x)}$ for all $x, y \in \mathbb{R}$ as well as the aforementioned replacement rules, and so we are done. \square

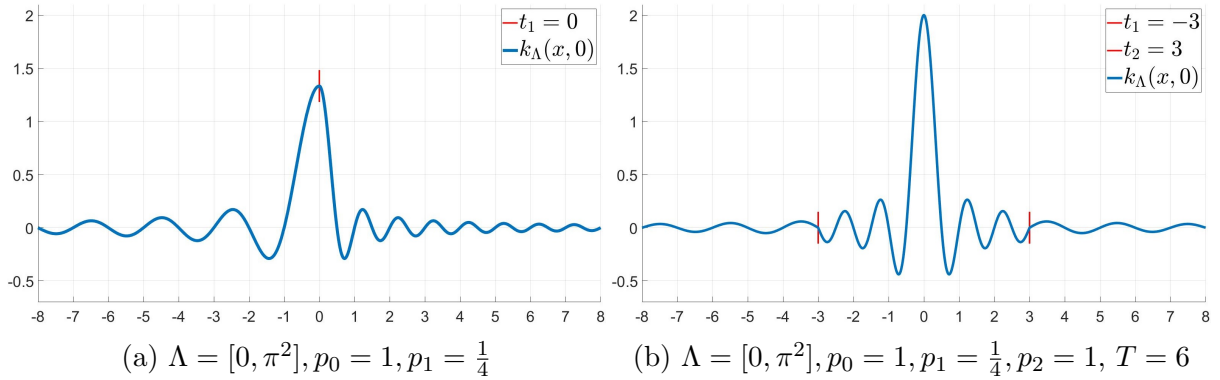


Figure 5.1.: Graph of the reproducing kernel $k_\Lambda(0, \cdot)$ when p has (a) two components, and (b) three components.

Plots of the reproducing kernels are shown in Figure 5.1. We also note the symmetry of the graph in (b) with respect to the y -axis. Theorem 5.2.5 also includes the following degenerate cases:

- If $p_1 = p_2$ ($q_1 = q_2$) and $T > 0$, then p reduces to

$$p(x) = \begin{cases} p_0, & x \leq -\frac{T}{2}, \\ p_1, & x > -\frac{T}{2}. \end{cases}$$

Using the formula (5.2.3) for J_{real} ,

$$\begin{aligned} k_{\Lambda,00}(x, y) &= \frac{q_0 \Omega^{1/2}}{\pi} \text{sinc}(q_0 \Omega^{1/2}(x - y)) + \frac{1}{2q_0} \left(1 - \frac{q_0^2}{q_1^2} \right) J_{\text{real}}(q_0(x + y + T)) \\ &= \frac{q_0 \Omega^{1/2}}{\pi} \text{sinc}(q_0 \Omega^{1/2}(x - y)) + \frac{q_1^2 - q_0^2}{2q_0 q_1^2} \cdot \frac{2q_0^2 q_1^2 \Omega^{1/2}}{\pi(q_0 + q_1)^2} \text{sinc } q_0 \Omega^{1/2}(x + y + T) \\ &= \frac{q_0 \Omega^{1/2}}{\pi} \left(\text{sinc}(q_0 \Omega^{1/2}(x - y)) - \frac{q_0 - q_1}{q_0 + q_1} \text{sinc } q_0 \Omega^{1/2}(x + y + T) \right). \end{aligned}$$

By performing similar computations on the remaining piecewise components $k_{\Lambda,jl}$

5.2. Case $n = 2$: three-component p

of k_Λ , one can verify that

$$k_\Lambda(x, y) = \begin{cases} \frac{q_0\Omega^{1/2}}{\pi} \left(\operatorname{sinc} q_0\Omega^{1/2}(x - y) - \frac{q_0 - q_1}{q_0 + q_1} \operatorname{sinc} q_0\Omega^{1/2}(x + y + T) \right), & x, y \leq -\frac{T}{2}, \\ \frac{q_1\Omega^{1/2}}{\pi} \left(\operatorname{sinc} q_1\Omega^{1/2}(x - y) + \frac{q_0 - q_1}{q_0 + q_1} \operatorname{sinc} q_1\Omega^{1/2}(x + y + T) \right), & x, y > -\frac{T}{2}, \\ \frac{2q_0q_1\Omega^{1/2}}{\pi(q_0 + q_1)} \operatorname{sinc} \Omega^{1/2} \left(q_0 \left(x + \frac{T}{2} \right) - q_1 \left(y + \frac{T}{2} \right) \right), & x \leq -\frac{T}{2}, y > -\frac{T}{2}, \\ \frac{2q_0q_1\Omega^{1/2}}{\pi(q_0 + q_1)} \operatorname{sinc} \Omega^{1/2} \left(q_1 \left(x + \frac{T}{2} \right) - q_0 \left(y + \frac{T}{2} \right) \right), & x > -\frac{T}{2}, y \leq -\frac{T}{2}. \end{cases}$$

This is precisely the toy example with shifts $x \mapsto x + \frac{T}{2}, y \mapsto y + \frac{T}{2}$.

- If $p_0 = p_1$ ($q_0 = q_1$) and $T > 0$, then p reduces to

$$p(x) = \begin{cases} p_1, & x \leq \frac{T}{2}, \\ p_2, & x > \frac{T}{2}. \end{cases}$$

Using the formula (5.2.4) for J_{real} , we analogously obtain

$$k_\Lambda(x, y) = \begin{cases} \frac{q_1\Omega^{1/2}}{\pi} \left(\operatorname{sinc} q_1\Omega^{1/2}(x - y) - \frac{q_1 - q_2}{q_1 + q_2} \operatorname{sinc} q_1\Omega^{1/2}(x + y - T) \right), & x, y \leq \frac{T}{2}, \\ \frac{q_2\Omega^{1/2}}{\pi} \left(\operatorname{sinc} q_2\Omega^{1/2}(x - y) + \frac{q_1 - q_2}{q_1 + q_2} \operatorname{sinc} q_2\Omega^{1/2}(x + y - T) \right), & x, y > \frac{T}{2}, \\ \frac{2q_1q_2\Omega^{1/2}}{\pi(q_1 + q_2)} \operatorname{sinc} \Omega^{1/2} \left(q_1 \left(x - \frac{T}{2} \right) - q_2 \left(y - \frac{T}{2} \right) \right), & x \leq \frac{T}{2}, y > \frac{T}{2}, \\ \frac{2q_1q_2\Omega^{1/2}}{\pi(q_1 + q_2)} \operatorname{sinc} \Omega^{1/2} \left(q_2 \left(x - \frac{T}{2} \right) - q_1 \left(y - \frac{T}{2} \right) \right), & x > \frac{T}{2}, y \leq \frac{T}{2}. \end{cases}$$

This is the toy example with shifts $x \mapsto x - \frac{T}{2}, y \mapsto y - \frac{T}{2}$.

- If $p_0 = p_1 = p_2$ ($q_0 = q_1 = q_2$), then all the terms of k_Λ collapse to

$$k_\Lambda(x, y) = \frac{q_0\Omega^{1/2}}{\pi} \operatorname{sinc}(q_0\Omega^{1/2}(x - y)), \quad x, y \in \mathbb{R}.$$

Again, this agrees to the well-known reproducing kernel of $PW_{q_0\Omega^{1/2}}(\mathbb{R})$ and is consistent with the degenerate case of $n = 1$.

In summary, we have shown that for two-component piecewise constant functions with an arbitrary knot, explicit formulas for the reproducing kernel k_Λ of $PW_\Lambda(A_p)$ can be derived. This follows from the fact that the integral J can be expressed using a cardinal sine function. Moreover, the reproducing kernel of $PW_{[0, \Omega]}(A_p)$ is given by a shifted version of the toy example. On the other hand, for three-component piecewise constant functions with symmetric knots, we were able to write J as an infinite sum that converges at a geometric rate. We can then use such a formula to numerically compute $J(s)$ for any $s \in \mathbb{R}$ up to any degree of accuracy. Hence, this evaluation method is better than the numerical quadratures for oscillatory integrals where high accuracy is only guaranteed in the highly oscillatory case. In turn, numerical calculations involving the reproducing kernel are now feasible and, more importantly, accurate up to tolerance.

6. Density theorems in $PW_\Lambda(A_p)$

In this chapter, we derive density conditions for sampling and interpolation in $PW_\Lambda(A_p)$ with piecewise constant p using techniques in [31]. Beurling and Landau's fundamental ideas on the density theorem can be adapted to many situations, particularly in the Hilbert space setting. It was observed in [31] that in a number of density theorems found in the literature, the proofs are rather similar and the common approach is to treat function spaces under study as reproducing kernel Hilbert spaces. These observations led the authors to investigate conditions for which a universal density theorem in reproducing kernel Hilbert spaces can be formulated. They presented an abstract approach to a general density theorem by showing that with natural conditions on both the geometry of the space and the reproducing kernel, necessary density conditions on sets of stable sampling and sets of interpolation can be derived. Moreover, a precise definition of a critical density and its existence were established. In the case of $PW_\Lambda(A_p)$ with piecewise constant p , we show that the natural conditions are indeed satisfied and an exact value for the critical density can be calculated. A density theorem for such variable bandwidth spaces immediately follows.

6.1. Density theorems for sampling and interpolation in reproducing kernel Hilbert spaces - variable bandwidth version

We first collect the aforementioned natural conditions in [31], stated in a form that is applicable for our purpose.

- **Assumptions on the metric and measure:** Let (\mathbb{R}, d, μ_p) be the metric measure space where $d : \mathbb{R} \times \mathbb{R} \rightarrow [0, \infty)$ is the standard metric $d(x, y) = |x - y|$, $x, y \in \mathbb{R}$ and μ_p is the positive measure

$$\mu_p(I) = \int_I \frac{dx}{\sqrt{p(x)}} \quad (6.1.1)$$

defined on the Borel σ -algebra of \mathbb{R} . The assumptions on the geometry of (\mathbb{R}, d, μ_p) are as follows:

- (a) *Open balls have finite μ_p -measure:* The metric d is $\mu_p \otimes \mu_p$ -measurable and the open balls

$$B_r(x) = \{y \in \mathbb{R} : d(x, y) < r\}$$

have finite μ_p -measure for all $x \in \mathbb{R}$, $r > 0$.

- (b) *Non-degeneracy of balls:* There exists $r > 0$ such that $\inf_{x \in \mathbb{R}} \mu_p(B_r(x)) > 0$.

6. Density theorems in $PW_\Lambda(A_p)$

- (c) *Weak annular decay property*: Spherical shells have smaller volumes compared to open balls, i.e.,

$$\limsup_{r \rightarrow \infty} \sup_{x \in \mathbb{R}} \frac{\mu_p(B_r(x) \setminus B_{r-1}(x))}{\mu_p(B_r(x))} = 0.$$

- **Assumptions on the reproducing kernel**: We consider a reproducing kernel Hilbert space $\mathcal{H} \subseteq L^2(\mathbb{R}, \mu_p)$ with inner product $\langle \cdot, \cdot \rangle_{\mathcal{H}}$ and reproducing kernel $k(x, y)$, i.e., for each $x \in \mathbb{R}$,

$$f(x) = \int_{\mathbb{R}} f(y) \overline{k(x, y)} d\mu_p(y) = \langle f, k_x \rangle_{\mathcal{H}}$$

where $k_x(y) = k(x, y) = \overline{k(y, x)}$ for all $y \in \mathbb{R}$. Assume k satisfies the following properties:

- (d) *Boundedness of diagonal*: There exist constants $C_1, C_2 > 0$ such that

$$C_1 \leq k(x, x) \leq C_2$$

for all $x \in \mathbb{R}$.

- (e) *Weak localization property*: For every $\epsilon > 0$, there exists $r(\epsilon) > 0$ such that

$$\sup_{x \in \mathbb{R}} \int_{\mathbb{R} \setminus B_{r(\epsilon)}(x)} |k(x, y)|^2 d\mu_p(y) < \epsilon^2.$$

- (f) *Homogeneous approximation property*: Let $X \subseteq \mathbb{R}$ such that $\{k(x, \cdot) : x \in X\}$ is a **Bessel sequence** for \mathcal{H} , i.e., for some $C > 0$,

$$\sum_{x \in X} |f(x)|^2 \leq C \|f\|_{\mathcal{H}}^2$$

for all $f \in \mathcal{H}$. Then for every $\epsilon > 0$ there exists $r(\epsilon) > 0$ such that

$$\sup_{y \in \mathbb{R}} \sum_{\substack{x \in X \\ |x-y| > r(\epsilon)}} |k(x, y)|^2 < \epsilon^2.$$

We also define the **upper, resp. lower Beurling densities**¹⁰

$$D_p^+(X) = \limsup_{r \rightarrow \infty} \sup_{x \in \mathbb{R}} \frac{\#(X \cap B_r(x))}{\mu_p(B_r(x))}, \quad D_p^-(X) = \liminf_{r \rightarrow \infty} \inf_{x \in \mathbb{R}} \frac{\#(X \cap B_r(x))}{\mu_p(B_r(x))} \quad (6.1.2)$$

of a discrete set X with respect to μ_p as well as the **upper, resp. lower averaged traces** of k given by

$$\begin{aligned} \text{tr}^+ &= \limsup_{r \rightarrow \infty} \sup_{x \in \mathbb{R}} \frac{1}{\mu_p(B_r(x))} \int_{B_r(x)} k(y, y) d\mu_p(y), \\ \text{tr}^- &= \liminf_{r \rightarrow \infty} \inf_{x \in \mathbb{R}} \frac{1}{\mu_p(B_r(x))} \int_{B_r(x)} k(y, y) d\mu_p(y). \end{aligned}$$

The following special case of [31, Thm. 2.2] will be used to derive the desired density theorems in $PW_\Lambda(A_p)$ with piecewise constant p .

¹⁰This definition of $D_p^\pm(X)$ is equivalent to the ones given in (3.2.2) and (3.2.3).

Theorem 6.1.1. *Let p be a piecewise constant function. Assume $\mathcal{H} \subseteq L^2(\mathbb{R}, \mu_p)$ is a reproducing kernel Hilbert space with reproducing kernel k and satisfies conditions (a)-(f).*

(i) *If X is a set of stable sampling for \mathcal{H} , then*

$$D_p^-(X) \geq \text{tr}^- \quad \text{and} \quad D_p^+(X) \geq \text{tr}^+.$$

(ii) *If X is a set of interpolation for \mathcal{H} , then*

$$D_p^-(X) \leq \text{tr}^- \quad \text{and} \quad D_p^+(X) \leq \text{tr}^+.$$

This result saves time and effort in deriving a density theorem in the reproducing kernel Hilbert space \mathcal{H} since we only need to verify six conditions as well as estimate the critical density using averaged traces. We shall see that we obtain the same conclusions as in Theorem 3.2.1 but with notable differences in the proofs. In particular, we do not transform τ_p into its Schrödinger form $\tilde{\tau}_q$ given at the beginning of Section 2.2 since we cannot do so for a piecewise constant p .

6.2. Conditions on the geometry of (\mathbb{R}, d, μ_p)

For a piecewise constant p , the geometric assumptions (a), (b) and (c) are immediate consequences of the equivalence¹¹ of μ_p and the Lebesgue measure.

Lemma 6.2.1. *Let p be a piecewise constant function. Then the metric measure space (\mathbb{R}, d, μ_p) with standard metric d and measure μ_p in (6.1.1) satisfies (a), (b) and (c).*

Proof. Let p be an $(n + 1)$ -component piecewise function for some $n \in \mathbb{N}$. Since p takes only finitely many values $\{p_k\}_{k=0}^n$, it follows that with $q_k = p_k^{-1/2}$,

$$\min_{0 \leq k \leq n} q_k |E| \leq \mu_p(E) \leq \max_{0 \leq k \leq n} q_k |E| \quad (6.2.1)$$

for any Borel set $E \subseteq \mathbb{R}$. The three geometric properties now follow.

(i) The continuity of d in \mathbb{R}^2 implies d is $\mu_p \otimes \mu_p$ -measurable. Moreover, it is immediate from the right-hand inequality of (6.2.1) that $\mu_p(B_r(x)) < \infty$ for all $x \in \mathbb{R}$, $r > 0$.

(ii) Non-degeneracy of balls holds for any $r > 0$ from the left-hand inequality of (6.2.1).

(iii) For any $r > 0$,

$$0 \leq \sup_{x \in \mathbb{R}} \frac{\mu_p(B_r(x) \setminus B_{r-1}(x))}{\mu_p(B_r(x))} \leq \max_{0 \leq j, k \leq n} \frac{q_j}{q_k} \sup_{x \in \mathbb{R}} \frac{|B_r(x) \setminus B_{r-1}(x)|}{|B_r(x)|} = \frac{1}{r} \max_{0 \leq j, k \leq n} \frac{q_j}{q_k}.$$

Taking the limit as $r \rightarrow \infty$ proves the weak annular decay property. □

In fact, Lemma 6.2.1 applies to any parametrizing function p that is bounded and bounded away from zero. Certainly, such a p implies that the Radon-Nikodym derivative $\frac{d\mu_p}{dm} = p^{-1/2}$ of μ_p with respect to the Lebesgue measure m is bounded and bounded away from zero.

¹¹We say two σ -finite measures μ and ν on a measurable space (X, \mathcal{E}) are equivalent if $\mu \ll \nu$ and $\nu \ll \mu$. In other words, μ and ν have the same collection of null sets. Moreover, it can be shown that $\frac{d\mu}{d\nu} \cdot \frac{d\nu}{d\mu} = 1$ a.e.

6.3. Properties of the reproducing kernel of $PW_\Lambda(A_p)$

We now go to assumptions (d), (e) and (f) on the reproducing kernel. Observe that we cannot directly apply Theorem 6.1.1 to $PW_\Lambda(A_p) \subseteq L^2(\mathbb{R})$ since the assumptions require $\mathcal{H} \subseteq L^2(\mathbb{R}, \mu_p)$. Again, the equivalence of μ_p and the Lebesgue measure ensures that this will not be an issue.

Proposition 6.3.1. *Let $\Lambda \subset \mathbb{R}_0^+$ and p a piecewise constant function. Then there exists an isometric isomorphism $\Psi : L^2(\mathbb{R}) \rightarrow L^2(\mathbb{R}, d\mu_p)$ such that $\Psi(PW_\Lambda(A_p))$ is a reproducing kernel Hilbert space. Moreover, if k_Λ is the reproducing kernel of $PW_\Lambda(A_p)$, then*

$$k_\Psi(x, y) = \sqrt[4]{p(x)p(y)}k_\Lambda(x, y), \quad x, y \in \mathbb{R}$$

is the reproducing kernel of $\Psi(PW_\Lambda(A_p))$ and satisfies conditions (d), (e) and (f) if and only if k_Λ does.

Proof. Consider the map

$$\Psi : L^2(\mathbb{R}) \rightarrow L^2(\mathbb{R}, d\mu_p), \quad \Psi f = \sqrt[4]{p}f, f \in L^2(\mathbb{R})$$

induced by the Radon-Nikodym derivative $\frac{dm}{d\mu_p} = \sqrt{p}$ of the Lebesgue measure m with respect to μ_p . Then Ψ is an isometric isomorphism between $L^2(\mathbb{R})$ and $L^2(\mathbb{R}, d\mu_p)$, since for $f, g \in L^2(\mathbb{R})$,

$$\langle \Psi f, \Psi g \rangle_{L^2(\mathbb{R}, d\mu_p)} = \int_{\mathbb{R}} \sqrt[4]{p(x)}f(x) \overline{\sqrt[4]{p(x)}g(x)} d\mu_p(x) = \int_{\mathbb{R}} f(x) \overline{g(x)} dx = \langle f, g \rangle_{L^2(\mathbb{R})}.$$

We can then identify $PW_\Lambda(A_p)$ as the subspace $\Psi(PW_\Lambda(A_p))$ of $L^2(\mathbb{R}, d\mu_p)$. Moreover, $\Psi(PW_\Lambda(A_p))$ is a reproducing kernel Hilbert space whose reproducing kernel k_Ψ we shall derive as in [31, Sec. 3.2]. If $f \in PW_\Lambda(A_p)$, then for all $x \in \mathbb{R}$,

$$\Psi f(x) = \sqrt[4]{p(x)}f(x) = \sqrt[4]{p(x)}\langle f, k_\Lambda(x, \cdot) \rangle_{L^2(\mathbb{R})} = \sqrt[4]{p(x)}\langle \Psi f, \Psi k_\Lambda(x, \cdot) \rangle_{L^2(\mathbb{R}, d\mu_p)}.$$

Thus, $\Psi(PW_\Lambda(A_p))$ is a reproducing kernel Hilbert space with

$$k_\Psi(x, y) = \sqrt[4]{p(x)p(y)}k_\Lambda(x, y), \quad x, y \in \mathbb{R}$$

as its reproducing kernel. As a consequence, we can rewrite the following expressions of k_Ψ in terms of k_Λ :

(i) The diagonal of k_Ψ is

$$k_\Psi(x, x) = \sqrt{p(x)}k_\Lambda(x, x).$$

Moreover, for any Borel set $I \subseteq \mathbb{R}$,

$$\int_I k_\Lambda(y, y) dy = \int_I k_\Psi(y, y) d\mu_p(y). \quad (6.3.1)$$

(ii) For the weak localization property,

$$\int_{|x-y|>r(\epsilon)} |k_\Psi(x, y)|^2 d\mu_p(y) = \sqrt{p(x)} \int_{|x-y|>r(\epsilon)} |k_\Lambda(x, y)|^2 dy.$$

6.3. Properties of the reproducing kernel of $PW_\Lambda(A_p)$

(iii) For the homogeneous approximation property,

$$\sum_{\substack{x \in X \\ |x-y| > r(\epsilon)}} |k_\Psi(x, y)|^2 = \sqrt{p(y)} \sum_{\substack{x \in X \\ |x-y| > r(\epsilon)}} \sqrt{p(x)} |k_\Lambda(x, y)|^2.$$

Since p is bounded and bounded away from zero, we conclude that k_Ψ satisfies the kernel properties (d), (e) and (f) if and only if k_Λ does. \square

It is now clear that $\mathcal{H} = \Psi(PW_\Lambda(A_p)) \subseteq L^2(\mathbb{R}, d\mu_p)$ is the correct space to apply Theorem 6.1.1. In addition, Proposition 6.3.1 implies that we can still exclusively use the more convenient reproducing kernel k_Λ in subsequent calculations since we have the isometric isomorphism Ψ to correctly translate the results to k_Ψ .

6.3.1. The diagonal and averaged traces

In axiomatic approach the diagonal $k_\Lambda(x, x)$, $x \in \mathbb{R}$ of the reproducing kernel plays a major role in deriving the necessary density conditions. A few results can be derived immediately from Chapter 4.

Lemma 6.3.2 (Boundedness of the diagonal). *Let $\Lambda \subset \mathbb{R}_0^+$ be of finite measure, p a piecewise constant function and k_Λ the reproducing kernel for $PW_\Lambda(A_p)$. Then there exist constants $C_1, C_2 > 0$ such that*

$$C_1 \leq k_\Lambda(x, x) \leq C_2$$

for all $x \in \mathbb{R}$.

Proof. The uniform boundedness of k_Λ in \mathbb{R}^2 (hence the existence of C_2) follows from the uniform boundedness of solutions by Lemma 4.2.6 and the reproducing kernel k_Λ in Theorem 4.4.1. On the other hand, the lower bound C_1 can be obtained using formula (4.4.4) for k_Λ :

$$\begin{aligned} k_\Lambda(x, x) &= \frac{1}{2\pi} \int_{\Lambda^{1/2}} \frac{\frac{1}{q_0} |\Phi^+(u^2, x)|^2 + \frac{1}{q_n} |\Phi^-(u^2, x)|^2}{\kappa(u)} du \\ &\geq \frac{1}{2\pi q_0} \int_{\Lambda^{1/2}} \frac{|\Phi^+(u^2, x)|^2}{\kappa(u)} du \\ &\geq \min_{0 \leq j \leq n} \inf_{x \in I_j} \frac{1}{2\pi q_0} \int_{\Lambda^{1/2}} \frac{|a_j^+(u^2) e^{iq_j x u} + b_j^+(u^2) e^{-iq_j x u}|^2}{\kappa(u)} du \\ &\geq \min_{0 \leq j \leq n} \frac{1}{2\pi q_0} \int_{\Lambda^{1/2}} \frac{||a_j^+(u^2)| - |b_j^+(u^2)||^2}{\kappa(u)} du = C_1. \end{aligned}$$

Since for all $u \in (0, \infty)$, $|a_j^+(u^2)| \neq |b_j^+(u^2)|$ by (4.3.3) and $\kappa(u) \geq \frac{1}{q_0 q_n} > 0$ by (4.3.11), we conclude that $C_1 > 0$. \square

6. Density theorems in $PW_\Lambda(A_p)$

Next, recall from Theorem 6.1.1 that the critical density can be derived or estimated using the upper and lower averaged traces

$$\mathrm{tr}^+ = \limsup_{r \rightarrow \infty} \sup_{x \in \mathbb{R}} \frac{1}{\mu_p(B_r(x))} \int_{B_r(x)} k_\Psi(y, y) d\mu_p(y),$$

$$\mathrm{tr}^- = \liminf_{r \rightarrow \infty} \inf_{x \in \mathbb{R}} \frac{1}{\mu_p(B_r(x))} \int_{B_r(x)} k_\Psi(y, y) d\mu_p(y)$$

of k_Ψ , respectively, which are invariants of $\Psi(PW_\Lambda(A_p))$. By (6.3.1), the averaged traces can be calculated using k_Λ , i.e.,

$$\mathrm{tr}^+ = \limsup_{r \rightarrow \infty} \sup_{x \in \mathbb{R}} \frac{1}{\mu_p(B_r(x))} \int_{B_r(x)} k_\Lambda(y, y) dy, \quad (6.3.2)$$

$$\mathrm{tr}^- = \liminf_{r \rightarrow \infty} \inf_{x \in \mathbb{R}} \frac{1}{\mu_p(B_r(x))} \int_{B_r(x)} k_\Lambda(y, y) dy. \quad (6.3.3)$$

We first prepare the known expression (4.4.4) to evaluate the diagonal of k_Λ . Fix $y \in \mathbb{R}$. Then there exists $0 \leq j \leq n$ such that $y \in I_j$. Recall the notation

$$\vartheta(u, x, y) = \frac{1}{q_0} \overline{\Phi^+(u^2, x)} \Phi^+(u^2, y) + \frac{1}{q_n} \overline{\Phi^-(u^2, x)} \Phi^-(u^2, y), \quad x, y \in \mathbb{R}.$$

Setting $x = y$ in ϑ yields

$$\begin{aligned} \vartheta(u, y, y) &= \frac{1}{q_0} |\Phi^+(u^2, y)|^2 + \frac{1}{q_n} |\Phi^-(u^2, y)|^2 \\ &= \frac{1}{q_0} |a_j^+(u^2) e^{iuq_j y} + b_j^+(u^2) e^{-iuq_j y}|^2 + \frac{1}{q_n} |a_j^-(u^2) e^{iuq_j y} + b_j^-(u^2) e^{-iuq_j y}|^2 \\ &= \left(\frac{|a_j^+(u^2)|}{q_0} + \frac{|b_j^+(u^2)|}{q_0} \right) + \left(\frac{|a_j^-(u^2)|}{q_n} + \frac{|b_j^-(u^2)|}{q_n} \right) \\ &\quad + 2\mathrm{Re} \left[\left(\frac{\overline{a_j^+(u^2)} b_j^+(u^2)}{q_0} + \frac{\overline{a_j^-(u^2)} b_j^-(u^2)}{q_n} \right) e^{-2iuq_j y} \right]. \end{aligned}$$

By (4.3.4),

$$\vartheta(u, y, y) = 2 \left(\frac{|a_j^+(u^2)|}{q_0} + \frac{|a_j^-(u^2)|}{q_n} \right) + 2\mathrm{Re} \left[\left(\frac{\overline{a_j^+(u^2)} b_j^+(u^2)}{q_0} + \frac{\overline{a_j^-(u^2)} b_j^-(u^2)}{q_n} \right) e^{-2iuq_j y} \right].$$

Define for $0 \leq j \leq n$ and $u \in (0, \infty)$ the auxiliary functions

$$\begin{aligned} h_j^{(1)}(u) &= \frac{|a_j^+(u^2)|}{q_0} + \frac{|a_j^-(u^2)|}{q_n} \\ h_j^{(2)}(u) &= \frac{\overline{a_j^+(u^2)} b_j^+(u^2)}{q_0} + \frac{\overline{a_j^-(u^2)} b_j^-(u^2)}{q_n}, \end{aligned}$$

As a consequence of Lemma 4.2.5, $h_j^{(1)}$ and $h_j^{(2)}$ are bounded on $(0, \infty)$ for $0 \leq j \leq n$. By (4.3.11), the integrals

$$\|h_j^{(r)}/\kappa\|_{L^1(\Lambda^{1/2})} = \int_{\Lambda^{1/2}} \frac{|h_j^{(r)}(u)|}{\kappa(u)} du, \quad 0 \leq j \leq n, r = 1, 2$$

are finite. We now have the following expression for the diagonal of k_Λ .

6.3. Properties of the reproducing kernel of $PW_\Lambda(A_p)$

Lemma 6.3.3. *Let $\Lambda \subset \mathbb{R}_0^+$ be of finite measure, p an $(n+1)$ -piecewise constant function for some $n \in \mathbb{N}$, and k_Λ the reproducing kernel for $PW_\Lambda(A_p)$. If $y \in I_j$ for some $0 \leq j \leq n$, then*

$$k_\Lambda(y, y) = \frac{1}{\pi} \int_{\Lambda^{1/2}} \frac{h_j^{(1)}(u)}{\kappa(u)} du + \frac{1}{\pi} \operatorname{Re} \mathcal{F} \left(\frac{h_j^{(2)}}{\kappa} \cdot \chi_{\Lambda^{1/2}} \right) (2q_j y). \quad (6.3.4)$$

Proof. Fix $y \in I_j$ for some $0 \leq j \leq n$. Then for $u \in (0, \infty)$,

$$\vartheta(u, y, y) = 2h_j^{(1)}(u) + 2\operatorname{Re}(h_j^{(2)}(u)e^{-2iq_j y u}).$$

Using the formula (4.4.6) for k_Λ , we have for fixed $y \in I_j$, $0 \leq j \leq n$,

$$\begin{aligned} k_\Lambda(y, y) &= \frac{1}{2\pi} \int_{\Lambda^{1/2}} \frac{\vartheta(u, y, y)}{\kappa(u)} du \\ &= \frac{1}{\pi} \int_{\Lambda^{1/2}} \frac{h_j^{(1)}(u)}{\kappa(u)} du + \frac{1}{\pi} \int_{\Lambda^{1/2}} \frac{\operatorname{Re}(h_j^{(2)}(u)e^{-2iq_j y u})}{\kappa(u)} du \\ &= \frac{1}{\pi} \int_{\Lambda^{1/2}} \frac{h_j^{(1)}(u)}{\kappa(u)} du + \frac{1}{\pi} \operatorname{Re} \left(\int_{\Lambda^{1/2}} \frac{h_j^{(2)}(u)e^{-2iq_j y u}}{\kappa(u)} du \right) \\ &= \frac{1}{\pi} \int_{\Lambda^{1/2}} \frac{h_j^{(1)}(u)}{\kappa(u)} du + \frac{1}{\pi} \operatorname{Re} \mathcal{F} \left(\frac{h_j^{(2)}}{\kappa} \cdot \chi_{\Lambda^{1/2}} \right) (2q_j y) \end{aligned}$$

as claimed. □

Finally, if p is an $(n+1)$ -piecewise constant function for some $n \in \mathbb{N}$ with components $\{p_k\}_{k=0}^n$, the measure $\mu_p(E)$ of a Borel set $E \subseteq \mathbb{R}$ is given by

$$\mu_p(E) = \sum_{k=0}^n q_k |E \cap I_k|, \quad q_k = p_k^{-1/2}.$$

The following theorem will be our main tool to compute the critical density in the next section.

Theorem 6.3.4. *Let $\Lambda \subset \mathbb{R}_0^+$ be of finite measure, p a piecewise constant function and k_Λ the reproducing kernel of $PW_\Lambda(A_p)$. Suppose I is a large interval such that $I \not\subset [t_1, t_n]$. Then there exists $C \geq 0$ independent of I such that*

$$\left| \frac{1}{\mu_p(I)} \int_I k_\Lambda(y, y) dy - \frac{|\Lambda^{1/2}|}{\pi} \right| \leq \frac{C}{\sqrt{\mu_p(I)}}.$$

In particular,

$$\operatorname{tr}^\pm = \frac{|\Lambda^{1/2}|}{\pi}.$$

Proof. Let p be an $(n+1)$ -component piecewise constant function for some $n \in \mathbb{N}$ with knots $\{t_k\}_{k=1}^n$. Since μ_p is equivalent to the Lebesgue measure, it suffices to consider a large, closed interval $I = [\alpha, \beta]$, $-\infty < \alpha < \beta < \infty$ such that $I \not\subset [t_1, t_n]$. Then

6. Density theorems in $PW_\Lambda(A_p)$

$I \cap (I_0 \cup I_n) \neq \emptyset$, i.e., I intersects I_0 or I_n . As the following computations contain several terms, most of which are irrelevant, we use $C_k \in \mathbb{R}$ to denote some constants in the course of the proof. First, consider the case when I intersects both I_0 and I_n , i.e., $[t_1, t_n] \subset I$. Then the μ_p -measure of I is

$$\begin{aligned} \mu_p(I) &= [q_0(t_1 - \alpha) + q_n(\beta - t_n)] + \sum_{j=1}^{n-1} q_j(t_{j+1} - t_j) \\ &= [q_0(t_1 - \alpha) + q_n(\beta - t_n)] + C_0. \end{aligned}$$

It is clear from (6.2.1) that $\mu_p(I)$ is large if and only if $|I|$ is large. We start from Lemma 6.3.3 by working on the terms of k_Λ separately. Integrating the first term of $k_\Lambda(y, y)$ (which is independent of y but dependent on I_j) in (6.3.4) with respect to y over the whole interval I yields

$$\begin{aligned} \tilde{T}_1(I) &= \frac{1}{\pi} \sum_{j=0}^n \int_{[\alpha, \beta] \cap I_j} \int_{\Lambda^{1/2}} \frac{h_j^{(1)}(u)}{\kappa(u)} du dy \\ &= \frac{t_1 - \alpha}{\pi} \int_{\Lambda^{1/2}} \frac{h_0^{(1)}(u)}{\kappa(u)} du + \frac{\beta - t_n}{\pi} \int_{\Lambda^{1/2}} \frac{h_n^{(1)}(u)}{\kappa(u)} du + C_1. \end{aligned}$$

Observe that

$$h_0^{(1)}(u) = \frac{|a_0^+(u^2)|^2}{q_0} + \frac{|a_0^-(u^2)|^2}{q_n}$$

and by identity (4.3.4) with $j = n$,

$$h_n^{(1)}(u) = \frac{|a_n^+(u^2)|^2}{q_0} + \frac{|a_n^-(u^2)|^2}{q_n} = \frac{|b_n^+(u^2)|^2}{q_0} + \frac{|b_n^-(u^2)|^2}{q_n}.$$

From the initial conditions $a_0^- = b_n^+ = 0$, $a_n^+ = b_0^- = 1$, we see that

$$h_0^{(1)}(u) = \frac{|a_0^+(u^2)|^2}{q_0}, \quad h_n^{(1)}(u) = \frac{|b_n^-(u^2)|^2}{q_n}$$

and hence, by definition of κ in (4.3.11), we have

$$h_0^{(1)}(u) = q_0 \kappa(u), \quad h_n^{(1)}(u) = q_n \kappa(u).$$

Thus,

$$\tilde{T}_1(I) = [q_0(t_1 - \alpha) + q_n(\beta - t_n)] \frac{|\Lambda^{1/2}|}{\pi} + C_1 = \mu_p(I) \frac{|\Lambda^{1/2}|}{\pi} - C_0 \frac{|\Lambda^{1/2}|}{\pi} + C_1$$

which in turn gives the estimate

$$T_1(I) = \left| \frac{\tilde{T}_1(I)}{\mu_p(I)} - \frac{|\Lambda^{1/2}|}{\pi} \right| = \frac{1}{\mu_p(I)} \left| \frac{|\Lambda^{1/2}|}{\pi} C_0 - C_1 \right| \leq \frac{C_2}{\sqrt{\mu_p(I)}}. \quad (6.3.5)$$

6.3. Properties of the reproducing kernel of $PW_\Lambda(A_p)$

For the second term, we make a similar computation. Let

$$\begin{aligned}\tilde{T}_2(I) &= \frac{1}{\pi} \sum_{j=1}^n \int_{[\alpha, \beta] \cap I_j} \operatorname{Re} \mathcal{F} \left(\frac{h_j^{(2)}}{\kappa} \cdot \chi_{\Lambda^{1/2}} \right) (2q_j y) dy \\ &= \frac{1}{\pi} \operatorname{Re} \left(\int_\alpha^{t_1} \int_{\Lambda^{1/2}} \frac{h_0^{(2)}(u) e^{-2iq_0 y u}}{\kappa(u)} du dy + \int_{t_n}^\beta \int_{\Lambda^{1/2}} \frac{h_n^{(2)}(u) e^{-2iq_n y u}}{\kappa(u)} du dy \right) + C_3.\end{aligned}$$

By interchanging the order of integration and performing the innermost integral on each of these integrals, we have

$$\begin{aligned}\tilde{T}_2(I) &= \frac{1}{\pi} \operatorname{Re} \int_{\Lambda^{1/2}} \frac{h_0^{(2)}(u) e^{-2iq_0(t_1 + \alpha)u}}{\kappa(u)} \cdot \frac{\sin(q_0(t_1 - \alpha)u)}{q_0 u} du \\ &\quad + \frac{1}{\pi} \operatorname{Re} \int_{\Lambda^{1/2}} \frac{h_n^{(2)}(u) e^{-2iq_n(\beta + t_n)u}}{\kappa(u)} \cdot \frac{\sin(q_n(\beta - t_n)u)}{q_n u} du + C_3.\end{aligned}$$

Considering integrals of the form

$$\mathcal{I}_j = \int_{\Lambda^{1/2}} \frac{h_j^{(2)}(u) e^{-2iq(b+a)u}}{\kappa(u)} \cdot \frac{\sin(q(b-a)u)}{qu} du$$

for $0 < a < b$ and $0 \leq j \leq n$, the following estimate follows from Cauchy-Schwarz inequality:

$$|\mathcal{I}_j| \leq \|h_j^{(2)}/\kappa\|_{L^2(\Lambda^{1/2})} \cdot \left(\frac{b-a}{q} \int_{q(b-a)\Lambda^{1/2}} \frac{\sin^2 \omega}{\omega^2} d\omega \right)^{1/2} \leq \left(\frac{(b-a)\pi}{q} \right)^{1/2} \|h_j^{(2)}/\kappa\|_{L^2(\Lambda^{1/2})}.$$

Therefore, as the norms above are finite, we have

$$\begin{aligned}|\tilde{T}_2(I)| &\leq \frac{1}{\sqrt{\pi}} \left\{ \left(\frac{t_1 - \alpha}{q_0} \right)^{1/2} \|h_0^{(2)}/\kappa\|_{L^2(\Lambda^{1/2})} + \left(\frac{\beta - t_n}{q_n} \right)^{1/2} \|h_n^{(2)}/\kappa\|_{L^2(\Lambda^{1/2})} \right\} + C_3 \\ &\leq C_4 \sqrt{\mu_p(I)}.\end{aligned}$$

Consequently, a straightforward estimate is obtained:

$$T_2(I) = \frac{|\tilde{T}_2(I)|}{\mu_p(I)} \leq \frac{C_4}{\sqrt{\mu_p(I)}}. \quad (6.3.6)$$

Finally, (6.3.5) and (6.3.6) with $C = C_2 + C_4 \geq 0$ independent of I yields

$$\left| \frac{1}{\mu_p(I)} \int_I k_\Lambda(y, y) dy - \frac{|\Lambda^{1/2}|}{\pi} \right| \leq T_1(I) + T_2(I) \leq \frac{C}{\sqrt{\mu_p(I)}} \quad (6.3.7)$$

for every large, closed interval I with $[t_1, t_n] \subset I$.

Meanwhile, if I intersects exactly one of I_0 and I_n , then some of the terms of $T_1(I)$ and $T_2(I)$ will be absent, but estimate (6.3.7) still holds since a term containing either $t_1 - \alpha$ (computations inside I_0) or $\beta - t_n$ (computations inside I_n) is always present.

6. Density theorems in $PW_\Lambda(A_p)$

For the second assertion, note that with $I = B_r(x)$ for some $x \in \mathbb{R}$ and $r > 0$ sufficiently large, there exists $C \geq 0$ independent of x and r such that

$$\left| \frac{1}{\mu_p(B_r(x))} \int_{B_r(x)} k_\Lambda(y, y) dy - \frac{|\Lambda^{1/2}|}{\pi} \right| \leq \frac{C}{\sqrt{\mu_p(B_r(x))}}.$$

By (6.2.1),

$$2r \min_{0 \leq k \leq n} q_k \leq \mu_p(B_r(x)) \leq 2r \max_{0 \leq k \leq n} q_k, \quad q_k = p_k^{-1/2}, 0 \leq k \leq n.$$

Therefore, from (6.3.2),

$$\begin{aligned} \text{tr}^+ &= \limsup_{r \rightarrow \infty} \sup_{x \in \mathbb{R}} \frac{1}{\mu_p(B_r(x))} \int_{B_r(x)} k(y, y) dy \\ &\leq \frac{|\Lambda^{1/2}|}{\pi} + \limsup_{r \rightarrow \infty} \sup_{x \in \mathbb{R}} \frac{C}{\sqrt{\mu_p(B_r(x))}} \\ &\leq \frac{|\Lambda^{1/2}|}{\pi} + \limsup_{r \rightarrow \infty} \frac{C}{\sqrt{2r \min_{0 \leq k \leq n} q_k}} \\ &= \frac{|\Lambda^{1/2}|}{\pi}. \end{aligned}$$

Analogously, we prove from (6.3.3) that $\text{tr}^- \geq \frac{|\Lambda^{1/2}|}{\pi}$. The inequalities

$$\frac{|\Lambda^{1/2}|}{\pi} \leq \text{tr}^- \leq \text{tr}^+ \leq \frac{|\Lambda^{1/2}|}{\pi}$$

imply $\text{tr}^\pm = \frac{|\Lambda^{1/2}|}{\pi}$ and we are done. □

6.3.2. Localization and approximation properties

Now that the necessary preparations are in place, we are ready to prove the remaining weak localization and homogeneous approximation properties of k_Λ . A version of the forthcoming lemmas was proved in [39, Sec. 7] in the context of variable bandwidth spaces $PW_\Lambda(A_p)$ where $p, p' \in AC_{loc}(\mathbb{R})$ and p is eventually constant. In this setting, one can apply a Liouville transformation [39, Prop. 6.6] to convert A_p into a Schrödinger operator $B_q = -D^2 + q$, where q has compact support contained on some interval $[-a, a]$. This paved way to use some scattering theory (see [82, Chap. 21]) to ultimately prove the lemmas. In our setting, however, we cannot apply these results directly since a piecewise constant p is not locally absolutely continuous on \mathbb{R} .

In this section it is instructive to consider spectral sets that are compact intervals, particularly $\Lambda = [0, \Omega]$ for some $\Omega > 0$ as most of the work has already been done in Section 4.4.1. In addition, k_Λ possesses off-diagonal decay with respect to the standard metric d , and as observed in [31, Sec. 4.1], assumptions (e) and (f) easy to verify. For general spectral sets, the proofs of the aforementioned properties of k_Λ are given in Appendix C.

6.3. Properties of the reproducing kernel of $PW_\Lambda(A_p)$

Proposition 6.3.5. *Let $\Lambda = [0, \Omega]$ for some $\Omega > 0$, p a piecewise constant function and k_Λ the reproducing kernel for $PW_{[0, \Omega]}(A_p)$. Then there exists $b, C > 0$ such that for all $x, y \in \mathbb{R}$ satisfying $|x - y| > b$,*

$$|k_\Lambda(x, y)| \leq \frac{C}{1 + |x - y|}. \quad (6.3.8)$$

Proof. Let p be an $(n + 1)$ -piecewise constant function for some $n \in \mathbb{N}$. Recall from Section 4.4.1 the integral

$$J(s) = \frac{1}{2\pi} \int_{\Lambda^{1/2}} \frac{e^{isu}}{\kappa(u)} du, \quad s \in \mathbb{R}$$

as well as the expression

$$k_\Lambda(x, y) = \sum_{k=1}^{m(x, y)} \alpha_k(x, y) J(\beta_k(x, y)), \quad m(x, y) \in \mathbb{N}, \alpha_k(x, y), \beta_k(x, y) \in \mathbb{R}, 1 \leq k \leq m(x, y)$$

for the reproducing kernel of $PW_\Lambda(A_p)$ in terms of J . By Remark 4.4.2, we prove (6.3.8) by showing that each $J(\beta_k(x, y))$ in the above expansion for k_Λ satisfies

$$|J(\beta_k(x, y))| \leq \frac{N_k}{1 + |x - y|}$$

for some $N_k, r_k > 0$ and for all $x, y \in \mathbb{R}$ satisfying $|x - y| > r_k$.

We proceed as follows: let $a > 0$ such that the knots $\{t_k\}_{k=1}^n$ of p are contained in $[-a, a]$. Consider cases where x and y take values on the intervals

$$(-\infty, -a) \subset I_0, \quad [-a, a] \supset I_1 \cup \dots \cup I_{n-1}, \quad (a, \infty) \subset I_n$$

with $|x - y|$ large. To reduce the number of cases to take, we apply the symmetry $k_\Lambda(x, y) = k_\Lambda(y, x)$ for all $x, y \in \mathbb{R}$.

- Suppose x and y belong to the same unbounded interval, i.e., $x, y < -a$ or $x, y > a$. It suffices to consider $x, y < -a$ as the other subcase is treated similarly. As observed in (4.4.8),

$$J(\beta_k(x, y)) = J(c_k \pm q_0(x \pm y))$$

for $c_k \in \mathbb{R}, 1 \leq k \leq m(x, y)$. We also know that $|x + y| = |x| + |y| \geq |x - y|$, and so $|x \pm y| \geq |x - y|$. By Lemma 4.4.3(iii), there exists $M_k > 0$ such that

$$|J(c_k \pm q_0(x \pm y))| \leq \frac{M_k}{|c_k \pm q_0(x \pm y)|} \leq \frac{M_k}{-|c_k| + q_0|x - y|}.$$

Choose $N_k > \frac{M_k}{q_0}$ and $r_k = \frac{M_k + N_k|c_k|}{q_0 N_k - M_k} > 0$. Then the inequality

$$|J(c_k \pm q_0(x \pm y))| \leq \frac{M_k}{-|c_k| + q_0|x - y|} \leq \frac{N_k}{1 + |x - y|}$$

6. Density theorems in $PW_\Lambda(A_p)$

holds for $|x - y| \geq r_k$. Now, take the constants

$$b_1 > \max_{1 \leq k \leq m(x,y)} r_k, \quad C_1 = \sum_{1 \leq k \leq m(x,y)} |\alpha_k(x, y)| N_k.$$

Thus,

$$|k_\Lambda(x, y)| \leq \frac{C_1}{1 + |x - y|}$$

for all $x, y < -a$ satisfying $|x - y| > b_1$.

- Suppose $x \in \mathbb{R}$ and $|y| \leq a$. Without loss of generality, fix $x \in I_j$, $y \in I_l \cap [-a, a]$ for some $0 \leq j, l \leq n$. Then by (4.4.8),

$$J(\beta_k(x, y)) = J(c_k \pm q_j x \pm q_l y)$$

for $c_k \in \mathbb{R}$, $1 \leq k \leq m(x, y)$. We also have

$$\begin{aligned} |q_j x \pm q_l y| &\geq q_j |x - y| - |q_j \pm q_l| |y| \\ &\geq q_j |x - y| - a |q_j \pm q_l|. \end{aligned}$$

By Lemma 4.4.3(iii), there exists $M_k > 0$ such that

$$|J(c_k \pm q_j x \pm q_l y)| \leq \frac{M_k}{|c_k \pm q_j x \pm q_l y|} \leq \frac{M_k}{-(|c_k| + a |q_j + q_l|) + q_j |x - y|}.$$

Following the remaining arguments as in the first case, there exist $b_2, C_2 > 0$ such that

$$|k_\Lambda(x, y)| \leq \frac{C_2}{1 + |x - y|}$$

for all $x \in I_j$, $y \in I_l \cap [-a, a]$ satisfying $|x - y| > b_2$.

- Suppose x and y are on distinct infinite intervals, i.e., $x < -a$ and $y > a$. Then $|q_0 x + q_n y|$ may not be large when $|x - y|$ is large, and (6.3.8) may not hold. We then turn our attention to the original formulation of k_Λ . From (4.2.15) and (4.2.16), write the components of $\Phi(u^2, \cdot) = (\Phi^+(u^2, \cdot), \Phi^-(u^2, \cdot))$ as

$$\begin{aligned} \Phi(u^2, x) &= \begin{bmatrix} \Phi^+(u^2, x) \\ \Phi^-(u^2, x) \end{bmatrix} = \begin{bmatrix} a_0^+(u^2) e^{iq_0 u x} + b_0^+(u^2) e^{-iq_0 u x} \\ e^{-iq_0 u x} \end{bmatrix} \\ \Phi(u^2, y) &= \begin{bmatrix} \Phi^+(u^2, y) \\ \Phi^-(u^2, y) \end{bmatrix} = \begin{bmatrix} e^{iq_n u y} \\ a_n^-(u^2) e^{iq_n u y} + b_n^-(u^2) e^{-iq_n u y} \end{bmatrix}. \end{aligned}$$

As in the computations in (5.2.11), we have

$$\begin{aligned} \vartheta(u, x, y) &= \frac{1}{q_0} \overline{\Phi^+(u^2, x)} \Phi^+(u^2, y) + \frac{1}{q_n} \overline{\Phi^-(u^2, x)} \Phi^-(u^2, y) \\ &= \frac{\overline{a_0^+(u^2)}}{q_0} e^{-i(q_0 x - q_n y)u} + \frac{a_0^+(u^2)}{q_0} e^{i(q_0 x - q_n y)u}. \end{aligned}$$

Hence, there are no exponential terms of the form $\beta_k(x, y) = c_k \pm (q_j x + q_l y)$. Now, observe that $|q_0 x - q_n y| = -q_0 x + q_n y$, and consider two sub-cases:

6.3. Properties of the reproducing kernel of $PW_\Lambda(A_p)$

(i) If $q_0 \geq q_n$, then

$$|q_0x - q_ny| = -q_n(x - y) - (q_0 - q_n)x \geq q_n|x - y| + a(q_0 - q_n) \geq q_n|x - y|.$$

(ii) Otherwise, if $q_n \geq q_0$, we have instead

$$|q_0x - q_ny| = -q_0(x - y) + (q_n - q_0)y \geq q_0|x - y| + a(q_n - q_0) \geq q_0|x - y|.$$

By Lemma 4.4.3, there exists $M_k \in \mathbb{R}$ such that

$$|J(c_k \pm (q_0x - q_ny))| \leq \frac{M_k}{|c_k \pm (q_0x - q_ny)|} \leq \frac{M_k}{-|c_k| + \min\{q_0, q_n\}|x - y|}.$$

From the rest of the arguments of the first case, we conclude that there exist $b_3, C_3 > 0$ such that

$$|k_\Lambda(x, y)| \leq \frac{C_3}{1 + |x - y|}$$

for all $x < -a, y > a$ satisfying $|x - y| > b_3$.

Finally, with $b \geq \max\{b_1, b_2, b_3\}$ and $C \geq \max\{C_1, C_2, C_3\}$, we conclude that for all $x, y \in \mathbb{R}$ satisfying $|x - y| > b$,

$$|k_\Lambda(x, y)| \leq \frac{C}{1 + |x - y|}$$

as we have claimed. \square

Lemma 6.3.5 shows that k_Λ exhibits off-diagonal decay with respect to the standard metric d , which by Proposition 6.3.1 is equivalent to off-diagonal decay of k_Ψ with respect to d whenever p is bounded and bounded away from zero. Moreover, one can show as a special case of [31, Sec. 4.1] that assumptions (d), (e) and (f) can be proved from assumptions (a), (b) and (c) on the geometry of (\mathbb{R}, d, μ_p) together with off-diagonal decay assumption on k_Λ .

Lemma 6.3.6 (Weak localization). *Let $\Lambda = [0, \Omega]$ for some $\Omega > 0$, p be a piecewise constant function and k_Λ the reproducing kernel for $PW_{[0, \Omega]}(A_p)$. Then for every $\epsilon > 0$, there exists $r(\epsilon) > 0$ such that*

$$\sup_{x \in \mathbb{R}} \int_{|x-y| > r(\epsilon)} |k_\Lambda(x, y)|^2 dy < \epsilon^2. \quad (6.3.9)$$

Proof. By Lemma 6.3.5, we can find $b, C > 0$ such that for all $x, y \in \mathbb{R}$ satisfying $|x - y| > b$,

$$|k_\Lambda(x, y)| \leq \frac{C}{1 + |x - y|}.$$

Let $\epsilon > 0$ and take $r(\epsilon) > \max\{b, \frac{4C^2}{\epsilon^2} - 1\}$. Then for a fixed $x \in \mathbb{R}$,

$$\begin{aligned} \int_{|x-y| > r(\epsilon)} |k_\Lambda(x, y)|^2 dy &\leq \int_{|x-y| > r(\epsilon)} \frac{C^2}{(1 + |x - y|)^2} dy = \int_{r(\epsilon)}^\infty \frac{2C^2}{(1 + z)^2} dz \\ &= \frac{2C^2}{1 + r(\epsilon)} < \frac{\epsilon^2}{2}. \end{aligned}$$

Taking the supremum over all $x \in \mathbb{R}$ proves (6.3.9). \square

6. Density theorems in $PW_\Lambda(A_p)$

For the proof of the homogeneous approximation property, we use an elementary approach. We recall some terminologies on sets. A set $X \subset \mathbb{R}$ is said to be **separated with separation** $\delta > 0$ (or **uniformly discrete**) if

$$\inf\{|x - x'| : x, x' \in X, x \neq x'\} = \delta.$$

A set is **relatively separated** if it is a finite union of separated sets. Relatively separated sets cannot have an accumulation point, hence a point may only be repeated a finite number of times. Moreover, for a relatively separated set X , the relative separation constant

$$\text{rel}(X) = \max_{x \in \mathbb{R}} \#(X \cap [x, x + 1]) \quad (6.3.10)$$

is always finite. The following lemma [31, Lem. 3.7] can be used to prove that a set is relatively separated. This will be used again in Section C.2.

Lemma 6.3.7. *Let \mathcal{H} be a reproducing kernel Hilbert space of functions from \mathbb{R} to \mathbb{C} with kernel k . Suppose $X \subset \mathbb{R}$ such that $\{k(x, \cdot) : x \in X\}$ is a Bessel sequence in \mathcal{H} . Then X is relatively separated.*

We are now ready to prove the homogeneous approximation property.

Lemma 6.3.8 (Homogeneous approximation). *Let $\Lambda = [0, \Omega]$ for some $\Omega > 0$, p a piecewise constant function and k_Λ the reproducing kernel for $PW_{[0, \Omega]}(A_p)$. Suppose $X \subset \mathbb{R}$ such that $\{k_\Lambda(x, \cdot) : x \in X\}$ is a Bessel sequence in $PW_{[0, \Omega]}(A_p)$. Then for every $\epsilon > 0$, there exists $r(\epsilon) > 0$ such that*

$$\sup_{y \in \mathbb{R}} \sum_{\substack{x \in X \\ |x - y| > r(\epsilon)}} |k_\Lambda(x, y)|^2 < \epsilon^2. \quad (6.3.11)$$

Proof. Fix $y \in \mathbb{R}$. By Lemma 6.3.5, there exists $r, C > 0$ such that

$$\sum_{\substack{x \in X \\ |x - y| > r}} |k_\Lambda(x, y)|^2 \leq \sum_{\substack{x \in X \\ |x - y| > r}} \frac{C^2}{1 + |x - y|^2}.$$

Let $\epsilon > 0$. Since $\sum_{n \in \mathbb{Z}} \frac{1}{1 + (n-1)^2}$ is a convergent series, we can find $r'(\epsilon) > 0$ sufficiently large such that

$$\sum_{n \in \mathbb{Z}: |n| > r'(\epsilon) - 1} \frac{1}{1 + (n-1)^2} < \frac{\epsilon^2}{2C^2}. \quad (6.3.12)$$

Take $r(\epsilon) > \max\{r, r'(\epsilon)\}$. If X is separated with separation $\delta = 1$, then each unit length interval contains at most one point $x - y$ for some $x \in X$. Thus, $x - y = n_x + s_x$ for some unique $n_x \in \mathbb{Z}$ and $s_x \in [0, 1)$. Since for all $x \in X$, $|n_x + s_x| > r(\epsilon)$ implies $|n_x| > |n_x + s_x| - |s_x| > r(\epsilon) - 1$, we get

$$\begin{aligned} \sum_{\substack{x \in X \\ |x - y| > r(\epsilon)}} \frac{1}{1 + |x - y|^2} &\leq \sum_{\substack{x \in X \\ |n_x + s_x| > r(\epsilon)}} \frac{1}{1 + |n_x + s_x|^2} \leq \sum_{\substack{x \in X \\ |n_x + s_x| > r(\epsilon)}} \frac{1}{1 + (|n_x| - 1)^2} \\ &\leq \sum_{\substack{x \in X \\ |n_x| > r(\epsilon) - 1}} \frac{1}{1 + (|n_x| - 1)^2} \leq \sum_{n \in \mathbb{Z}: |n| > r(\epsilon) - 1} \frac{1}{1 + (n - 1)^2}. \end{aligned}$$

6.4. Necessary density conditions for sampling and interpolation

Taking the supremum over all $y \in \mathbb{R}$, we have

$$\sup_{y \in \mathbb{R}} \sum_{\substack{x \in X \\ |x-y| > r(\epsilon)}} |k_\Lambda(x, y)|^2 \leq \frac{\epsilon^2}{2} < \epsilon^2 \quad (6.3.13)$$

which is precisely (6.3.11). Now, by Lemma 6.3.7, X is relatively separated. Hence, with the relative separation constant $\text{rel}(X)$ defined in (6.3.10) we replace $\frac{\epsilon^2}{2C^2}$ in (6.3.12) by $\frac{\epsilon^2}{2C^2 \text{rel}(X)}$ so that (6.3.13) still holds. \square

For spectral sets that are not compact intervals, Proposition 6.3.5 does not hold, and therefore the proofs of Lemmas 6.3.6 and 6.3.8 will not work for general spectral sets. We prove in Appendix C the following general versions of the weak localization and homogeneous approximation properties of k_Λ :

Lemma 6.3.9 (Weak localization). *Let $\Lambda \subset \mathbb{R}_0^+$ be a Borel set of finite measure. Let p be a piecewise constant function and k_Λ be the reproducing kernel for $PW_\Lambda(A_p)$. Then for every $\epsilon > 0$, there exists $r(\epsilon) > 0$ such that*

$$\sup_{x \in \mathbb{R}} \int_{|x-y| > r(\epsilon)} |k_\Lambda(x, y)|^2 dy < \epsilon^2.$$

Lemma 6.3.10 (Homogeneous approximation). *Let $\Lambda \subset \mathbb{R}_0^+$ be a bounded Borel set, p be a piecewise constant function and k_Λ be the reproducing kernel for $PW_\Lambda(A_p)$. Suppose X is a set of stable sampling for $PW_\Lambda(A_p)$. Then for every $\epsilon > 0$, there exists $r(\epsilon) > 0$ such that*

$$\sup_{y \in \mathbb{R}} \sum_{\substack{x \in X \\ |x-y| > r(\epsilon)}} |k_\Lambda(x, y)|^2 < \epsilon^2.$$

As in the case of bandlimited functions (see discussion in [31, Sec. 5.1]), the homogeneous approximation property of k_Λ does not hold for unbounded spectral sets.

6.4. Necessary density conditions for sampling and interpolation

In Section 6.2, we verified that the metric measure space (\mathbb{R}, d, μ_p) satisfies finiteness of μ_p -measure of balls, non-degeneracy of balls and weak annular decay property. On the other hand, in Section 6.3 we proved that k_Λ has bounded diagonal, and when Λ is a compact interval, k_Λ satisfies the weak localization and homogeneous approximation properties. We also mentioned a version of these properties for general spectral sets. We are now ready to collect all these results and finally derive necessary density conditions for sampling and interpolation in $PW_\Lambda(A_p)$.

Theorem 6.4.1 (Density theorem in $PW_\Lambda(A_p)$). *Let $\Lambda \subseteq \mathbb{R}_0^+$ be a Borel set of finite measure and p a piecewise constant function.*

- (i) *If X is a set of stable sampling for $PW_\Lambda(A_p)$, then $D_p^-(X) \geq \frac{|\Lambda^{1/2}|}{\pi}$.*

6. Density theorems in $PW_\Lambda(A_p)$

(ii) If X is a set of interpolation for $PW_\Lambda(A_p)$, then $D_p^+(X) \leq \frac{|\Lambda^{1/2}|}{\pi}$.

Proof. Let p be a piecewise constant function. By Lemma 6.2.1, (\mathbb{R}, d, μ_p) satisfies conditions (a), (b) and (c). On the other hand, k_Λ satisfies (d) by Lemma 6.3.2. We now proceed by cases.

- Case 1: Suppose $\Lambda \subseteq \mathbb{R}_0^+$ is bounded. Then by Lemmas 6.3.9 and 6.3.10, k_Λ satisfies (e) and (f). By Theorem 6.3.4, $\text{tr}^\pm = \frac{|\Lambda^{1/2}|}{\pi}$. The density theorem for $PW_\Lambda(A_p)$ now follows from Theorem 6.1.1.
- Case 2: Suppose $\Lambda \subset \mathbb{R}_0^+$ is unbounded. To prove (i), consider the bounded spectral set $\Lambda_\Omega = \Lambda \cap [0, \Omega] \subseteq \Lambda$. Then $PW_{\Lambda_\Omega}(A_p)$ is a closed subspace of $PW_\Lambda(A_p)$. Moreover, if X is a set of stable sampling for $PW_\Lambda(A_p)$, then X is a set of stable sampling for $PW_{\Lambda_\Omega}(A_p)$. By the density theorem for $PW_{\Lambda_\Omega}(A_p)$ we have

$$D_p^-(X) \geq \frac{|\Lambda_\Omega^{1/2}|}{\pi} = \frac{|\Lambda^{1/2} \cap [0, \Omega^{1/2}]|}{\pi}.$$

Since Ω is arbitrary, we conclude that $D_p^-(X) \geq \frac{|\Lambda^{1/2}|}{\pi}$. To prove (ii), fix $x \in \mathbb{R}$. Following the proof in [39, Sec. 6.4(A)] (cf. [31, Rem. 4.3]) one can show that for all $\epsilon > 0$ sufficiently small we can choose $r > r(\epsilon)$ as in Lemma 6.3.9 and $C' > 0$ such that

$$\frac{1}{\mu_p(B_r(x))} \int_{B_r(x)} k_\Lambda(y, y) dy \geq (1 - C'\epsilon) \frac{\#(X \cap B_r(x))}{\mu_p(B_r(x))}.$$

By Theorem 6.3.4, there exists $C \geq 0$ independent of x such that

$$\frac{\#(X \cap B_r(x))}{\mu_p(B_r(x))} \leq (1 - C'\epsilon)^{-1} \left(\frac{|\Lambda^{1/2}|}{\pi} + \frac{C}{\sqrt{\mu_p(B_r(x))}} \right).$$

Finally, taking the supremum over all $x \in \mathbb{R}$ and the limit superior as $r \rightarrow \infty$ gives us $D_p^+(X) \leq (1 - C'\epsilon)^{-1} \frac{|\Lambda^{1/2}|}{\pi}$. Since ϵ is arbitrary, we conclude that $D_p^+(X) \leq \frac{|\Lambda^{1/2}|}{\pi}$.

□

7. Numerical implementation and simulations

In this chapter, we consider the problem of reconstructing a function from its point samples in the space of functions variable bandwidth via least squares approximation. Our goal is to show that for functions that behave locally as bandlimited functions, approximation by variable bandwidth functions with appropriately chosen piecewise constant parametrizing function performs significantly better than approximation by bandlimited functions. We adopt a finite-dimensional numerical reconstruction algorithm as in [4, 5] that is based on frames, oversampling, and regularization. Oversampling allows the number of point samples to exceed the number of reconstruction vectors spanning a finite-dimensional subspace of functions of variable bandwidth, which leads to least squares approximation. On the other hand, the inherent redundancy of frames offers flexibility in terms of function representation at the cost of ill-conditioning. By regularization we mean thresholding on the singular values of the corresponding finite-dimensional least squares problem. The resulting algorithm then produces a variable bandwidth reconstruction whose representation has bounded¹² norm coefficients and are thus computable in floating point arithmetic.

A crucial part of the aforementioned reconstruction algorithm is a robust and accurate evaluation of the reproducing kernel of a variable bandwidth space at any point. Due to computational limitations, we limit our discussion to variable bandwidth spaces with either two-component or three-component piecewise constant functions. Hence, all the necessary calculations involving the reproducing kernel can be carried out directly using the results in Chapter 5. In particular, we have Theorem 5.1.1 (toy example) for the two-component case, while the reproducing kernel for the three-component case with symmetric knots can be computed numerically via Theorem 5.2.5 and the formula (5.2.9) for J_{real} .

A summary of the numerical simulations is as follows. We show experimentally that bandlimited functions can be reasonably reconstructed in a variable bandwidth space whose local bandwidths are sufficiently close to the bandwidth of the function. For functions that locally behave like bandlimited functions, an approximation in some reasonably chosen variable bandwidth space performs significantly better than approximation by bandlimited functions. In the case of uniform sampling, any numerical reconstruction using the Shannon sampling theorem is expected to interpolate uniform samples of a function within machine precision. However, it is observed that with a finer grid, notable errors are present as we get close to the transition points where the abrupt changes in oscillatory behavior occur. We shall see that if said points are the knots of a parametrizing function p with appropriately chosen piecewise constant components, we obtain a more accurate approximation in the corresponding variable bandwidth space. Next, we investigate experimentally how the parametrizing function affects the accuracy of reconstructing a function

¹²In [4, 5], the authors also used the term *small norm coefficients*.

7. Numerical implementation and simulations

in some space of variable bandwidth. This is done by performing reconstruction in several variable bandwidth spaces and take the (local) bandwidth(s) of the function to be reconstructed as our reference (local) bandwidth(s). It is expected that if the parametrizing functions of these variable spaces are taken so that the corresponding local bandwidths approach the reference bandwidth, then the reconstruction improves. We also take a look at reconstructing functions from samples of varying Beurling densities, particularly when the lower Beurling density approaches the critical density.

Lastly, we expressly note that the experiments done in this chapter are proofs of concept of our notion of variable bandwidth. Hence, there are no attempts to optimize sampling and reconstruction algorithms and no large examples were considered.

7.1. General reconstruction theory

We present relevant theory on numerical approximation of functions using frames [4, 5]. More precisely, given reproducing kernel Hilbert subspaces $\mathcal{H}_1, \mathcal{H}_2$ of $L^2(\mathbb{R})$, we consider the problem of reconstructing a function $f \in \mathcal{H}_1$ by elements of \mathcal{H}_2 given its point samples $\{f(x_j)\}_{j \in \mathbb{Z}}$. We also recall some notations. Let \mathcal{H} and \mathcal{K} be Hilbert spaces. Given an operator $T : \mathcal{H} \rightarrow \mathcal{K}$, we define its **kernel** (or **nullspace**) \mathcal{N}_T by

$$\mathcal{N}_T = \{x \in \mathcal{H} : Tx = 0\}$$

and its **range** \mathcal{R}_T by

$$\mathcal{R}_T = \{Tx : x \in \mathcal{H}\}.$$

We also define the pseudoinverse of T as follows [9, Def. 5.1], [22, Sec. 2.5]. Suppose $T : \mathcal{H} \rightarrow \mathcal{K}$ is a bounded operator with closed range. The **pseudoinverse** of T is the unique bounded operator $T^\dagger : \mathcal{K} \rightarrow \mathcal{H}$ satisfying

$$\mathcal{N}_{T^\dagger} = \mathcal{R}_T^\perp, \quad \mathcal{R}_{T^\dagger} = \mathcal{N}_T^\perp, \quad \text{and} \quad TT^\dagger x = x, x \in \mathcal{R}_T.$$

The following lemma shows that pseudoinverses can be used to find minimal norm least squares solutions of linear systems [14, Cor. 1.1].

Lemma 7.1.1. *Let $T : \mathcal{H} \rightarrow \mathcal{K}$ be a bounded operator with closed range and $b \in \mathcal{K}$. Then $\tilde{x} = T^\dagger b$ is the unique minimal norm solution of the least squares problem $\min_{x \in \mathcal{H}} \|Tx - b\|_{\mathcal{K}}$.*

We now formulate the reconstruction problem. Let \mathcal{H}_1 and \mathcal{H}_2 be reproducing kernel Hilbert spaces¹³ with reproducing kernels k_1 and k_2 , respectively. Suppose we are given samples

$$d_j = \langle f, k_1(x_j, \cdot) \rangle_{\mathcal{H}_1} = f(x_j), \quad j \in \mathbb{Z}$$

of an unknown function $f \in \mathcal{H}_1$ at fixed, possibly non-uniform sampling points $X = \{x_j\}_{j \in \mathbb{Z}} \subset \mathbb{R}$. We wish to approximate f by an element of \mathcal{H}_2 . A reconstruction $\tilde{f} \in \mathcal{H}_2$ of f can be obtained by means of a least squares problem, i.e.,

$$\tilde{f} = \arg \min_{g \in \mathcal{H}_2} \sum_{j \in \mathbb{Z}} |\langle g, k_2(x_j, \cdot) \rangle_{\mathcal{H}_2} - d_j|^2 = \arg \min_{g \in \mathcal{H}_2} \sum_{j \in \mathbb{Z}} |g(x_j) - d_j|^2. \quad (7.1.1)$$

¹³In general, \mathcal{H}_1 may be taken as a dense subspace of a Hilbert space where pointwise evaluations are well defined. See [5, Sec. 1.2] for details.

In the literature, we refer to \mathcal{H}_1 as the **sampling space** and \mathcal{H}_2 the **reconstruction space**.

In this study, we assume that $d = \{d_j\}_{j \in \mathbb{Z}} \in \ell^2(\mathbb{Z})$. This holds precisely if $\{k_1(x_j, \cdot)\}_{j \in \mathbb{Z}}$ is a Bessel sequence for \mathcal{H}_1 . Furthermore, we also assume that there exist constants $A, B > 0$ such that

$$A \|g\|_2^2 \leq \sum_{j \in \mathbb{Z}} |g(x_j)|^2 \leq B \|g\|_2^2 \quad (7.1.2)$$

for all $g \in \mathcal{H}_2$, i.e., X is a set of stable sampling for \mathcal{H}_2 . Hence,

$$\mathcal{H}_2 = \overline{\text{span}}\{k_2(x_j, \cdot)\}_{j \in \mathbb{Z}}.$$

Let $T : \ell^2(\mathbb{Z}) \rightarrow \mathcal{H}_2$ be the synthesis operator defined as

$$Tc = \sum_{j \in \mathbb{Z}} c_j k_2(x_j, \cdot), \quad c = \{c_j\}_{j \in \mathbb{Z}} \in \ell^2(\mathbb{Z}).$$

By (7.1.2), T is well-defined and bounded. The analysis operator $T^* : \mathcal{H}_2 \rightarrow \ell^2(\mathbb{Z})$ is given by

$$T^*g = \{\langle g, k_2(x_j, \cdot) \rangle_{\mathcal{H}_2}\}_{j \in \mathbb{Z}} = \{g(x_j)\}_{j \in \mathbb{Z}}, \quad g \in \mathcal{H}_2.$$

Assuming (7.1.2) holds, (7.1.1) can be rephrased as follows. Since $\mathcal{R}_T = \mathcal{H}_2$, there exists $\tilde{c} \in \ell^2(\mathbb{Z})$ such that $\tilde{f} = T\tilde{c}$ and satisfies

$$\tilde{c} \in \arg \min_{c \in \ell^2(\mathbb{Z})} \sum_{j \in \mathbb{Z}} \left| \sum_{l \in \mathbb{Z}} c_l k_2(x_l, x_j) - d_j \right|^2. \quad (7.1.3)$$

Define the Gramian $G : \ell^2(\mathbb{Z}) \rightarrow \ell^2(\mathbb{Z})$ by $G = T^*T$, i.e.,

$$Gc = T^*Tc = \left\{ \sum_{l \in \mathbb{Z}} c_l k_2(x_l, x_j) \right\}_{j \in \mathbb{Z}}, \quad c = \{c_l\}_{l \in \mathbb{Z}}.$$

Thus, (7.1.3) can be written as

$$\tilde{c} \in \arg \min_{c \in \ell^2(\mathbb{Z})} \|Gc - d\|_2^2, \quad d = \{d_j\}_{j \in \mathbb{Z}} \in \ell^2(\mathbb{Z}).$$

Moreover, G is bounded and $\mathcal{R}_G = \mathcal{R}_{T^*T} = \mathcal{R}_{T^*}$ is closed. Therefore, Lemma 7.1.1 applies. Among all possible coefficient sequences satisfying (7.1.3), we form the reconstruction $\tilde{f} \in \mathcal{H}_2$ using the unique minimal norm coefficient vector $\hat{c} = G^\dagger d$. Finally, we define the reconstruction operator $\mathcal{Q} : \ell^2(\mathbb{Z}) \rightarrow \mathcal{H}_2$ by

$$\tilde{f} = \mathcal{Q}d = TG^\dagger d = \sum_{l \in \mathbb{Z}} \hat{c}_l k_2(x_l, \cdot). \quad (7.1.4)$$

Let us now compare this reconstruction method to the best approximation of $f \in \mathcal{H}_1$ in \mathcal{H}_2 obtained via the orthogonal projection.

7. Numerical implementation and simulations

Theorem 7.1.2. *Let $\mathcal{H}_1, \mathcal{H}_2 \subset L^2(\mathbb{R})$ be reproducing kernel Hilbert spaces. Suppose $f \in \mathcal{H}_1$ and $X = \{x_j\}_{j \in \mathbb{Z}} \subset \mathbb{R}$ such that*

(i) $d = \{f(x_j)\}_{j \in \mathbb{Z}} \in \ell^2(\mathbb{Z})$, and

(ii) X is a set of stable sampling for \mathcal{H}_2 with lower bound A .

Let $\mathcal{Q} : \ell^2(\mathbb{Z}) \rightarrow \mathcal{H}_2$ be the reconstruction operator given in (7.1.4) and $\tilde{f} = \mathcal{Q}d$. Then

$$\|f - \tilde{f}\|_2 \leq \inf_{g \in \mathcal{H}_2} \left(\|f - g\|_2 + \frac{1}{\sqrt{A}} \left\{ \sum_{j \in \mathbb{Z}} |g(x_j) - \tilde{f}(x_j)|^2 \right\}^{1/2} \right). \quad (7.1.5)$$

In particular, if T^* is the analysis operator, $P_{\mathcal{H}_2} : L^2(\mathbb{R}) \rightarrow \mathcal{H}_2$ is the orthogonal projection onto \mathcal{H}_2 and k_2 the reproducing kernel for \mathcal{H}_2 , then

$$\|f - \tilde{f}\|_2 \leq \|f - P_{\mathcal{H}_2}f\|_2 + \frac{1}{\sqrt{A}} \|T^* \tilde{f} - d\|_2 + \frac{1}{\sqrt{A}} \left\{ \sum_{j \in \mathbb{Z}} |\langle f, k_2(x_j, \cdot) \rangle - d_j|^2 \right\}^{1/2}. \quad (7.1.6)$$

Proof. For any $g \in \mathcal{H}_2$, inequality (7.1.2) implies

$$\begin{aligned} \|f - \tilde{f}\|_2 &\leq \|f - g\|_2 + \|g - \tilde{f}\|_2 \\ &= \|f - g\|_2 + \frac{1}{\sqrt{A}} \left\{ \sum_{j \in \mathbb{Z}} |g(x_j) - \tilde{f}(x_j)|^2 \right\}^{1/2}. \end{aligned}$$

Taking the infimum over all $g \in \mathcal{H}_2$ yields (7.1.5). Now, write $f = P_{\mathcal{H}_2}f + h$, where $h \in \mathcal{H}_2^\perp$. Then for any $x \in \mathbb{R}$, $k_2(x, \cdot) \in \mathcal{H}_2$ and

$$\langle f, k_2(x, \cdot) \rangle = \langle P_{\mathcal{H}_2}f, k_2(x, \cdot) \rangle = P_{\mathcal{H}_2}f(x).$$

Choosing $g = P_{\mathcal{H}_2}f$ in (7.1.5) yields

$$\begin{aligned} \|f - \tilde{f}\|_2 &\leq \|f - P_{\mathcal{H}_2}f\|_2 + \frac{1}{\sqrt{A}} \left\{ \sum_{j \in \mathbb{Z}} |\langle f, k_2(x_j, \cdot) \rangle - \tilde{f}(x_j)|^2 \right\}^{1/2} \\ &\leq \|f - P_{\mathcal{H}_2}f\|_2 + \frac{1}{\sqrt{A}} \left\{ \sum_{j \in \mathbb{Z}} |\tilde{f}(x_j) - d_j|^2 \right\}^{1/2} + \frac{1}{\sqrt{A}} \left\{ \sum_{j \in \mathbb{Z}} |\langle f, k_2(x_j, \cdot) \rangle - d_j|^2 \right\}^{1/2}. \end{aligned}$$

The second term can be expressed using the analysis operator T^* . □

We see that the error in approximating f by \tilde{f} is bounded by three quantities: the first term of (7.1.6) takes care of the part of f outside of \mathcal{H}_2 , the second term is the minimal residual of the least squares problem by (7.1.3), and the third term is the discrepancy between the point samples $d_j = f(x_j)$ and sampling f via inner products with $k_2(x_j, \cdot)$.

In the case where $\{k_1(x_j, \cdot)\}_{j \in \mathbb{Z}}$ is indeed a Bessel sequence, we can analogously define the synthesis and analysis operators

$$\begin{aligned} L : \ell^2(\mathbb{Z}) &\rightarrow \mathcal{H}_1, & Lc &= \sum_{j \in \mathbb{Z}} c_j k_1(x_j, \cdot), \\ L^* : \mathcal{H}_1 &\rightarrow \ell^2(\mathbb{Z}), & L^*g &= \{\langle g, k_1(x_j, \cdot) \rangle\}_{j \in \mathbb{Z}} = \{g(x_j)\}_{j \in \mathbb{Z}} \end{aligned}$$

respectively. Hence, the mapping $F : \mathcal{H}_1 \rightarrow \mathcal{H}_2$ given by

$$F(f) = \tilde{f} = TG^\dagger L^* f, \quad f \in \mathcal{H}_1$$

is bounded. Moreover, by Theorem 7.1.2,

$$\|f - F(f)\|_2 \leq \|f - P_{\mathcal{H}_2} f\|_2 + \frac{1}{\sqrt{A}} \|T^* F(f) - L^* f\|_2 + \frac{1}{\sqrt{A}} \|T^* f - L^* f\|_2.$$

In particular, if $f \in \mathcal{H}_1 \cap \mathcal{H}_2$, then $F(f) = f$.

7.1.1. Finite-dimensional reconstruction algorithm

In practice, we only have access to a finite number of point samples of $f \in \mathcal{H}_1$. We adopt the reconstruction procedure in [5] on best approximations with regularization using oversampling. We shall shortly see that this choice of numerical reconstruction gives us some control over the ill-conditioning of the resulting linear system. Let $m, n \in \mathbb{N}$ with $m \geq n$. From $2m + 1$ samples

$$d_j = \langle f, k_1(x_j, \cdot) \rangle = f(x_j), \quad j = -m, \dots, m,$$

we define the reconstruction $\tilde{f}^{[m,n]}$ of f in the finite-dimensional subspace

$$\mathcal{T}_n = \text{span}\{k_2(x_l, \cdot) : l = -n, \dots, n\}$$

of \mathcal{H}_2 as

$$\tilde{f}^{[m,n]} = \arg \min_{g \in \mathcal{T}_n} \sum_{j=-m}^m |g(x_j) - d_j|^2.$$

As in the infinite-dimensional case, this reconstruction vector can be written as

$$\tilde{f}^{[m,n]} = \sum_{l=-n}^n c_l^{[m,n]} k_2(x_l, \cdot),$$

where $c^{[m,n]} \in \mathbb{C}^{2n+1}$ satisfies

$$c^{[m,n]} \in \arg \min_{c \in \mathbb{C}^{2n+1}} \sum_{j=-m}^m \left| \sum_{l=-n}^n c_l k_2(x_l, x_j) - d_j \right|^2. \quad (7.1.7)$$

For $r \in \mathbb{N}$, define the synthesis operator $T^{[r]} : \mathbb{C}^{2r+1} \rightarrow \mathcal{T}_r$ as

$$T^{[r]} c = \sum_{l=-r}^r c_l k_2(x_l, \cdot), \quad c = \{c_l\}_{l=-r}^r \in \mathbb{C}^{2r+1}$$

and the analysis operator $(T^{[r]})^* : \mathcal{T}_r \rightarrow \mathbb{C}^{2r+1}$ by

$$(T^{[r]})^* g = \{\langle g, k_2(x_l, \cdot) \rangle\}_{l=-r}^r, \quad g \in \mathcal{T}_r.$$

7. Numerical implementation and simulations

Now, with $m \geq n$, set $G^{[m,n]} \in \mathbb{C}^{(2m+1) \times (2n+1)}$ to be the matrix whose entries are

$$G^{[m,n]}(j, l) = k_2(x_l, x_j), \quad j = -m, \dots, m, l = -n, \dots, n. \quad (7.1.8)$$

In other words,

$$G^{[m,n]} = (T^{[m]})^* T^{[n]}.$$

We call $G^{[m,n]}$ an **uneven section** of G if $m \neq n$. If $m = n$, $G^{[n,n]}$ is called a **finite section** of G . Set $d^{[m]} \in \mathbb{C}^{2m+1}$ to be the vector of samples

$$d_j^{[m]} = f(x_j), \quad j = -m, \dots, m.$$

It is now evident from (7.1.7) that $c^{[m,n]}$ is a least squares solution of the linear system

$$G^{[m,n]} c = d^{[m]}. \quad (7.1.9)$$

Overcomplete frames have the advantage of flexibility over orthonormal bases due to redundant representations. However, corresponding linear systems are in general ill-conditioned. It was shown in [5, Rem. 3.4] that whenever $G^{[n,n]}$ is ill-conditioned for some n , $G^{[m,n]}$ inherits this ill-conditioning for large m . Moreover, norms of solutions of (7.1.9) may also grow arbitrarily large as we take larger uneven sections of G . This causes computations in floating point arithmetic to be impossible (see also [4, Sec. 5.1]). In order to control the growth of solutions of (7.1.9), we use a variant of the singular value decomposition (SVD), called the truncated SVD [41, 61]. This yields a reconstruction of f whose representation has bounded norm coefficients.

We briefly recall the singular value decomposition for rectangular matrices. For a thorough review, consult [16, Thm. 1.2.1], [22, Cor. 1.6.4], or [35, Thm. 2.4.1].

Theorem 7.1.3 (Singular value decomposition). *Let $m \geq n$. If $A \in \mathbb{C}^{m \times n}$ and $\text{rank}(A) = r$, then there exist unitary matrices $U \in \mathbb{C}^{m \times m}$, $V \in \mathbb{C}^{n \times n}$ and n nonnegative real numbers $\sigma_1 \geq \dots \geq \sigma_r > \sigma_{r+1} = \dots = \sigma_n = 0$ such that*

$$A = U \Sigma V^*, \quad \Sigma = \text{diag}(\sigma_1, \dots, \sigma_r, 0, \dots, 0) \in \mathbb{C}^{m \times n}.$$

The numbers $\sigma_i, i = 1, \dots, n$ are called the **singular values** of A . The columns of U are the **left singular vectors** of A and the columns of V are the **right singular vectors** of A . If we write U and V in terms of their column vectors as $U = [u_1 | \dots | u_m]$ and $V = [v_1 | \dots | v_n]$, these vectors satisfy [35, Cor. 2.4.2]

$$A v_i = \sigma_i u_i, \quad A^* u_i = \sigma_i v_i, \quad i = 1, \dots, n.$$

Consequently, the nonzero singular values are the square roots of the eigenvalues of $A^* A$ (same as the nonzero eigenvalues of AA^* , including multiplicities). Moreover, A can be expressed as

$$A = \sum_{i=1}^r \sigma_i u_i v_i^*, \quad r = \text{rank}(A).$$

The SVD provides information on the rank as well as the kernel and range of a matrix [35, Cor. 2.4.6], and the above representation of A is commonly used to construct low-rank approximations of A [35, Thm. 2.4.8]. Furthermore, the decomposition yields a

straightforward computation of the pseudoinverse A^\dagger of A [35, Sec. 5.5.2]: given $A = U\Sigma V^*$ as above, we have

$$A^\dagger = V\Sigma^\dagger U^* = \sum_{i=1}^r \frac{1}{\sigma_i} v_i u_i^*, \quad r = \text{rank}(A), \quad (7.1.10)$$

where

$$\Sigma^\dagger = \text{diag} \left(\frac{1}{\sigma_1}, \dots, \frac{1}{\sigma_r}, 0, \dots, 0 \right) \in \mathbb{C}^{n \times n}.$$

We now apply the SVD to uneven sections of the Gramian. Suppose $G^{[m,n]} \in \mathbb{C}^{(2m+1) \times (2n+1)}$ has SVD

$$G^{[m,n]} = U^{[m]} \Sigma^{[m,n]} (V^{[n]})^*$$

for some unitary matrices $U^{[m]} \in \mathbb{C}^{(2m+1) \times (2m+1)}$, $V^{[n]} \in \mathbb{C}^{(2n+1) \times (2n+1)}$ and matrix of singular values $\Sigma^{[m,n]} \in \mathbb{C}^{(2m+1) \times (2n+1)}$ of $G^{[m,n]}$. The truncated SVD is computed as follows. Given a threshold $\epsilon > 0$, we form the matrix

$$G_\epsilon^{[m,n]} = U^{[m]} \Sigma_\epsilon^{[m,n]} (V^{[n]})^*,$$

where $\Sigma_\epsilon^{[m,n]} \in \mathbb{C}^{(2m+1) \times (2n+1)}$ is obtained by replacing all the diagonal entries of $\Sigma^{[m,n]}$ below ϵ by zero. This corresponds to a possibly low-rank approximation of $G^{[m,n]}$. The so-called **regularized reconstruction** $\tilde{f}_\epsilon^{[m,n]} \in \mathcal{T}_n$ of f is given by

$$\tilde{f}_\epsilon^{[m,n]} = \sum_{l=-n}^n (\tilde{c}_\epsilon^{[m,n]})_l k_2(x_l, \cdot),$$

where $\tilde{c}_\epsilon^{[m,n]} \in \mathbb{C}^{2n+1}$ satisfies

$$\tilde{c}_\epsilon^{[m,n]} \in \arg \min_{c \in \mathbb{C}^{2n+1}} \sum_{j=-m}^m \left| \sum_{l=-n}^n c_l G_\epsilon^{[m,n]}(j, l) - d_j \right|^2. \quad (7.1.11)$$

Among all possible coefficient vectors satisfying (7.1.11), we choose the minimal norm solution

$$\hat{c}_\epsilon^{[m,n]} = (G_\epsilon^{[m,n]})^\dagger d^{[m]} = V^{[m]} (\Sigma_\epsilon^{[m,n]})^\dagger (U^{[n]})^* d^{[m]}. \quad (7.1.12)$$

Hence, the regularized reconstruction operator $\mathcal{Q}_\epsilon^{[m,n]} : \mathbb{C}^{2m+1} \rightarrow \mathcal{T}_n$ is defined as

$$\tilde{f}_\epsilon^{[m,n]} = \mathcal{Q}_\epsilon^{[m,n]} d^{[m]} = T^{[n]} (G_\epsilon^{[m,n]})^\dagger d^{[m]} = \sum_{l=-n}^n (\hat{c}_\epsilon^{[m,n]})_l k_2(x_l, \cdot). \quad (7.1.13)$$

We can also express the above reconstruction using the singular vectors of $G^{[m,n]}$. Write $U^{[m]} = [u_1^{[m]} | \dots | u_m^{[m]}]$ and $V^{[n]} = [v_1^{[n]} | \dots | v_n^{[n]}]$. By (7.1.10),

$$\hat{c}_\epsilon^{[m,n]} = \sum_{i: \sigma_i \geq \epsilon} \frac{\langle u_i^{[m]}, d^{[m]} \rangle}{\sigma_i} v_i^{[n]}. \quad (7.1.14)$$

7. Numerical implementation and simulations

Applying $T^{[n]}$ yields

$$\tilde{f}_\epsilon^{[m,n]} = \sum_{i:\sigma_i \geq \epsilon} \frac{\langle u_i^{[m]}, d^{[m]} \rangle}{\sigma_i} T^{[n]} v_i^{[n]}.$$

Therefore, $\tilde{f}_\epsilon^{[m,n]}$ can be thought of as a reconstruction of f in the (possibly proper) subspace $\{T^{[n]} v_i^{[n]} : \sigma_i \geq \epsilon\}$ of \mathcal{T}_n . Furthermore, $\tilde{f}_\epsilon^{[m,n]}$ is formed using bounded norm coefficients (7.1.14). Indeed, by orthonormality of columns of unitary matrices, we have

$$\|\hat{c}_\epsilon^{[m,n]}\|_2^2 = \sum_{i:\sigma_i \geq \epsilon} \frac{|\langle u_i^{[m]}, d^{[m]} \rangle|^2}{\sigma_i^2} \leq \epsilon^{-2} \sum_{i:\sigma_i \geq \epsilon} |\langle u_i^{[m]}, d^{[m]} \rangle|^2 \leq \epsilon^{-2} \|d^{[m]}\|_2^2.$$

This yields an upper bound estimate

$$\|\hat{c}_\epsilon^{[m,n]}\|_2 \leq \epsilon^{-1} \|d^{[m]}\|_2. \quad (7.1.15)$$

In contrast, without regularization, i.e., $\epsilon = 0$, the norm $\|\hat{c}_\epsilon^{[m,n]}\|_2$ may grow without bound as n increases (m also increases since we always assume $m \geq n$) due to the presence of arbitrarily small singular values.

For further discussion on the approximation error, growth of coefficients as well as stable sampling rate, we refer the reader to [5, Sec. 3].

7.1.2. A note on selecting the regularization parameter

An important aspect of the regularized reconstruction is choosing a reasonable value for the tolerance ϵ . To this end, we mention a relevant result in [61, Secs. 4, 6] and [76, Sec. 2.1]. Let $A \in \mathbb{C}^{m \times n}$ and $b \in \mathbb{C}^m$. In solving the ill-conditioned system $Ax = b$, one needs additional information in order to obtain a satisfactory solution. One possibility is to qualitatively describe the so-called ‘‘smoothness’’ of a solution. For linear systems, we consider for $r \in \mathbb{N}$ the smoothing matrix

$$\mathcal{S} = \begin{cases} (A^* A)^{r/2}, & r \text{ even,} \\ (A^* A)^{(r-1)/2} A^*, & r \text{ odd.} \end{cases}$$

Typically, it suffices to take $r = 1$ or $r = 2$. As a consequence of results in [61, Thm. 4.1, Sec. 6], we assert the following. Let $\delta > 0$ and b^δ a perturbation of b such that $\|b - b^\delta\|_2 \leq \delta \|b\|_2$. Suppose

$$x = \mathcal{S}z, \quad \|Ax - b^\delta\|_2 \leq \Delta \|z\|_2 \quad (7.1.16)$$

for some $r \in \mathbb{N}$ defining \mathcal{S} , $\Delta > 0$ and vector z (in \mathbb{C}^n if r is even, in \mathbb{C}^m if r is odd. In any case, $x \in \mathbb{C}^n$). Then the optimal threshold ϵ_{opt} for the truncated SVD is given by

$$\epsilon_{opt} = \left(\frac{\Delta}{r} \right)^{1/(r+1)}.$$

It is generally observed that in estimate (7.1.16), z is not known and Δ may be difficult to estimate [61, Sec. 7]. If one is eager to find the optimal threshold, one may naively use estimates involving b and δ instead. Together with an additional crude assumption

$$\Delta \|z\|_2 \leq \delta \|b\|_2, \quad (7.1.17)$$

we see that for $0 < \delta < \frac{1}{2}$,

$$\|b\|_2 \leq \|b - b^\delta\|_2 + \|Ax - b^\delta\|_2 + \|Ax\|_2 \leq 2\delta \|b\|_2 + \|Ax\|_2.$$

Thus,

$$\|b\|_2 \leq \frac{\|Ax\|_2}{1 - 2\delta} = \frac{\|ASz\|_2}{1 - 2\delta} \leq \frac{\|A\|_2^{r+1} \|z\|_2}{1 - 2\delta}.$$

Consequently,

$$\Delta \leq \frac{\delta \|A\|_2^{r+1}}{1 - 2\delta} \quad \text{and} \quad \epsilon_{opt} \leq \|A\|_2 \left(\frac{\delta}{r(1 - 2\delta)} \right)^{1/(r+1)}. \quad (7.1.18)$$

We now apply (7.1.18) in the setting of $G^{[m,n]}_C = d^{[m]}$. Let B be an upper frame bound for the frame $\{k_2(x_l, \cdot) : l \in \mathbb{Z}\}$. Then $\|G^{[m,n]}\|_2 \leq B$ for all $m, n \in \mathbb{N}$ with $m \geq n$. By setting $r = 1$ and $r = 2$, we may take the values

$$B \left(\frac{\delta}{1 - 2\delta} \right)^{1/2} \leq \epsilon \leq B \left(\frac{\delta}{2(1 - 2\delta)} \right)^{1/3}.$$

In particular, using the machine precision $\delta = 10^{-16}$, we have approximately

$$1.0000 \times 10^{-8} \leq \frac{\epsilon}{B} \leq 3.6840 \times 10^{-6}.$$

With the knowledge of an upper frame bound B , the above estimate can be used as a guide in choosing singular value tolerances. In the forthcoming simulations, we do not know if (7.1.17) is realized, but in view of the above arguments, we fix a uniform value $\epsilon = 10^{-8}$ as tolerance across all numerical experiments.

7.2. Generating sets of stable sampling

In order to perform reconstruction methods, we need to carefully choose our sampling set. In the forthcoming numerical simulations, we use sets of stable sampling for our reconstruction algorithms. Theorem 3.3.1 provides sufficient conditions for $X = \{x_j\}_{j \in \mathbb{Z}}$ to be a set of stable sampling. For piecewise constant parametrizing functions, boundedness away from zero is automatically satisfied. We have the following corollary.

Corollary 7.2.1. *Let $\Omega > 0$ and p a piecewise constant function. If $X = \{x_j\}_{j \in \mathbb{Z}} \subset \mathbb{R}$ such that*

$$\delta(X, p) = \sup_{j \in \mathbb{Z}} \frac{x_{j+1} - x_j}{\inf_{x \in [x_j, x_{j+1}]} \sqrt{p(x)}} < \frac{\pi}{\Omega^{1/2}} \quad (7.2.1)$$

7. Numerical implementation and simulations

and in addition, there exist $\gamma_1, \gamma_2 > 0$ satisfying

$$\gamma_1 \leq x_{j+1} - x_j \leq \gamma_2, \quad \text{for all } j \in \mathbb{Z}, \quad (7.2.2)$$

then X is a set of stable sampling for $PW_{[0,\Omega]}(A_p)$ with lower and upper bounds $\gamma_2^{-1} \left(1 - \frac{\delta\Omega^{1/2}}{\pi}\right)^2$ and $\gamma_1^{-1} \left(1 + \frac{\delta\Omega^{1/2}}{\pi}\right)^2$, respectively.

In our reconstruction simulations, we consider two specific sampling sets: for $\gamma > 0$, we either take

- uniform samples $X_\gamma = \gamma\mathbb{Z}$, or
- perturbed samples $\tilde{X}_{\gamma,\eta} = \{\gamma j + \eta_j\}_{j \in \mathbb{Z}}$, where each η_j is chosen uniformly at random on the interval $(-\frac{\eta}{2}, \frac{\eta}{2})$ for some $\eta > 0$.

In reference to (7.2.2), we have $\gamma_1 = \gamma_2 = \gamma$ for X_γ . On the other hand, if $\eta < \gamma$, then $\gamma_1 = \gamma - \eta$, $\gamma_2 = \gamma + \eta$ for $\tilde{X}_{\gamma,\eta}$. Moreover, if p is an $(n+1)$ -component piecewise function for some $n \in \mathbb{N}$, then the maximum gaps are

$$\delta(X_\gamma, p) < \frac{\pi}{\Omega^{1/2}}, \quad \text{if } \gamma < \frac{\pi \min_{1 \leq j \leq n} \sqrt{p_j}}{\Omega^{1/2}} \quad (7.2.3)$$

and

$$\delta(\tilde{X}_{\gamma,\eta}, p) < \frac{\pi}{\Omega^{1/2}}, \quad \text{if } 0 < \eta < \gamma \leq \frac{\pi \min_{1 \leq j \leq n} \sqrt{p_j}}{2\Omega^{1/2}}. \quad (7.2.4)$$

Consequently, (7.2.3) and (7.2.4) respectively imply X_γ and $\tilde{X}_{\gamma,\eta}$ are sets of stable sampling for $PW_{[0,\Omega]}(A_p)$ by Corollary 7.2.1.

7.2.1. Sets of prescribed Beurling density

In another experiment, we investigate the behavior of the reconstruction algorithm as we take a family of sets of stable sampling whose lower Beurling densities approach the critical density. First, we mention a result in [39, Prop. 6.5] that relates the maximum gap and the lower Beurling density of a set.

Theorem 7.2.2. *Let $X = \{x_j\}_{j \in \mathbb{Z}} \subset \mathbb{R}$ such that $x_j < x_{j+1}$ for all $j \in \mathbb{Z}$ and $\lim_{j \rightarrow \infty} x_j = \pm\infty$. If $\delta(X, p) = \eta$ for some $\eta > 0$, then $D_p^-(X) \geq \eta^{-1}$.*

With an $(n+1)$ -component piecewise constant p , we give an algorithm to generate a discrete set Y with prescribed maximum gap $\delta(Y, p) = \eta$ and lower Beurling density $D_p^\pm(Y) = \eta^{-1}$. The construction can be thought of as semi-uniform sampling: for a fixed $\eta > 0$ and for each $j = 1, \dots, \leq n-1$, we start from the right endpoint of $I_j = (t_j, t_{j+1}]$ and generate uniformly spaced points

$$Y_j = \{t_{j+1} - k\eta\sqrt{p_j}\}_{k=0}^\infty \cap I_j, \quad 1 \leq j \leq n-1.$$

Additionally, if the pair of points t_j and $y_j^* = \min\{y : y \in Y_j\}$ satisfy

$$y_j^* - t_j > \eta \min\{\sqrt{p_{j-1}}, \sqrt{p_j}\},$$

we append another point $w_j \in (t_j, y_j^*) \subset Y_j$ given by

$$w_j = t_j + \eta \min\{\sqrt{p_{j-1}}, \sqrt{p_j}\}. \quad (7.2.5)$$

Meanwhile, on unbounded intervals I_0 and I_n we take the points

$$Y_0 = \{t_1 - k\eta\sqrt{p_0}\}_{k=0}^\infty \subset I_0, \quad Y_n = \{t_n + k\eta\sqrt{p_n}\}_{k=1}^\infty \subset I_n.$$

By construction, the set $Y = Y_0 \cup \dots \cup Y_n = \{y_j\}_{j \in \mathbb{Z}}$ satisfies $\delta(Y, p) = \eta$. Now, suppose $r > \frac{t_n - t_1}{2}$. We take a look at the following configurations:

- If $x \in \mathbb{R}$ such that $[t_1, t_n] \subset B_r(x)$, then

$$\frac{\#(Y \cap B_r(x))}{\mu_p(B_r(x))} = \frac{\sum_{k=1}^{n-1} \#(Y \cap I_k \cap B_r(x)) + \left\lfloor \frac{t_1 - (x-r)}{\eta\sqrt{p_0}} \right\rfloor + \left\lfloor \frac{(x+r) - t_n}{\eta\sqrt{p_n}} \right\rfloor}{\sum_{k=1}^{n-1} \frac{|I_k \cap B_r(x)|}{\sqrt{p_k}} + \frac{t_1 - (x-r)}{\sqrt{p_0}} + \frac{(x+r) - t_n}{\sqrt{p_n}}}.$$

- Otherwise, we know by our choice of r that $B_r(x) \cap (I_0 \cup I_n) \neq \emptyset$ for all $x \in \mathbb{R}$. Hence, terms corresponding to either $k = 0$ or $k = n$ (but not both) found in the numerator and denominator are absent. For the extreme cases $B_r(x) \subset I_0$ or $B_r(x) \subset I_n$, one has

$$\frac{\#(Y \cap B_r(x))}{\mu_p(B_r(x))} = \frac{\left\lfloor \frac{2r}{\eta\sqrt{p_k}} \right\rfloor}{\frac{2r}{\sqrt{p_k}}}, \quad k = 0 \text{ or } n.$$

In any case, since the number of consecutive points where local uniform spacing may not occur (i.e., the points t_j , y_j^* and a possible additional point w_j in (7.2.5)) is finite and only occurs at finite intervals I_k , $k = 1, \dots, n-1$, we get from (6.1.2) that $D_p^\pm(Y) = \eta^{-1}$. It is also clear that

$$0 < \eta \min_{0 \leq k \leq n} \sqrt{p_k} \leq y_{j+1} - y_j \leq \eta \max_{0 \leq k \leq n} \sqrt{p_k}, \quad j \in \mathbb{Z}.$$

Finally, if $0 < \eta < \frac{\pi}{\Omega^{1/2}}$, Corollary 7.2.1 implies that Y is a set of stable sampling for $PW_{[0, \Omega]}(A_p)$ with lower frame bound

$$\frac{1}{\eta \max_{0 \leq k \leq n} \sqrt{p_k}} \left(1 - \frac{\Omega^{1/2} \eta}{\pi}\right)^2 \downarrow 0 \quad \text{as } \eta \uparrow \frac{\pi}{\Omega^{1/2}}.$$

Take note that this is not the optimal lower frame bound; in fact, we show in a forthcoming experiment that the condition number of the Gramian even improves as we get close to the critical density $\frac{\Omega^{1/2}}{\pi}$.

We summarize the above construction of Y in the following routine.

Algorithm 3 Constructing semi-uniform sampling sets with prescribed maximum gap

Input: positive parameters $p = [p_0, p_1, \dots, p_n]$ and knots $t = [t_1, t_2, \dots, t_n]$
 $L > 0$ for the local interval $[-\frac{L}{2}, \frac{L}{2}]$, assume $[t_1, t_n] \subset [-\frac{L}{2}, \frac{L}{2}]$
Prescribed maximum gap η

Output: Set Y with maximum gap η and density η^{-1} .

- 1: **function** SEMIREGSAMP(p, t, η, L)
- 2: $Y_0 = \{t_1 - k\eta\sqrt{p_0}\}_{k=0}^\infty \cap [-\frac{L}{2}, t_1]$
- 3: **for** $j = 1$ to $n - 1$ **do**
- 4: $Y_j = \{t_{j+1} - k\eta\sqrt{p_j}\}_{k=0}^\infty \cap (t_j, t_{j+1}]$
- 5: Let $y_j^* = \min Y_j$
- 6: **if** $y_j^* - t_j > \eta \min\{\sqrt{p_{j-1}}, \sqrt{p_j}\}$ **then**
- 7: $Y_j = Y_j \cup \{t_j + \eta \min\{\sqrt{p_{j-1}}, \sqrt{p_j}\}\}$
- 8: **end if**
- 9: **end for**
- 10: $Y_n = \{t_1 + k\eta\sqrt{p_n}\}_{k=0}^\infty \cap (t_n, \frac{L}{2}]$
- 11: **end function**

7.3. Numerical simulations

In this section, we take a closer look at some aspects of approximation by variable bandwidth functions by means of numerical simulations. The piecewise constant nature of the parametrizing function suggests that variable bandwidth spaces are good candidates as reconstruction spaces for functions formed by continuously splicing bandlimited functions of different bandwidths. Our main point is to show experimentally that for such functions where distinct, local bandwidths are observed, reconstruction by variable bandwidth functions performs better than reconstruction by bandlimited functions.

We have the following pseudocode that encapsulates the general numerical procedure in Section 7.1.1.

Algorithm 4 Regularized reconstruction in $PW_{[0,\Omega]}(A_p)$

Input: Piecewise constant function p and singular value threshold $\epsilon > 0$
Numbers $m, n \in \mathbb{N}$ with $m \geq n$, and sampling points $\{x_j\}_{j=-m}^m$
Noiseless measurements $d^{[m]} = [f(x_j)]^T \in \mathbb{C}^{2m+1}$ of f

Output: Regularized reconstruction $\tilde{f}_\epsilon^{[m,n]}$ of f

- 1: Let k be the reproducing kernel for $PW_{[0,\Omega]}(A_p)$.
- 2: Build the Gramian $G^{[m,n]} = [k(x_l, x_j)]_{j,l} \in \mathbb{C}^{(2m+1) \times (2n+1)}$.
- 3: Write $G^{[m,n]} = U^{[m]} \Sigma^{[m,n]} (V^{[n]})^*$ using SVD.
- 4: Replace $\Sigma^{[m,n]}$ by $\Sigma_\epsilon^{[m,n]}$ by thresholding on the singular values.
- 5: Compute $\hat{c}_\epsilon^{[m,n]} = V^{[n]} (\Sigma_\epsilon^{[m,n]})^\dagger (U^{[m]})^* d^{[m]} \in \mathbb{C}^{2n+1}$.
- 6: **return** $\tilde{f}_\epsilon^{[m,n]} = \sum_{l=-n}^n (\hat{c}_\epsilon^{[m,n]})_l k(x_l, \cdot)$.

We then apply this finite-dimensional reconstruction procedure using variable bandwidth spaces as reconstruction spaces. The reconstruction is computed by regularized least squares fit as described in (7.1.12) and (7.1.13) using sets of stable sampling as

discussed in Section 7.2. In our simulations, we mostly consider $m = 2n$ (linear oversampling) and $\epsilon = 10^{-8}$. When we study the influence of the sampling rate $\frac{2m+1}{2n+1}$ on the performance of the algorithm, we take $m = \lfloor \varsigma n \rfloor$, $1 < \varsigma < 2$, so that the sampling rate is approximately ς for large n . Since Step 3 involves evaluating the reproducing kernel at sampling points, we only consider the case of two-component and three-component piecewise constant p . We also remind the reader that in Step 4, thresholding is performed by replacing singular values of $G^{[m,n]}$ that are less than ϵ by zero. The coefficient solution in Step 5 is precisely the minimal-norm least squares solution of the regularized linear system $G_\epsilon^{[m,n]} c = d^{[m]}$. In Step 6, we can form the regularized reconstruction by resampling: we plot $\tilde{f}_\epsilon^{[m,n]}$ using a uniform grid $\{hj\}_{j \in \mathbb{Z}}$ with fixed $h > 0$ as

$$\tilde{f}_\epsilon^{[m,n]}(hj) = \sum_{l=-n}^n (\hat{c}_\epsilon^{[m,n]})_l k(x_l, hj) = [k(x_l, hj)]_{j,l} \hat{c}_\epsilon^{[m,n]}.$$

Ideally, we choose a sufficiently small h so that the plot of $\tilde{f}_\epsilon^{[m,n]}$ is visually smooth on a plot window. Alternatively, by defining $\tilde{f}_\epsilon^{[m,n]}$ as a function handle, MATLAB's `fplot` command will automatically generate a smooth plot of $\tilde{f}_\epsilon^{[m,n]}$.

One can measure the accuracy of any finite-dimensional reconstruction \tilde{f} of f by computing from finite sampling points $\{x_j\}_{j=-m}^m$ the approximation errors

$$E_{\text{samp}}^2 = \left\{ \sum_{-m \leq j \leq m} |\tilde{f}(x_j) - f(x_j)|^2 \right\}^{1/2}, \quad E_{\text{samp}}^\infty = \max_{-m \leq j \leq m} |\tilde{f}(x_j) - f(x_j)|. \quad (7.3.1)$$

The empirical errors in (7.3.1) can be thought of a measure of how good the reconstruction interpolates the finite data $f(x_j)$. However, these errors may not reflect the quality of the reconstruction in between samples. Since in our artificial examples we know the original function f beforehand, it is more insightful to look at the discretized errors in a uniform grid $\{hl\}_{l \in \mathbb{Z}}$ on a fixed interval $[-\frac{L}{2}, \frac{L}{2}]$, $L > 0$ given by

$$E_{\text{grid}}^2 = \left\{ \sum_{-\frac{L}{2} \leq hl \leq \frac{L}{2}} |\tilde{f}(hl) - f(hl)|^2 \right\}^{1/2}, \quad E_{\text{grid}}^\infty = \max_{-\frac{L}{2} \leq hl \leq \frac{L}{2}} |\tilde{f}(hl) - f(hl)|. \quad (7.3.2)$$

We will mainly use (7.3.2) to measure the quality of regularized reconstructions together with the growth of $\|\hat{c}_\epsilon^{[2n,n]}\|_2$ as n increases.

Lastly, we mention that all simulations are performed using MATLAB R2021a (Academic Use - Individual) installed on a laptop computer with the following technical specifications:

Operating system	Windows 10 Home 64-Bit
Processor	Intel Core i7-7700HQ
Memory	32768 MB
Storage	Samsung SSD 870 EVO 1TB

In Appendix A we list important MATLAB routines used in all our simulations¹⁴.

¹⁴The Matlab Codes folder containing all the routines used in this dissertation can be downloaded via the link <https://www.dropbox.com/sh/57utba39ytkh0yf/AADK8upEumLqKaGhop489VKpa?dl=1>. Some parts of the discussion refer to a number of files in this downloadable folder.

7.3.1. Simulations for two-component piecewise constant p

In this section, we perform some experiments on reconstructing functions in some variable bandwidth space corresponding to a two-component piecewise constant p . Without loss of generality, it is enough to consider the reconstruction space $PW_{[0,\Omega]}(A_p)$ where p is a two-component piecewise function of the form

$$p(x) = \begin{cases} p_0, & x \leq 0, \\ p_1, & x > 0 \end{cases}$$

for some $p_0, p_1 > 0$. We recall the notation $q_k = p_k^{-1/2}$, $k = 0, 1$ and from Theorem 5.1.1 the formula

$$k_\Lambda(x, y) = \begin{cases} \frac{q_0\Omega^{1/2}}{\pi} \left(\operatorname{sinc} q_0\Omega^{1/2}(x - y) - \frac{q_0 - q_1}{q_0 + q_1} \operatorname{sinc} q_0\Omega^{1/2}(x + y) \right), & x, y \leq 0, \\ \frac{q_1\Omega^{1/2}}{\pi} \left(\operatorname{sinc} q_1\Omega^{1/2}(x - y) + \frac{q_0 - q_1}{q_0 + q_1} \operatorname{sinc} q_1\Omega^{1/2}(x + y) \right), & x, y > 0, \\ \frac{2q_0q_1\Omega^{1/2}}{\pi(q_0 + q_1)} \operatorname{sinc} \Omega^{1/2}(q_0x - q_1y), & x \leq 0, y > 0, \\ \frac{2q_0q_1\Omega^{1/2}}{\pi(q_0 + q_1)} \operatorname{sinc} \Omega^{1/2}(q_1x - q_0y), & x > 0, y \leq 0 \end{cases}$$

for the reproducing kernel k_Λ of $PW_{[0,\Omega]}(A_p)$. In particular,

$$k_\Lambda(0, x) = \begin{cases} \frac{2q_0q_1\Omega^{1/2}}{\pi(q_0 + q_1)} \operatorname{sinc}(q_0\Omega^{1/2}x), & x \leq 0, \\ \frac{2q_0q_1\Omega^{1/2}}{\pi(q_0 + q_1)} \operatorname{sinc}(q_1\Omega^{1/2}x), & x > 0 \end{cases} \quad (7.3.3)$$

is an element of $PW_{[0,\Omega]}(A_p)$. For nonzero knots, we can use the reproducing kernels found below Figure 5.1. Algorithm 4 is used to approximate a function from its point samples taken on some interval of interest.

In the forthcoming experiments, we study a number of problems from a numerical perspective.

- (i) Is a bandlimited function perfectly reconstructible in a variable bandwidth space whose local bandwidths are greater than or equal to the bandwidth of the function? Analogously, is a function of variable bandwidth perfectly reconstructible in a variable bandwidth space whose local bandwidths are greater than or equal to the respective local bandwidths of the function?
- (ii) If f is a $\frac{\pi}{\sqrt{c}}$ -bandlimited function for some $c > 0$ and p is a piecewise constant function, is the error in reconstructing f in the space $PW_{[0,\pi]}(A_p)$ commensurate to $\|p - c\|_\infty$? Similarly, let p and \tilde{p} be piecewise constant, positive functions with the same set of knots. Is the error in reconstructing a function $g \in PW_{[0,\pi]}(A_p)$ in the space $PW_{[0,\pi]}(A_{\tilde{p}})$ commensurate to $\|p - \tilde{p}\|_\infty$?
- (iii) If a function is formed by continuously joining two bandlimited functions with distinct bandwidths, can variable bandwidth spaces outperform Paley-Wiener spaces of constant bandwidth in terms of reconstructing the function?
- (iv) What happens to the quality of reconstruction of a function of variable bandwidth as we take sets of stable sampling whose lower Beurling densities approach the critical density $\frac{\Omega^{1/2}}{\pi}$?

With these guiding questions we now proceed to the simulations.

7.3.1.1. Reconstructing bandlimited functions in $PW_\Lambda(A_p)$

Our first set of simulations deal with reconstructing bandlimited functions in $PW_\Lambda(A_p)$ and provides some insights into answering problems (i) and (ii). Our focus is not on finding optimal Λ and p so that a bandlimited function is perfectly reconstructed in $PW_\Lambda(A_p)$, but rather on the interplay of the parametrizing function and the regularized reconstruction. To this end, let $\Lambda = [0, \pi^2]$ and consider the π -bandlimited function

$$f(x) = \text{sinc } \pi x = \frac{\sin \pi x}{\pi x}, \quad f \in PW_\pi(\mathbb{R}).$$

We wish to find the regularized reconstruction of f in the space $PW_{[0, \pi^2]}(A_p)$ with

$$p(x) = \begin{cases} 1, & x \leq 0, \\ p_1, & x > 0 \end{cases} \quad (7.3.4)$$

as p_1 approaches 1 in both directions and observe how the quality of reconstruction behaves.

By Proposition 3.1.3, functions in $PW_{[0, \pi^2]}(A_p)$ can locally be viewed as elements of B_π for $x < 0$ and $B_{\pi/\sqrt{p_1}}$ for $x > 0$. Since $PW_{[0, \pi^2]}(A_p) = PW_\pi(\mathbb{R})$ when $p_1 = 1$, we expect that the reconstruction improves as $p_1 \downarrow 1$, i.e., E_{grid}^2 and E_{grid}^∞ decrease as $p_1 \downarrow 1$. On the other hand, since $p_1 \uparrow 1$ means we have local bandwidth $\pi/\sqrt{p_1} > \pi$ on $I_1 = (0, \infty)$, it is natural to think that perfect reconstruction of f occurs. However, elements of $PW_\pi(\mathbb{R})$ are analytic functions, while the piecewise nature of p implies that elements of $PW_{[0, \pi^2]}(A_p)$ are not analytic. This means that a reconstruction of f in $PW_{[0, \pi^2]}(A_p)$ may be distorted due to Gibbs phenomenon, i.e., oscillations near the knots of p , and hence the reconstruction may be far from perfect. Therefore, as p_1 tends to 1 in both directions the best we can expect is that E_{grid}^2 and E_{grid}^∞ decrease.

The numerical setup starts by taking values

$$p_1 \in \{4, 2, 1.1, 1.0001, 1.0000001, 1.00000001, 1.000000001, 1\}, \quad (7.3.5)$$

$$p_1 \in \{0.25, 0.5, 0.9, 0.9999, 0.9999999, 0.99999999, 0.999999999, 1\} \quad (7.3.6)$$

to simulate the limiting processes $p_1 \downarrow 1$ and $p_1 \uparrow 1$, respectively. Uniformly-spaced sampling points

$$X_{\frac{1}{4}} = \frac{1}{4}\mathbb{Z} = \left\{ \frac{j}{4} \right\}_{j \in \mathbb{Z}}$$

are used so that for all choices of p_1 in (7.3.5) and (7.3.6), $\delta(X_{\frac{1}{4}}, p) < 1$ and $X_{\frac{1}{4}}$ is a set of stable sampling for $PW_{[0, \pi^2]}(A_p)$ by (7.2.3). For $n \in \mathbb{N}$, we take $4n + 1$ ($m = 2n$) noiseless samples

$$d_j^{[2n]} = f\left(\frac{j}{4}\right) = \text{sinc } \frac{\pi j}{4}, \quad j = -2n, \dots, 2n \quad (7.3.7)$$

of f and reconstruction space

$$\mathcal{T}_n = \text{span}\{k_\Lambda\left(\frac{l}{4}, \cdot\right) : l = -n, \dots, n\}$$

of dimension at most $2n + 1$. With $\epsilon = 10^{-8}$, we apply Algorithm 4 to calculate the regularized reconstruction $\tilde{f}_\epsilon^{[2n, n]}$ of f as

$$\tilde{f}_\epsilon^{[2n, n]}(x) = \sum_{l=-n}^n (\hat{c}_\epsilon^{[2n, n]})_l k_\Lambda\left(\frac{l}{4}, x\right),$$

7. Numerical implementation and simulations

where the coefficient vector $\hat{c}_\epsilon^{[2n,n]} \in \mathbb{C}^{2n+1}$ is computed as

$$\hat{c}_\epsilon^{[2n,n]} = (G_\epsilon^{[2n,n]})^\dagger d^{[2n]}.$$

To assess how the reconstruction performs as we approach the correct constant bandwidth π when $p_1 = 1$, we use the discretized errors E_{grid}^2 and E_{grid}^∞ as well as the norm $\|\hat{c}_\epsilon^{[2n,n]}\|_2$ of the coefficients of the regularized reconstruction on a uniform grid on the interval $[-25, 25]$ with $10^5 + 1$ points, i.e., $L = 50$ and $h = 0.0005$. We refer the reader to attached file `Trend2pBL.m` on the implementation of Algorithm 4 in MATLAB.

With minor modifications, we can perform the above numerical setup using the perturbed sampling set

$$\tilde{X}_{\frac{1}{4}, \frac{1}{8}} = \left\{ \frac{j}{4} + \eta_j, \eta_j \in \left(-\frac{1}{16}, \frac{1}{16}\right) \text{ uniformly random} \right\}_{j \in \mathbb{Z}}.$$

By (7.2.4), $\tilde{X}_{\frac{1}{4}, \frac{1}{8}}$ also a set of stable sampling for all choices of p_1 in (7.3.5) and (7.3.6). Noisy measurements

$$\tilde{d}_j^{[2n]} = f\left(\frac{j}{4} + \eta_j\right) + \theta_j, \quad |\eta_j| \leq \frac{1}{16}, j = -2n, \dots, 2n$$

are then used instead of (7.3.7), where each θ_j is chosen uniformly at random and satisfies $|\theta_j| \leq \theta$ for some $\theta > 0$ small.

In Figure 7.1 we display plots of E_{grid}^2 , E_{grid}^∞ , and $\|\hat{c}_\epsilon^{[2n,n]}\|_2$ for $n = 5, 6, \dots, 100$ using the uniform sampling set $X_{\frac{1}{4}}$, while in Figure 7.2 we show plots of the same quantities using the perturbed sampling set $\tilde{X}_{\frac{1}{4}, \frac{1}{8}}$ and noise bound $\theta = 10^{-8}$. Upon inspecting both figures, using $\tilde{X}_{\frac{1}{4}, \frac{1}{8}}$ with noisy samples produces slightly higher errors than using $X_{\frac{1}{4}}$ with noiseless samples, particularly when p_1 is very close to 1. Some remarkable findings from Figure 7.1 are as follows:

- For each $p_1 \neq 1$ in (7.3.5) and (7.3.6), the discretized errors E_{grid}^2 and E_{grid}^∞ decrease as n increases and then eventually stabilize to their respective constant values. For $p_1 = 1$, E_{grid}^2 and E_{grid}^∞ fluctuate close to 10^{-8} and 10^{-10} , respectively. The norms $\|\hat{c}_\epsilon^{[2n,n]}\|_2$ exhibit significant decrease as p_1 approaches 1 in both directions and do not exceed $\epsilon^{-1} = 10^8$ as we know from (7.1.15).
- As $p_1 \downarrow 1$, the local bandwidth $\pi/\sqrt{p_1} < \pi$ on $I_2 = (0, \infty)$ increasingly approaches π . This behavior is reflected by the steady decrease in E_{grid}^2 , E_{grid}^∞ and $\|\hat{c}_\epsilon^{[2n,n]}\|_2$ as $p_1 \downarrow 1$.
- As $p_1 \uparrow 1$, $\pi/\sqrt{p_1} > \pi$ and decreasingly approaches π . It is evident from both figures that taking local bandwidths, no matter how large or close to π , does not guarantee perfect or even reasonable reconstruction in the corresponding variable bandwidth space. This is counter-intuitive to perfect recovery of bandlimited functions in Paley-Wiener spaces of larger constant bandwidth.

Viewing f as a $\frac{\pi}{\sqrt{c}}$ -bandlimited function with $c = 1$, the experiments suggest that the quantity $\|p - c\|_\infty$ is commensurate to the discretized errors E_{grid}^2 and E_{grid}^∞ , and is a rough representation of the model mismatch between f and the reconstruction space $PW_{[0, \pi^2]}(A_p)$.

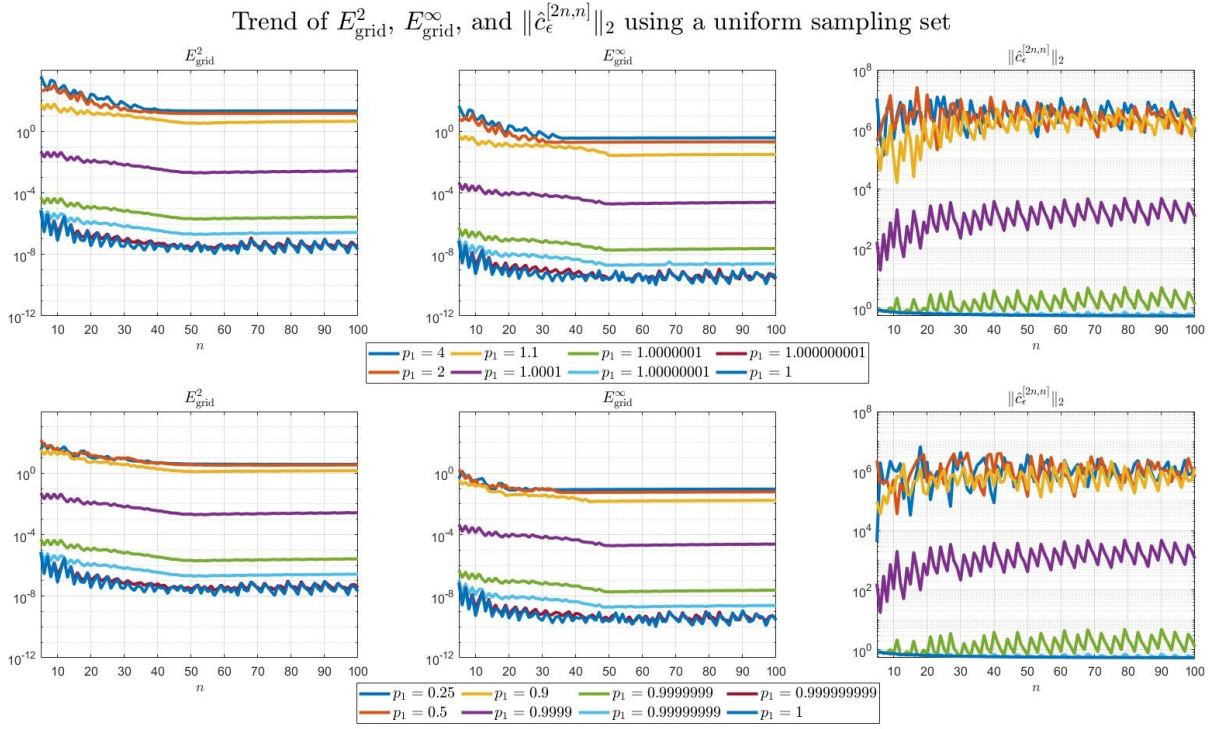


Figure 7.1.: Plots of E_{grid}^2 (col 1), E_{grid}^∞ (col 2), and $\|\hat{c}_\epsilon^{[2n,n]}\|_2$ (col 3) using the uniform sampling set $X_{\frac{1}{4}}$ and different values of p_1 approaching $p_1 = 1$.

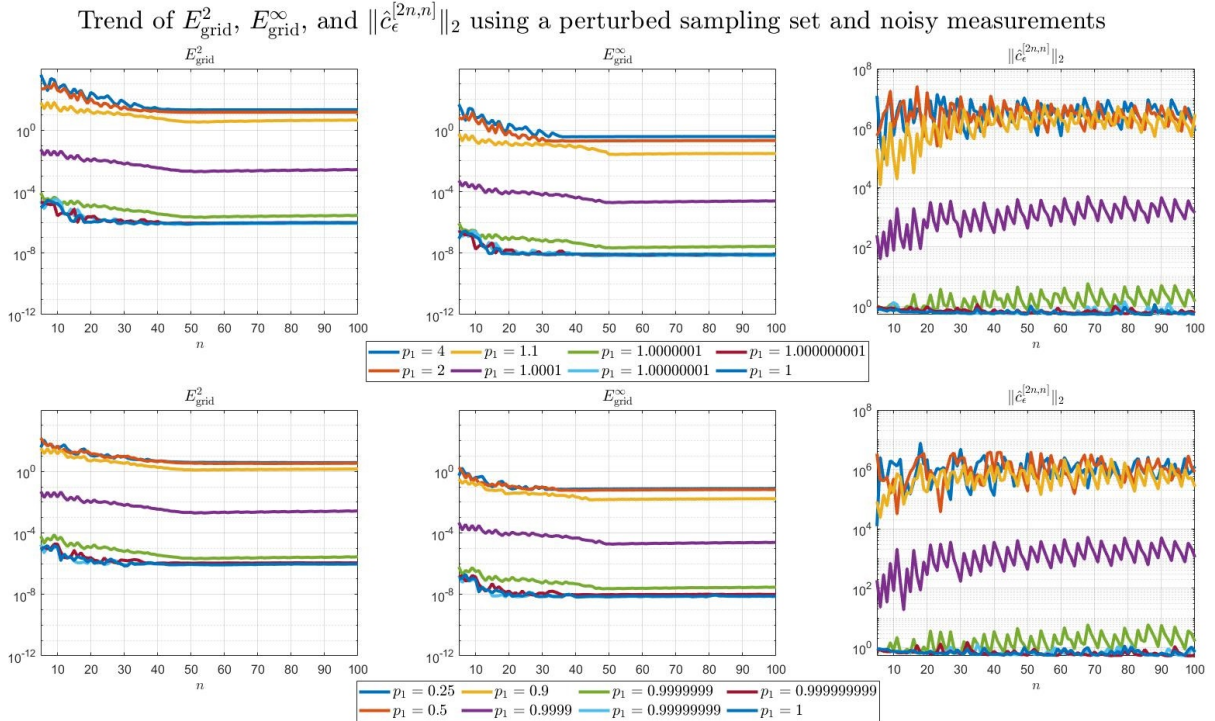


Figure 7.2.: Plots of E_{grid}^2 (col 1), E_{grid}^∞ (col 2), and $\|\hat{c}_\epsilon^{[2n,n]}\|_2$ (col 3) using the perturbed sampling set $\tilde{X}_{\frac{1}{4}, \frac{1}{8}}$ and noisy samples as well as different values of p_1 approaching $p_1 = 1$.

7. Numerical implementation and simulations

Interestingly, Figure 7.3 below shows that the reconstruction algorithm seems to perform stably even with decreasing sampling rates. We performed the same simulation from Figure 7.1 but replaced $m = 2n$ by $m = \lfloor \zeta n \rfloor$, where $\zeta = 2, 1.75, 1.5, 1.25$, in that order. We only considered $p_1 \downarrow 1$ but the same can be said for $p_1 \uparrow 1$. The reader may consult `Trend2pRedund.m` for additional simulations.

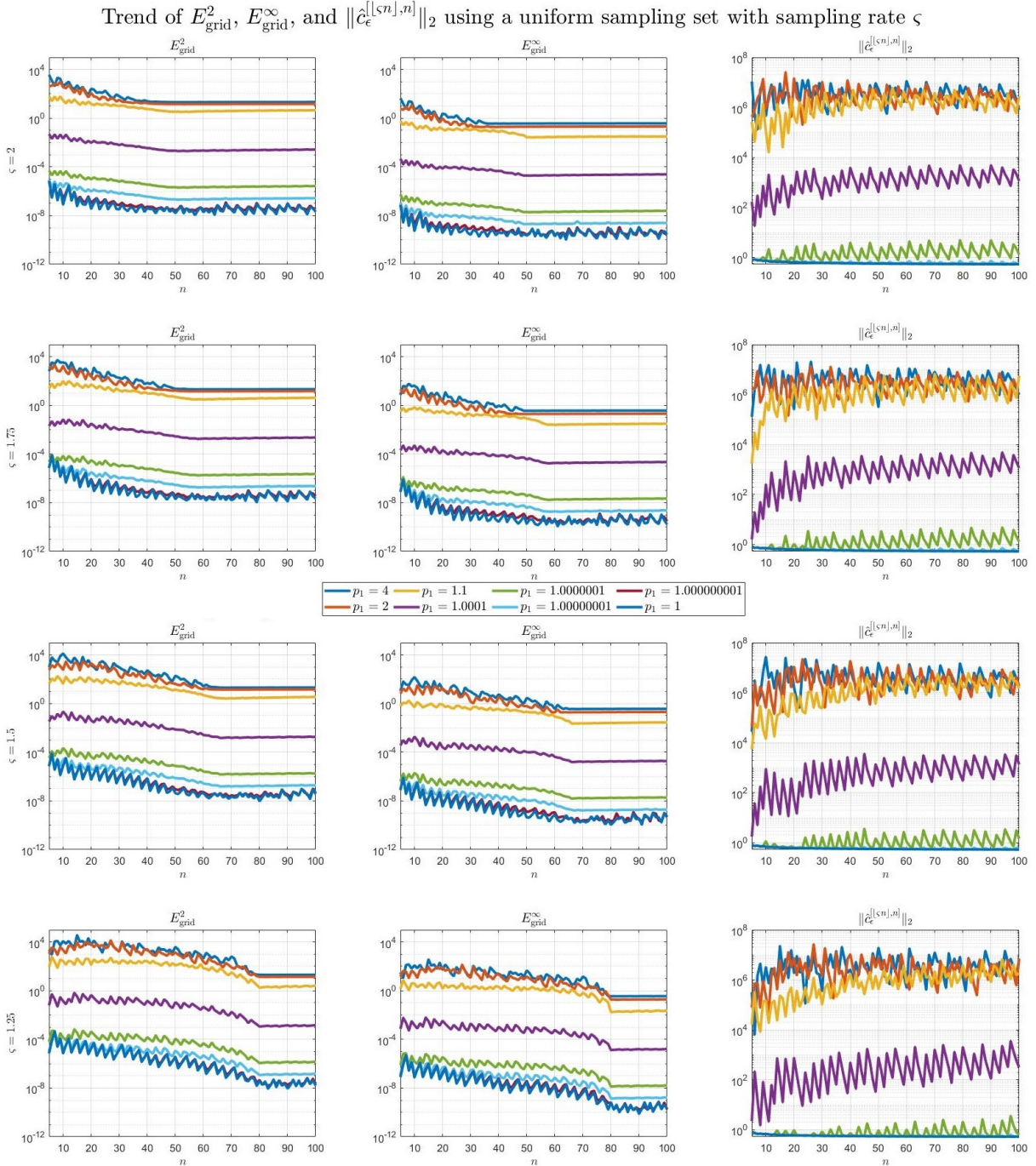


Figure 7.3.: Plots of E_{grid}^2 (col 1), E_{grid}^∞ (col 2), and $\|\hat{c}_\epsilon^{\lfloor \zeta n \rfloor, n}\|_2$ (col 3) using the uniform sampling set $X_{\frac{1}{4}}$, sampling rates $\zeta = 2$ (row 1), $\zeta = 1.75$ (row 2), $\zeta = 1.5$ (row 3), $\zeta = 1.25$ (row 4), and $p_1 \downarrow 1$.

A slight improvement in the numerical reconstruction can be achieved by replacing the MATLAB command `pinv` by `lsqminnorm` in Routine A.6. Since `lsqminnorm` is based on complete orthogonal decompositions (a form of rank-revealing QR decomposition, see [16, Secs. 1.3.1, 2.7.6] for details), it is more computationally efficient¹⁵ than `pinv` when computing minimum norm least square solutions. Figure A.1 shows that E_{grid}^2 and E_{grid}^∞ fluctuate close to 10^{-10} and 10^{-12} , respectively, which better reflect perfect recovery of f when $p_1 = 1$. The rest of the plots are visually unchanged.

The reader might have expected that for $p_1 = 1$, the discretized errors are within machine precision. Unfortunately, the errors in Figures 7.1, 7.2, and A.1 show significantly higher values, particularly with E_{grid}^∞ around 10^{-10} using `pinv` (and 10^{-12} using `lsqminnorm`). To some extent, this occurrence may be attributed to ill-conditioning and rank-deficiency of uneven sections of the Gramian. One way to further improve the errors is to generate reconstruction vectors using the following result [39, Thm. 4.1]:

Theorem 7.3.1. *Let p be a two-component piecewise constant function with components $p_0, p_1 > 0$. Fix the sampling set*

$$S_{\text{onb}} = \{s_l\}_{l \in \mathbb{Z}}, \quad s_l = \begin{cases} \frac{\pi l \sqrt{p_0}}{\Omega^{1/2}}, & l \leq 0, \\ \frac{\pi l \sqrt{p_1}}{\Omega^{1/2}}, & l > 0 \end{cases} \quad (7.3.8)$$

for some $\Omega > 0$ and the weights

$$w_l = \begin{cases} \sqrt{p_0}, & l < 0, \\ \frac{1}{2}(\sqrt{p_0} + \sqrt{p_1}), & l = 0, \\ \sqrt{p_1}, & l > 0. \end{cases}$$

Then the set

$$\left\{ \sqrt{\frac{\pi w_l}{\Omega^{1/2}}} k_\Lambda(s_l, \cdot) : l \in \mathbb{Z} \right\}$$

is an orthonormal basis for $PW_{[0, \Omega]}(A_p)$ with reproducing kernel k_Λ . The orthogonal expansion

$$f(x) = \frac{\pi}{\Omega^{1/2}} \sum_{l \in \mathbb{Z}} w_l f(s_l) k_\Lambda(s_l, x)$$

converges in $L^2(\mathbb{R})$ and uniformly for every $f \in PW_{[0, \Omega]}(A_p)$.

In particular, taking $\Omega = \pi^2$ and p given in (7.3.4) implies the set

$$S_{\text{onb}} = \{s_l\}_{l \in \mathbb{Z}}, \quad s_l = \begin{cases} \frac{\pi l}{\Omega^{1/2}}, & l \leq 0, \\ \frac{\pi l \sqrt{p_1}}{\Omega^{1/2}}, & l > 0 \end{cases}$$

¹⁵This tip is mentioned in the `lsqminnorm` documentation available at <https://www.mathworks.com/help/matlab/ref/lsqminnorm.html>. In theory, both methods yield the same minimum-norm least square solution but may have different numerical results in MATLAB.

7. Numerical implementation and simulations

generates an orthogonal system $\{k_\Lambda(s_l, \cdot) : l \in \mathbb{Z}\}$ for $PW_{[0, \pi^2]}(A_p)$. In turn, we have for $n \in \mathbb{N}$ the invertible matrix $G^{[n, n]} \in \mathbb{C}^{(2n+1) \times (2n+1)}$ given by

$$G^{[n, n]}(j, l) = k_\Lambda(s_l, s_j) = \begin{cases} 1, & j = l < 0, \\ \frac{2}{1 + \sqrt{p_1}}, & j = l = 0, \\ \frac{1}{\sqrt{p_1}}, & j = l > 0, \\ 0, & j \neq l, \end{cases} \quad G^{[n, n]} = \begin{bmatrix} I_n & & \\ & \frac{2}{1 + \sqrt{p_1}} & \\ & & \frac{1}{\sqrt{p_1}} I_n \end{bmatrix}$$

for $j, l = -n, \dots, n$. Figure A.2 confirms the error values obtained in Figure 7.1 for $p_1 \neq 1$, perfect reconstruction of f is achieved as E_{grid}^2 is around 10^{-14} and E_{grid}^∞ is within machine precision, and the norm of coefficients converges to 1 as p_1 approaches 1.

In summary, we observe that the closer the local bandwidths of the reconstruction space $PW_{[0, \pi^2]}(A_p)$ to π , the smaller the discretized errors of regularized reconstructions of f . Surprisingly, variable bandwidth spaces with arbitrarily large local bandwidths may not contain a satisfactory reconstruction of f .

We also mention that variations of this simulation can be done by replacing (7.3.4) by a different family of parametrizing functions. For instance, we can take

$$p(x) = \begin{cases} p_0, & x \leq 0, \\ p_1, & x > 0 \end{cases}$$

where $p_0 \uparrow 1$ and $p_1 \downarrow 1$, i.e., the local bandwidths on $(-\infty, 0)$ and $(0, \infty)$ approach π from above, resp. from below. We performed an independent simulation¹⁶ with this family of parametrizing functions and the observations are no different from what are stated previously. Lastly, it is natural to ask if these observations still hold if f is a function of variable bandwidth. It can analogously be shown as an example that the regularized reconstruction of

$$f(x) = \begin{cases} \text{sinc } \frac{\pi}{3}x, & x \leq 0, \\ \text{sinc } \pi x, & x > 0 \end{cases}$$

in the space $PW_{[0, \pi^2]}(A_p)$, where

$$p(x) = \begin{cases} 9, & x \leq 0, \\ p_1, & x > 0 \end{cases}$$

and p approaches 1 in both directions, behaves in a similar fashion¹⁷.

What we have seen so far from the experiments is that if one of the local bandwidths is fixed and we let the other vary, then the corresponding regularized reconstruction worsens as we deviate from the correct bandwidth. What we have not tested yet is the reconstruction of a function $f \in PW_\Lambda(A_p)$ in another variable bandwidth space $PW_\Lambda(A_{\tilde{p}})$, where $\tilde{p} = c^{-2}p$ for some $c > 0$. The following theorem states that if p is a piecewise constant function and Λ is an interval of the form $[0, \Omega]$, then there is a subspace inclusion between variable bandwidth spaces generated by p and \tilde{p} .

¹⁶See further instructions in `Trend2pBL.m` to run this simulation.

¹⁷See `Trend2pVB.m`.

Theorem 7.3.2. *Let $\Lambda \subset \mathbb{R}_0^+$ and p a piecewise constant function. Then*

$$PW_\Lambda(A_{c^{-2}p}) = PW_{c^2\Lambda}(A_p).$$

In particular, if $\Lambda = [0, \Omega]$ for some $\Omega > 0$, then $PW_{[0, \Omega]}(A_{c^{-2}p}) \subseteq PW_{[0, \Omega]}(A_p)$ for all $0 < c \leq 1$.

Proof. Let $\tilde{p} = c^{-2}p$ for some $0 < c \leq 1$. Then by definition,

$$A_{\tilde{p}} = -D(c^{-2}pD) = c^2(-D(pD)) = c^{-2}A_p.$$

We can verify using results from Chapter 4 the following adjustments when p is replaced by \tilde{p} :

Quantity	p	$p \mapsto \tilde{p} = c^{-2}p$	Reference
$d\mu$	$d\mu(\lambda)$	$d\mu(c^2\lambda)$	(4.3.11)
\mathcal{F}_{A_p}	$\mathcal{F}_{A_p}f(\lambda)$	$\mathcal{F}_{A_p}f(c^2\lambda)$	(4.3.12)
$\chi_\Lambda(A_p)$	$\chi_\Lambda(A_p)f$	$\chi_{c^2\Lambda}(A_p)f$	(2.2.7)

As a consequence, the spectral projection $\chi_\Lambda(A_{\tilde{p}}) : L^2(\mathbb{R}) \rightarrow PW_\Lambda(A_{\tilde{p}})$ amounts to projecting $f \in L^2(\mathbb{R})$ onto the variable bandwidth space generated by p but with a scaled spectral set $c^2\Lambda$. In particular, if $\Lambda = [0, \Omega]$ for some $\Omega > 0$, then $c^2\Lambda \subseteq \Lambda$ and so $PW_{[0, \Omega]}(A_{c^{-2}p}) = PW_{[0, c^2\Omega]}(A_p)$ is a closed subspace of $PW_{[0, \Omega]}(A_p)$. \square

As a special case, if $\Lambda = [0, \omega^2]$ and $p \equiv 1$, then from (2.2.11) we have for $0 < c \leq 1$ the known fact that

$$PW_{c\omega}(\mathbb{R}) = PW_{[0, c^2\omega^2]}(A_p) \subseteq PW_{[0, \omega^2]}(A_p) = PW_\omega(\mathbb{R}).$$

We now check if we can further support the above theorem using numerical simulations. Let

$$p(x) = \begin{cases} \frac{1}{16}, & x \leq 0, \\ 1, & x > 0 \end{cases}$$

and consider the regularized reconstruction of

$$f(x) = \begin{cases} \text{sinc } \pi x, & x \leq 0, \\ \text{sinc } \frac{\pi}{4}x, & x > 0 \end{cases} \in PW_{[0, \pi^2]}(A_{16p})$$

in the spaces

$$PW_{[0, \pi^2]}(A_{16p}) \subseteq PW_{[0, \pi^2]}(A_{8p}) \subseteq PW_{[0, \pi^2]}(A_{4p}) \subseteq PW_{[0, \pi^2]}(A_{2p}) \subseteq PW_{[0, \pi^2]}(A_p).$$

These nested inclusions are guaranteed by Theorem 7.3.2 with $c = 2^{-1/2}$ for each inclusion. The reconstruction of f in these three spaces must be perfect, at least in theory. In the following experiment we use orthogonal reconstruction vectors generated via Theorem 7.3.1 and singular value threshold $\epsilon = 10^{-8}$ to compute $\tilde{f}_\epsilon^{[n, n]}$ for $n = 5, \dots, 200$ via Algorithm 4. Figure 7.4 shows that perfect reconstruction is evident with the parametrizing function $16p$. On the other hand, there is an observable but surprisingly very slow downward trend for both E_{grid}^2 and E_{grid}^∞ for the remaining parametrizing functions. By (7.3.3), the correct coefficient is $\frac{5}{2}$ and is attained only when we use $16p$. We encourage the reader to use `PerfRec2pVB.m` as well as adjust the parameters to verify the results for even larger values of n . This may take a few hours to complete but the discretized errors are expected to display a consistent downward trend. The reconstructions in the above spaces have virtually overlapping graphs.

7. Numerical implementation and simulations

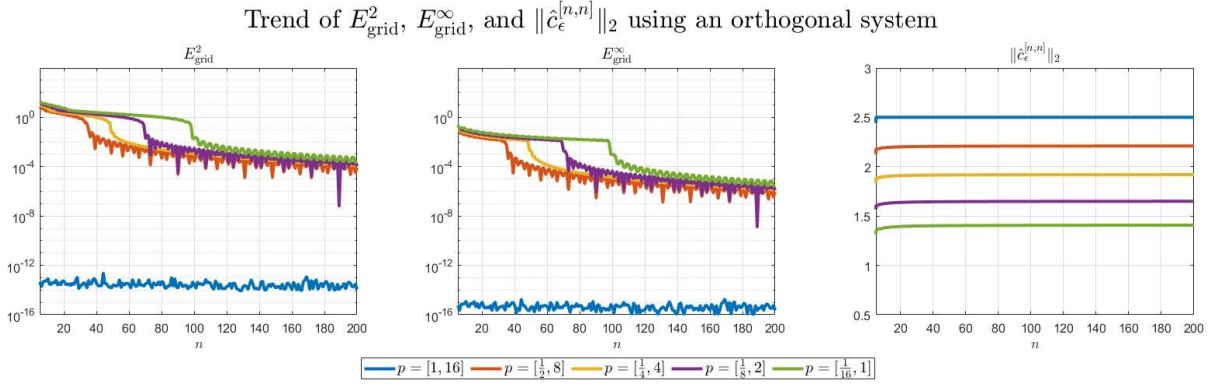


Figure 7.4.: Plots of E_{grid}^2 (col 1), E_{grid}^∞ (col 2), and $\|\hat{c}_\epsilon^{[n,n]}\|_2$ (col 3) using orthogonal reconstruction vectors and using multiples of a fixed parametrizing function.

7.3.1.2. Reconstructing non-bandlimited functions in $PW_\Lambda(A_p)$

Perhaps the most important simulation in this section is to show that given point samples as data, some functions are better reconstructed by functions of variable bandwidth than by functions of constant bandwidth. Define the continuous function

$$g(x) = \begin{cases} \text{sinc } \pi x, & x \leq 0, \\ \text{sinc } \frac{\pi}{10} x, & x > 0. \end{cases}$$

While the piecewise component functions of g are in itself bandlimited, g is not bandlimited since it is not smooth at $x = 0$. This is due to the Paley-Wiener Theorem [63, Thm. X]. Indeed, since $\text{sinc}_a x = \text{sinc } ax$, $a > 0$ has the Taylor series expansion

$$\text{sinc}_a x = \sum_{k=0}^{\infty} \frac{(-1)^k (ax)^{2k}}{(2k+1)!}, \quad x \in \mathbb{R},$$

we have the even-order derivatives

$$\text{sinc}_a^{(2k)}(0) = \frac{(-1)^k a^{2k}}{2k+1}, \quad k \in \mathbb{N}_0$$

while all odd-order derivatives are zero. Since we have $a = \pi$ on the left part of g and $a = \frac{\pi}{10}$ on the right, $D^2 g(0)$ does not exist as the left and right derivatives at $x = 0$ are not equal. Upon closer inspection, we see from (7.3.3) that with $\Omega = \pi^2$ and parametrizing function

$$p(x) = \begin{cases} 1, & x \leq 0, \\ 100, & x > 0, \end{cases} \quad (7.3.9)$$

we have

$$g(x) = \frac{11}{2} k_\Lambda(0, x), \quad x \in \mathbb{R}. \quad (7.3.10)$$

Hence, g can be perfectly reconstructed in $PW_{[0, \pi^2]}(A_p)$ with this p .

In order to provide a proper comparison between reconstructing g in variable bandwidth spaces and in Paley-Wiener spaces of constant bandwidth, we propose the following modified setup for the regularized reconstruction. Consider the uniform sampling sets

$$X_\gamma = \{\gamma j\}_{j \in \mathbb{Z}}, \quad \gamma = 0.5, 0.6, 0.7, 0.8, 0.9, 0.99, 0.999, 0.9999. \quad (7.3.11)$$

By (7.2.3), X_γ is a set of stable sampling for $PW_{[0, \pi^2]}(A_p)$, where (i) p is given by (7.3.9), and (ii) $p \equiv 1$, i.e., $PW_{[0, \pi^2]}(A_p) = PW_\pi(\mathbb{R})$. Now, we slightly modify how we build the Gramian in (7.1.8). For each $n \in \mathbb{N}$, we take the middle $4n + 1$ ($m = 2n$) sampling points

$$\{x_j\}_{j=-2n}^{2n} = \{\gamma j\}_{j=-2n}^{2n}$$

in X_γ and form the $(2n + 1)$ -dimensional reconstruction subspace

$$\mathcal{T}_n = \{k_\Lambda(s_l, \cdot) : l = -n, \dots, n\}$$

where s_l is given in (7.3.8). As a result, for each $n \in \mathbb{N}$ we can form the cross-Gramian $\tilde{G}^{[2n, n]} \in \mathbb{C}^{(4n+1) \times (2n+1)}$ with entries

$$\tilde{G}^{[2n, n]}(j, l) = k_\Lambda(s_l, x_j), \quad j = -2n, \dots, 2n, l = -n, \dots, n.$$

We then compute the regularized reconstruction $\tilde{g}_\epsilon^{[2n, n]}$ for $n = 5, 6, \dots, 100$ via Algorithm 4 with singular value threshold $\epsilon = 10^{-8}$ and the Gramian in Step 2 replaced by the cross-Gramian above. Taking p as in (7.3.9) corresponds to reconstructing g in $PW_{[0, \pi^2]}(A_p)$ while taking $p \equiv 1$ corresponds to reconstructing g in $PW_\pi(\mathbb{R})$. The increasing uniform sampling width γ in (7.3.11) simulates a steady decrease in sampling density, which permits us to observe if taking fewer samples has consequential effects on the regularized reconstruction of g .

Before we discuss the results, we emphasize that in both reconstructions we used a fixed spectral set $\Lambda = [0, \pi^2]$, the same set of stable sampling, the same dimension for the reconstruction subspaces, and the same regularized reconstruction procedure. The only difference is the reproducing kernel k_Λ used to form elements of the finite-dimensional reconstruction subspaces since k_Λ is dependent on the choice of p .

Figure 7.5 displays the trends of E_{grid}^2 , E_{grid}^∞ , and $\|\hat{c}_\epsilon^{[2n, n]}\|_2$ of the proposed reconstruction method for two different reconstruction spaces for $n = 5, 6, \dots, 100$. We also have on the left of Figure 7.6 the graphs of $\tilde{g}_\epsilon^{[2n, n]}$ with $n = 100$ in the reconstruction space $PW_\pi(\mathbb{R})$ using the sampling set X_γ given in (7.3.11). On the right we have a magnified version of the same plots to understand how the reconstructions behave near the point $x = 0$.

Our findings from Figure 7.5 are as follows:

- In the first row we have the regularized reconstruction procedure using $PW_{[0, \pi^2]}(A_p)$ with p in (7.3.9) as reconstruction space. We see as expected that the orthogonal system results in small discretized errors E_{grid}^2 and E_{grid}^∞ around 10^{-10} and 10^{-12} , respectively. In addition, the norms $\|\hat{c}_\epsilon^{[2n, n]}\|_2$ are steady at $\frac{11}{2}$ which is consistent with the original expansion of g in (7.3.10). The decreasing density of the sampling set has no observable effect on the discretized errors and is a direct consequence of using an orthogonal system to form finite-dimensional reconstruction spaces.

7. Numerical implementation and simulations

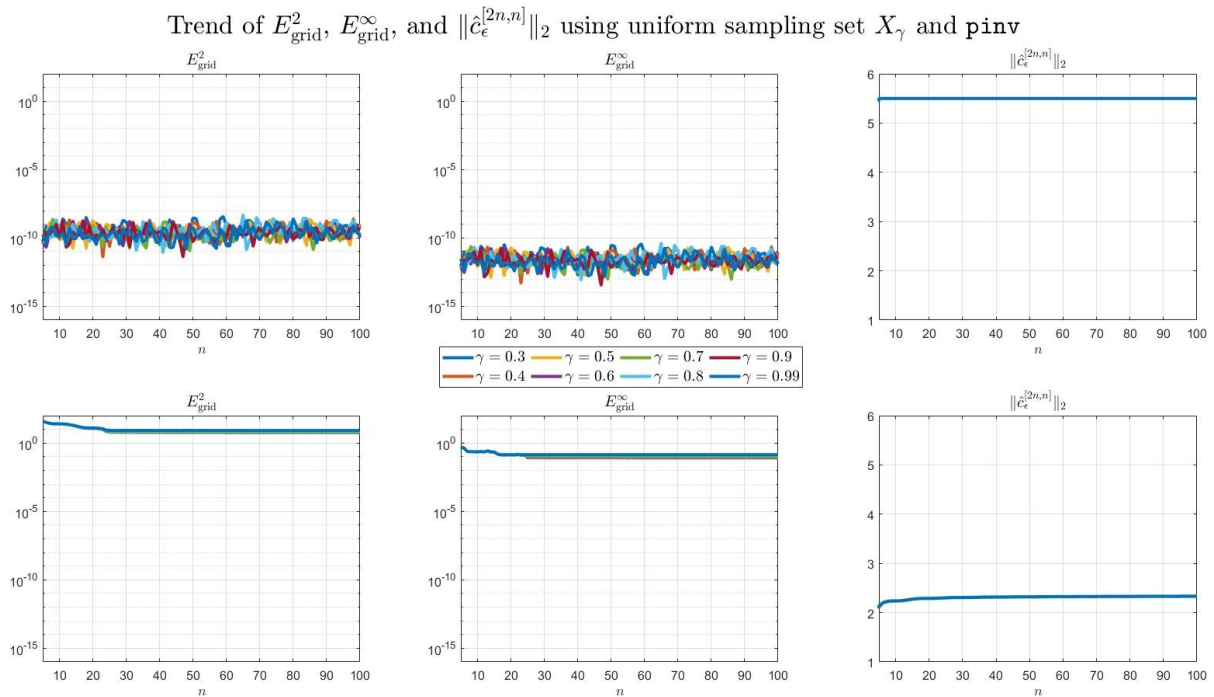


Figure 7.5.: Plots of E_{grid}^2 (col 1), E_{grid}^∞ (col 2), and $\|\hat{c}_\epsilon^{[2n,n]}\|_2$ (col 3) when g is reconstructed in $PW_{[0, \pi^2]}(A_p)$ (row 1) and $PW_\pi(\mathbb{R})$ (row 2) using uniform sampling sets X_γ with increasing γ and MATLAB command `pinv`.

Plot of $y = g(x)$ and $y = \tilde{g}_\epsilon^{[200,100]}(x)$ using uniform sampling sets approaching near-critical density

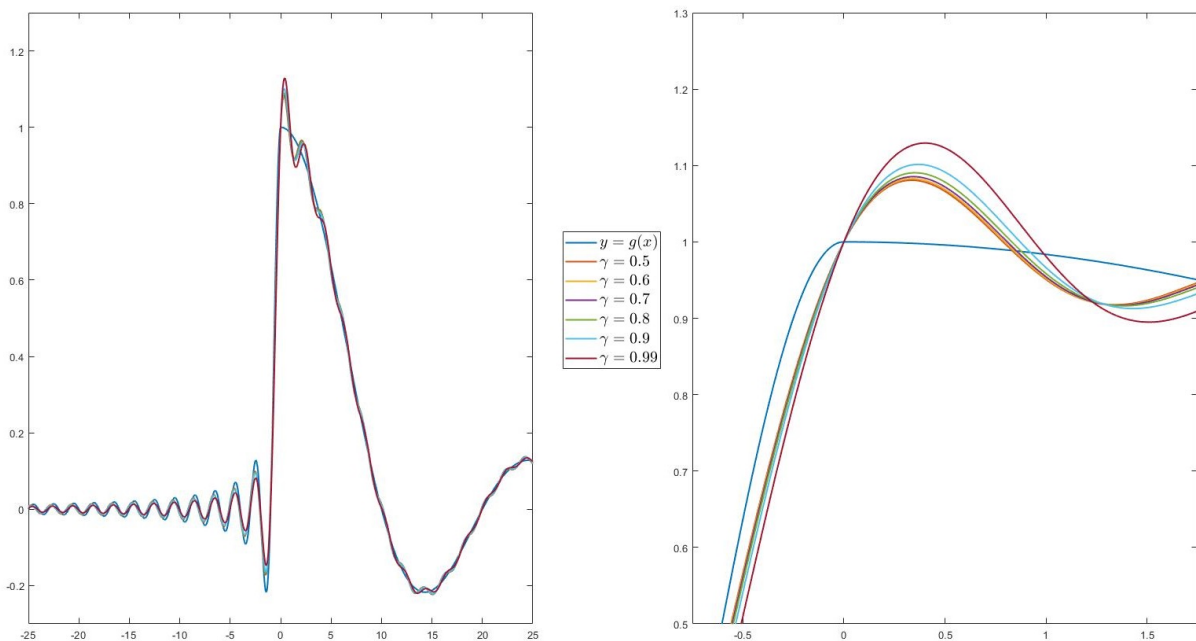


Figure 7.6.: (Left) Plot of g and its regularized reconstructions $\tilde{g}_\epsilon^{[200,100]}$ using uniform sampling sets X_γ with increasing γ . (Right) A closer look at the reconstructions near $x = 0$.

- In the second row we perform the same reconstruction setup with $PW_\pi(\mathbb{R})$ as reconstruction space. Although the local bandwidths π and $\frac{\pi}{10}$ are less than or equal to π , we always have significant reconstruction error due to Gibbs phenomenon (see Figure 7.6) that does not resolve as n increases. The plots suggest that for all values of γ in (7.3.11), the reconstruction $\tilde{g}_\epsilon^{[200,100]}$ attempts to minimize the errors near $x = 0$ at the cost of substantial errors on other parts of the reconstruction. In this case, the compensatory behavior is mostly on the left side of the graphs of the reconstructions.

We now have verified numerically that the regularized reconstruction of g in the correct variable bandwidth space outperforms the regularized reconstruction of g in $PW_\pi(\mathbb{R})$.

7.3.1.3. On the quality of regularized reconstruction on sets of stable sampling with near-critical densities

The last simulation deals with the behavior of the reconstruction as we take sets of stable sampling whose lower Beurling densities approach the critical density. Section 7.2.1 includes a method to generate such sets. Let p be a two-component piecewise constant function. By Theorem 6.4.1, we have the critical density $\frac{\Omega^{1/2}}{\pi}$ for $PW_{[0,\Omega]}(A_p)$. Fix $r > 1$. By Algorithm 3, we can generate a sequence of semi-uniform sampling sets $\{S_{r,k}\}_{k=0}^\infty$ such that

$$\delta(S_{r,k}, p) = \frac{\pi}{\Omega^{1/2}} \left(\frac{1}{1+r^{-k}} \right) \quad \text{and} \quad D_p^\pm(S_{r,k}) = \frac{\Omega^{1/2}}{\pi} (1+r^{-k}). \quad (7.3.12)$$

By construction, $\{S_{r,k}\}_{k=0}^\infty$ is a sequence of sets of stable sampling for $PW_{[0,\Omega]}(A_p)$ such that $D_p^\pm(S_{r,k}) \rightarrow \frac{\Omega^{1/2}}{\pi}$ as $k \rightarrow \infty$.

With the above construction we consider the following setup: let $\Omega = \pi^2$ and take the previously defined function

$$g(x) = \begin{cases} \operatorname{sinc} \pi x, & x \leq 0, \\ \operatorname{sinc} \frac{\pi}{10} x, & x > 0 \end{cases} \in PW_{[0,\pi^2]}(A_p), \quad p(x) = \begin{cases} 1, & x \leq 0, \\ 100, & x > 0. \end{cases}$$

As before, we examine E_{grid}^2 , E_{grid}^∞ and $\|\hat{c}_\epsilon^{[\lceil 100\varsigma \rceil, 100]}\|_2$ using the sets $S_{\frac{4}{3},k}$, $k = 0, \dots, 30$ satisfying (7.3.12) and taking sampling rates $\varsigma = 2, 1.75, 1.5, 1.25$. We see from Figure 7.7 that E_{grid}^2 and E_{grid}^∞ display a downward trend, and for $k \geq 12$ there is a noticeable drop to 10^{-13} and 10^{-15} , respectively. In addition, the norms $\|\hat{c}_\epsilon^{[\lceil 100\varsigma \rceil, n]}\|_2$ abruptly jump and stabilize to $\frac{11}{2}$, while $D_p^\pm(S_{\frac{4}{3},k})$ steadily decreases and approaches 1 but does not seem to improve that much beyond $k = 12$. Figure 7.8 shows that the condition number $\kappa(G^{[\lceil 100\varsigma \rceil, 100]})$ of the Gramian drastically improves for $k \geq 8$, hence the reconstruction procedure becomes more well-conditioned as k increases. Such observations are not surprising since with a two-component piecewise constant p and $k \rightarrow \infty$, $S_{\frac{4}{3},k}$ is the same as S_{onb} in (7.3.8) with the exception of possibly one point added by Step 7 of Algorithm 3.

In conclusion, this experiment shows that g can be perfectly reconstructed from $S_{r,k}$ (with r fixed) and with decreasing Beurling densities, so long as these densities do not fall below the critical density 1. The decreasing sampling rates do not present any significant effect on E_{grid}^2 , E_{grid}^∞ , $\|\hat{c}_\epsilon^{[\lceil 100\varsigma \rceil, 100]}\|_2$, and $\kappa(G^{[\lceil 100\varsigma \rceil, 100]})$.

7. Numerical implementation and simulations

Trend of E_{grid}^2 , E_{grid}^∞ , $\|\hat{c}_\epsilon^{[100\zeta],100}\|_2$, and $D_p^\pm(S_{\frac{4}{3},k})$ for sampling sets $S_{\frac{4}{3},k}$ having near-critical densities

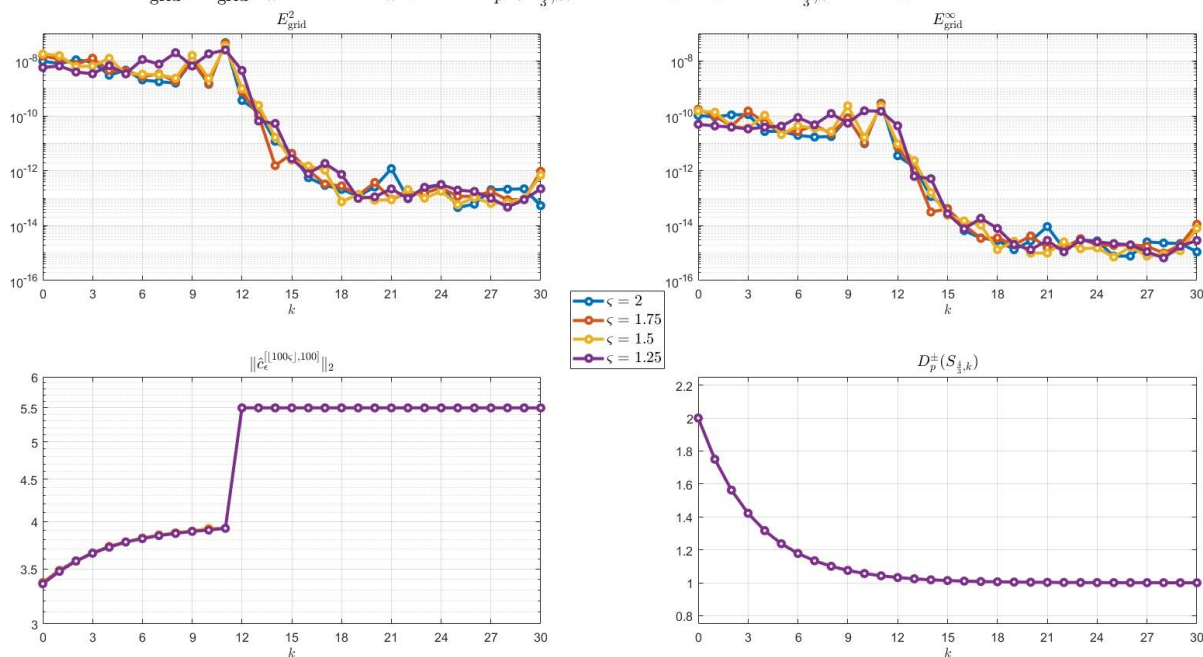


Figure 7.7.: Plots of E_{grid}^2 , E_{grid}^∞ , $\|\hat{c}_\epsilon^{[100\zeta],100}\|_2$, and $D_p^\pm(S_{\frac{4}{3},k})$ when g is reconstructed from sampling sets $S_{\frac{4}{3},k}$, $k = 0, \dots, 20$ whose Beurling densities approach the critical density 1 and taking decreasing sampling rates $\zeta = 2, 1.75, 1.5, 1.25$.

Trend of $\kappa(G^{[100\zeta],100})$ for sampling sets $S_{\frac{4}{3},k}$ having near-critical densities and decreasing sampling rates

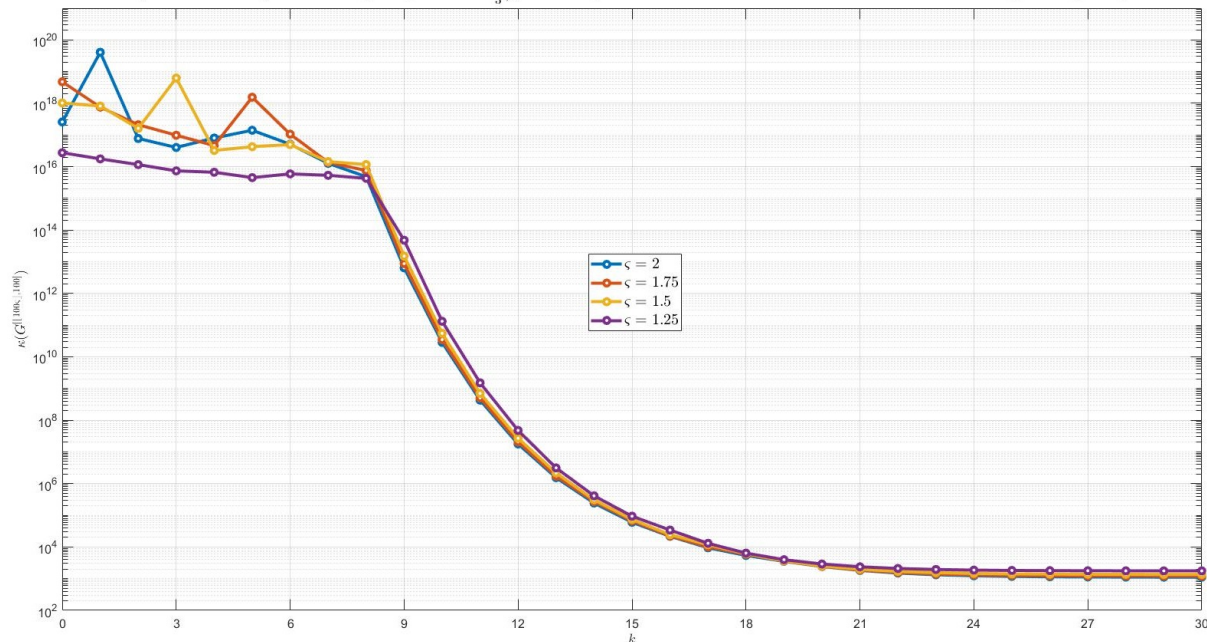


Figure 7.8.: Plot of $\kappa(G^{[100\zeta],100})$ when g is reconstructed from sampling sets $S_{\frac{4}{3},k}$, $k = 0, \dots, 20$ whose Beurling densities approach the critical density 1 and taking decreasing sampling rates $\zeta = 2, 1.75, 1.5, 1.25$.

7.3.2. Numerical implementation for three-component piecewise constant p

The previous simulations for two-component piecewise constant p answer some of the basic questions on reconstructing functions in variable bandwidth spaces from a numerical perspective. In this section, our focus is to demonstrate actual numerical computability of necessary quantities to perform sampling and reconstruction in $PW_\Lambda(A_p)$ with a three-component piecewise constant p . We consider the reconstruction space $PW_{[0,\Omega]}(A_p)$ where p is the three-component piecewise function

$$p(x) = \begin{cases} p_0, & x \in (-\infty, -\frac{T}{2}], \\ p_1, & x \in (-\frac{T}{2}, \frac{T}{2}], \\ p_2, & x \in (\frac{T}{2}, \infty) \end{cases}$$

for some $T, p_0, p_1, p_2 > 0$. As before, we use the notation $q_k = p_k^{-1/2}$, $k = 0, 1, 2$ and recall the constants

$$C = \frac{1}{16q_0^2} \left[\left(1 + \frac{q_0}{q_1}\right)^2 \left(1 + \frac{q_1}{q_2}\right)^2 + \left(1 - \frac{q_0}{q_1}\right)^2 \left(1 - \frac{q_1}{q_2}\right)^2 \right],$$

$$K = \frac{1}{8q_0^2} \left(1 - \frac{q_0^2}{q_1^2}\right) \left(1 - \frac{q_1^2}{q_2^2}\right),$$

$\zeta = 2q_1T$, and $r = \frac{K}{C}$. By Lemma 5.2.1 and Theorem 5.2.3, we know that for any $s \in \mathbb{R}$,

$$J(s) = \frac{1}{2\pi} \int_{\Lambda^{1/2}} \frac{e^{isu}}{C + K \cos \zeta u} du$$

$$= \frac{\Omega^{1/2}}{2C\pi} \sum_{m=0}^{\infty} \sum_{l=0}^m \left(-\frac{r}{2}\right)^m \binom{m}{l} e^{i\frac{\Omega^{1/2}}{2}(s+(m-2l)\zeta)} \operatorname{sinc} \left(\frac{\Omega^{1/2}}{2}(s + (m-2l)\zeta)\right).$$

For $M \in \mathbb{N}_0$, the M^{th} partial sum J_M of J satisfies the error estimate

$$|J(s) - J_M(s)| \leq \frac{\Omega^{1/2} |r|^{M+1}}{2C\pi (1 - |r|)}$$

for any $s \in \mathbb{R}$. Finally, Theorem 5.2.5 states explicit formulas for each piecewise component of the reproducing kernel k_Λ in terms of the real part

$$J_{\text{real}}(s) = \frac{\Omega^{1/2}}{2C\pi} \sum_{m=0}^{\infty} \sum_{l=0}^m \left(-\frac{r}{2}\right)^m \binom{m}{l} \operatorname{sinc} (\Omega^{1/2}(s + (m-2l)\zeta))$$

of J . Figure 7.9 shows the graph of $y = J_{\text{real}}(x)$ on the interval $[-50, 50]$ for a given set of parameters. We used Routine A.5 with accuracy set to machine precision to plot the graph below. Routine A.4 is an auxiliary code used to compute $\frac{1}{2^m} \binom{m}{l}$ via floating point arithmetic and to avoid warnings when M is large. As observed in Remark 5.2.4, the graph of J_{real} resembles that of sinc aside from the occasional spikes at $s = k\zeta$, $k \in \mathbb{Z}$ that degrade as $|s| \rightarrow \infty$. In Figure 7.9 we see the spikes occur at $s = 24k$, $k \in \mathbb{Z}$ and the zeros at any other integer points.

7. Numerical implementation and simulations

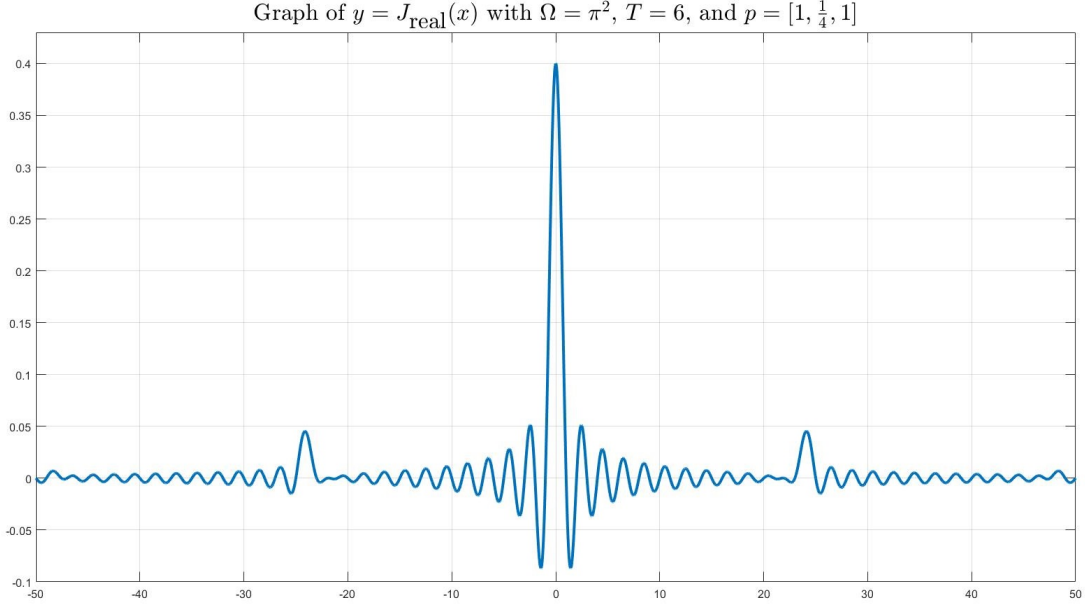


Figure 7.9.: Graph of J_{real} for $\Omega = \pi^2$, $T = 6$, $p_0 = p_2 = 1$ and $p_1 = \frac{1}{4}$ on the interval $[-50, 50]$.

To demonstrate that the numerical calculations are indeed functioning, we apply Algorithm 4 to calculate the regularized reconstruction $g_\epsilon^{[2n,n]}$ of

$$g(x) = k_\Lambda(0, x) \in PW_{[0, \pi^2]}(A_p), \quad p(x) = \begin{cases} 1, & x \in (-\infty, -15], \\ \frac{1}{4}, & x \in (-15, 15], \\ 1, & x \in (15, \infty) \end{cases}$$

from point samples in the uniform sampling set $X_{\frac{1}{8}}$, i.e.,

$$d_j^{[2n]} = g\left(\frac{j}{8}\right) = k_\Lambda\left(0, \frac{\pi j}{8}\right), \quad j = -2n, \dots, 2n. \quad (7.3.13)$$

We consider the reconstruction spaces $PW_{[0, \pi^2]}(A_{\tilde{p}})$ where

$$\tilde{p}(x) = \begin{cases} 1, & x \in (-\infty, -15], \\ p_1, & x \in (-15, 15], \\ 1, & x \in (15, \infty) \end{cases}, \quad p_1 = \frac{1}{2}, \frac{1}{4}, \frac{1}{8}.$$

With the above values of p_1 , $X_{\frac{1}{8}}$ is a set of stable sampling by (7.2.3). As before, we set $\epsilon = 10^{-8}$ and plot the discretized errors E_{grid}^2 and E_{grid}^∞ on a uniform grid on the interval $[-25, 25]$ with $10^4 + 1$ points, i.e., $L = 50$ and $h = 0.005$, as well as the norms $\|\hat{c}_\epsilon^{[2n,n]}\|_2$ for $n = 5, \dots, 100$. Clearly, perfect reconstruction should occur for $p_1 = \frac{1}{4}$. Figure 7.10 displays the trends of E_{grid}^2 , E_{grid}^∞ and $\|\hat{c}_\epsilon^{[2n,n]}\|_2$. Plots of the reconstruction show that the blue and yellow ones nearly overlap. We observe that deviating from the correct reconstruction space still yields significant reconstruction errors and the expansion has coefficients of norm bounded above by 10^8 . As noted previously, this is counter-intuitive from perfect recovery of bandlimited functions in Paley-Wiener spaces of larger constant bandwidths.

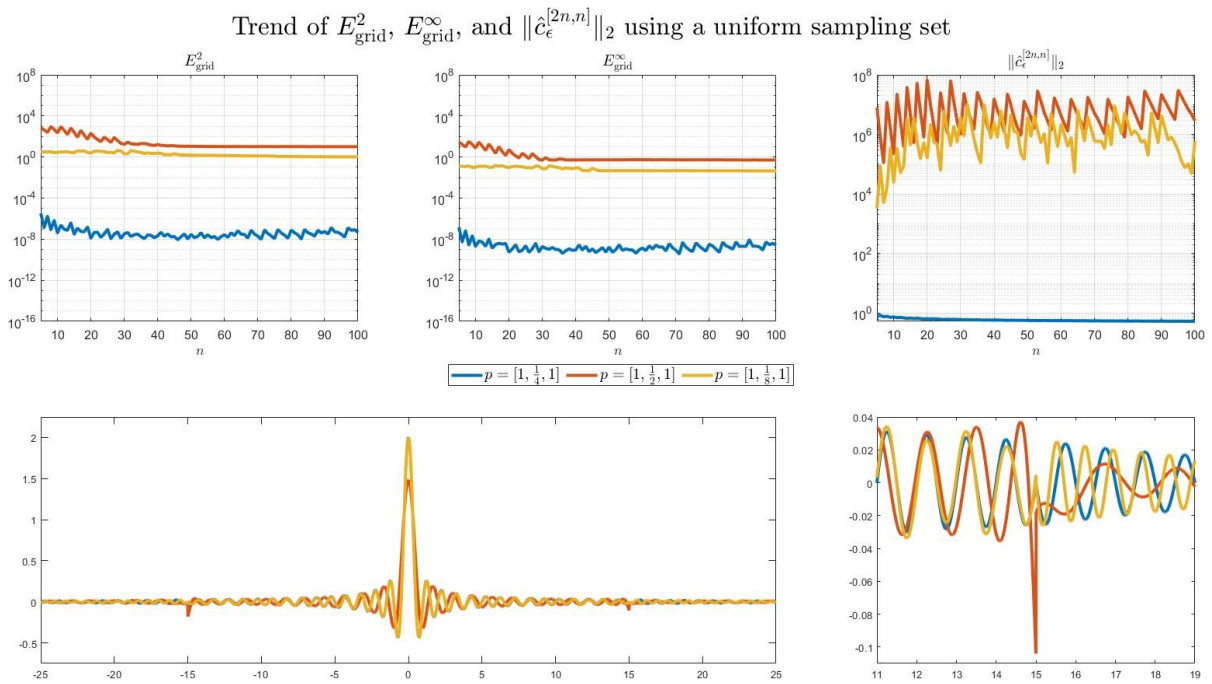


Figure 7.10.: Plots of E_{grid}^2 (col 1), E_{grid}^∞ (col 2), $\|\hat{c}_\epsilon^{[2n,n]}\|_2$ (col 3) and the reconstructions (row 2) when g is reconstructed using the uniform sampling set $X_{\frac{1}{8}}$ and different values of p_1 .

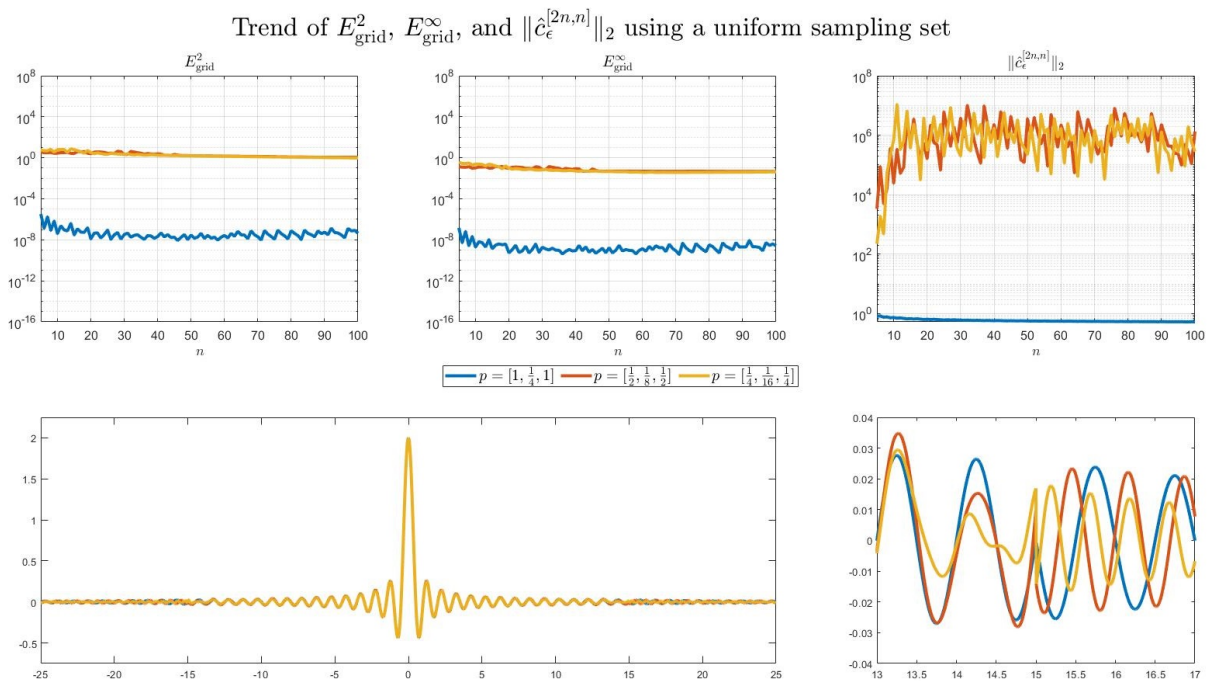


Figure 7.11.: Plots of E_{grid}^2 (col 1), E_{grid}^∞ (col 2), $\|\hat{c}_\epsilon^{[2n,n]}\|_2$ (col 3), and the reconstructions (row 2) when g is reconstructed using the uniform sampling set $X_{\frac{1}{8}}$ and multiples of a fixed p .

7. Numerical implementation and simulations

The reader may consult `Trend3p.m` and explore other values of parameters to see how the reconstruction performs given different configurations. We end this chapter by looking at a numerical simulation related to Theorem 7.3.2 for the three-component case. Consider the same g as above and reconstruction spaces

$$PW_{[0,\pi^2]}(A_p) \subseteq PW_{[0,\pi^2]}(A_{\frac{1}{2}p}) \subseteq PW_{[0,\pi^2]}(A_{\frac{1}{4}p}).$$

With the same numerical setup as above, Figure 7.11 shows that the reconstructions visually overlap on the middle interval $[-15, 15]$ while some noticeable errors occur near the knots $x = \pm 15$ of p . Perfect reconstruction is not observed for the multiples $\frac{1}{2}p$ and $\frac{1}{4}p$, although we see that the three plots mostly virtually overlap. Astonishingly, a downward trend of E_{grid}^2 and E_{grid}^∞ is not observed. This may be due to the errors that occur near the knots. We invite the reader to again use `Trend3p.m` and check that in the case of $\frac{1}{4}p$, the plot of the reconstruction slightly improves as we take even larger values of n (at the cost of longer computation time and higher memory usage). In contrast, reconstructions corresponding to $\frac{1}{2}p$ occasionally produce high spikes at the knots.

8. Summary and outlook

In this dissertation we studied the theoretical and computational aspects of sampling and reconstruction in spaces of functions of variable bandwidth parametrized by a piecewise constant function.

In Chapter 4 we showed that in contrast to arbitrary parametrizing functions, piecewise constant parametrizing functions offer a direct approach to assigning local bandwidths of a signal. Moreover, the quantities needed to compute the reproducing kernel of the resulting variable bandwidth space are directly computable from the spectral set Λ and the piecewise components of p . In Chapter 5 we derived explicit formulas for the reproducing kernel when p has two or three piecewise components.

In Chapter 6 we derived necessary density conditions for sampling and interpolation in variable bandwidths spaces with piecewise constant parametrizing functions. We then used this as a guide to generate sets of stable sampling and consequently performed numerical simulations on approximating functions by functions of variable bandwidth. Chapter 7 tackles most of the numerical aspects of the reconstruction problem and provided some insights on how the parametrizing function influences the quality of reconstruction as well as the feasibility of performing numerical approximation in variable bandwidth spaces.

While we tried to cover the important details on variable bandwidth spaces with piecewise constant parametrizing functions, there are still some open problems for future research. We enumerate some of these questions and describe our preliminary approach to answer them.

8.1. Constructing orthonormal bases for $PW_{[0,\Omega]}(A_p)$

Theorem 7.3.1 is an explicit construction of orthonormal bases for $PW_{[0,\Omega]}(A_p)$ with p a two-component piecewise constant function with knot at $t_1 = 0$. By translation, this result can be extended to arbitrary nonzero knots. The heart of the proof lies on carefully choosing points $\{s_j\}_{j \in \mathbb{Z}}$ so that the reproducing kernel k_Λ of $PW_{[0,\Omega]}(A_p)$ satisfies $k_\Lambda(s_j, s_l) = 0$ for $j \neq l$. This is precisely achieved by the choice (7.3.8) that is easy to derive since we have an explicit formula for k_Λ in terms of the cardinal sine function.

It is then natural to ask if such an orthonormal basis construction can be extended to arbitrary number of piecewise components. In the case of three-component piecewise constant functions with symmetric knots, the piecewise components of k_Λ are written in terms of J_{real} in Theorem 5.2.3. Inspired by the proof of Theorem 7.3.1, a possible construction of an orthogonal system in $PW_{[0,\Omega]}(A_p)$ involves finding the zeros of J_{real} , some of which are identified by Remark 5.2.4 as the points

$$s \in \left(\frac{\pi}{\Omega^{1/2}} \mathbb{Z} + \zeta \mathbb{Z} \right) \setminus \zeta \mathbb{Z}.$$

One has to figure out how to choose a sequence of points $\{s_j\}_{j \in \mathbb{Z}}$ so that $k_\Lambda(s_j, s_l) = 0$ for $j \neq l$ holds.

8. Summary and outlook

If orthonormal bases are out of reach, the next best thing is to find Riesz bases for $PW_{[0,\Omega]}(A_p)$. We still do not have an idea how to generate such a family, and we are open to discussions and future work on this topic.

8.2. Subspace relations between variable bandwidth spaces

Theorem 7.3.2 states that if the spectral set Λ is an interval, then any piecewise constant function p generates a nested sequence $\{PW_\Lambda(A_{c^{-2p}})\}_{0 < c \leq 1}$ of variable bandwidth spaces. We are interested to know if there are other subspace relations that can be derived in the case of piecewise constant parametrizing functions. Another related problem is to derive relations between $PW_\Lambda(A_p)$ and $PW_\Lambda(A_{\tilde{p}})$ if p and \tilde{p} are close with respect to some norm, say $\|\cdot\|_\infty$. So far, our simulation in Section 7.3.1.1 only suggests that the error in reconstructing a function $f \in PW_\Lambda(A_p)$ in the space $PW_\Lambda(A_{\tilde{p}})$ is commensurate to $\|p - \tilde{p}\|_\infty$. We wish to know if there is indeed some general truth behind this observation.

One possible general approach in deriving subspace relations that may not require additional assumptions on the spectral set is to relate the reproducing kernels of two variable bandwidth spaces. We describe this method in detail. Let $\Lambda \subset \mathbb{R}_0^+$ be of finite measure. Suppose p and \tilde{p} are piecewise constant functions. We wish to find conditions for which the inclusion

$$PW_\Lambda(A_p) \subseteq PW_\Lambda(A_{\tilde{p}})$$

holds. It turns out that it is possible to derive such conditions using the reproducing kernels of these spaces. We introduce the following notion. Let K be the reproducing kernel for the reproducing kernel Hilbert space \mathcal{H} . Then K is positive definite (or a kernel function), i.e.,

$$\sum_{j,l=1}^n \xi_l \bar{\xi}_j K(x_l, x_j) \geq 0$$

for all $\{x_j\}_{j=1}^n \subset \mathbb{R}$, $\{\xi_j\}_{j=1}^n \subset \mathbb{C}$ and for all $n \in \mathbb{N}$. In other words, for any finite collection $\{x_j\}_{j=1}^n$ of points in \mathbb{R} , the matrix $[K(x_l, x_j)]_{j,l=1}^n \in \mathbb{C}^{n \times n}$ is positive semidefinite. Now, given two kernel functions K_1 and K_2 , we write $K_1 \ll K_2$ if $K_2 - K_1$ is positive definite. The following result [8, Thms. I,II] establishes subspace inclusion between reproducing kernel Hilbert spaces based on this relation.

Theorem 8.2.1. *Let K_1 and K_2 be reproducing kernels for \mathcal{H}_1 and \mathcal{H}_2 , respectively. Then $K_1 \ll K_2$ if and only if $\mathcal{H}_1 \subseteq \mathcal{H}_2$ and $\|f\|_{\mathcal{H}_2} \leq \|f\|_{\mathcal{H}_1}$ for all $f \in \mathcal{H}_1$.*

When $\Lambda = [0, \Omega]$ for some $\Omega > 0$, Theorem 7.3.2 follows from the above theorem. To see this, fix a piecewise constant function p and $0 < c < 1$. Let K_1 and K_2 be the reproducing kernels of $PW_\Lambda(A_{c^{-2p}})$ and $PW_\Lambda(A_p)$, respectively. By (4.4.2) and the table

found in proof of Theorem 7.3.2, we have

$$\begin{aligned} K(x_l, x_j) &= K_2(x_l, x_j) - K_1(x_l, x_j) \\ &= \int_{\Lambda} \overline{\Phi(\lambda, x_l)} \cdot \Phi(\lambda, x_j) d\mu(\lambda) - \int_{\Lambda} \overline{\Phi(c^2\lambda, x_l)} \cdot \Phi(c^2\lambda, x_j) d\mu(c^2\lambda) \\ &= \int_{\Lambda \setminus c^2\Lambda} \overline{\Phi(\lambda, x_l)} \cdot \Phi(\lambda, x_j) d\mu(\lambda) \end{aligned}$$

for all $n \in \mathbb{N}$ and $\{x_j\}_{j=1}^n \subset \mathbb{R}$. Thus, for all $\{\xi_j\}_{j=1}^n \subset \mathbb{C}$,

$$\sum_{j,l=1}^n \xi_l \bar{\xi}_j K(x_l, x_j) = \left\langle \sum_{j=1}^n \bar{\xi}_j \Phi(\cdot, x_j), \sum_{l=1}^n \xi_l \Phi(\cdot, x_l) \right\rangle_{L^2(\Lambda \setminus c^2\Lambda, d\mu)} \geq 0,$$

i.e., $K_1 \ll K_2$. Therefore, $PW_{\Lambda}(A_{c^{-2}p}) \subseteq PW_{\Lambda}(A_p)$ by Theorem 8.2.1. Other subspace relations can potentially be proved using this method but may require additional knowledge of the reproducing kernel. We also refer the reader to [10, Sec. 4.5] on other equivalent conditions related to subspace inclusions between reproducing kernel Hilbert spaces.

8.3. Reconstructions using other sets of stable sampling

In classical Paley-Wiener spaces of dimension one, a result of Beurling [12] asserts that if $D^-(X) > 1$, then X is a set of stable sampling for the Paley-Wiener space. This suggests that such a result might also hold in certain spaces of variable bandwidth. We conjecture that if $D_p(X) > \frac{\Omega^{1/2}}{\pi}$, then X is a set of stable sampling for $PW_{[0,\Omega]}(A_p)$. Several experiments confirm this conjecture when p is a piecewise constant function.

A. Matlab codes and additional plots

The following MATLAB codes are simplified versions of routines used in the numerical simulations in Section 7.3. The complete collection can be downloaded from the Dropbox folder <https://www.dropbox.com/sh/57utba39ytkh0yf/AADK8upEumLqKaGhop489VKpa?dl=1>.

Routine A.1: Computing the reproducing kernel for two-component piecewise constant p from vector inputs as well as forming uneven sections of the Gramian

```

1 function z = Ker2p(p, Omega, u, v)
2 %%%%%%%%%%%%%%%%%%%%%%%%%%%%%%%%%%%%%%%%%%%%%%%%%%%%%%%%%%%%%%%%%%%%%%%%%
3 %Computes the reproducing kernel k(u,v) for the two-component piecewise
4 %constant p with knot at t = 0 and spectral set [0, Omega]. Accepts row
5 %vectors u and v whose lengths may be different. If u has length n and
6 %v has length m, the output is an mxn matrix whose entries are
7 %k(u(j), v(i)). This way, the output can also be treated as the uneven mxn
8 %section of the Gramian G(i, j) = <k(u(j), .), k(v(i), .)>.
9 %%%%%%%%%%%%%%%%%%%%%%%%%%%%%%%%%%%%%%%%%%%%%%%%%%%%%%%%%%%%%%%%%%%%%%%%%
10 q = sqrt(1./p);
11 Y = meshgrid(v, u)';
12 z = zeros(size(Y));
13
14 [r1, c1] = find((Y <= 0 & u <= 0) == 1);
15 [r2, c2] = find((Y > 0 & u > 0) == 1);
16 [r3, c3] = find((Y > 0 & u <= 0) == 1);
17 [r4, c4] = find((Y <= 0 & u > 0) == 1);
18
19 a = q(1)*sqrt(Omega)/pi;
20 b = ((q(2) - q(1))/(q(1) + q(2)));
21 z(sub2ind(size(z), r1, c1)) = ...
    a*(sinc(q(1)*sqrt(Omega)*(u(c1)-v(r1))/pi) + ...
    b*sinc(q(1)*sqrt(Omega)*(u(c1)+v(r1))/pi));
22
23 c = q(2)*sqrt(Omega)/pi;
24 z(sub2ind(size(z), r2, c2)) = ...
    c*(sinc(q(2)*sqrt(Omega)*(u(c2)-v(r2))/pi) - ...
    b*sinc(q(2)*sqrt(Omega)*(u(c2)+v(r2))/pi));
25
26 g = 2*q(1)*q(2)*sqrt(Omega)/(pi*(q(1) + q(2)));
27 z(sub2ind(size(z), r3, c3)) = g*sinc(sqrt(Omega)*(q(1)*u(c3) - ...
    q(2)*v(r3))/pi);
28 z(sub2ind(size(z), r4, c4)) = g*sinc(sqrt(Omega)*(q(2)*u(c4) - ...
    q(1)*v(r4))/pi);
29 end

```

To form uneven sections of the Gramian, take u as the row vector of points generating the frame elements and v as the row vector of sampling points.

A. MATLAB codes and additional plots

Routine A.2: Truncated SVD with threshold `tol`

```

1 function G = tsvd(A,tol)
2 %%%%%%%%%%%%%%%%%%%%%%%%%%%%%%%%%%%%%%%%%%%%%%%%%%%%%%%%%%%%%%%%%%%%%%%%%%
3 %Performs singular value thresholding on A, i.e., replaces all singular
4 %values of A below the threshold tol by zero. The output is the matrix
5 %G with the same left/right singular vectors as that of A but whose
6 %nonzero singular values are the singular values of A with value at
7 %least tol.
8 %%%%%%%%%%%%%%%%%%%%%%%%%%%%%%%%%%%%%%%%%%%%%%%%%%%%%%%%%%%%%%%%%%%%%%%%%%
9 [U,S,V] = svd(A);
10 d = diag(S);
11 [m,n] = size(A);
12
13 i = 1;
14 while i <= length(d) && d(i) >= tol
15     i = i+1;
16 end
17 if i <= min(m,n)
18     for j = i:min(m,n)
19         S(j,j) = 0;
20     end
21 end
22 G = U*S*V';
23 end

```

This routine is only used when `pinv` is replaced by `lsqminnorm`. Alternatively, one can use `pinv(pinv(A,tol))` to obtain G . However, for large, rank-deficient matrices A , it is often the case that `norm(tsvd(A,tol) - pinv(pinv,tol))` is small (around 10^{-12}) but is not within machine precision.

Routine A.3: Constructing points generating an orthogonal system for two-component piecewise constant p

```

1 function samp = ONB2p(p, Omega, N)
2 %%%%%%%%%%%%%%%%%%%%%%%%%%%%%%%%%%%%%%%%%%%%%%%%%%%%%%%%%%%%%%%%%%%%%%%%%%
3 d = pi*sqrt(p)/sqrt(Omega);
4 samp = [flip(-d(1):-d(1):-N*d(1)) 0:d(2):N*d(2)]; %sampling
5 end

```

These points are precisely the middle $2N + 1$ elements (with center at the origin) of X_{onb} in (7.3.8).

Routine A.4: Alternative way to compute $2^{-n} \binom{n}{k}$ in floating point arithmetic and without warning messages

```

1 function y = modnchoosek(n,k)
2 %%%%%%%%%%%%%%%%%%%%%%%%%%%%%%%%%%%%%%%%%%%%%%%%%%%%%%%%%%%%%%%%%%%%%%%%%
3 %Computes binom(n,k)/2^n using floating point arithmetic
4 %%%%%%%%%%%%%%%%%%%%%%%%%%%%%%%%%%%%%%%%%%%%%%%%%%%%%%%%%%%%%%%%%%%%%%%%%
5 if k == 0
6     y = 2^-n;
7     return
8 elseif 2*k > n
9     k = n-k; %reduce number of iterative multiplications
10 end
11 y = 2^(k-n);
12 for i = 1:k
13     y = y*(n-k+i)/(2*i);
14 end
15 end

```

Routine A.5: Approximating $J_{\text{real}}(s)$ for any $s \in \mathbb{R}$ up to machine precision

```

1 function J = Jreal(Omega,p,T,s)
2 %%%%%%%%%%%%%%%%%%%%%%%%%%%%%%%%%%%%%%%%%%%%%%%%%%%%%%%%%%%%%%%%%%%%%%%%%
3 %Computes the partial sum of the the real part of J(s) given a
4 %three-component piecewise p with knots at -T/2 and T/2. The truncation
5 %is determined as the least M such that geometric error estimate is
6 %within machine precision. Once M is determined, the routine computes the
7 %output as directed.
8 %%%%%%%%%%%%%%%%%%%%%%%%%%%%%%%%%%%%%%%%%%%%%%%%%%%%%%%%%%%%%%%%%%%%%%%%%
9 q = sqrt(1./p);
10 zeta = 2*q(2)*T;
11 C = ((1+q(1)/q(2))^2*(1+q(2)/q(3))^2 + ...
12     (1-q(1)/q(2))^2*(1-q(2)/q(3))^2)/(16*q(1)^2);
13 K = (1-q(1)^2/q(2)^2)*(1-q(2)^2/q(3)^2)/(8*q(1)^2);
14 r = K/C;
15 fac = sqrt(Omega)/(2*C*pi);
16 M = 0; %determines the truncation level
17 Err = fac*abs(r)^(M+1)/(1-r); %geometric error estimate
18 while Err >= eps %machine precision accuracy
19     Err = Err*abs(r);
20     M = M+1;
21 end
22 J=0;
23 for m = 1:M+1
24     increm = 0;
25     for l = 1:m
26         increm = increm + ...
27             modnchoosek(m-1,l-1)*sinc((s+(m-2*l+1)*zeta)*sqrt(Omega)/pi);
28     end
29     J = J+(-r)^(m-1)*fac*increm;
30 end
31 end

```

A. MATLAB codes and additional plots

Routine A.6: Reconstruction routine for two- and three-component piecewise constant p

```

1 function [Recf, lsqgrid, supgrid, coef] = ...
   Rec(f, p, t, Omega, gamma, tol, div, N, s, a, b, inp, eta, bnd, pars)
2 %%%%%%%%%%%%%%%%%%%%%%%%%%%%%%%%%%%%%%%%%%%%%%%%%%%%%%%%%%%%%%%%%%%%%%%%%
3 %Trend of the least squares error (grid), supremum norm error (grid),
4 %and growth of coefficient solutions of the regularized reconstruction
5 %with SVD threshold tol as n ranges from s to N on the interval [a,b].
6 %Several options for the sampling set are offered. The sampling rate eta
7 %can also be adjusted and plotting the reconstruction is also possible.
8 %%%%%%%%%%%%%%%%%%%%%%%%%%%%%%%%%%%%%%%%%%%%%%%%%%%%%%%%%%%%%%%%%%%%%%%%%
9 lsqgrid = zeros(1,N);
10 supgrid = zeros(1,N);
11 coef = zeros(1,N);
12
13 M = floor(eta*N); %sampling rate eta
14 %Prompt 1: unif., pinv 2: unif., lsqminnorm, 3: perturbed, noisy, 4: ONB
15 samp = -M*gamma:gamma:M*gamma; %uniform by default
16 if inp == 3
17     samp = samp - gamma/4 + gamma/2*rand(1,length(samp)); %perturbed ...
   samples
18 else
19     samp = ONB2p(p, Omega, M); %orthogonal
20 end
21
22 %Quantities needed to compute the reconstruction
23 frames = samp(M-N+1:M+N+1); %frame elements
24 y = f(samp).'; %noiseless samples of f
25 if inp == 3
26     y = y - bnd + 2*bnd*rand(length(y),1);
27 end
28
29 %Plotting the reconstruction on a uniform grid
30 mesh = a:(b-a)/div:b;
31 fgrid = f(mesh);
32 G = zeros(length(y), length(frames)+2);
33 gridG = zeros(length(mesh), length(frames)+2);
34 if pars == 2 %two-component
35     G(:, 2:end-1) = Ker2p(p, Omega, frames, samp); %Gramian
36     gridG(:, 2:end-1) = Ker2p(p, Omega, frames, mesh); %Resampling
37 else %three-component
38     G(:, 2:end-1) = Ker3p(p, t, Omega, frames, samp); %Gramian
39     gridG(:, 2:end-1) = Ker3p(p, t, Omega, frames, mesh); %Resampling
40 end
41
42 mset = M;
43 for n = N:-1:s
44     G = G(:, 2:end-1);
45     mn = floor(eta*n);
46     if mn < mset
47         r = mset - mn;
48         y = y(1+r:end-r);
49         G = G(1+r:end-r, :);
50         mset = mn;
51     end
52     if inp == 2

```

```
53     regG = tsvd(G, tol);
54     xn = lsqminnorm(regG, y);
55 else
56     xn = pinv(G, tol)*y;
57 end
58 gridG = gridG(:,2:end-1);
59 recf = (gridG*xn).';
60 if n == N
61     Recf = recf;
62 end
63 lsqgrid(n) = norm(recf - fgrid);
64 supgrid(n) = norm(recf - fgrid, inf);
65 coef(n) = norm(xn);
66 end
67 end
```

A. MATLAB codes and additional plots

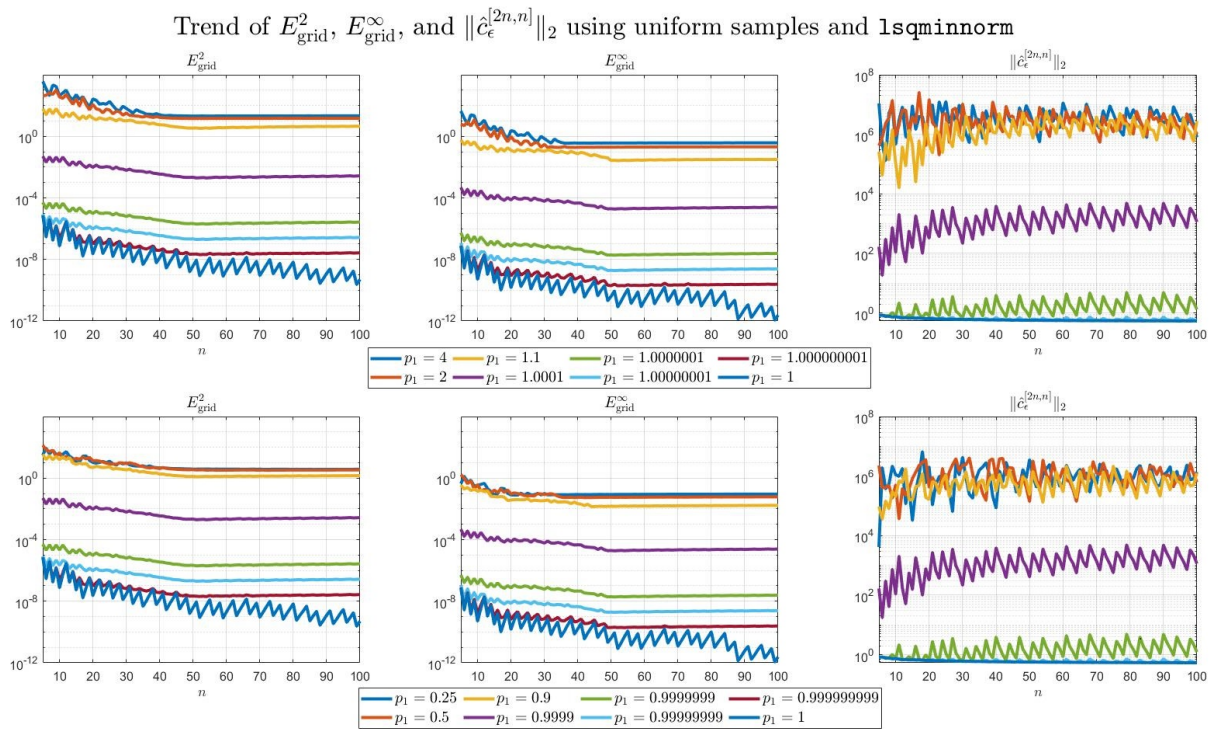


Figure A.1.: Plots of E_{grid}^2 (col. 1), E_{grid}^∞ (col. 2), and $\|\hat{c}_\epsilon^{[2n,n]}\|_2$ (col. 3) using the uniform sampling set $X_{\frac{1}{4}}$ with different values of p_1 approaching $p_1 = 1$ and MATLAB command `lsqminnorm`

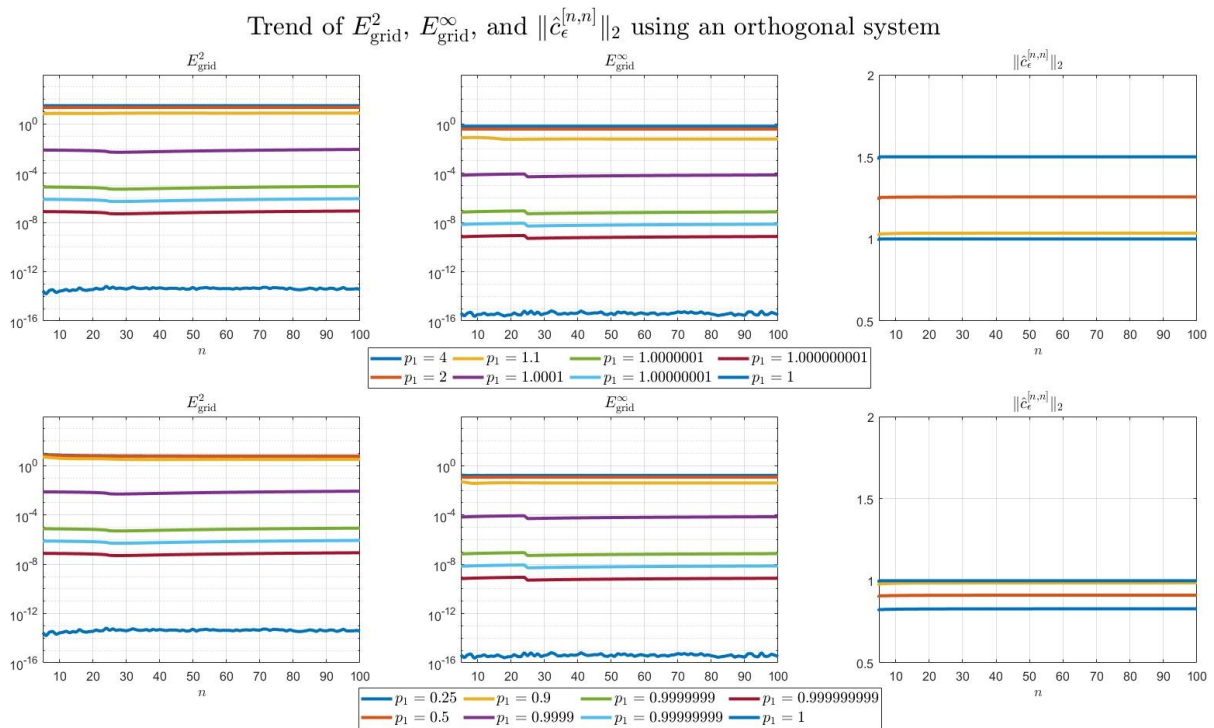


Figure A.2.: Plots of E_{grid}^2 (col. 1), E_{grid}^∞ (col. 2), and $\|\hat{c}_\epsilon^{[n,n]}\|_2$ (col. 3) using the sampling set X_{onb} and different values of p_1 approaching $p_1 = 1$.

B. Evaluating J : complex analysis

In this section, we consider a special case of a three-component piecewise constant p with symmetric knots and derive an alternative formula for the parameter integral J using complex analysis and special functions. Recall from Theorem 5.2.3 that evaluations of J can be computed using a series expansion. Moreover, the formula works for any choice of parameters p_0, p_1, p_2 and T . It only assumes that the spectral set is $\Lambda = [0, \Omega]$ for some $\Omega > 0$, but it actually applies to arbitrary Borel sets of finite measure as long as one can compute $\mathcal{F}^{-1}(\chi_{\Lambda^{1/2}})(\omega)$ for any $\omega \in \mathbb{R}$. For any $s \in \mathbb{R}$, the partial sums $J_M(s)$, $M \in \mathbb{N}$ of the series expansion also converge to $J(s)$ at a geometric rate, hence one can use a finite number of terms to approximate $J(s)$ up to desired accuracy.

With additional assumptions on the three-component piecewise p , a closed-form expression for J may be obtained using contour integrals. We review some fundamental concepts (see [32, Chap. VII]). A point $z_0 \in \mathbb{C}$ is an **isolated singularity** of a function f if f is analytic on some punctured disc

$$\{z \in \mathbb{C} : 0 < |z - z_0| < R\}.$$

If f is analytic on the open annulus

$$B_{r,R}(z_0) = \{z \in \mathbb{C} : r < |z - z_0| < R\}$$

for some $0 \leq r < R$, then f has the Laurent series expansion

$$f(z) = \sum_{j=-\infty}^{\infty} a_j (z - z_0)^j, \quad r < |z - z_0| < R$$

that converges absolutely at each point in $B_{r,R}(z_0)$ and uniformly on every closed subannular domain $\overline{B_{s,S}(z_0)}$ where $r \leq s < S \leq R$ [32, Chap. VI]. The **residue** $\text{Res}(f, z_0)$ of f at an isolated singularity z_0 is defined as

$$\text{Res}(f, z_0) = a_{-1} = \frac{1}{2\pi i} \oint_{|z-z_0|=r} f(z) dz$$

for any fixed $0 < r < R$. Instead of computing the Laurent series or the above contour integral, we can use the following rule in computing residues [32, Chap. VII, Rule 3]: if f and g are analytic at z_0 and g has a simple zero at z_0 , i.e., $g(z) = (z - z_0)\tilde{g}(z)$ for some analytic \tilde{g} with $\tilde{g}(z_0) \neq 0$, then

$$\text{Res}\left(\frac{f}{g}, z_0\right) = \frac{f(z_0)}{g'(z_0)}. \quad (\text{B.0.1})$$

With the above terminologies we can now state our main computational tool.

B. Evaluating J : complex analysis

Theorem B.0.1 (Residue Theorem). *Let U be a bounded domain in the complex plane with piecewise smooth boundary ∂U . Suppose that f is analytic in an open set containing $U \cup \partial U$ except for a finite number of isolated singularities $z_1, z_2, \dots, z_m \in U$. Then*

$$\int_{\partial U} f(z) dz = 2\pi i \sum_{j=1}^m \operatorname{Res}(f, z_j).$$

We will also need a few formulas for special functions. For $k \in \mathbb{N}$ and $q \in \mathbb{R}$, the quantity $(q)_k$ denotes the **Pochhammer symbol** or the **rising factorial** given by

$$(q)_k = \begin{cases} q(q+1) \cdots (q+k-1), & k \in \mathbb{N} \\ 1, & k = 0. \end{cases}$$

The **Gaussian hypergeometric function** ${}_2F_1$ with parameters $a, b, c \in \mathbb{R}$ is the power series

$${}_2F_1(a, b, c; z) = \sum_{k=0}^{\infty} \frac{(a)_k (b)_k}{(c)_k} \frac{z^k}{k!}, \quad |z| < 1. \quad (\text{B.0.2})$$

It is known that the sum in (B.0.2) converges absolutely for all $|z| < 1$ as well as for $|z| = 1$ if $a + b - c > 0$ [34]. We refer the reader to [33] on topics in basic hypergeometric series. For our purpose, the following lemmas will suffice.

Lemma B.0.2. *Let $\alpha < 1$ and $c > 0$. Then*

$$H(\alpha, c) = \int_0^1 \frac{u^{-\alpha}}{u+c} du = \frac{{}_2F_1\left(1, 1, 2-\alpha; \frac{1}{1+c}\right)}{(1-\alpha)(1+c)}.$$

Proof. Let $\beta = 1 - \alpha > 0$. Observe that for $|1 - u| < 1 + c$, we have the convergent expansion

$$\frac{u^{-\alpha}}{u+c} = \frac{1}{1+c} \cdot \frac{u^{\beta-1}}{1 - \frac{1-u}{1+c}} = \frac{1}{1+c} \sum_{k=0}^{\infty} u^{\beta-1} (1-u)^k \left(\frac{1}{1+c}\right)^k.$$

Recalling the beta function

$$B(x, y) = \int_0^1 t^{x-1} (1-t)^{y-1} dt, \quad \operatorname{Re} x, \operatorname{Re} y > 0,$$

we get

$$\int_0^1 \frac{u^{-\alpha}}{u+c} du = \frac{1}{1+c} \sum_{k=0}^{\infty} B(\beta, k+1) \left(\frac{1}{1+c}\right)^k.$$

Repeated application of the identity $B(x, y+1) = \frac{y}{x+y} B(x, y)$ and $B(\beta, 1) = \frac{1}{\beta}$ yields the formula

$$B(\beta, k+1) = \frac{k!}{\beta(1+\beta)_k}, \quad k \in \mathbb{N}_0.$$

Consequently, by rewriting $k! = (1)_k$, we have from (B.0.2) that

$$\int_0^1 \frac{u^{-\alpha}}{u+c} du = \frac{1}{\beta(1+c)} \sum_{k=0}^{\infty} \frac{(k!)^2}{(1+\beta)_k k!} \left(\frac{1}{1+c}\right)^k = \frac{{}_2F_1\left(1, 1, 1+\beta; \frac{1}{1+c}\right)}{\beta(1+c)}$$

and the proof is complete. □

Next, we recall from Section 5.2 the constants $q_k = p_k^{-1/2}$, $k = 0, 1, 2$ and

$$C = \frac{1}{16q_0^2} \left[\left(1 + \frac{q_0}{q_1}\right)^2 \left(1 + \frac{q_1}{q_2}\right)^2 + \left(1 - \frac{q_0}{q_1}\right)^2 \left(1 - \frac{q_1}{q_2}\right)^2 \right],$$

$$K = \frac{1}{8q_0^2} \left(1 - \frac{q_0^2}{q_1^2}\right) \left(1 - \frac{q_1^2}{q_2^2}\right).$$

With the above lemma, the following parameter integrals can be directly computed.

Lemma B.0.3. *Let $\alpha < 1$ and suppose $c_{\pm} = \frac{C}{K} \pm \sqrt{\frac{C^2}{K^2} - 1} > 0$. Then*

$$\int_1^{\infty} \frac{r^{\alpha}}{Kr^2 + 2Cr + K} dr = \frac{H(\alpha, c_-) - H(\alpha, c_+)}{2\sqrt{C^2 - K^2}}.$$

Proof. For $\alpha < 1$, the substitution $u = r^{-1}$ yields

$$\begin{aligned} \int_1^{\infty} \frac{r^{\alpha}}{Kr^2 + 2Cr + K} dr &= \int_0^1 \frac{u^{-\alpha}}{Ku^2 + 2Cu + K} du \\ &= \frac{1}{2\sqrt{C^2 - K^2}} \int_0^1 \left(\frac{u^{-\alpha}}{u + c_-} - \frac{u^{-\alpha}}{u + c_+} \right) du. \end{aligned}$$

Applying Lemma B.0.2 proves the assertion. \square

We now show by means of special functions that for a special case of parameters, we can derive a formula for $J(s)$ for any $s \in \mathbb{R}$. Consider the following simplified setup. Let $\Omega = \pi^2$ and $p_0, p_1, p_2 > 0$ such that either $p_0 > p_1 > p_2$ or $p_0 < p_1 < p_2$. Suppose we are given the piecewise constant function

$$p(x) = \begin{cases} p_0, & x \in (-\infty, -\frac{T}{2}], \\ p_1, & x \in (-\frac{T}{2}, \frac{T}{2}], \\ p_2, & x \in (\frac{T}{2}, \infty), \end{cases}$$

where $T = \sqrt{p_1}$. Then $\zeta = 2q_1T = 2$. By Theorem 5.2.3, J takes the form

$$J(s) = \frac{1}{2\pi} \int_0^{\pi} \frac{e^{ius}}{C + K \cos 2u} du = \frac{1}{\pi} \int_0^{\pi} \frac{e^{iu(s+2)}}{Ke^{4ui} + 2Ce^{2ui} + K} du. \quad (\text{B.0.3})$$

Basically, we have chosen p so that $\Lambda^{1/2} = [0, \pi]$ covers exactly one period of $\kappa(u) = C + K \cos 2u$. We apply the residue theorem and Lemma B.0.2 to the integral (B.0.3), and the following result is a formula for $J(s)$ for any $s \in \mathbb{R}$.

Theorem B.0.4. *Let $\Lambda = [0, \pi^2]$, p a monotone piecewise constant function, and $c_{\pm} = \frac{C}{K} \pm \sqrt{\frac{C^2}{K^2} - 1}$. Then J in (B.0.3) is given by*

$$J(s) = \begin{cases} \frac{e^{i\frac{s}{2}\pi} e^{\frac{s}{2} \text{Argcosh} \frac{C}{K}}}{2\sqrt{C^2 - K^2}} - \frac{i}{4\pi} \frac{1 - e^{\pi is}}{\sqrt{C^2 - K^2}} (H(\frac{s}{2}, c_-) - H(\frac{s}{2}, c_+)), & s < 2, \\ -\frac{e^{-\text{Argcosh} \frac{C}{K}}}{2\sqrt{C^2 - K^2}}, & s = 2, \\ \frac{e^{i\frac{s}{2}\pi} e^{-\frac{s}{2} \text{Argcosh} \frac{C}{K}}}{2\sqrt{C^2 - K^2}} + \frac{i}{4\pi} \frac{1 - e^{\pi is}}{\sqrt{C^2 - K^2}} (H(-\frac{s}{2}, c_-) - H(-\frac{s}{2}, c_+)), & s > 2. \end{cases}$$

B. Evaluating J : complex analysis

This is the closest that we can get to deriving a formula for J , though admittedly, one has every right to feel somewhat deceived by the appearance of a special function that is defined using a convergent series. Nonetheless, hypergeometric functions are frequently used in number theory and combinatorics, and mathematical computing software such as MATLAB and Mathematica have build-in commands for numeric and symbolic computations involving special functions.

Proof. For $s \in \mathbb{R}$, we take the above integrand as a complex function, i.e.,

$$F_s(z) = \frac{e^{iz(s+2)}}{Ke^{4iz} + 2Ce^{2iz} + K}.$$

As regards to the poles, we solve for the zeros of the denominator.

$$0 = Ke^{4iz} + 2Ce^{2iz} + K \quad \rightarrow \quad e^{2iz} = -\frac{C}{K} \pm \sqrt{\left(\frac{C}{K}\right)^2 - 1}$$

Since the components of p are strictly monotone, $K > 0$ and consequently $e^{2iz} = -c_{\mp} < 0$. Hence, the poles $\{z_m\}_{m \in \mathbb{Z}}$ of F_s are

$$\begin{aligned} z_m^{\pm} &= \frac{(2m+1)\pi}{2} \pm \frac{i}{2} \ln \left(\frac{C}{K} + \sqrt{\left(\frac{C}{K}\right)^2 - 1} \right) \\ &= \frac{(2m+1)\pi}{2} \pm \frac{i}{2} \ln c_+ = \frac{(2m+1)\pi}{2} \pm \frac{i}{2} \operatorname{Argcosh} \frac{C}{K}, \end{aligned}$$

utilizing the function $\operatorname{Argcosh} x = \ln(x + \sqrt{x^2 - 1})$ for $x \geq 1$. Now, for $m \in \mathbb{Z}$, define

$$h_m^{\pm}(z) = \sum_{n=1}^{\infty} \frac{2C(2i)^n e^{2iz_m^{\pm}} + K(4i)^n e^{4iz_m^{\pm}}}{n!} (z - z_m^{\pm})^{n-1}.$$

Then h_m^{\pm} is analytic, and for $m \in \mathbb{Z}$,

$$h_m^{\pm}(z_m^{\pm}) = 4ie^{2iz_m^{\pm}}(Ke^{2iz_m^{\pm}} + C) \neq 0.$$

We see that writing the denominator of F_s as a power series centered at each pole z_m^{\pm} yields

$$\begin{aligned} Ke^{4iz} + 2Ce^{2iz} + K &= K + \sum_{n=0}^{\infty} \frac{2C(2i)^n e^{2iz_m^{\pm}} + K(4i)^n e^{4iz_m^{\pm}}}{n!} (z - z_m^{\pm})^n \\ &= (z - z_m^{\pm}) \sum_{n=1}^{\infty} \frac{2C(2i)^n e^{2iz_m^{\pm}} + K(4i)^n e^{4iz_m^{\pm}}}{n!} (z - z_m^{\pm})^{n-1} \\ &= (z - z_m^{\pm}) h_m^{\pm}(z). \end{aligned}$$

Thus, all poles $\{z_m^{\pm}\}_{m \in \mathbb{Z}}$ of F_s are simple and lie on the parallel lines

$$\ell^{\pm} = \left\{ z \in \mathbb{C} : \operatorname{Im} z = \frac{1}{2} \operatorname{Argcosh} \frac{C}{K} \right\}.$$

By (B.0.1), the residue of F_s at z_m^\pm is

$$\operatorname{Res}(F_s, z_m^\pm) = \frac{e^{i(s+2)z_m^\pm}}{4ie^{2iz_m^\pm}(Ke^{2iz_m^\pm} + C)} = \frac{e^{isz_m^\pm}}{4i(Ke^{2iz_m^\pm} + C)} = \pm \frac{e^{isz_m^\pm}}{4i\sqrt{C^2 - K^2}}, \quad m \in \mathbb{Z}.$$

We now derive J using contour integrals. Let $L > 0$ be large. Referring to Figure B.1, let γ^+ be the blue rectangular contour with vertices $(0, 0)$, $(\pi, 0)$, (π, L) and $(0, L)$, oriented in the counter-clockwise direction. Similarly, let γ^- be the orange contour with vertices $(0, 0)$, $(0, -L)$, $(\pi, -L)$ and $(\pi, 0)$, also oriented counter-clockwise. Observe that γ^+ and

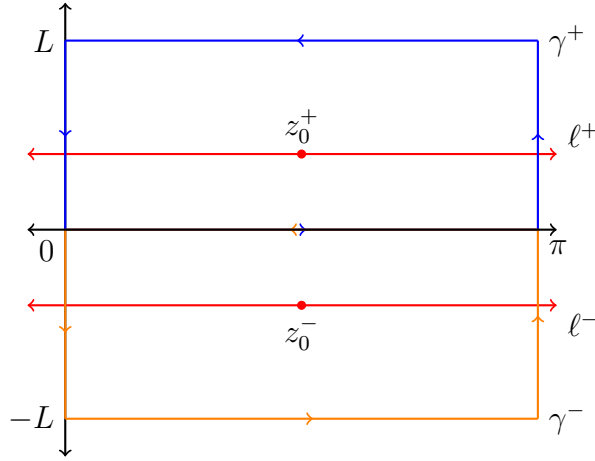


Figure B.1.: Contours γ^+ (in blue) and γ^- (in orange) enclosing the poles z_0^\pm of F_s .

γ^- encloses the poles

$$z_0^+ = \frac{\pi}{2} + \frac{i}{2} \operatorname{Argcosh} \frac{C}{K}, \quad z_0^- = \frac{\pi}{2} - \frac{i}{2} \operatorname{Argcosh} \frac{C}{K},$$

respectively. By the residue theorem, we have

$$\int_{\gamma} F_s(z) dz = \begin{cases} \frac{\pi e^{i\frac{\pi}{2}s} e^{-\frac{s}{2} \operatorname{Argcosh} \frac{C}{K}}}{2\sqrt{C^2 - K^2}}, & \gamma = \gamma^+, \\ -\frac{\pi e^{i\frac{\pi}{2}s} e^{\frac{s}{2} \operatorname{Argcosh} \frac{C}{K}}}{2\sqrt{C^2 - K^2}}, & \gamma = \gamma^-. \end{cases} \quad (\text{B.0.4})$$

We next have to deal with the contour integrals, which we have to consider by cases.

- Case 1: $s > 2$. We appropriately choose γ^+ as our contour and write

$$\gamma^+ = \gamma_1^+ \cup \gamma_2^+ \cup \gamma_3^+ \cup \gamma_4^+,$$

as shown in Figure B.2 and with the counter-clockwise orientation. We also list down the computations on the line integrals for each subcontour.

$$\gamma_1^+ : \int_{\gamma_1^+} F_s(z) dz = \pi J(s).$$

B. Evaluating J : complex analysis

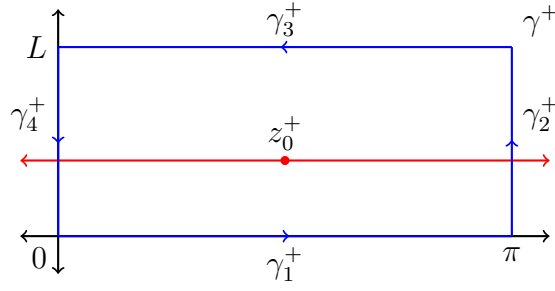


Figure B.2.: Contour γ^+ split into four oriented segments and the pole z_0^+ of F_s (in red dots) in the upper half-plane enclosed by γ^+ .

γ_2^+ : with $z(t) = \pi + it, 0 \leq t \leq L$, we obtain

$$\begin{aligned} \int_{\gamma_2^+} F_s(z) dz &= ie^{\pi is} \int_0^L \frac{e^{-(s+2)t}}{Ke^{-4t} + 2Ce^{-2t} + K} dt \\ &= ie^{\pi is} \int_0^L \frac{e^{-(s-2)t}}{Ke^{4t} + 2Ce^{2t} + K} dt \\ &= \frac{ie^{\pi is}}{2} \int_1^{e^{2L}} \frac{r^{-s/2}}{Kr^2 + 2Cr + K} dr. \end{aligned}$$

γ_3^+ : with $\tilde{\gamma}_3^+ : z(t) = t + iL, 0 \leq t \leq \pi$ and $\gamma_3^+ = -\tilde{\gamma}_3^+$, we observe that

$$\begin{aligned} \int_{\gamma_3^+} F_s(z) dz &= -e^{-(s+2)L} \int_0^\pi \frac{e^{i(s+2)t}}{Ke^{4it}e^{-4L} + 2Ce^{2it}e^{-2L} + K} dt \\ &= -e^{-(s-2)L} \int_0^\pi \frac{e^{i(s+2)t}}{Ke^{4it} + 2Ce^{2it}e^{2L} + Ke^{4L}} dt. \end{aligned}$$

As L is large, we have

$$\left| \int_{\gamma_3^+} F_s(z) dz \right| \leq \frac{\pi e^{-(s-2)L}}{e^{2L}(Ke^{2L} - 2C - Ke^{-2L})}.$$

γ_4^+ : similar approach to γ_2^+ but with reversal of orientation and without the exponential factors involving π . We get

$$\int_{\gamma_4^+} F_s(z) dz = -\frac{i}{2} \int_1^{e^{2L}} \frac{r^{-s/2}}{Kr^2 + 2Cr + K} dr.$$

Summing all four contours and letting $L \rightarrow \infty$, we obtain

$$\int_{\gamma^+} F_s(z) dz = \pi J(s) + \frac{i}{2} (e^{\pi is} - 1) \int_1^\infty \frac{r^{-s/2}}{Kr^2 + 2Cr + K} dr.$$

By (B.0.4) and the residue theorem, we have for $s > 2$ that

$$J(s) = \frac{e^{i\frac{s}{2}\pi} e^{-\frac{s}{2} \operatorname{Argcosh} \frac{C}{K}}}{2\sqrt{C^2 - K^2}} + \frac{i}{2\pi} (1 - e^{\pi is}) \int_1^\infty \frac{r^{-s/2}}{Kr^2 + 2Cr + K} dr.$$

By Lemma B.0.3, we finally obtain

$$J(s) = \frac{e^{i\frac{s}{2}\pi} e^{-\frac{s}{2} \operatorname{Argcosh} \frac{C}{K}}}{2\sqrt{C^2 - K^2}} + \frac{i}{4\pi} \frac{1 - e^{\pi is}}{\sqrt{C^2 - K^2}} \left(H\left(-\frac{s}{2}, c_-\right) - H\left(-\frac{s}{2}, c_+\right) \right), \quad s > 2.$$

- Case 2: $s < 2$. In this case, we use γ^- . Similar to the previous case, we take

$$\gamma^- = \gamma_1^- \cup \gamma_2^- \cup \gamma_3^- \cup \gamma_4^-$$

as shown in the Figure B.3, but is now oriented clockwise. We propose to keep this clockwise orientation as to preserve the correct orientation for the real integral, and afterwards introduce a negative sign on the sum of the residues once we use the residue theorem.

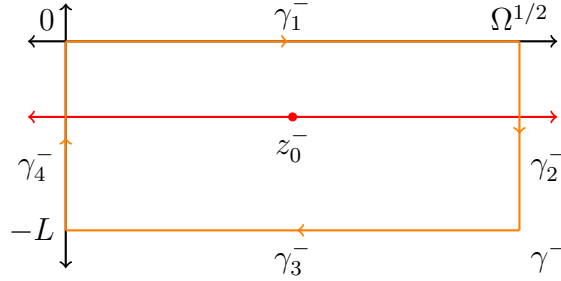


Figure B.3.: Contour γ^- split into four oriented segments and the poles z_0^- of F (in red dots) in the lower half-plane enclosed by γ^- .

We obtain the following computations on the line integrals for each subcontour.

$$\gamma_1^- : \int_{\gamma_1^-} F_s(z) dz = \pi J(s).$$

γ_2^- : with $z(t) = \Omega^{1/2} - it, 0 \leq t \leq L$, we obtain

$$\int_{\gamma_2^-} F_s(z) dz = -ie^{\pi is} \int_0^L \frac{e^{(s+2)t}}{Ke^{4t} + 2Ce^{2t} + K} dt = -\frac{ie^{\pi is}}{2} \int_1^{e^{2L}} \frac{r^{s/2}}{Kr^2 + 2Cr + K} dr.$$

γ_3^- : with $\tilde{\gamma}_3^- : z(t) = t - iL, 0 \leq t \leq \pi$ and $\gamma_3^- = -\tilde{\gamma}_3^-$, we observe that

$$\begin{aligned} \int_{\gamma_3^-} F_s(z) dz &= -e^{(s+2)L} \int_0^\pi \frac{e^{i(s+2)t}}{Ke^{4it}e^{4L} + 2Ce^{2it}e^{2L} + K} dt \\ &= -e^{(s-2)L} \int_0^\pi \frac{e^{i(s+2)t}}{Ke^{4it} + 2Ce^{2it}e^{-2L} + Ke^{-4L}} dt. \end{aligned}$$

Again, if L is sufficiently large so that $K > 2Ce^{-2L} + Ke^{-4L}$, then

$$\left| \int_{\gamma_3^-} F_s(z) dz \right| \leq \frac{\pi e^{(s-2)L}}{K - 2Ce^{-2L} - Ke^{-4L}}.$$

B. Evaluating J : complex analysis

γ_4^- : with $z(t) = it$, $-L \leq t \leq 0$, we have

$$\int_{\gamma_4^-} F_s(z) dz = i \int_{-L}^0 \frac{e^{-(s+2)t}}{K e^{-4t} + 2C e^{-2t} + K} dt = \frac{i}{2} \int_1^{e^{2L}} \frac{r^{s/2}}{K r^2 + 2C r + K} dr.$$

Summing all four contours and letting $L \rightarrow \infty$, we obtain

$$\int_{\gamma^-} F_s(z) dz = \pi J(s) - \frac{i}{2} (e^{\pi i s} - 1) \int_1^\infty \frac{r^{s/2}}{K r^2 + 2C r + K} dr.$$

As in the previous case, we have by the residue theorem (with negative sign) that for $s < 2$,

$$J(s) = \frac{e^{i\frac{s}{2}\pi} e^{\frac{s}{2} \operatorname{Argcosh} \frac{C}{K}}}{2\sqrt{C^2 - K^2}} - \frac{i}{2\pi} (1 - e^{\pi i s}) \int_1^\infty \frac{r^{s/2}}{K r^2 + 2C r + K} dr.$$

Analogously, Lemma B.0.3 yields

$$J(s) = \frac{e^{i\frac{s}{2}\pi} e^{\frac{s}{2} \operatorname{Argcosh} \frac{C}{K}}}{2\sqrt{C^2 - K^2}} - \frac{i}{4\pi} \frac{1 - e^{\pi i s}}{\sqrt{C^2 - K^2}} (H(\frac{s}{2}, c_-) - H(\frac{s}{2}, c_+)), \quad s < 2.$$

- Case 3: $s = 2$. It is straightforward to apply Weierstrass substitution to compute the real and imaginary parts of $J(2)$. Alternatively, we have

$$\begin{aligned} J(2) &= \frac{1}{2\pi} \int_0^\pi \frac{\cos 2u}{C + K \cos 2u} du + \frac{i}{2\pi} \int_0^\pi \frac{\sin 2u}{C + K \cos 2u} du \\ &= \frac{1}{2\pi K} \int_0^\pi \left(1 - \frac{C}{C + K \cos 2u}\right) du + \frac{i}{4\pi} \int_0^{2\pi} \frac{\sin t}{C + K \cos t} dt \\ &= \frac{1 - 2CJ(0)}{2K} - \frac{i}{4\pi K} \ln |C + K \cos t| \Big|_0^{2\pi} \\ &= -\frac{1}{2\sqrt{C^2 - K^2}} \left(\frac{C}{K} - \sqrt{\left(\frac{C}{K}\right)^2 - 1} \right) \\ &= -\frac{c_-}{2\sqrt{C^2 - K^2}} = -\frac{e^{-\operatorname{Argcosh} \frac{C}{K}}}{2\sqrt{C^2 - K^2}} \end{aligned}$$

and we are done. □

It is also possible to generalize Theorem B.0.4 for a class of parametrizing functions. Let Ω , $p_0, p_1, p_2 > 0$ such that either $p_0 > p_1 > p_2$ or $p_0 < p_1 < p_2$. Define

$$p(x) = \begin{cases} p_0, & x \in (-\infty, -\frac{T}{2}], \\ p_1, & x \in (-\frac{T}{2}, \frac{T}{2}], \\ p_2, & x \in (\frac{T}{2}, \infty), \end{cases}$$

where $T = n\pi \left(\frac{p_1}{\Omega}\right)^{1/2}$ for some $n \in \mathbb{N}$. Then C and K stay the same, while $\zeta = \frac{2n\pi}{\Omega^{1/2}}$. By construction, there are exactly n complete cycles of $\kappa(u) = C + K \cos \zeta u$ on the interval $\Lambda^{1/2} = [0, \Omega^{1/2}]$. The resulting J is now

$$J(s) = \frac{1}{2\pi} \int_0^{\Omega^{1/2}} \frac{e^{ius}}{C + K \cos \zeta u} du = \frac{1}{\pi} \int_0^{\Omega^{1/2}} \frac{e^{iu(s+\zeta)}}{K e^{2\zeta ui} + 2C e^{\zeta ui} + K} du.$$

We present the following theorem without proof.

Theorem B.0.5. *Let $\Lambda = [0, \Omega^2]$ for some $\Omega > 0$, p a monotone piecewise constant function, $c_{\pm} = \frac{C}{K} \pm \sqrt{\frac{C^2}{K^2} - 1}$, and $\zeta = \frac{2n\pi}{\Omega^{1/2}}$ for some $n \in \mathbb{N}$. Define*

$$\Theta_n(s) = \sum_{0 \leq j \leq n-1} e^{(2j+1)\pi i \frac{s}{\zeta}} = e^{\pi i \frac{s}{\zeta}} \sum_{0 \leq j \leq n-1} e^{2j\pi i \frac{s}{\zeta}}.$$

Then

$$J(s) = \begin{cases} \frac{\Theta_n(s) e^{\frac{s}{\zeta} \operatorname{Argcosh} \frac{C}{K}}}{\zeta \sqrt{C^2 - K^2}} - \frac{i}{2\pi} \frac{1 - e^{i\Omega^{1/2}s}}{\zeta \sqrt{C^2 - K^2}} \left(H\left(\frac{s}{\zeta}, c_{-}\right) - H\left(\frac{s}{\zeta}, c_{+}\right) \right), & s < \zeta, \\ -\frac{n e^{-\operatorname{Argcosh} \frac{C}{K}}}{\zeta \sqrt{C^2 - K^2}}, & s = \zeta, \\ \frac{\Theta_n(s) e^{-\frac{s}{\zeta} \operatorname{Argcosh} \frac{C}{K}}}{\zeta \sqrt{C^2 - K^2}} + \frac{i}{2\pi} \frac{1 - e^{i\Omega^{1/2}s}}{\zeta \sqrt{C^2 - K^2}} \left(H\left(-\frac{s}{\zeta}, c_{-}\right) - H\left(-\frac{s}{\zeta}, c_{+}\right) \right), & s > \zeta. \end{cases}$$

Theorem B.0.4 is a special case of Theorem B.0.5, where the values $\Omega = \pi^2$, $n = 1$ and $\zeta = 2$ were used. Aside from additional poles as well as minor computational adjustments, the proofs of both theorems are the same. It is also possible to derive a similar theorem as above for the case where the components p_1 , p_2 and p_3 are not monotone. However, this requires delicate work as one needs to compute principal value integrals.

We end this section to mention that the connection between J and hypergeometric functions is no coincidence. A power series $\sum a_j z^j$ is a Gaussian hypergeometric function if and only if $a_0 = 1$ and

$$\frac{a_{j+1}}{a_j} = \frac{(j+a)(j+b)}{(j+c)(j+1)} \cdot \alpha, \quad j \in \mathbb{N}_0$$

for some $a, b, c \in \mathbb{R}$ and $\alpha \neq 0$ (cf. [33]). By induction, $\sum_{j=0}^{\infty} a_j z^j = {}_2F_1(a, b, c; \alpha z)$. Now, consider the power series

$$\sum_{j=0}^{\infty} \binom{2j+|k|}{j} x^j, \quad k \in \mathbb{Z}. \tag{B.0.5}$$

Note that with $a_j = \binom{2j+|k|}{j}$, $j \in \mathbb{N}_0$, we get $a_0 = 1$ and

$$\begin{aligned} \frac{a_{j+1}}{a_j} &= \frac{\binom{2(j+1)+|k|}{j+1}}{\binom{2j+|k|}{j}} = \frac{(2j+2+|k|)(2j+1+|k|)}{(j+1+|k|)(j+1)} \\ &= \frac{\left(j + \frac{|k|}{2} + 1\right) \left(j + \frac{|k|}{2} + \frac{1}{2}\right)}{(j+|k|+1)(j+1)} \cdot 4. \end{aligned}$$

B. Evaluating J : complex analysis

Therefore, (B.0.5) can be computed as

$$\sum_{j=0}^{\infty} \binom{2j+|k|}{j} x^j = {}_2F_1 \left(\frac{|k|}{2} + 1, \frac{|k|}{2} + \frac{1}{2}, |k| + 1; 4x \right), \quad k \in \mathbb{Z}.$$

Consequently,

$$J_{\text{real}}(s) = \sum_{k=-\infty}^{\infty} c_k \text{sinc}(\Omega^{1/2}(s - k\zeta)),$$

where the coefficients previously defined in (5.2.8) is given by

$$\begin{aligned} c_k &= \frac{\Omega^{1/2}}{2C\pi} \sum_{j=0}^{\infty} \binom{2j+|k|}{j} \left(-\frac{r}{2}\right)^{2j+|k|} \\ &= \frac{\Omega^{1/2}}{2C\pi} \left(-\frac{r}{2}\right)^{|k|} {}_2F_1 \left(\frac{|k|}{2} + 1, \frac{|k|}{2} + \frac{1}{2}, |k| + 1; r^2 \right), \quad k \in \mathbb{Z}. \end{aligned}$$

C. Localization and approximation lemmas for general spectral sets

In this section, we prove that the reproducing kernel k_Λ satisfies the weak localization property when Λ is a Borel set of finite measure, as well as the homogeneous approximation property when Λ is a bounded Borel set. The reason for the distinction between compact intervals and sets of finite measure/bounded sets is that estimates such as Lemma 6.3.5 may not be true for spectral sets that are not compact intervals. The proof closely follows the proof in [39, Sec. 7] but with key differences. In the course of the proofs we will repeatedly use the spectral projection formula (4.3.23) corresponding to the spectral set Λ given by

$$\begin{aligned}\chi_\Lambda(A_p)f(x) &= \int_\Lambda \mathcal{F}_{A_p}f(\lambda) \cdot \Phi(\lambda, x) d\mu(\lambda) \\ &= \frac{1}{2\pi} \int_{\Lambda^{1/2}} \frac{\frac{1}{q_0}F_1(u^2)\Phi^+(u^2, x) + \frac{1}{q_n}F_2(u^2)\Phi^-(u^2, x)}{\kappa(u)} du,\end{aligned}\tag{C.0.1}$$

where $f \in L^2(\mathbb{R})$ and $F = (F_1, F_2) = \mathcal{F}_{A_p}f \in L^2(\mathbb{R}, d\mu)$. In particular, $f = \chi_\Lambda(A_p)f$ for $f \in PW_\Lambda(A_p)$. We also recall the following notation used in Chapter 5. We define as in (4.4.5) the function

$$\vartheta(u, x, y) = \frac{1}{q_0} \overline{\Phi^+(u^2, x)}\Phi^+(u^2, y) + \frac{1}{q_n} \overline{\Phi^-(u^2, x)}\Phi^-(u^2, y), \quad x, y \in \mathbb{R}$$

so that the reproducing kernel k_Λ in (4.4.4) reads

$$k_\Lambda(x, y) = \frac{1}{2\pi} \int_{\Lambda^{1/2}} \frac{\vartheta(u, x, y)}{\kappa(u)} du, \quad x, y \in \mathbb{R}.\tag{C.0.2}$$

Parts of the proof of Theorem 5.2.5 turn out to be useful here as they can be generalized to piecewise constant functions p with arbitrary number of components.

C.1. Weak localization property

Before we start with the statement and proof of the weak localization lemma, we first recall the following. A subset \mathcal{M} of a metric space \mathcal{X} is said to be **totally bounded** or **precompact** if \mathcal{M} admits a finite ϵ -cover for each $\epsilon > 0$, i.e., for every $\epsilon > 0$ there exists $n_\epsilon \in \mathbb{N}$ and a collection $\{\mathcal{M}_k\}_{k=1}^{n_\epsilon}$ of subsets of \mathcal{X} with diameter at most ϵ such that $\mathcal{M} \subseteq \cup_{k=1}^{n_\epsilon} \mathcal{M}_k$. For the proof, we shall use a special case of [41, Thm. 1].

Theorem C.1.1 (Kolmogorov-Riesz-Sudakov). *A set $\mathcal{M} \subseteq L^2(\mathbb{R})$ is totally bounded if and only if*

C. Localization and approximation lemmas for general spectral sets

(a) for every $\epsilon > 0$, there exists $b_\epsilon > 0$ such that

$$\sup_{f \in \mathcal{M}} \int_{|y| > b_\epsilon} |f(y)|^2 dy < \epsilon^2,$$

(b) for every $\epsilon > 0$, there exists $b_\epsilon > 0$ such that for $|y_0| < b_\epsilon$,

$$\sup_{f \in \mathcal{M}} \int_{\mathbb{R}} |f(y + y_0) - f(y)|^2 dy < \epsilon^2.$$

For the proof of the weak localization lemma, we only need the first part of Theorem C.1.1.

Lemma C.1.2 (Weak localization). *Let $\Lambda \subset \mathbb{R}_0^+$ be a Borel set of finite measure. Let p be a piecewise constant function and k_Λ be the reproducing kernel for $PW_\Lambda(A_p)$. Then for every $\epsilon > 0$, there exists $r(\epsilon) > 0$ such that*

$$\sup_{x \in \mathbb{R}} \int_{|x-y| > r(\epsilon)} |k_\Lambda(x, y)|^2 dy < \epsilon^2.$$

Proof. We show that for every $\epsilon > 0$, there exists $r(\epsilon) > 0$ such that

$$\int_{|x-y| > r(\epsilon)} |k_\Lambda(x, y)|^2 dy < \frac{3\epsilon^2}{4} \tag{C.1.1}$$

holds for all $x \in \mathbb{R}$. Let p be an $(n + 1)$ -component piecewise constant function for some $n \in \mathbb{N}$. Fix $a > 0$ sufficiently large so that $\{t_k\}_{k=1}^n \subset [-a, a]$ and work on three cases: $x < -a$, $|x| \leq a$, and $x > a$.

(i) Case 1: $|x| \leq a$. Consider the map $x \mapsto k_\Lambda(x, \cdot)$ from $[-a, a]$ to $PW_\Lambda(A_p) \subseteq L^2(\mathbb{R})$. We claim that this map is continuous, i.e., for any $\epsilon > 0$ there exists $\delta > 0$ such that if $x_1, x_2 \in [-a, a]$ satisfy $|x_1 - x_2| < \delta$, then

$$\|k_\Lambda(x_1, \cdot) - k_\Lambda(x_2, \cdot)\|_2 < \epsilon.$$

Indeed, observe that for all $x_1, x_2 \in [-a, a]$, we have

$$\begin{aligned} \|k_\Lambda(x_1, \cdot) - k_\Lambda(x_2, \cdot)\|_2 &= \sup_{f \in PW_\Lambda(A_p), \|f\|_2 \leq 1} |\langle f, k_\Lambda(x_1, \cdot) - k_\Lambda(x_2, \cdot) \rangle| \\ &= \sup_{f \in PW_\Lambda(A_p), \|f\|_2 \leq 1} |f(x_1) - f(x_2)|. \end{aligned} \tag{C.1.2}$$

We then work on the right-hand side of (C.1.2). Let $f \in PW_\Lambda(A_p)$ with $\|f\|_2 \leq 1$. By (4.3.21) and (C.0.1),

$$\begin{aligned} f(x) &= \int_{\Lambda} \mathcal{F}_{A_p} f(\lambda) \cdot \Phi(\lambda, x) d\mu(\lambda) \\ &= \int_{\Lambda \setminus [0, \lambda_0^2]} \mathcal{F}_{A_p} f(\lambda) \cdot \Phi(\lambda, x) d\mu(\lambda) + \int_{\Lambda \cap [0, \lambda_0^2]} \mathcal{F}_{A_p} f(\lambda) \cdot \Phi(\lambda, x) d\mu(\lambda) \\ &= \chi_{\Lambda \setminus [0, \lambda_0^2]} f(x) + \chi_{\Lambda \cap [0, \lambda_0^2]} f(x) \end{aligned} \tag{C.1.3}$$

for a.e. $x \in \mathbb{R}$ and every $\lambda_0 \geq 0$. We inspect the above summands one at a time. Observe that for $x_1, x_2 \in [-a, a]$,

$$\begin{aligned} |\chi_{\Lambda \setminus [0, \lambda_0^2]} f(x_1) - \chi_{\Lambda \setminus [0, \lambda_0^2]} f(x_2)| &\leq \int_{\Lambda \setminus [0, \lambda_0^2]} |\mathcal{F}_{A_p} f(\lambda) \cdot (\Phi(\lambda, x_1) - \Phi(\lambda, x_2))| d\mu(\lambda) \\ &\leq \|\mathcal{F}_{A_p} f\|_{L^1(\Lambda \setminus [0, \lambda_0^2], d\mu)} \|\Phi(\cdot, x_1) - \Phi(\cdot, x_2)\|_{L^\infty(\Lambda \setminus [0, \lambda_0^2], d\mu)}. \end{aligned}$$

By Lemma 4.2.6, there exists $C_\Phi > 0$ such that

$$\|\Phi(\cdot, x_1) - \Phi(\cdot, x_2)\|_{L^\infty([0, \infty), d\mu)} \leq C_\Phi.$$

Now, let $\epsilon > 0$. Choose $\lambda_0 > 0$ such that

$$|\Lambda^{1/2} \setminus [0, \lambda_0]| < \frac{\pi \epsilon^2}{8C_\Phi^2(q_0 + q_n)}.$$

Using the fact from (4.3.11) that $\kappa(u) \geq \frac{1}{q_0 q_n}$ for all $u \in (0, \infty)$ and \mathcal{F}_{A_p} is unitary, we have

$$\begin{aligned} \|\mathcal{F}_{A_p} f\|_{L^1(\Lambda \setminus [0, \lambda_0^2], d\mu)} &\leq \left(\frac{1}{2\pi} \int_{\Lambda^{1/2} \setminus [0, \lambda_0]} \frac{\frac{1}{q_0} + \frac{1}{q_n}}{\kappa(u)} du \right)^{1/2} \cdot \|\mathcal{F}_{A_p} f\|_{L^2(\Lambda \setminus [0, \lambda_0^2], d\mu)} \\ &\leq \left(\frac{q_0 + q_n}{2\pi} \right)^{1/2} |\Lambda^{1/2} \setminus [0, \lambda_0]|^{1/2} \|\mathcal{F}_{A_p} f\|_{L^2(\Lambda, d\mu)} \\ &< \frac{\epsilon}{4C_\Phi} \|f\|_2 < \frac{\epsilon}{4C_\Phi}. \end{aligned}$$

Hence,

$$|\chi_{\Lambda \setminus [0, \lambda_0^2]} f(x_1) - \chi_{\Lambda \setminus [0, \lambda_0^2]} f(x_2)| < \frac{\epsilon}{4}. \quad (\text{C.1.4})$$

Meanwhile, using the same λ_0 we similarly obtain

$$|\chi_{\Lambda \cap [0, \lambda_0^2]} f(x_1) - \chi_{\Lambda \cap [0, \lambda_0^2]} f(x_2)| \leq \|\mathcal{F}_{A_p} f\|_{L^1(\Lambda \cap [0, \lambda_0^2], d\mu)} \|\Phi(\cdot, x_1) - \Phi(\cdot, x_2)\|_{L^\infty(\Lambda \cap [0, \lambda_0^2], d\mu)}.$$

The functions Φ^\pm are uniformly continuous on the compact set $[0, \lambda_0^2] \times [-a, a]$. Thus, with the same ϵ there exists $\delta > 0$ such that for $u \in [0, \lambda_0^2]$ and for all $x_1, x_2 \in [-a, a]$ with $|x_1 - x_2| < \delta$,

$$\|\Phi(\cdot, x_1) - \Phi(\cdot, x_2)\|_{L^\infty([0, \lambda_0^2], d\mu)} < \frac{\epsilon}{2\sqrt{2}} \left(\frac{\pi}{\lambda_0(q_0 + q_n)} \right)^{1/2}.$$

We also see that

$$\begin{aligned} \|\mathcal{F}_{A_p} f\|_{L^1(\Lambda^{1/2} \cap [0, \lambda_0^2], d\mu)} &\leq \left(\frac{1}{2\pi} \int_{\Lambda \cap [0, \lambda_0]} \frac{\frac{1}{q_0} + \frac{1}{q_n}}{\kappa(u)} du \right)^{1/2} \cdot \|\mathcal{F}_{A_p} f\|_{L^2(\Lambda \cap [0, \lambda_0^2], d\mu)} \\ &\leq \left(\frac{q_0 + q_n}{2\pi} \right)^{1/2} |\Lambda^{1/2} \cap [0, \lambda_0]|^{1/2} \|\mathcal{F}_{A_p} f\|_{L^2(\Lambda, d\mu)} \\ &< \left(\frac{\lambda_0(q_0 + q_n)}{2\pi} \right)^{1/2}. \end{aligned}$$

C. Localization and approximation lemmas for general spectral sets

Thus, as δ is independent of f ,

$$|\chi_{\Lambda \cap [0, \lambda_0^2]} f(x_1) - \chi_{\Lambda \cap [0, \lambda_0^2]} f(x_2)| < \frac{\epsilon}{4}. \quad (\text{C.1.5})$$

It is clear from (C.1.3), (C.1.4) and (C.1.5) that for every $\epsilon > 0$ there exists $\delta > 0$ such that for all $f \in PW_\Lambda(A_p)$ with $\|f\|_2 \leq 1$,

$$|f(x_1) - f(x_2)| < |\chi_{\Lambda \setminus [0, \lambda_0^2]} f(x_1) - \chi_{\Lambda \setminus [0, \lambda_0^2]} f(x_2)| + |\chi_{\Lambda \cap [0, \lambda_0^2]} f(x_1) - \chi_{\Lambda \cap [0, \lambda_0^2]} f(x_2)| < \frac{\epsilon}{2}.$$

We finally conclude from (C.1.2) that for every $\epsilon > 0$ there exists $\delta > 0$ such that

$$\|k_\Lambda(x_1, \cdot) - k_\Lambda(x_2, \cdot)\|_2 \leq \frac{\epsilon}{2} < \epsilon.$$

Now that the continuity of $x \mapsto k_\Lambda(x, \cdot)$ is proved, the desired result follows almost instantly. The claim implies that the set $\{k_\Lambda(x, \cdot) : |x| \leq a\}$ is compact in $PW_\Lambda(A_p)$, hence totally bounded. By Theorem C.1.1, with the above $\epsilon > 0$ there exists $b_\epsilon > 0$ such that

$$\sup_{x \in [-a, a]} \int_{|y| > b_\epsilon} |k_\Lambda(x, y)|^2 dy < \frac{\epsilon^2}{2}.$$

Since $|x| \leq a$ and $|x - y| > a + b_\epsilon$ imply $|y| \geq |x - y| - |x| > b_\epsilon$, we conclude that

$$\sup_{x \in [-a, a]} \int_{|x-y| > a+b_\epsilon} |k_\Lambda(x, y)|^2 dy \leq \sup_{x \in [-a, a]} \int_{|y| > b_\epsilon} |k_\Lambda(x, y)|^2 dy < \frac{\epsilon^2}{2}. \quad (\text{C.1.6})$$

For later reference, let us take $r_1(\epsilon) = a + b_\epsilon$.

(ii) Case 2: $x > a$. We use the form (C.0.2) of $k_\Lambda(x, y)$ and split the integral of $k_\Lambda(x, y)$ over $|x - y| > b$ for some $b > 0$ into three parts:

$$\int_{|x-y| > b} |k_\Lambda(x, y)|^2 dy = \underbrace{\int_{\substack{|x-y| > b \\ y < -a}} |k_\Lambda(x, y)|^2 dy}_A + \underbrace{\int_{\substack{|x-y| > b \\ y > a}} |k_\Lambda(x, y)|^2 dy}_B + \underbrace{\int_{\substack{|x-y| > b \\ |y| \leq a}} |k_\Lambda(x, y)|^2 dy}_C.$$

Then we make some estimates accordingly. In the following subcases we let $\epsilon > 0$.

- Integral A: We take a similar approach as in the last part of the proof of Lemma 6.3.5. From (4.2.15) and (4.2.16), we write $\Phi(u^2, \cdot) = (\Phi^+(u^2, \cdot), \Phi^-(u^2, \cdot))$ as a column vector. Since $x > a$ and $y < -a$, i.e., $x \in I_n$ and $y \in I_0$, we get

$$\begin{aligned} \Phi(u^2, x) &= \begin{bmatrix} \Phi^+(u^2, x) \\ \Phi^-(u^2, x) \end{bmatrix} = \begin{bmatrix} e^{iq_n u x} \\ a_n^-(u^2) e^{iq_n u x} + b_n^-(u^2) e^{-iq_n u x} \end{bmatrix} \\ \Phi(u^2, y) &= \begin{bmatrix} \Phi^+(u^2, y) \\ \Phi^-(u^2, y) \end{bmatrix} = \begin{bmatrix} a_0^+(u^2) e^{iq_0 u y} + b_0^+(u^2) e^{-iq_0 u y} \\ e^{-iq_0 u y} \end{bmatrix}. \end{aligned}$$

Performing similar calculations as in (5.2.11) yields

$$\begin{aligned} \vartheta(u, x, y) &= \frac{1}{q_0} \overline{\Phi^+(u^2, x)} \Phi^+(u^2, y) + \frac{1}{q_n} \overline{\Phi^-(u^2, x)} \Phi^-(u^2, y) \\ &= \frac{a_0^+(u^2)}{q_0} e^{-i(q_n x - q_0 y)u} + \frac{a_0^+(u^2)}{q_0} e^{i(q_n x - q_0 y)u}, \end{aligned}$$

where the vanishing of $e^{iu(-q_0x - q_ny)}$ follows from identity (4.3.5). Therefore, (C.0.2) can be interpreted as

$$k_\Lambda(x, y) = \frac{1}{2\pi} \int_{\Lambda^{1/2}} \frac{\vartheta(u, x, y)}{\kappa(u)} du \quad (\text{C.1.7})$$

$$\begin{aligned} &= \mathcal{F} \left(\underbrace{\frac{a_0^+(\cdot^2)}{2q_0\pi\kappa}}_{f_1} \chi_{\Lambda^{1/2}} \right) (-q_nx + q_0y) + \mathcal{F} \left(\underbrace{\frac{\overline{a_0^+(\cdot^2)}}{2q_0\pi\kappa}}_{\overline{f_1}} \chi_{\Lambda^{1/2}} \right) (q_nx - q_0y) \\ &= \mathcal{F} f_1(-q_nx + q_0y) + \overline{\mathcal{F} f_1(-q_nx + q_0y)} = 2\text{Re} \mathcal{F} f_1(-q_nx + q_0y). \end{aligned} \quad (\text{C.1.8})$$

In addition, a_0 is an almost periodic polynomial by Lemma 4.2.5, Λ has finite measure, and κ is bounded below. Thus, $f_1 \in L^2(\mathbb{R})$ and consequently $\mathcal{F} f_1 \in L^2(\mathbb{R})$. Hence, there exists $b'_1 > 0$ such that

$$\int_{|z| > b'_1} |\mathcal{F} f_1(z)|^2 dz < \frac{\epsilon^2 q_0}{16} \quad (\text{C.1.9})$$

Now, choose $b_1 > 0$ such that

$$b_1 \min\{q_0, q_n\} + a|q_n - q_0| > b'_1.$$

Recall the assumptions $x > a$ and $y < -a$. We consider two cases:

(i) Suppose $q_n \geq q_0$. If $x - y > b_1$,

$$\begin{aligned} q_nx - q_0y &> q_nx + q_0(b_1 - x) = x(q_n - q_0) + b_1q_0 \\ &> b_1 \min\{q_0, q_n\} + a(q_n - q_0) > b'_1. \end{aligned}$$

Otherwise, if $x - y < -b_1$, then

$$\begin{aligned} q_nx - q_0y &< q_n(y - b_1) - q_0y = (q_n - q_0)y - b_1q_n \\ &< -b_1 \min\{q_0, q_n\} - a(q_n - q_0) < -b'_1. \end{aligned}$$

(ii) Suppose $q_n < q_0$. If $x - y > b_1$,

$$\begin{aligned} q_nx - q_0y &> q_n(b_1 + y) - q_0y = (q_0 - q_n)(-y) + b_1q_n \\ &> b_1 \min\{q_0, q_n\} + a(q_0 - q_n) > b'_1. \end{aligned}$$

Otherwise, if $x - y < -b_1$

$$\begin{aligned} q_nx - q_0y &< q_nx + q_0(-b_1 - x) = (q_0 - q_n)(-x) - b_1q_0 \\ &< -b_1 \min\{q_0, q_n\} - a(q_0 - q_n) < -b'_1. \end{aligned}$$

Therefore, the conditions $x > a$, $y < -a$ and $|x - y| > b_1$ imply $|q_nx - q_0y| > b'_1$. In turn, the substitution $z = -q_nx + q_0y$ implies

$$\begin{aligned} \int_{\substack{|x-y| > b_1 \\ y < -a}} |k_\Lambda(x, y)|^2 dy &= \int_{\substack{|x-y| > b_1 \\ y < -a}} |2\text{Re} \mathcal{F} f_1(-q_nx + q_0y)|^2 dy \\ &\leq \frac{4}{q_0} \int_{|z| > b'_1} |\mathcal{F} f_1(z)|^2 dz < \frac{\epsilon^2}{4}. \end{aligned} \quad (\text{C.1.10})$$

C. Localization and approximation lemmas for general spectral sets

- Integral B: This one is similar to Integral A, but now we have $x, y > a$, i.e., $x, y \in I_n$. We have

$$\begin{aligned}\Phi(u^2, x) &= \begin{bmatrix} e^{iq_n u x} \\ a_n^-(u^2)e^{iq_n u x} + b_n^-(u^2)e^{-iq_n u x} \end{bmatrix} \\ \Phi(u^2, y) &= \begin{bmatrix} e^{iq_n u y} \\ a_n^-(u^2)e^{iq_n u y} + b_n^-(u^2)e^{-iq_n u y} \end{bmatrix}.\end{aligned}$$

By mimicking (5.2.10) and applying Corollary 4.3.2, we get

$$\begin{aligned}\vartheta(u, x, y) &= q_n \kappa(u) (e^{q_n(x-y)u} + e^{-q_n(x-y)u}) \\ &\quad + \frac{1}{q_n} \left(a_n^-(u^2) \overline{b_n^-(u^2)} e^{iq_n(x+y)u} + \overline{a_n^-(u^2)} b_n^-(u^2) e^{-iq_n(x+y)u} \right).\end{aligned}$$

Hence,

$$\begin{aligned}k_\Lambda(x, y) &= \mathcal{F} \underbrace{\left(\frac{q_0}{2\pi} \chi_{\Lambda^{1/2}} \right)}_{f_2} (q_n(x-y)) + \mathcal{F} \left(\frac{q_0}{2\pi} \chi_{\Lambda^{1/2}} \right) (-q_n(x-y)) \\ &\quad + \mathcal{F} \underbrace{\left(\frac{a_n^-(\cdot) \overline{b_n^-(\cdot)}}{2q_n \pi \kappa} \chi_{\Lambda^{1/2}} \right)}_{f_3} (q_n(x+y)) + \mathcal{F} \underbrace{\left(\frac{\overline{a_n^-(\cdot)} b_n^-(\cdot)}{2q_n \pi \kappa} \chi_{\Lambda^{1/2}} \right)}_{\overline{f_3}} (-q_n(x+y)) \\ &= \mathcal{F} f_2(q_n(x-y)) + \mathcal{F} f_2(-q_n(x-y)) + \mathcal{F} f_3(q_n(x+y)) + \overline{\mathcal{F} f_3(q_n(x+y))} \\ &= 2\operatorname{Re} \mathcal{F} f_2(q_n(x-y)) + 2\operatorname{Re} \mathcal{F} f_3(q_n(x+y))\end{aligned}\tag{C.1.11}$$

since f_2 is real-valued. Moreover, $f_2, f_3 \in L^2(\mathbb{R})$, implies $\mathcal{F} f_2, \mathcal{F} f_3 \in L^2(\mathbb{R})$. Therefore, there exists $b_2 > 0$ such that

$$\int_{|z|>b_2} |\mathcal{F} f_2(-q_n z)|^2 dz < \frac{\epsilon^2}{64} \quad \text{and} \quad \int_{|z|>b_2} |\mathcal{F} f_3(q_n z)|^2 dz < \frac{\epsilon^2}{64}.\tag{C.1.12}$$

We also know that with $x, y > a$ and $|x-y| \geq b_2$, we obtain $x+y \geq |x-y| \geq b_2$. Thus, from (C.1.12) and using the fact that $\|u+v\|_2^2 \leq 2\|u\|_2^2 + 2\|v\|_2^2$,

$$\int_{\substack{|x-y|>b_2 \\ y>a}} |k_\Lambda(x, y)|^2 dy \leq 8 \int_{|z|>b_2} |\mathcal{F} f_2(-q_n z)|^2 dz + 8 \int_{|z|>b_2} |\mathcal{F} f_3(q_n z)|^2 dz < \frac{\epsilon^2}{4},\tag{C.1.13}$$

where for the first integral we have the substitution $z = y - x$ and $z = x + y$ for the second.

- Integral C: Using the more general form (3.1.1) of k_Λ , we have

$$\begin{aligned}\int_{|y|\leq a} |k_\Lambda(x, y)|^2 dy &= \int_{|y|\leq a} \left[\int_\Lambda \overline{\Phi(\lambda, x)} \cdot \Phi(\lambda, y) d\mu(\lambda) \int_\Lambda \overline{\Phi(\omega, x)} \cdot \Phi(\omega, y) d\mu(\omega) \right] dy \\ &= \int_{|y|\leq a} \int_{\Lambda \times \Lambda} \overline{\Phi(\lambda, x)} \cdot \Phi(\lambda, y) \Phi(\omega, x) \cdot \overline{\Phi(\omega, y)} d(\mu \otimes \mu)(\lambda, \omega) dy,\end{aligned}$$

where $\mu \otimes \mu$ is the product measure¹⁸ of μ with itself. Define for $\lambda, \omega \in \Lambda$ the functions

$$Z_{jl}(\lambda, \omega) = \int_{|y| \leq a} \Phi_j(\lambda, y) \overline{\Phi_l(\omega, y)} dy, \quad j, l = 1, 2, \quad (\text{C.1.14})$$

where we used $(\Phi_1, \Phi_2) = (\Phi^+, \Phi^-)$ for ease of representation. By interchanging the order of integration and applying change of variables, we get that

$$\begin{aligned} \int_{|y| \leq a} |k_\Lambda(x, y)|^2 dy &= \sum_{j,l=1}^2 \int_{\Lambda^{1/2} \times \Lambda^{1/2}} Z_{jl}(u^2, \omega^2) \cdot \overline{\Phi_j(u^2, x)} \Phi_l(\omega^2, x) d\mu_{jj}(u^2) d\mu_{ll}(\omega^2) \\ &= \sum_{j,l=1}^2 \int_{\Lambda^{1/2} \times \Lambda^{1/2}} c_{jl} \frac{Z_{jl}(u^2, \omega^2)}{\kappa(u)\kappa(\omega)} \cdot \overline{\Phi_j(u^2, x)} \Phi_l(\omega^2, x) du d\omega, \end{aligned} \quad (\text{C.1.15})$$

where

$$C = [c_{jl}]_{j,l=1,2} = \frac{1}{4\pi^2 q_0^2 q_n^2} \begin{bmatrix} q_n^2 & q_0 q_n \\ q_0 q_n & q_0^2 \end{bmatrix} \quad (\text{C.1.16})$$

is obtained from (4.3.21). By Lemma 4.2.5, each $\overline{\Phi_j(u^2, x)} \Phi_l(\omega^2, x)$, $x > a$ for $j, l = 1, 2$ is an almost periodic polynomial of the form

$$\begin{aligned} \overline{\Phi_j(u^2, x)} \Phi_l(\omega^2, x) &= A_{jl}(u, \omega) e^{iq_n(u+\omega)x} + B_{jl}(u, \omega) e^{iq_n(u-\omega)x} \\ &\quad + C_{jl}(u, \omega) e^{-iq_n(u+\omega)x} + D_{jl}(u, \omega) e^{-iq_n(u-\omega)x}, \end{aligned}$$

where each A_{jl} , B_{jl} , C_{jl} , D_{jl} are functions in u and ω formed by some products of $a_n^\pm(u^2)$, $b_n^\pm(u^2)$ and $a_n^\pm(\omega^2)$, $b_n^\pm(\omega^2)$ including their complex conjugates. Thus, for a fixed $x > a$, (C.1.15) may be viewed as a linear combination of two-dimensional Fourier transforms of finitely many functions

$$\frac{e^{i(\alpha u + \beta \omega)} Z_{jl}(u^2, \omega^2)}{\kappa(u)\kappa(\omega)} \chi_{\Lambda^{1/2} \times \Lambda^{1/2}}(u, \omega) \in L^1(\Lambda^{1/2} \times \Lambda^{1/2}), \quad \alpha, \beta \in \mathbb{R}, j, l = 1, 2$$

with evaluations occurring at $(\pm q_n x, \pm q_n x)$. By the Riemann-Lebesgue lemma,

$$\lim_{|x| \rightarrow \infty} \int_{|y| \leq a} |k_\Lambda(x, y)|^2 dy = 0.$$

In particular, there exists $b'_3 > 0$ such that for $|x| > b'_3$

$$\int_{|y| \leq a} |k_\Lambda(x, y)|^2 dy < \frac{\epsilon^2}{4}. \quad (\text{C.1.17})$$

Choose $b_3 = b'_3 + a > 0$. Then as in Case 1, $|y| \leq a$ and $|x - y| > b_3$ imply $|x| \geq |x - y| - |y| > b'_3$, and so (C.1.17) can be applied. Thus,

$$\int_{\substack{|x-y| > b_3 \\ |y| \leq a}} |k_\Lambda(x, y)|^2 dy \leq \sup_{|x| > b'_3} \int_{|y| \leq a} |k_\Lambda(x, y)|^2 dy \leq \frac{\epsilon^2}{4}. \quad (\text{C.1.18})$$

¹⁸If μ_1 and μ_2 are measures on respective measure spaces (X_1, \mathcal{E}_1) and (X_2, \mathcal{E}_2) , the product measure $\mu_1 \otimes \mu_2$ is a measure on the measure space $(X_1 \times X_2, \mathcal{E}_1 \otimes \mathcal{E}_2)$ (tensor product σ -algebra) with the property that for all $E_1 \in \mathcal{E}_1$, $E_2 \in \mathcal{E}_2$, we have $(\mu_1 \otimes \mu_2)(E_1, E_2) = \mu_1(E_1)\mu_2(E_2)$.

C. Localization and approximation lemmas for general spectral sets

Lastly, combining the estimates (C.1.10), (C.1.13) and (C.1.18) for A , B and C , respectively, the choice $r_2(\epsilon) = \max\{b_1, b_2, b_3\}$ yields

$$\int_{|x-y|>r_2(\epsilon)} |k_\Lambda(x, y)|^2 dy < \frac{3\epsilon^2}{4}, \quad x > a. \quad (\text{C.1.19})$$

(iii) Case 3: $x < -a$: The proof of this case is similar to Case 2, and we can conclude that there exists $r_3(\epsilon) > 0$ such that

$$\int_{|x-y|>r_3(\epsilon)} |k_\Lambda(x, y)|^2 dy < \frac{3\epsilon^2}{4}, \quad x < -a. \quad (\text{C.1.20})$$

In summary, we have shown from (C.1.6), (C.1.19) and (C.1.20) that for any $\epsilon > 0$, choosing $r(\epsilon) > \max\{r_1(\epsilon), r_2(\epsilon), r_3(\epsilon)\}$ works so that (C.1.1) holds for all $x \in \mathbb{R}$. Taking the supremum over all $x \in \mathbb{R}$, we get

$$\sup_{x \in \mathbb{R}} \int_{|x-y|>r(\epsilon)} |k_\Lambda(x, y)|^2 dy \leq \frac{3\epsilon^2}{4} < \epsilon^2$$

which is exactly what we wish to prove. \square

We now comment on key differences between the above proof of the weak localization lemma and the proof of the same lemma in [39, Sec. 7].

- (i) In our proof, the estimates in Case 2 were computed using the original spectral measure μ . In [39, Sec. 6.3], the authors used fundamental solutions $\Phi = (\Phi^+, \Phi^-)$ of $(\tilde{\tau}_q - \omega^2)f = 0$, $\tilde{\tau}_q = -D^2 + q$ with $\text{supp}(q) \subseteq [-a, a]$ of the form

$$\Phi^+(\omega, x) = \begin{cases} e^{i\omega x} + R_1(\omega)e^{-i\omega x}, & x < -a, \\ T(\omega)e^{i\omega x}, & x > a, \end{cases}$$

$$\Phi^-(\omega, x) = \begin{cases} T(\omega)e^{-i\omega x}, & x < -a, \\ R_2(\omega)e^{i\omega x} + e^{-i\omega x}, & x > a, \end{cases}$$

where T, R_1 and R_2 are analytic in $\mathbb{C} \setminus (-\infty, 0]$. They also formed the so-called scattering matrix S given by the unitary matrix

$$S(\omega) = \begin{bmatrix} T(\omega) & R_1(\omega) \\ R_2(\omega) & T(\omega) \end{bmatrix}.$$

With this fundamental system and using scattering theory (see [82, Chap. 21]), the corresponding spectral matrix measure reduces to an identity matrix multiplied by the Lebesgue measure [39, Prop. 6.9], which then simplified most of their work. Our proof does not require knowledge of the scattering theory, though the reader may see some resemblance on how some identities similar to those on the scattering matrix S were used. For instance, a crucial part of the proof of Integral A is the vanishing of $e^{iu(-q_n x - q_0 y)}$ (which by symmetry is similar to the vanishing of $e^{iu(q_0 x + q_n y)}$ as in (5.2.11) with $n = 2$) and is a consequence of single identity.

- (ii) Because the solutions found at the infinite intervals may have different frequencies, we had to be very careful in dealing with terms such as $q_n x - q_0 y$ in order to prove our estimates. Nonetheless, the train of thought is the same as the proof of the same lemma in [39, Sec. 7].

C.2. Homogeneous approximation property

We now move on to the proof of the homogeneous approximation property for bounded spectral sets. For the proof, we will apply two results. The first one is a version of Theorem C.1.1 applied to $\ell^2(X)$ (see [7, Thm. 3.4]) and restated for our purpose.

Theorem C.2.1. *A subset $\mathcal{M} \subseteq \ell^2(X)$ is totally bounded if and only if \mathcal{M} is uniformly bounded and for every $\epsilon > 0$, there exists $b_\epsilon > 0$ such that*

$$\sup_{f \in \mathcal{M}} \sum_{x \in X: |x| > b_\epsilon} |f(x)|^2 < \epsilon^2.$$

The second one is the following one-dimensional version of a result in [40, Lem. 1] extended to relatively separated sets.

Lemma C.2.2. *Let $f^\#(x) = \sup_{|x-y| \leq 1} |f(y)|$. If $f \in L^2(\mathbb{R})$ is bandlimited with $\text{supp } \widehat{f} \subseteq [-\Omega, \Omega]$, then $f^\# \in L^2(\mathbb{R})$ and $\|f^\#\|_2 \leq C \|f\|_2$ for some $C > 0$. Moreover, if $X \subseteq \mathbb{R}$ is relatively separated, then there exists $\delta, C_\delta > 0$ such that*

$$\sum_{x \in X: |x| \geq R} |f(x)|^2 \leq C_\delta \int_{|x| \leq R-\delta} |f^\#(x)|^2 dx$$

for all $R > 0$.

The constant δ is determined by writing X as a finite union of separated sets with separation at least δ , while C_δ depends on δ as well as the relative separation constant $\text{rel}(X)$ defined in (6.3.10).

We now restate and prove the homogeneous approximation property.

Lemma C.2.3 (Homogeneous approximation). *Let $\Lambda \subset \mathbb{R}_0^+$ be a bounded Borel set, p be a piecewise constant function and k_Λ be the reproducing kernel for $PW_\Lambda(A_p)$. Suppose X is a set of stable sampling for $PW_\Lambda(A_p)$. Then for every $\epsilon > 0$, there exists $r(\epsilon) > 0$ such that*

$$\sup_{y \in \mathbb{R}} \sum_{\substack{x \in X \\ |x-y| > r(\epsilon)}} |k_\Lambda(x, y)|^2 < \epsilon^2.$$

Proof. This is the discrete analogue of Lemma 6.3.6 and is proved almost exactly the same way. Therefore, some details may be omitted. We fix a sufficiently large $a > 0$ such that $\{t_k\}_{k=1}^n \subseteq [-a, a]$ and work again by cases, but now on the variable y : we have $y < -a$, $|y| \leq a$ and $y > a$. This choice is taken so that the index x is naturally assigned to the indexing set X .

(i) Case 1: $|y| \leq a$. Case 1 of the proof of Lemma C.1.2 shows that the map $y \mapsto k_\Lambda(\cdot, y)$ from $[-a, a]$ to $PW_\Lambda(A_p)$ is compact, since k_Λ is symmetric. Now, if X is a set of stable sampling for $PW_\Lambda(A_p)$, the map $f \mapsto \{f(x)\}_{x \in X}$ from $PW_\Lambda(A_p)$ to $\ell^2(X)$ is also continuous. Hence, the set of sequences $\{\{k_\Lambda(x, y)\}_{x \in X} : |y| \leq a\}$ is compact in $\ell^2(X)$, thus totally bounded. By Theorem C.2.1, we conclude that for any $\epsilon > 0$, there exists $b_\epsilon > 0$ such that

$$\sup_{y \in [-a, a]} \sum_{x \in X: |x| > b_\epsilon} |k_\Lambda(x, y)|^2 < \frac{\epsilon^2}{2}.$$

C. Localization and approximation lemmas for general spectral sets

Taking again $r_1(\epsilon) = a + b_\epsilon$, we have $|x - y| > r_1(\epsilon)$ and $|y| \leq a$ imply $|x| \geq |x - y| - |y| > b_\epsilon$. Consequently,

$$\sup_{y \in [-a, a]} \sum_{\substack{x \in X \\ |x - y| > r_1(\epsilon)}} |k_\Lambda(x, y)|^2 \leq \sup_{y \in [-a, a]} \sum_{x \in X: |x| > b_\epsilon} |k_\Lambda(x, y)|^2 \leq \frac{\epsilon^2}{2}. \quad (\text{C.2.1})$$

(ii) Case 2: $y > a$. The sum is split again into three parts.

$$\sum_{\substack{x \in X \\ |x - y| > b}} |k_\Lambda(x, y)|^2 = \underbrace{\sum_{\substack{x \in X: x < -a \\ |x - y| > b}} |k_\Lambda(x, y)|^2}_A + \underbrace{\sum_{\substack{x \in X: x > a \\ |x - y| > b}} |k_\Lambda(x, y)|^2}_B + \underbrace{\sum_{\substack{x \in X: |x| \leq a \\ |x - y| > b}} |k_\Lambda(x, y)|^2}_C.$$

- Sum A: We perform the same calculations as in (C.1.8), but instead, we write $k_\Lambda(x, y)$, $x < -a, y > a$ in terms of \mathcal{F}^{-1} . If $x < -a$ and $y > a$, i.e., $x \in I_0$ and $y \in I_n$, then the same calculations yield the expression

$$\vartheta(u, x, y) = \frac{\overline{a_0^+(u^2)}}{q_0} e^{-i(q_0 x - q_n y)u} + \frac{a_0^+(u^2)}{q_0} e^{i(q_0 x - q_n y)u}.$$

Hence, for $x < -a, y > a$,

$$\begin{aligned} k_\Lambda(x, y) &= \underbrace{\mathcal{F}^{-1} \left(\frac{a_0^+(\cdot^2)}{q_0 \kappa} \chi_{\Lambda^{1/2}} \right)}_{g_1} (q_0 x - q_n y) + \underbrace{\mathcal{F}^{-1} \left(\frac{\overline{a_0^+(\cdot^2)}}{q_0 \kappa} \chi_{\Lambda^{1/2}} \right)}_{\tilde{g}_2} (-q_0 x + q_n y) \\ &= g_1(q_0 x - q_n y) + g_2(q_0 x - q_n y), \quad g_2(x) = \tilde{g}_2(-x). \end{aligned}$$

By definition, $g_1, g_2 \in L^2(\mathbb{R})$ are bandlimited functions with bandwidth

$$\max\{\omega : \omega^2 \in \Lambda\} < \infty$$

due to the boundedness of Λ . Applying Lemma C.2.2 to g_j , $j = 1, 2$, we have $g_j^\# \in L^2(\mathbb{R})$ for $j = 1, 2$. Moreover, since X is a set of stable sampling for $PW_\Lambda(A_p)$, X is relatively separated by Lemma 6.3.7. Hence, the collection of sets

$$Z_y = -q_n y + q_0 X = \{q_0 x - q_n y : x \in X\}, \quad y > a$$

is a family of relatively separated sets with $\text{rel}(Z_y) = \text{rel}(q_0 X)$ for all $y > a$. By the second conclusion of Lemma C.2.2, there exist $\delta, C_\delta > 0$ such that

$$\sum_{z \in Z_y: |z| \geq R} |g_j(z)|^2 \leq C_\delta \int_{|z| \geq R - \delta} |g_j^\#(z)|^2 dz \quad j = 1, 2 \quad (\text{C.2.2})$$

for all $R > 0$ and for all $y > a$. As each $g_j^\#$ is square-integrable, we have that for every $\epsilon > 0$, there exists $b'_1 > 0$ such that

$$\int_{|z| \geq b'_1 - \delta} |g_j^\#(z)|^2 dz < \frac{\epsilon^2}{16C_\delta} \quad j = 1, 2. \quad (\text{C.2.3})$$

C.2. Homogeneous approximation property

In particular, if we take $R = b'_1$, (C.2.2) and (C.2.3) combined become

$$\sum_{z \in Z_y: |z| \geq b'_1} |g_j(z)|^2 < \frac{\epsilon^2}{16}, \quad j = 1, 2.$$

Again, if we choose $b_1 > 0$ such that

$$b_1 \min\{q_0, q_n\} + a|q_n - q_0| > b'_1,$$

we recall from the arguments of (C.1.8) that $x < -a, y > a$ and $|x - y| > b_1$ imply $|q_0x - q_ny| > b'_1$. Hence, setting $z = q_0x - q_ny$ gives

$$\begin{aligned} \sum_{\substack{x \in X: x < -a \\ |x-y| > b_1}} |k_\Lambda(x, y)|^2 &\leq 2 \sum_{\substack{x \in X \\ |q_0x - q_ny| > b'_1}} (|g_1(q_0x - q_ny)|^2 + |g_2(q_0x - q_ny)|^2) \\ &\leq 2 \sum_{z \in Z_y: |z| > b'_1} (|g_1(z)|^2 + |g_2(z)|^2) < \frac{\epsilon^2}{4} \end{aligned} \quad (\text{C.2.4})$$

for all $y > a$.

- Sum B: By a similar approach as in Sum A applied to the functions analogous to f_2 and f_3 in (C.1.11), we can work our way to conclude that there exists $b_2 > 0$ such that

$$\sum_{\substack{x \in X: x > a \\ |x-y| > b_2}} |k_\Lambda(x, y)|^2 < \frac{\epsilon^2}{4} \quad (\text{C.2.5})$$

for all $y > a$.

- Sum C: We replace the integrals in Integral C by sums and with the appropriate index as well. As in (C.1.14), define for $\lambda, \omega \in \Lambda$ the function

$$W_{jl}(\lambda, \omega) = \sum_{x \in X: |x| \leq a} \Phi_j(\lambda, x) \overline{\Phi_l(\omega, x)} dy, \quad j, l = 1, 2.$$

Since X is relatively separated, W_{jl} has a finite number of terms, each of which is continuous and uniformly bounded on $\mathbb{R}^+ \times \mathbb{R}$ by Lemma 4.2.6. The additional assumption that Λ is a bounded Borel set implies W_{jl} is continuous and bounded in $\Lambda \times \Lambda$. By proceeding exactly as what we did in Integral C, we have from (C.1.15) that

$$\begin{aligned} \sum_{x \in X: |x| \leq a} |k_\Lambda(x, y)|^2 dy &= \sum_{|x| \leq a} \int_\Lambda \overline{\Phi(\lambda, x)} \cdot \Phi(\lambda, y) d\mu(\lambda) \int_\Lambda \overline{\Phi(\omega, x)} \cdot \Phi(\omega, y) d\mu(\omega) \\ &= \sum_{j,l=1}^2 \int_{\Lambda^{1/2} \times \Lambda^{1/2}} W_{jl}(u^2, \omega^2) \cdot \overline{\Phi_j(u^2, y)} \Phi_l(\omega^2, y) d\mu_{jj}(u^2) d\mu_{ll}(\omega^2) \\ &= \sum_{j,l=1}^2 \int_{\Lambda^{1/2} \times \Lambda^{1/2}} c_{jl} \frac{W_{jl}(u^2, \omega^2)}{\kappa(u)\kappa(\omega)} \overline{\Phi_j(u^2, y)} \Phi_l(\omega^2, y) du d\omega, \end{aligned} \quad (\text{C.2.6})$$

C. Localization and approximation lemmas for general spectral sets

with c_{jl} defined exactly as in (C.1.16). Since $y > a$, (C.2.6) is also a linear combination of two-dimensional Fourier transforms of finitely many continuous functions

$$e^{i(\alpha u + \beta \omega)} \frac{W_{jl}(u^2, \omega^2)}{\kappa(u)\kappa(\omega)} \chi_{\Lambda^{1/2} \times \Lambda^{1/2}}(u, \omega), \quad \alpha, \beta \in \mathbb{R}, j, l = 1, 2$$

with evaluations occurring at $(\pm q_n y, \pm q_n y)$. By the Riemann-Lebesgue lemma,

$$\lim_{|y| \rightarrow \infty} \sum_{x \in X: |x| \leq a} |k_\Lambda(x, y)|^2 = 0$$

and by following the same arguments in Integral C, we conclude that there exists $b_3 > 0$ so that

$$\sum_{\substack{x \in X: |x| \leq a \\ |x-y| > b_3}} |k_\Lambda(x, y)|^2 < \frac{\epsilon^2}{4}. \quad (\text{C.2.7})$$

Finally, taking $r_2(\epsilon) > \max\{b_1, b_2, b_3\}$, we get from (C.2.4), (C.2.5) and (C.2.7) that

$$\sup_{y > a} \sum_{\substack{x \in X \\ |x-y| > r_2(\epsilon)}} |k_\Lambda(x, y)|^2 \leq \frac{3\epsilon^2}{4}. \quad (\text{C.2.8})$$

(iii) Case 3: $y < -a$. Using the same arguments as in Case 2, we find $r_3(\epsilon) > 0$ such that

$$\sup_{y < -a} \sum_{\substack{x \in X \\ |x-y| > r_3(\epsilon)}} |k_\Lambda(x, y)|^2 \leq \frac{3\epsilon^2}{4}. \quad (\text{C.2.9})$$

In view of the estimates (C.2.1), (C.2.8) and (C.2.9), $r(\epsilon) > \max\{r_1(\epsilon), r_2(\epsilon), r_3(\epsilon)\}$ does the job and yields the desired result. \square

Bibliography

- [1] L. D. Abreu and A. S. Bandeira. Landau's necessary density conditions for the Hankel transform, 2011.
- [2] R. Aceska and H. Feichtinger. Functions of variable bandwidth via time-frequency analysis tools. *Journal of Mathematical Analysis and Applications*, 382(1):275 – 289, 2011.
- [3] R. Aceska and H. Feichtinger. Reproducing kernels and variable bandwidth. *Journal of Function Spaces and Applications*, 2012, 2012.
- [4] B. Adcock and D. Huybrechs. Frames and numerical approximation. *SIAM Review*, 61(3):443–473, 2019.
- [5] B. Adcock and D. Huybrechs. Frames and numerical approximation ii: Generalized sampling. *Journal of Fourier Analysis and Applications*, 26(6):87, Nov 2020. ISSN 1531-5851.
- [6] L. Amerio and G. Prouse. *Almost-Periodic Functions and Functional Equations*. The university series in higher mathematics. Springer New York, 2013.
- [7] J. Appell and M. Väth. *Elemente der Funktionalanalysis: Vektorräume, Operatoren und Fixpunktsätze*. Vieweg+Teubner Verlag, 2012.
- [8] N. Aronszajn. Theory of reproducing kernels. *Transactions of the American Mathematical Society*, 68(3):337–404, 1950.
- [9] P. Berger, K. Gröchenig, and G. Matz. Sampling and reconstruction in distinct subspaces using oblique projections. *J Fourier Anal Appl*, 25:1090–1112, 2019.
- [10] A. Berlinet and C. Thomas-Agnan. *Reproducing Kernel Hilbert Spaces in Probability and Statistics*. Springer US, 2011.
- [11] A. Besicovitch. *Almost Periodic Functions*. Dover Publications, 1954.
- [12] A. Beurling. On balayage of measures in Fourier transforms. *Notes from a seminar at the Institute for Advanced Study, Princeton, N.J.*, 1959-60 (unpublished).
- [13] A. Beurling. Local harmonic analysis with some applications to differential operators. In *Some Recent Advances in the Basic Sciences*, volume 1, pages 109 – 125. Belfer Graduate School of Science, Yeshiva University, New York, 1966.
- [14] F. J. Beutler and W. L. Root. The operator pseudoinverse in control and systems identification. In M. Z. Nashed, editor, *Generalized inverse and applications*. Academic Press, 1976.
- [15] P. Billingsley. *Probability and Measure*. Wiley Series in Probability and Statistics. Wiley, 2012.
- [16] Å. Björck. *Numerical Methods for Least Squares Problems*. Society for Industrial and Applied Mathematics, 1996.
- [17] R. Blahut. *Principles and Practice of Information Theory*. Addison-Wesley series in electrical and computer engineering. Addison-Wesley Publishing Company, 1987.
- [18] H. Bohr, A. Society, H. Cohn, and F. Steinhardt. *Almost Periodic Functions*. AMS Chelsea Publishing Series. Chelsea Publishing Company, 1947.

Bibliography

- [19] N. N. Brueller, N. Peterfreund, and M. Porat. Non-stationary signals: optimal sampling and instantaneous bandwidth estimation. In *Proceedings of the IEEE-SP International Symposium on Time-Frequency and Time-Scale Analysis (Cat. No.98TH8380)*, pages 113–115, Oct 1998.
- [20] T. Bühler and D. Salamon. *Functional Analysis*. Graduate Studies in Mathematics. American Mathematical Society, 2018.
- [21] B. Buttkus. *Spectral Analysis and Filter Theory in Applied Geophysics*. Springer Berlin Heidelberg, 2012.
- [22] O. Christensen. *An Introduction to Frames and Riesz Bases*. Applied and Numerical Harmonic Analysis. Springer International Publishing, 2016.
- [23] J. Clark, M. Palmer, and P. Lawrence. A transformation method for the reconstruction of functions from nonuniformly spaced samples. *IEEE Transactions on Acoustics, Speech, and Signal Processing*, 33(5):1151–1165, October 1985.
- [24] L. Cohen and C. Lee. Local bandwidth and optimal windows for the short time fourier transform. In F. T. Luk, editor, *Advanced Algorithms and Architectures for Signal Processing IV*, volume 1152, pages 401 – 425. International Society for Optics and Photonics, SPIE, 1989.
- [25] A. Deitmar. *Analysis*. Springer-Lehrbuch. Springer Berlin Heidelberg, 2016.
- [26] E. DiBenedetto. *Real Analysis*. Birkhäuser Advanced Texts Basler Lehrbücher. Springer New York, 2016.
- [27] D. L. Donoho and P. B. Stark. Uncertainty principles and signal recovery. *SIAM Journal on Applied Mathematics*, 49(3):906–931, 1989.
- [28] N. Dunford and J. Schwartz. *Linear Operators, Part 2: Spectral Theory, Self Adjoint Operators in Hilbert Space*. Wiley Classics Library. Wiley, 1988.
- [29] J. Elstrodt. *Maß- und Integrationstheorie*. Springer Berlin Heidelberg, 2018.
- [30] L. N. G. Filon. III.—on a quadrature formula for trigonometric integrals. *Proceedings of the Royal Society of Edinburgh*, 49:38–47, 1930.
- [31] H. Führ, K. Gröchenig, A. Haimi, A. Klotz, and J. L. Romero. Density of sampling and interpolation in reproducing kernel Hilbert spaces. *Journal of the London Mathematical Society*, 96(3):663–686, 2017.
- [32] T. Gamelin. *Complex Analysis*. Undergraduate Texts in Mathematics. Springer New York, 2003.
- [33] G. Gasper, M. Rahman, C. U. Press, G. Rota, G. George, B. Doran, P. Flajolet, M. Ismail, T. Lam, and E. Wutwak. *Basic Hypergeometric Series*. Encyclopedia of Mathematics and its Applications. Cambridge University Press, 2004.
- [34] C. Gauss. *Disquisitiones generales circa seriem infinitam ...*, volume 3, pages 123–162. Göttingen: Königlichem Gesellschaft der Wissenschaften, 1866.
- [35] G. Golub and C. Van Loan. *Matrix Computations*. Johns Hopkins Studies in the Mathematical Sciences. Johns Hopkins University Press, fourth edition edition, 2013.
- [36] R. Gonzalez and R. Woods. *Digital Image Processing*. Pearson/Prentice Hall, 2008.
- [37] K. Gröchenig. Reconstruction algorithms in irregular sampling. *Mathematics of Computation*, 59(199):181–194, 1992.
- [38] K. Gröchenig. *Foundations of Time-Frequency Analysis*. Applied and Numerical Harmonic Analysis. Birkhäuser Boston, 2013.

- [39] K. Gröchenig and A. Klotz. What is variable bandwidth? *Communications on Pure and Applied Mathematics*, 70(11):2039–2083, 2017.
- [40] K. Gröchenig and H. Razafinjatovo. On Landau’s necessary density conditions for sampling and interpolation of band-limited functions. *Journal of the London Mathematical Society*, 54(3):557–565, 1996.
- [41] H. Hanche-Olsen, H. Holden, and E. Malinnikova. An improvement of the Kolmogorov-Riesz compactness theorem. *Expositiones Mathematicae*, 37(1):84 – 91, 2019.
- [42] J. Hogan and J. Lakey. *Duration and Bandwidth Limiting: Prolate Functions, Sampling, and Applications*. Applied and Numerical Harmonic Analysis. Birkhäuser Boston, 2011.
- [43] K. Horiuchi. Sampling principle for continuous signals with time-varying bands. *Information and Control*, 13:53–61, 1968.
- [44] R. Horn and C. Johnson. *Matrix Analysis*. Matrix Analysis. Cambridge University Press, 2013.
- [45] I. Pesenson and A. Zayed. Paley–Wiener subspace of vectors in a Hilbert space with applications to integral transforms. *Journal of Mathematical Analysis and Applications*, 353(2):566 – 582, 2009.
- [46] A. Iserles. On the numerical quadrature of highly-oscillating integrals I: Fourier transforms. *IMA Journal of Numerical Analysis*, 24(3):365–391, 07 2004.
- [47] A. Iserles and S. P. Nørsett. On quadrature methods for highly oscillatory integrals and their implementation. *BIT Numerical Mathematics*, 44(4):755–772, Dec 2004.
- [48] A. Iserles, S. Nørsett, and S. Olver. Highly oscillatory quadrature: The story so far. In A. B. de Castro, D. Gómez, P. Quintela, and P. Salgado, editors, *Numerical Mathematics and Advanced Applications*, pages 97–118, Berlin, Heidelberg, 2006. Springer Berlin Heidelberg.
- [49] A. Jerri. The Shannon sampling theorem—its various extensions and applications: A tutorial review. *Proceedings of the IEEE*, 65:1565 – 1596, 12 1977.
- [50] K. Jörgens, J. Weidmann, and F. Rellich. *Eigenwerttheorie gewöhnlicher Differentialgleichungen*. Hochschultext. Springer Berlin Heidelberg, 2013.
- [51] E. Lai. Converting analog to digital signals and vice versa. In *Practical Digital Signal Processing*, pages 14 – 49. Newnes, Oxford, 2003.
- [52] H. J. Landau. Necessary density conditions for sampling and interpolation of certain entire functions. *Acta Math.*, 117:37–52, 1967.
- [53] H. J. Landau. Sampling, data transmission, and the Nyquist rate. *Proceedings of the IEEE*, 55(10): 1701–1706, 1967.
- [54] D. Levin. Fast integration of rapidly oscillatory functions. *Journal of Computational and Applied Mathematics*, 67(1):95 – 101, 1996.
- [55] D. Levin. Analysis of a collocation method for integrating rapidly oscillatory functions. *Journal of Computational and Applied Mathematics*, 78(1):131–138, 1997.
- [56] R. Martin and A. Kempf. Function spaces obeying a time-varying bandlimit. *Journal of Mathematical Analysis and Applications*, 458(2):1597 – 1638, 2018.
- [57] J. Marzo, S. Nitzan, and J.-F. Olsen. Sampling and interpolation in de Branges spaces with doubling phase. *Journal d’Analyse Mathématique*, 117(1):365–395, Jun 2012.
- [58] M. Mintchev. *Sampling Theorem and Aliasing in Biomedical Signal Processing*. American Cancer Society, 2006.

Bibliography

- [59] V. Moretti. *Spectral Theory and Quantum Mechanics: With an Introduction to the Algebraic Formulation*. UNITEXT. Springer Milan, 2013.
- [60] M. Z. Nashed and G. G. Walter. General sampling theorems for functions in reproducing kernel Hilbert spaces. *Mathematics of Control, Signals and Systems*, 4(4):363, Dec 1991.
- [61] A. Neumaier. Solving ill-conditioned and singular linear systems: A tutorial on regularization. *SIAM Rev.*, 40(3):636–666, Sept. 1998.
- [62] A. Olevskii and A. Ulanovskii. Interpolation in Bernstein and Paley–Wiener spaces. *Journal of Functional Analysis*, 256(10):3257 – 3278, 2009.
- [63] R. Paley and N. Wiener. *Fourier Transforms in the Complex Domain*. Number v. 19 in Amer. Math. Soc. Colloquium pub. American Mathematical Society, 1934.
- [64] A. Papoulis. Error analysis in sampling theory. *Proceedings of the IEEE*, 54(7):947–955, July 1966.
- [65] G. Pedersen. *Analysis Now*. Graduate Texts in Mathematics. Springer New York, 2012.
- [66] I. Pesenson. Sampling of band-limited vectors. *Journal of Fourier Analysis and Applications*, 7(1): 93–100, Jan 2001.
- [67] M. A. Poletti. The development of instantaneous bandwidth via local signal expansion. *Signal Processing*, 31(3):273 – 281, 1993.
- [68] M. Reed and B. Simon. *II: Fourier Analysis, Self-Adjointness*. Methods of Modern Mathematical Physics. Elsevier Science, 1975.
- [69] M. Reed and B. Simon. *I: Functional Analysis*. Methods of Modern Mathematical Physics. Elsevier Science, 1981.
- [70] H. Royden and P. Fitzpatrick. *Real Analysis*. Prentice Hall, 2010.
- [71] J. Russ. *The Image Processing Handbook*. CRC Press, 2016.
- [72] K. Seip. Density theorems for sampling and interpolation in the Bargmann-Fock space II. *J. Reine. Angew. Math.*, 1992:107–114, 01 1992.
- [73] E. Sejdic, I. Djurovic, and L. Stankovic. Quantitative performance analysis of scalogram as instantaneous frequency estimator. *IEEE Transactions on Signal Processing*, 56(8):3837–3845, 2008.
- [74] M. Sonka, V. Hlavac, and R. Boyle. *Image Processing, Analysis, and Machine Vision*. PWS Pub., 1999.
- [75] E. Stein, G. Weiss, G. Mather, and P. Griffiths. *Introduction to Fourier Analysis on Euclidean Spaces*. Mathematical Series. Princeton University Press, 1971.
- [76] T. Strohmer. Numerical analysis of the non-uniform sampling problem. *Journal of Computational and Applied Mathematics*, 122(1):297 – 316, 2000. Numerical Analysis in the 20th Century Vol. II: Interpolation and Extrapolation.
- [77] G. Teschl. *Mathematical Methods in Quantum Mechanics*. Graduate Studies in Mathematics. American Mathematical Society, 2014.
- [78] D. Wei and A. V. Oppenheim. Sampling based on local bandwidth. In *2007 Conference Record of the Forty-First Asilomar Conference on Signals, Systems and Computers*, pages 1103–1107, Nov 2007.
- [79] J. Weidmann. *Linear Operators in Hilbert Spaces*. Graduate texts in mathematics. Springer-Verlag, 1980.

- [80] J. Weidmann. *Spectral theory of ordinary differential operators*. Lecture notes in mathematics. Springer, 1987.
- [81] J. Weidmann. *Lineare Operatoren in Hilberträumen: Teil 1 Grundlagen*. Mathematische Leitfäden. Vieweg+Teubner Verlag, 2013.
- [82] J. Weidmann. *Lineare Operatoren in Hilberträumen: Teil 2 Anwendungen*. Mathematische Leitfäden. Vieweg+Teubner Verlag, 2013.
- [83] H. Weyl. Über gewöhnliche differentialgleichungen mit singularitäten und die zugehörigen entwicklungen willkürlicher funktionen. *Mathematische Annalen*, 68:220–269, 1910.
- [84] J. J. Wolf. Speech signal processing and feature extraction. In J. C. Simon, editor, *Spoken Language Generation and Understanding*, pages 103–128, Dordrecht, 1980. Springer Netherlands.
- [85] S. Xiang. On the Filon and Levin methods for highly oscillatory integral. *Journal of Computational and Applied Mathematics*, 208(2):434 – 439, 2007.
- [86] Y. Y. Zeevi and E. Shlomot. Nonuniform sampling and antialiasing in image representation. *IEEE Transactions on Signal Processing*, 41(3):1223–1236, March 1993.
- [87] K. Zhu. *Analysis on Fock Spaces*. Graduate Texts in Mathematics. Springer US, 2012.